Pontocerebellar hypoplasia: from gene to disease

Namavar, Y.

Publication date
2011
Document Version
Final published version

Yasmin Namavar

Pontocerebellar Hypoplasia: from gene to disease

Pontocerebellar Hypoplasia:

from gene to disease

Yasmin Namavar

Pontocerebellar Hypoplasia: from gene to disease

This thesis should be cited as:

Namavar, Y 2011. Pontocerebellar Hypoplasia: from gene to disease. PhD-thesis, University of Amsterdam, Amsterdam, The Netherlands.

This research was supported financially by generous donations from the Family Heijdeman, the AMC graduate school of the University of Amsterdam and the Hersenstichting Nederland KS2009(1)-81.

Cover illustration: Yasmin Namavar

Lay-out: Rob van Bemmelen & Yasmin Namavar

Printed by: Ipskamp Drukkers B.V. Amsterdam, The Netherlands

ISBN: 978-94-6191-014-1

Pontocerebellar Hypoplasia: from gene to disease

ACADEMISCH PROEFSCHRIFT

ter verkrijging van de graad van doctor
aan de Universiteit van Amsterdam
op gezag van de Rector Magnificus

prof.dr. D.C. van den Boom

ten overstaan van een door het college voor promoties
ingestelde commissie, in het openbaar te verdedigen
in de Aula der Universiteit

op vrijdag 2 december 2011, te 11:00 uur

door

Yasmin Namavar
geboren te Amstelveen

Promotiecommissie

Promotores	Prof. Dr. F. Baas
	Prof. Dr. B.T. Poll-The
Co-promotor	Prof. Dr. P.G. Barth
Overige leden	Prof. Dr. R.C.M. Hennekam
	Prof. Dr. M.S. van der Knaap
	Dr. J. Martinez
	Prof. Dr. R.J. Oostra
	Prof. Dr. I.N. van Schaik
	Prof. Dr. R.J.A. Wanders

Faculteit der Geneeskunde

Contents

Chapter 1

General introduction

Yasmin Namavar, Peter G. Barth, Bwee Tien Poll-The & Frank Baas

Published as "Classification, diagnosis and potential mechanisms
in pontocerebellar hypoplasia" in 2011
in The Orphanet Journal of Rare Diseases 6: 50.

Abstract

Pontocerebellar Hypoplasia (PCH) is group of very rare, inherited progressive neurodegenerative disorders with prenatal onset. Up to now seven different subtypes have been reported (PCH1-7). The incidence of each subtype is unknown. All subtypes share common characteristics, including hypoplasia/atrophy of cerebellum and pons, progressive microcephaly, and variable cerebral involvement. Patients have severe cognitive and motor handicaps and seizures are often reported. Treatment is only symptomatic and prognosis is poor, as most patients die during infancy or childhood. The genetic basis of different subtypes has been elucidated, which makes prenatal testing possible in families with mutations. Mutations in three tRNA splicing endonuclease subunit genes were found to be responsible for PCH2, PCH4 and PCH5. Mutations in the nuclear encoded mitochondrial arginyl-tRNA synthetase gene underlie PCH6. The tRNA splicing endonuclease, the mitochondrial arginyl-tRNA synthetase and the vaccinia related kinase1 are mutated in the minority of PCH1 cases. Most of these genes are involved in essential processes in protein synthesis in general and tRNA processing in particular. In this review we describe the neuroradiological, neuropathological, clinical and genetic features of the different PCH subtypes and we report on *in vitro* and *in vivo* studies on the tRNA splicing endonuclease and mitochondrial arginyl-tRNA synthetase and discuss their relation to pontocerebellar hypoplasia.

Pontocerebellar Hypoplasias

The name Pontocerebellar Hypoplasia (PCH) originates from a report of Brun almost a century ago, in which he described human brain development and abnormalities associated with brain development. Cerebellar Hypoplasia is described as dwarfed growth of the cerebellum [1]. Seven years later Brouwer suggested that pontocerebellar hypoplasia is possibly due to degeneration rather than to hypoplasia [2]. Subsequent reports described the pathology as atrophy of cerebellar hemispheres with relative sparing of the flocculi and vermis and apparent fragmentation of the cerebellar dentate nucleus [3-5]. The first reported case of PCH which included specific clinical details was probably by Krause [4]. He reported a child with swallowing problems, spasticity and complete absence of cognitive and voluntary motor development with the pathological profile of PCH. In retrospect this may have been the first documented case on PCH type 2. Pfeiffer and Pfeiffer first reported the extrapyramidal component [5-8]. Barth *et al.* described a cluster of related families with PCH from a genetic isolate in the Netherlands as an inherited syndrome of microcephaly, dyskinesia and pontocerebellar hypoplasia [9]. A first attempt for classification was based on two subtypes; this divided PCH in cases with accompanying spinal anterior horn disease (type 1) and cases with chorea/dyskinesia (type 2) [10]. This classification was extended into five subtypes in 2006 and in 2007 a sixth was added [11,12]. The latest subtype that may be classified as PCH7, has been recently added to this list [13]. PCH now includes seven (PCH1-7) disorders. In most cases, especially in PCH1, PCH2, PCH4 and PCH5 prenatal onset of structural decline is well documented. In some milder cases cerebellar images suggest a perinatal or early postnatal onset. The clinical diagnosis is made on neuroradiological, neuropathological and neurological findings [14-18]. Neuroradiological findings in all subtypes are pontocerebellar hypoplasia and atrophy of ventral pons, cerebellum and to a lesser extent also the cerebral cortex (Fig. 1). Neuropathologically, there is segmental degeneration of the cerebellar cortex with loss of Purkinje cells, fragmentation of the dentate nucleus and degeneration with neuronal loss and decreased folding of the inferior olivary nuclei in PCH1, PCH2, PCH4 and PCH5. Neuropathological studies in the other types are scarce or absent. Cerebellar hemispheres are usually more severely affected than the vermis and there is progressive loss of the ventral nuclei and transverse fibers in the pons [19]. Furthermore there is severe progressive microcephaly and variable ventriculomegaly. Severe intellectual deficit, swallowing problems and seizures are clinical features of all subtypes [9,18,20].

Clinical features of the PCH subtypes

PCH1

PCH type 1 (Table 1) (PCH1, previously known as Norman's disease, ORPHA2254, MIM 607596) is characterised by pontocerebellar hypoplasia with additional loss of motor neurons in the anterior horn of the spinal cord, pathologically similar to the

spinal muscular atrophies (SMA) [6,7]. Magnetic resonance imaging (MRI) of PCH1 patients always shows cerebellar hypoplasia in which the cerebellar hemispheres are variably affected; in some cases more flat and in other cases more preserved (Fig. 1a-c). There is variable involvement of pons and cerebrum [21]. Patients suffer from severe hypotonia, pareses, central visual failure, dysphagia, respiratory insufficiency, psychomotor retardation and they usually die within the first year. The majority of patients also exhibits prenatal onset of symptoms such as congenital contractures and polyhydramnios. Microcephaly in most reported cases is not present at birth, but develops postnatally [7,10,21-25].

PCH2

PCH type 2 (PCH2, ORPHA2524, MIM 277470, 612389, 612390) is the most frequently reported and therefore the best studied subtype (Table 1) [10,18-20,26]. So far at least 81 families have been reported [20,27,28]. Extrapyramidal dyskinesias and dystonia are the major features of PCH2, pure spasticity is reported in a minority. Other clinical features include impairment of swallowing from birth on, jitteriness in the neonatal period, central visual failure and seizures. There is no involvement of the spinal anterior horn cells in any of the cases that have been studied post-mortem. Life expectancy is unpredictable, as age of death ranges from the neonatal period to well into adulthood; most patients however do not reach puberty [20]. Recently chances for survival have become greater due to improved care, such as tube feeding and gastrostomy. Typical brain MRI findings are a dragonfly-like cerebellar pattern on coronal sections, in which the cerebellar hemispheres are flat and severely reduced in size and the vermis is relatively spared (Fig. 1d-f) [20]. Mild or severe atrophy of the cerebral cortex is observed in 40% of the PCH2 cases. On MRI myelination is delayed, but demyelination has not been observed [20].

Prenatal diagnosis by ultrasound imaging is not yet possible in the second trimester of pregnancy, therefore molecular genetic testing is required for prenatal diagnosis in high risk pregnancies [29].

PCH3

PCH type 3 (PCH3, ORPHA97249, MIM 608027) also known as cerebellar atrophy with progressive microcephaly (CLAM), is a very rare subtype of PCH (Table 1). Only three families have been described so far. All cases had short stature, seizures, hypotonia and in four of the five cases optic atrophy was reported [30-32]. In the most recent reported case, the patient suffered from an additional severe Vitamin A deficiency with unknown cause [32].

PCH4

PCH type 4 (PCH4, olivopontocerebellar hypoplasia (OPCH), ORPHA166063, MIM 225753) shares similarities with PCH2; however PCH4 is more rare and the disease course is more severe (Table 1). Up to now 18 families have been reported with a PCH4

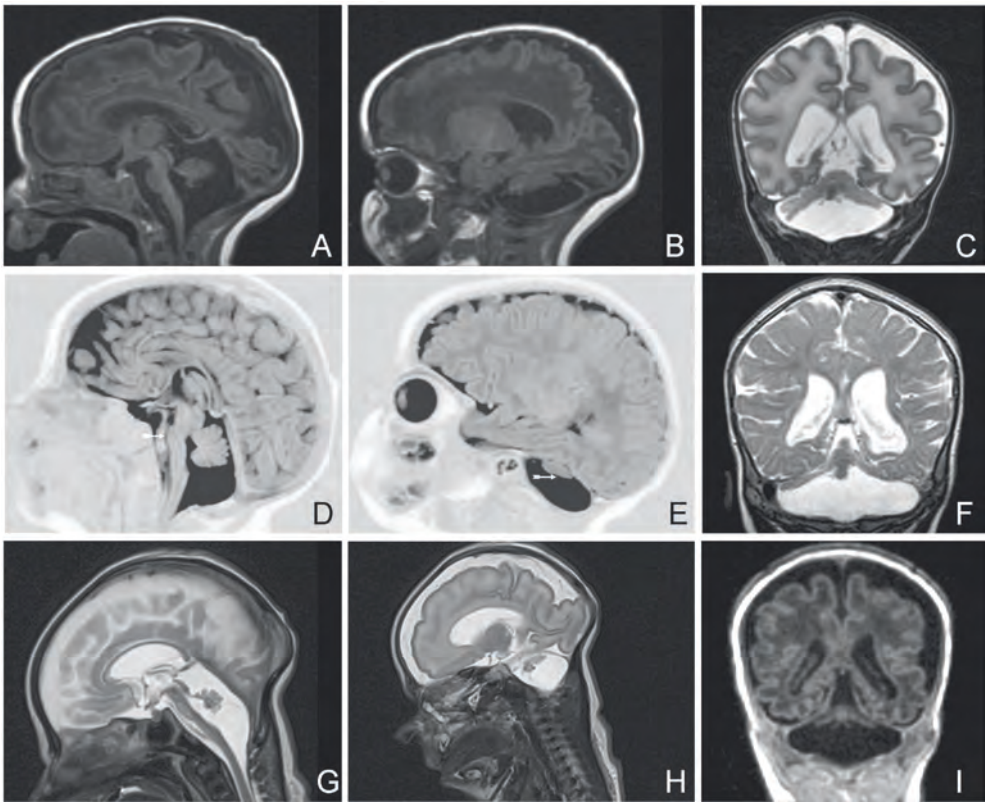

Figure 1. MRI sections of cases with PCH type 1, type 2 and type 4. The images of the PCH1 case were kindly provided by Professor Darin, The Queen Silvia Children's Hospital, Gothenburg University, Sweden. (a-c) Images of a 2 wk old neonate with PCH1. (a) Mid-sagittal section (T_1) shows vermal hypoplasia and marked cerebellar hypoplasia. (b) Lateral sagittal section (T_1) shows severe hypoplasia of the cerebellar hemispheres. (c) Coronal section (T_2) shows flattened cerebellar hemispheres which also display some atrophy. The vermis is relatively spared. (d-e) Images of a 2 months old baby with PCH2. (d) Mid-sagittal section (T_1IR) shows a flat ventral pons and vermal hypoplasia. (e) Lateral sagittal section (T_1IR) shows severely hypoplastic cerebellar hemispheres (arrow) leaving most of the posterior fossa empty. (f) Coronal section (T_2) of a 9 months old infant with PCH2 shows flat cerebellar hemispheres and mild vermal hypoplasia (dragonfly configuration). Cerebral cortical atrophy is also present. (g-i) Images of a 31+5 weeks neonate with PCH4. (g) Mid-sagittal section (T_2) shows severe vermal hypoplasia and ventral pontine flattening. (h) Lateral sagittal section (T_2) shows severe hypoplasia of the cerebellar hemispheres. Above the tentorium there is an increased distance between the cortical surface and the skull visible, which is probably due to diminished brain growth in utero. (i) Coronal section (T_1) shows extremely small and flattened cerebellar hemispheres and severe vermal hypoplasia. Immaturity of cerebral cortex and enlarged ventricles are also visible.

Table 1. PCH subtypes. Adapted and extended from Namavar *et al.* [38].

PCH	**Clinical features**	**Pathological features**	**Gene(s)**	**Ref.**
PCH1	*Neonatal period*: Hypotonia, impaired swallowing, congenital contractures and/or polyhydramnios, primary hypoventilation, progressive microcephaly. *MRI*: Pontocerebellar hypoplasia.	*Cerebellar hypoplasia*: hemispheres >> vermis, areas of stunted or absent folial development. Cerebellar dentate nucleus present as tiny remnants. *Olivary nucleus*: absent folding and gliosis. *Pons*: loss of ventral nuclei and transverse fibers. *Spinal cord*: Anterior horn cell degeneration. *Peripheral nerves and muscle*: chronic denervation.	One family with the common *TSEN54* mutation. One case with missense plus splice site mutations in *RARS2.* One atypical mild family with nonsense mutations in *VRK1.* Locus unknown in the majority .	[6,7,10,20, 21,40,42]
PCH2	*Neonatal period*: Clonus, impaired swallowing. *Infancy and later*: Chorea, variable spastic pareses; progressive microcephaly. Severe impairment of cognitive and motor development. *MRI*: Variable neocortical atrophy, pontocerebellar hypoplasia.	*Cerebellar hypoplasia*: hemispheres >> vermis. Segmental degeneration of cerebellar cortex. Fragmentation of cerebellar dentate nucleus. *Olivary nucleus*: neuron loss and decreased folding. *Pons*: progressive loss of ventral nuclei and transverse fibers. *Cerebral cortex*: progressive atrophy	*TSEN54:* p.A307S, A307S most common in 75 families. Rarely: Other *TSEN54* missense mutations in 3 families, *TSEN2* mutations in 2 families , *TSEN34* mutations in 1 family.	[15,18-20,28,37]
PCH3	*Neonatal period*: Hypotonia, impaired swallowing. *Infancy and later*: Short stature progressive microcephaly, optic atrophy. *MRI*: Neocortical and cerebellar atrophy, pontocerebellar hypoplasia; Pons and cerebellum equally affected.	No autopsies performed.	Locus on chromosome 7q in 2 families.	[30-32]

Table 1. (continued)

PCH	Clinical features	Pathological features	Gene(s)	Ref.
PCH4	*Neonatal period*: Hypertonia, severe clonus, polyhydramnios and/or contractures; primary hypoventilation. *MRI*: Delayed neocortical maturation, pontocerebellar hypoplasia; microcephaly on autopsy.	*Cerebellar hypoplasia*: hemispheres >> vermis, areas of stunted or absent folial development. Cerebellar dentate nucleus present as tiny remnants *Olivary nucleus*: absent folding and gliosis. *Pons*: loss of ventral nuclei and transverse fibers.	*TSEN54:* Compound heterozygosity for p.A307S plus nonsense or splice site mutations in 10 families. Three missense mutations in 1 family.	[14,16,19, 20,37]
PCH5	*Prenatal/neonatal period*: Clonus or seizures. *Neonatal period*: Persistent clonus, microcephaly and pontocerebellar hypoplasia on autopsy.	*Cerebellar hypoplasia*: cortical involvement as in PCH4, but vermal cortex more extensively affected than hemispheric cortex; subtotal loss of cerebellar dentate nucleus. *Olivary nucleus*: absent folding. *Pons*: loss of ventral nuclei and transverse fibers.	*TSEN54*: Compound heterozygosity for p.A307S plus splice site mutation in 1 family.	[11,20]
PCH6	*Neonatal period*: Hypotonia, clonus, impaired swallowing. *Infancy and later*: Progressive microcephaly, spasticity, elevated CSF lactate, edema of extremities. *MRI*: Neocortical and cerebellar atrophy, pontocerebellar hypoplasia; Pons and cerebellum equally affected.	No autopsies performed.	Missense and splice site mutations in *RARS2* in 2 families.	[12,39]
PCH7	*Neonatal period*: No palpable gonads with a micropenis. Hypotonia. *Infancy and later*: Regression of penis. Progressive microcephaly, seizures, respiratory distress, poor feeding. *MRI*: Pontocerebellar hypoplasia.	*Cerebellar hypoplasia*: absence of cerebellar hemispheres with neuronal loss. *Olivary nucleus*: absent. *Pons*: loss of ventral nuclei and transverse fibers. *Cerebral cortex*: progressive atrophy.	No locus.	[13]

phenotype [14,16,20,28,33-36]. Patients exhibit more severe perinatal symptoms such as excessive, prolonged general clonus, congenital contractures, polyhydramnios and primary hypoventilation the latter necessitating prolonged mechanical ventilation. Weaning from ventilatory support is often impossible making survival through the neonatal period exceptional [20]. The pathology seen in PCH4 deviates in some regards from PCH2. A striking pathological distinction in PCH4 is the C-shaped form of the inferior olives and large denuded areas without folia in the cerebellar hemispheric cortex, both phenomena suggesting an early prenatal onset [14,19,37]. Other striking features in PCH4 are pericerebral cerebrospinal fluid (CSF) accumulation, wide midline cava and delayed neocortical maturation; all suggesting prenatal decline of cerebral growth. Additionally the cerebellar vermis is more severely affected (Fig. 1g-i) [20,38]. MRI analysis is therefore helpful in the clinical diagnosis of PCH4.

PCH5

Only one family with PCH type 5 (PCH5, ORPHA166068, MIM 610204) has been described (Table 1). In this subtype of PCH, patients displayed foetal onset of seizure-like activity in combination with severe olivopontocerebellar hypoplasia and a severely affected cerebellar vermis [11]. Autopsy of the three published siblings showed diffuse brain volume loss, C-shaped inferior olivary nuclei, absent or immature dentate nuclei and cell death which was more pronounced in the cerebellar vermis than in the hemispheres. No evidence was found for spinal cord involvement.

In retrospect there is an arbitrary difference between PCH4 and PCH5 [38]. In PCH5 the vermis was more affected than the hemispheres, whereas in PCH4 the vermis and the hemispheres are both severely affected, with the emphasis on the hemispheres. The prenatal seizure-like activity observed in PCH5 appears similar to the severe neonatal clonus observed in PCH4 [16]. The primary hypoventilation observed in PCH5 is also a typical aspect of PCH4 [20].

PCH6

PCH type 6 (PCH6, ORPHA166073, MIM 611523) is a rare subtype of PCH (Table 1). The first published family with PCH6 is a Sephardic Jewish family with three siblings exhibiting cerebellar and vermal hypoplasia, infantile encephalopathy, dysphagia, seizures, progressive microcephaly and generalised hypotonia followed by spasticity [12]. No developmental milestones were reached. Biochemical investigation of mitochondrial complexes showed reduced activity of mitochondrial complexes I, III, and IV in muscle, while activity of complex II was normal. Elevated CSF lactate levels were found. Another case by Rankin *et al.* with a PCH6 phenotype in combination with progressive encephalopathy and edema, was suggestive of PEHO syndrome (Progressive Encephalopathy with Oedema, Hypsarrhythmia and Optic atrophy) [39]. No autopsies have been performed in PCH6 cases so far.

PCH7

A new subtype was proposed based on a profile combining genital abnormalities in combination with PCH. We tentatively classify this as PCH7 (Table 1). The male patient had impalpable testes with a micropenis at birth and an XY karyotype. In the following weeks he developed progressive microcephaly, swallowing problems, hypotonia, respiratory distress, absent tracking movements, a head lag and seizures. MRI at the age of 16 weeks showed pontocerebellar hypoplasia and cerebral atrophy. At 19 weeks of age, regression of penile corporeal tissue was noted. He died at 5 ½ months of age [13].

Genetics of PCH

TSEN-related PCH and genotype-phenotype correlations

Through homozygosity mapping in a cluster of related families with PCH2, the genetic basis for PCH2 was identified [37]. All patients were homozygous mutant for an amino acid change of an alanine into a serine at position 307 (p.A307S, common mutation) in the transferRNA (tRNA) splicing endonuclease subunit 54 gene (*TSEN54*) (Table 2). Ninety percent of the well-defined PCH2 cases carried this mutation [37]. This *TSEN54* mutation correlated strongly with jitteriness, clonus, dyskinesia and/or dystonia and with flat cerebellar hemispheres on coronal MRI compared to those PCH cases where no mutation was identified (Fig. 1f) [20].

In rare occasions, mutations are found in two of the three other subunit genes of the tRNA splicing endonuclease, *TSEN2* and *TSEN34* (Table 2) [20,37]. Four patients have been described so far; three with *TSEN2* mutations and one with a *TSEN34* mutation [20]. These cases have a PCH2 phenotype, as they exhibited spasticity and/or dyskinesias. Other missense mutations than the p.A307S in *TSEN54*, have been associated with PCH2 as well (Table 2). Some of these patients with a rare mutation in *TSEN54* and the patient with a *TSEN34* mutation have relatively mild involvement of pons and cerebellum. On early coronal MRI the cerebellar hemispheres are not completely flat, but fill the posterior fossa almost completely, suggestive of postnatal atrophy rather than hypoplasia [20]. Because only a few patients with *TSEN2*, *TSEN34* and rare *TSEN54* missense mutations other than p.A307S have been diagnosed thus far, one should be cautious with generalisations about their phenotypes.

Whereas missense mutations in *TSEN54* underlie PCH2, heterozygous missense- plus heterozygous nonsense or splice site mutations in *TSEN54* underlie the more severe PCH4 (Table 1, Table 2) [20,27,37]. In one case, three *TSEN54* missense mutations were found in PCH4. This case was homozygous mutant for the common mutation, plus another missense mutation (p.S93P) on one of the alleles, giving rise to a PCH4 phenotype. Nonsense and splice site mutations in *TSEN54* are associated with increased severity of hypoplasia of pons and cerebellum and immaturity of the cerebral cortex

Table 2. Pathogenic mutations in PCH. Note that in PCH4 and PCH5 there is compound heterozygosity for a nonsense or a splice site mutation plus a missense mutation (p.A307S, *TSEN54*).

Gene	**Nucleotide position**	**Protein position**	**Subtype**
TSEN54	c.178_215del	p.E60AfsX109	PCH4
TSEN54	c.285G>C	p.A95A Splice site mutation	PCH4
TSEN54	c.277T>C	p.S93P	PCH4
TSEN54	c.371G>T	p.G124V	PCH2
TSEN54	c.370-2A>G	p.G124_Q138del	PCH4
TSEN54	c.468+2T>C	Splice site mutation	PCH5
TSEN54	c.736C>T	p.Q246X	PCH4
TSEN54	c.919G>T	p.A307S (common)	PCH1, PCH2, PCH4, PCH5
TSEN54	c.953delC	p.P318QfsX23	PCH4
TSEN54	c.1027C>T	p.Q343X	PCH4
TSEN54	c.1056_1057del	p.R353GfsX81	PCH4
TSEN54	c.1170_1183del	p.V390fsX39	PCH4
TSEN54	c.1251A>G	p.P417P Splice site mutation	PCH4
TSEN54	c.1430+2T>A	Splice site mutation	PCH4
TSEN54	c.1537T>G	p.Y513D	PCH4
TSEN34	c.172C>T	p.R58W	PCH2
TSEN2	c.926A>G	p.Y309C	PCH2
TSEN2	c.960+1delGTAAG	Splice site mutation	PCH2
RARS2	c.35A>G	p.Q12R	PCH1, PCH6
RARS2	c.110+5A>G	Splice site mutation	PCH1, PCH6
RARS2	c.1024A>G	p.M342V	PCH6
VRK1	c.1072C>T	p.R358X	PCH1

with more perinatal symptoms and an earlier lethality than seen in PCH2.

As in PCH4, a heterozygous missense mutation (p.A307S) plus a heterozygous splice site mutation (c.468+2T>C) in *TSEN54* has been found to be responsible for PCH5 (Table 2) [38]. Although milder, the clinical findings in PCH2 are similar to PCH4 and PCH5. Therefore PCH5, PCH4 and PCH2 represent a spectrum of clinical manifestations caused by different mutations in the *TSEN* genes (Table 1). It is still unclear whether PCH1 is part of this spectrum too, as the common mutation in *TSEN54* was identified in one case from a family with three siblings with a PCH1

phenotype [40]. DNA was only available in one of the three siblings. Post-mortem examination revealed neuronal cell loss of the anterior horns of the cervical cord [40]. PCH1 seems to be more heterogeneous than PCH2/PCH4 and several genes are already involved in the minority of the PCH1 cases.

Reliable estimations of the incidence of the common/p.A307S mutation (*TSEN54*) are difficult to obtain. Although PCH2 with this underlying mutation is the most common form of PCH, it is still a rare disease and clusters in isolated communities. In the Dutch and German population the carrier frequency of the common mutation is 0.004 [37]. With 184 915 newborns in the Netherlands in the year 2009 one would expect 3 affected children *per annum* [41]. However, since the p.A307S mutation occurs in closed communities, where consanguinity occurs, probably more affected children are born per year, than one would expect based on carrier frequency in unrelated Caucasian individuals. Therefore preconceptional testing with prenatal diagnosis for this disease in selected regions is advised.

RARS2-related PCH

Following homozygosity mapping in the first published PCH6 family, a homozygous intronic splice site mutation (c.110+5A>G) was found in the nuclear encoded gene for the mitochondrial arginyl-tRNA synthetase (*RARS2*) (Table 2) [12]. A second PCH6 case with additional progressive encephalopathy and edema was compound heterozygote for *RARS2* missense mutations (Table 2) [39].

Mutations in *RARS2* were identified in one case with a PCH1 phenotype [20]. Although this case had high CSF lactate levels, which is normally not reported in PCH1, post-mortem examination revealed a neuropathological profile that fits a PCH1 phenotype with loss of spinal anterior horn neurons.

Other genes and loci involved in PCH

Nonsense mutations in the Vaccinia Related Kinase1 gene (*VRK1*) were reported to be associated with pontocerebellar hypoplasia plus SMA in one atypical PCH1 family of Ashkenazi Jewish origin [42]. Despite the severe microcephaly at birth (fronto-occipital circumference -3SD and –6SD), the three affected children were mildly delayed in their developmental milestones. The proband was e.g. able to walk at the age of 3 years; however she became wheelchair bound later in life and eventually died at the age of 11 years. Cognitive impairment was stated as mild mental retardation, whereas in typical PCH1 cases there is severe mental retardation and no developmental milestones will be achieved [7,10,21-25]. Up to now no other cases with *VRK1* mutations have been reported.

Mutations or deletions in the survival motor neuron gene (*SMN1*) cause SMA. In PCH1 linkage to the *SMN* genes has been excluded; although the motor neuron loss observed in PCH1 is morphologically similar to the motor neuron loss in SMA [43,44].

Table 3. Differential diagnostic options for PCH (*right page*).

There is no locus for the majority of the PCH1 cases and no other genes have been linked to PCH1 yet, with the exception of rare cases with *TSEN54*, *RARS2* and *VRK1* mutations (Table 2). Fifteen families with a PCH1 phenotype have been published thus far; only in 3 families mutations were identified [6,7,10,20-25,34,40,42,44-51]. Further research on these and other candidate genes in PCH1 is necessary to identify mutations involved in the remaining majority of the PCH1 cases.

Linkage on chromosome 7q was found in two of the three families with PCH3, but no causative gene has been found [30,31]. Unfortunately no linkage analysis was performed in the most recently published case with PCH3 [32].

There is no locus yet for PCH7, however sequencing of the coding regions in *TSEN54*, *TSEN34*, *TSEN2*, *TSEN15* and *RARS2* yielded no mutations. FISH analysis of *SRY* and *Xq12* and a CGH-array appeared to be normal, as well as ARX expansion analysis [13].

Management and Treatment

There is no cure for PCH: Management is only symptomatic and includes nutritional support by percutaneous endoscopic gastrostomy (PEG feeding), treatment of dystonia, dyskinesias and seizures. Sometimes respiratory support is provided. The chorea in PCH2 is difficult to treat, but physiotherapy may ease cases with severe dystonia or spasticity. Levodopa treatment appeared beneficial in some cases [52].

Life-threatening complications of PCH are cot death, sleep apnea and malignant hyperthermia with rhabdomyolysis with extreme elevation of plasma creatine kinase. Sleep apnea can be detected by sleep monitoring. Malignant hyperthermia should be prevented by sufficient hydration and monitoring especially during periods of infection [26].

Other diseases with (ponto)cerebellar hypoplasia

There are several other diseases that one may consider when a patient presents with pontocerebellar hypoplasia, see also Table 3 for an indication.

Genetic diseases with cerebellar hypoplasia and/or atrophy and variable cerebral cortical atrophy

Recently a new PCH-like phenotype has been described: Progressive Cerebello-Cereberal Atrophy (PCCA). Patients with PCCA have postnatal atrophy of the cerebellar hemispheres, which is not typical for PCH, but some PCH patients do have this feature [20,30]. Patients with PCCA have progressive microcephaly, severe

Differential diagnosis	Cerebellar Hypoplasia plus:	Gene(s)	Pathways involved	Ref.
Genetic diseases with cerebellar hypoplasia and/or atrophy and variable cerebral cortical atrophy				
PCCA	Progressive Cerebello-cerebral atrophy, progressive microcephaly, spasticity, seizures, mental retardation and seizures.	Missense mutations in *SEPSECS.*	Selenocysteine synthesis	[53]
ICCA	Severe atrophy of cerebrum and cerebellum. Psychomotor retardation, clonus, seizures, spasticity, progressive microcephaly.	Missense mutations in *MED17*	Transcripition initiation	[54]
CDG type 1A and 1D	Hypotonia, ataxia, developmental delay, failure to thrive, microcephaly.	*PMM2* (type 1a), *ALG3* (type 1d)	Glycoprotein biosynthesis	[55,56]
Phosphoserine aminotransferase deficiency	Low CSF concentrations of serine and glycine, seizures, progressive microcephaly, hypertonia and psychomotor retardation. White matter immaturity and cerebral atrophy.	*PSAT*	Serine biosynthesis	[59]
Different congenital mitochondrial disorders	Respiratory chain deficiencies plus several other abnormalities.	-	n/a	[60]
PEHO-syndrome	Progressive cerebellar atrophy, progressive encephalopathy, hypsarrythmie, edema and optic atrophy.	Unknown	Unknown	[62,63]
Genetic diseases with cerebellar hypoplasia plus neocortical dysplasia				
Dystroglanopathies: Walker-Warburg syndrome, MEB-disease, Fukuyama	Neocortical dysplasia. Mental retardation, eye abnormalities, seizures, impaired motor control.	*FKRP, LARGE, POMGNT1, POMT1, POMT2, FKTN*	Dystroglycan synthesis	[64,65]
Lissencephaly	Lissencephaly phenotype.	*RELN*	Neuronal migration	[67]
X-linked brain malformation phenotype with microcephaly and hypoplasia of the brainstem and cerebellum	Microcephaly, optic atrophy, sensorineural hearing loss, simplified gyri, developmental delay.	*CASK*	Neuronal migration; Part of MAGUK protein family, involved in signaling in both, pre- and post-synapses.	[66]
Congenital fibrosis of the extraocular muscles 3 with extraocular involvement	Ocular motility disorder, facial weakness, axonal peripheral neuropathy, delayed development, neocortical dysplasia and other neuronal migration disorders.	*TUBB3*	Neuronal migration	[68,69]
Acquired cerebellar hypoplasia				
Extreme prematurity (<32 weeks)	Extreme prematurity.	n/a	n/a	[70]

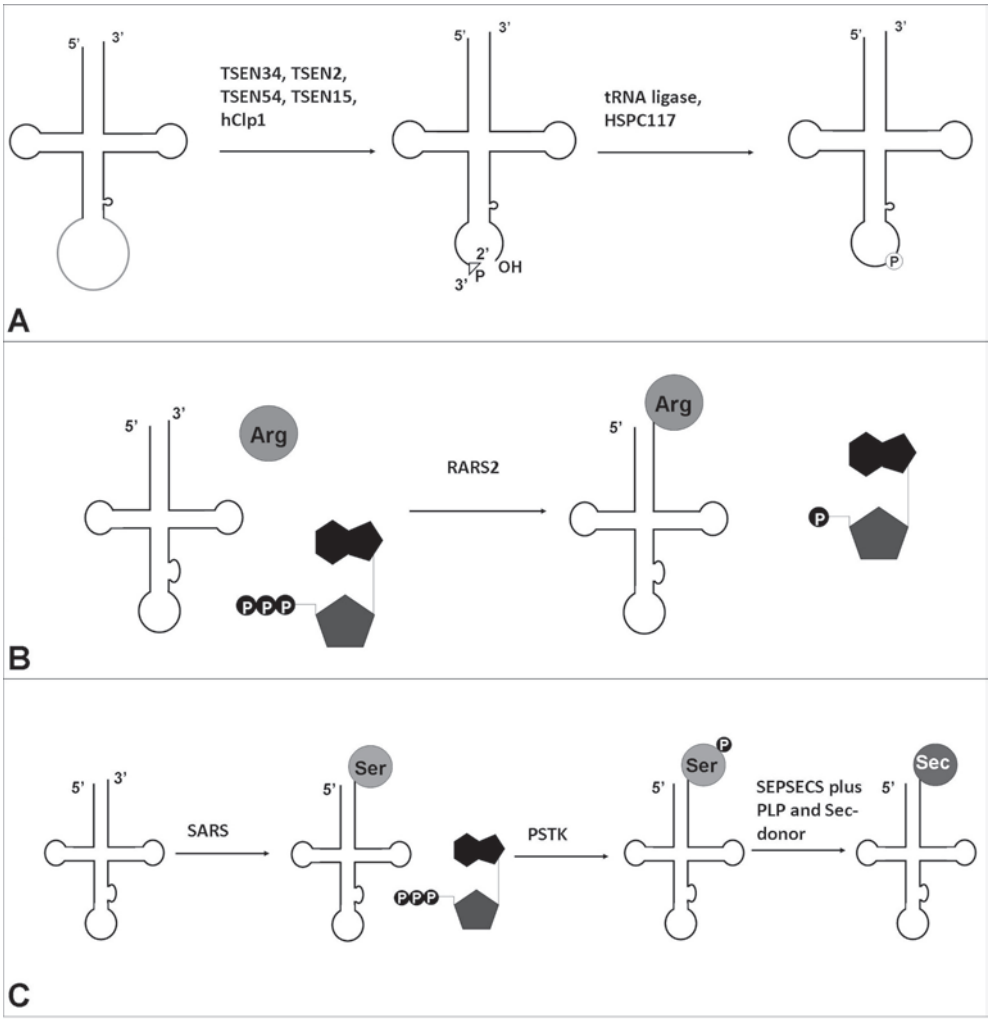

Figure 2. Different RNA processing events in mammals. (a) Eukaryotic splicing pathway of tRNA splicing in mammals. The TSEN complex is involved in the maturation of premature tRNAs and excises the tRNA into two halves; one 5'tRNA half with a 2'-3'cyclic phosphate at one exon-end and a 3'tRNA half with a 5'OH-group at the other exon-end. The final processing of tRNA maturation involves either direct ligation of the two tRNA halves by ligation through the Archaea-like pathway (by HSPC117, depicted) or indirect ligation through the yeast-like pathway (not depicted) [104]. Adapted from Calvin *et al.* [105]. (b) tRNA aminoacylation in mammals. RARS2 can bind to its cognate amino acid in an ATP dependent matter. This complex of ATP, RARS2 and arginine binds to the mt-tRNA-Arg and arginine will be transferred to its tRNA. Adapted from Antonellis *et al.* [83]. (c) Selenocysteine synthesis. Serine (Ser) is aminoacylated to tRNA-Sec by a seryl-tRNA synthetase (SARS). This Ser-tRNA-Sec complex is then converted by a kinase to a Sep-tRNA-Sec complex. In the presence of the cofactor pyridoxal phosphate (PLP) and the selenium donor selenophosphate (Se-donor) the SEPSECS enzyme converts the Sep-tRNA-Sec to Sec-tRNA-Sec. Adapted from Allmang *et al.* [87].

spasticity, mental retardation and in some cases seizures. Sequential brain MRI of patients shows the progressive nature of the cerebellar and cerebral atrophy. Missense mutations in the *O*-phosphoseryl-tRNA selenocysteine tRNA synthase gene (*SEPSECS*) are associated with this disease (Table 3) [53].

In infantile cerebral and cerebellar atrophy (ICCA) there is also cerebellar volume loss with psychomotor retardation, seizures, jitteriness, clonus, severe spasticity, visual problems, hypertonia and progressive postnatal microcephaly. Brain MRI shows severe atrophy of cerebrum and cerebellum (Table 3) [54].

Certain subtypes of the congenital disorders of glycosylation (CDG) disorders manifest with cerebellar hypoplasia as well. CDG-1a patients have generalised hypotonia, developmental delay, swallowing problems, failure to thrive and cerebellar hypoplasia, next to variable external dysmorphia and hematologic problems [55]. Cerebellar hypoplasia is also present in patients with CDG-1d, a rare form of CDG (Table 3) [56-58].

Phosphoserine aminotransferase deficiency is associated with low CSF concentrations of serine and glycine. Clinically patients exhibit seizures, progressive microcephaly, hypertonia and psychomotor retardation. MRI shows cerebral atrophy, poor white matter development and vermal hypoplasia. The authors did not mention the size and morphology of the cerebellar hemispheres (Table 3) [59]. Also in various paediatric mitochondrial disorders predominant cerebellar volume loss is relatively common, together with respiratory chain deficiencies (Table 3) [60,61]. Progressive cerebellar atrophy is commonly found in patients with PEHO-syndrome (Table 3) [62,63].

Genetic diseases with cerebellar hypoplasia plus neocortical dysplasia

Dystroglycanopathies cause neocortical dysplasia and variable pontocerebellar hypoplasia and microcephaly or hydrocephalus (Table 3) [64,65]. An X-linked brain malformation phenotype with a moderately simplified gyral pattern and mild cortical dysplasia, only visible on autopsy is due to mutations in the calcium/calmodulin dependent serine protein kinase gene (*CASK*). It can manifests with microcephaly, optic atrophy, sensorineural hearing loss and pontocerebellar hypoplasia (Table 3) [66]. Other diseases with cerebellar hypoplasia and additional neocortical dysplasia but easier to differentiate from PCH, are lissencephaly with agyria or very wide gyria and congenital fibrosis of the extraocular muscles type 3 (CFEOM3) with extraocular involvement like neocortical dysplasia and neuronal migration defects (Table 3) [67-69].

Acquired cerebellar hypoplasia

Extreme prematurity (<32 weeks) in infants can also lead to cerebellar hypoplasia, due to disruption of normal brain development. One should be aware of this when a prematurely born neonate presents with these features (Table 3) [70,71].

Pathogenesis

The function of the tRNA splicing endonuclease

The tRNA splicing endonuclease (*TSEN*) complex is mutated in the majority of the PCH cases. The endonuclease complex is encoded by four different *TSEN* genes (*TSEN2*, *15*, *34*, *54*) and consists of four protein subunits. Together they form one heterotetramic enzyme, consisting of two catalytic subunits (TSEN2 and TSEN34) and two structural subunits (TSEN54 and TSEN15) [72-74]. In mammals, maturation of tRNA necessitates removal of the 5'leader and 3'trailer sequences, addition of a CCA tail and various modifications [75]. Six percent of the human tRNA genes are intron-containing; this intron is not removed by the conventional splicing machinery, but by the TSEN complex. Only these intron-containing tRNAs require the TSEN complex for excising the tRNA into two halves; one 5'tRNA half with a 2'-3'cyclic phosphate at the cleavage site and a 3'tRNA half with a 5'OH-group at the other cleavage site (Fig. 2a). The individual halves of the tRNA are ligated together again. Mature tRNAs are essential for translation of messengerRNA (mRNA) into proteins, as they transfer the correct amino acid to the ribosome to incorporate these amino acids at the growing peptide chain. Each amino acid has its own cognate tRNA and each tRNA has an anticodon sequence that can interact to the corresponding codon on mRNA sequence. In humans there are 506 different tRNA genes, meaning that there are more tRNA genes than codons. For certain tRNA species the majority of the tRNA genes are intron-containing: For example, 13 of the 14 tRNA-Tyr (GTA) genes contain an intron (Table 4). For other tRNAs there are no intron-containing tRNA genes at all: For example all tRNA-Gly (GCC, CCC, TCC) genes are not intron-containing. For further information on intron-containing and intronless tRNA genes, see [76].

Table 4. Overview of the number of human tRNA genes with an intron and the remaining corresponding tRNAs without an intron. Adapted from the Genomic tRNA database [76].

Human tRNA species with an intron (*anticodon*)	**Number of human tRNA genes with an intron**	**Number of the remaining human tRNA genes without an intron (same anticodon)**
Pro - *AGG*	1	9
Arg - *TCT*	5	1
Leu - *CAA*	5	2
Ile - *TAT*	5	0
Tyr - *ATA*	1	0
Tyr - *GTA*	13	1
Cys - *ACA*	1	0
Trp - *CCA*	1	8

The TSEN complex is not only involved in tRNA splicing, it is also involved in mRNA 3'end formation. Knockdown of *TSEN2* results in impaired mRNA 3'end formation of two housekeeping transcripts *GAPDH* and *EF1A* mRNA in HEK293 cells [73]. Furthermore the TSEN complex interacts with a lot of factors associated with the mRNA 3'end processing machinery [73,77].

In 2007, the human cleavage and polyadenylation factor I subunit (hClp1) was identified as siRNA kinase. hClp1 is a binding partner of the TSEN complex and its kinase activity is also active on 3'tRNA halves, furthermore hClp1 participates in mRNA 3'end formation [78-80]. It seems that multiple enzymes involved in RNA processing assemble into a molecular equivalent of a 'Swiss Army Knife', creating a complex that can cleave and process several different RNA species [79].

The TSEN complex and PCH

In vitro studies of the TSEN complex

In 2006 the yeast Sen complex was purified and different mutations in the complex were introduced; this showed that certain mutations abolished tRNA splicing activity whereas others do not affect tRNA splicing at all [74]. The authors also show that the same mutation can have a different effect on tRNA splicing, depending on the different tRNA: E.g. tRNA-Phe is usually not as strongly affected by mutations as tRNA-Tyr. Certain tRNA transcripts are perhaps spliced more readily than other tRNA transcripts [74]. This illustrates that it is difficult to predict how mutations in the TSEN complex will affect tRNA splicing in PCH patients. It is likely that tRNA splicing activity in patients is reduced, and not completely abolished as no patients to date have been described with two nonsense mutations in one of the *TSEN* subunits; this would abrogate tRNA splicing completely and lead to deprivation of certain amino acids, which would be non-compatible with life.

Generally, PCH4 patients have a null allele and a missense mutation in *TSEN54* and are therefore more severely affected than PCH2 patients who carry two missense mutations in *TSEN54*. This genotype-phenotype correlation suggests that loss of TSEN function is the underlying disease mechanism in PCH2 and PCH4. One could hypothesise that a defective TSEN complex would lead to insufficient tRNA splicing, mainly affecting intron-rich tRNA genes, like tRNA-Tyr (Table 4). However Northern blot analysis of tRNA-Tyr from fibroblasts of three patients homozygous for the common mutation in *TSEN54* did not show unspliced products. No significant difference was found in mature tRNA-Tyr levels in fibroblasts of patients and controls either [37]. To summarise, there is no evidence for a tRNA maturation defect in *TSEN*-mutated fibroblasts. Neuronal cells derived from patients would be a better substrate for tRNA maturation analysis, but unfortunately brain material is scarce and usually severely affected at the time of death. Induced pluripotent stem cell (iPS) technology

might circumvent this problem, but even when patient fibroblasts can be converted to neuronal cells, there is no guarantee that these cells will show a phenotype. After all, not all neurons in a PCH case are affected.

It remains possible that other unknown (cell type specific) functions of the TSEN complex may play a role in the disease pathogenesis of PCH cases.

Zebrafish models of TSEN related PCH

Recently we established a zebrafish model for PCH. Knockdown of *tsen54* by antisense morpholino injections in zebrafish embryos resulted in abnormalities in the mid-hindbrain and a developmental delay. The zebrafish embryos showed head hypoplasia and loss of structural integrity in the brain. The loss of structural definition in the brain is not due to a patterning defect, since fibroblast growth factor 8 (*fgf8*) and orthodenticle homeobox 2 (*otx2*), two developmental markers, were expressed in the correct regions. Instead the developing zebrafish embryo's showed increased levels of cell death, bearing comparisons to the neurodegeneration observed in PCH. This neurodegenerative phenotype is partially rescued by co-injecting human *TSEN54* mRNA in zebrafish embryos [81].

Expression analysis of *tsen54* in zebrafish shows a ubiquitous expression pattern, but higher expression in brain, primarily in the telencephalon and mid-hindbrain boundary. This is in line with the expression of human *TSEN54* mRNA at eight weeks of gestation, in which high expression in the developing telencephalon and metencephalon is observed [81]. The human cerebellum begins its development at six weeks of gestation and continues growing into the postnatal period [82]. With careful monitoring in PCH4/PCH5 cases, one can already measure a decline in transverse cerebellar diameter at 16 weeks of gestation, indicating a very early onset of the neurodegeneration [11].

Antisense morpholino effects diminish after a few days post-injection. Therefore we also developed a stable *tsen54* knockout zebrafish carrying a premature stop codon. When bred to homozygosity these zebrafish mutants were viable at 9 days post fertilization (dpf). The absence of a major brain phenotype and survival up to 9 dpf may be explained by the presence of maternal tsen54 during embryogenesis [81]. Redundancy of the protein in zebrafish is not likely, as eventually these mutant zebrafish die after 9 days.

RARS2 and PCH

RARS2, mutated in PCH6 and PCH1, is one of the 36 human tRNA synthetases. By the usage of ATP, the tRNA synthetase binds to its cognate amino acid. This complex of ATP, tRNA synthetase and amino acid, binds to the appropriate tRNA whereto the amino acid will be transferred (Fig. 2b) [83]. RARS2 is involved in the aminoacylation of arginine (Arg) to its mitochondrial-tRNA-Arg. In *RARS2* mutated (c.110+5A>G)

fibroblasts, a reduction in the amount of the mt-tRNA-Arg was observed. Despite this reduction, the residual mt-tRNA-Arg transcript was almost completely acylated, suggesting that uncharged mt-tRNA-Arg transcripts are unstable [12]. Morpholino-directed knockdown of *rars2* in zebrafish resulted in a similar neurodegenerative phenotype as *tsen54* knockdown, suggesting the same pathogenesis for PCH2/4 and PCH6, although it is still not understood how RARS2 is involved in the development of the pons and cerebellum [81].

Alternative functions of RARS2 compromising the same biological pathway as the TSEN complex could also be the underlying mechanism in PCH [73,78,81]. For some of the tRNA synthetases alternative functions are known in processes like conventional splicing, apoptosis, viral assembly, regulation of transcriptional and translational processes and angiogenic signaling [83-85].

SEPSECS and PCCA

Mutations in *SEPSECS* are associated with PCCA (progressive cerebello-cerebral atrophy). The SEPSECS enzyme (Fig. 2c) is involved in the final step of the selenocysteine (Sec) synthesis [86,87]. Selenocysteine lacks its own tRNA synthetase and in contrast to the other amino acids selenocysteine is synthesised on its cognate tRNA. The codon for selenocysteine is UGA, normally encoding for translation termination, however depending on the flanking sequences of the UGA, this codon is recoded for a selenocysteine. Prior to selenocysteine synthesis, serine (Ser) is aminoacylated to tRNA-Sec by a seryl-tRNA synthetase; this Ser-tRNA-Sec complex is then converted by a kinase to a Sep-tRNA-Sec complex. As a final step SEPSECS converts the Sep-tRNA-Sec to Sec-tRNA-Sec. It is not likely that *SEPSECS* missense mutations (p.A239T, p.Y334K) completely abolish its function, as deprivation of selenocysteins is associated with lethality in mice [88].

Discussion

The identification of mutations in genes involved in transcription and translation in neurological disorders shows that these processes are important in (developing) neurons [83,89-94]. The TSEN complex, RARS2 and SEPSECS proteins, all share involvement in essential processes in protein synthesis and mutations in the corresponding genes all lead to a severe phenotype of pontocerebellar hypoplasia, often in combination with cortical involvement. One explanation could be that developing neuronal tissue is sensitive to dysregulation of protein synthesis [83,92-94]. This hypothesis is supported by mice with a homozygous missense mutation in the alanyl-tRNA synthetase gene (*AARS*). This mouse has increased levels of mischarged tRNAs which lead to intracellular accumulation of misfolded proteins in neurons, this induces the unfolded protein response (UPR) and these mice develop a neurodegenerative phenotype, with

Purkinje cell death and subsequent ataxia [95]. However UPR activation has not been detected in postmortem brain of PCH2 patients carrying a *TSEN* mutation, but one can argue that UPR activation is an early event in the pathogenesis of PCH and that postmortem studies do not capture this event [19].

On the other hand it is possible that there is a time frame during embryogenesis in which there is an extra high demand for protein synthesis in neuronal tissue in the early post-migratory stage. Human brain tissue expresses relatively high overall levels of nuclear and mitochondrial encoded tRNAs, which might be due to higher levels of translation in the CNS compared to other tissue [96]. Moreover, malnutrition in rats during the prenatal period has severe consequences for brain development and the cerebellum in particular [97]. Protein malnutrition both prenatally and postnatally, results in reduced brain weight, thinner cerebral and cerebellar cortices, reduced numbers of neurons, deficient myelination and reduced dendritic spines of cortical neurons [98,99]. Therefore it is very likely that nutrients and proteins are highly essential for normal brain development.

Why mutations in other genes involved in protein synthesis lead to completely different phenotypes remains unclear. For example, mutations in other genes involved in tRNA charging like *KARS*, *YARS* and *GARS* lead to different types of Charcot-Marie-Tooth neuropathy [83,100,101]. Mitochondrial aspartyl-tRNA synthetase (*DARS2*) mutations cause leukoencephalopathy with brain stem and spinal cord involvement and lactate elevation (LBSL). Patients with LBSL have profound white matter abnormalities in their cerebrum, pons and spinal cord. There are some similarities between LBSL and PCH, like cerebellar involvement and spasticity, but the differences are more evident. Patients have slowly progressive cerebellar ataxia, dorsal column dysfunction, occasionally a mild cognitive decline and the age of onset is usually during childhood or even later. It is unclear how mutations in *DARS2* lead to LBSL [89].

Not all mutations in tRNA synthetase genes result in a neurological phenotype. Missense mutations in the mitochondrial Seryl-tRNA Synthetase gene (*SARS2*) give rise to a multi-organ disease with Hyperuricemia, Pulmonary Hypertension, Renal Failure and Alkalosis (HUPRA-syndrome). Although there is failure to thrive and a global developmental delay, patients exhibit no neurological symptoms and brain ultrasound was reported to be normal [102]. Compound heterozygote mutations in mitochondrial histidyl-tRNA synthetase gene (*HARS2*) were found in one family with ovarian dysgenesis and progressive sensorineural hearing loss (Perrault syndrome) [103].

In summary, the most likely explanation for the neurological phenotype in the disorders described above is that maturing neurons are more vulnerable for defects in protein synthesis than other tissues, but this does not explain the difference between disease presentation shared by mutations of *TSEN*, *RARS2* and *SEPSECS*, in which the cerebellum appears to be preferentially affected and other diseases (*KARS, YARS,*

GARS, SARS2), with a different disease presentation.

Conclusions and Outlook

During the last decade many genes involved in protein synthesis have been associated with different neurological diseases. Several genes of PCH subtypes have been described, in view of the shared function in tRNA processing, a defect in protein synthesis seems the most likely pathomechanism in PCH. Hopefully identification of new genes in PCH subtypes will provide further insight and lead us to a common disease pathway. Also further research on TSEN and/or RARS2 function in PCH models is necessary to elucidate the question why solely the brain, and specifically the cerebellum and pons are affected in PCH.

Aim and Outline

The aim of this thesis is to identify the gene(s) responsible for Pontocerebellar Hypoplasia (PCH) and to understand the pathogenesis of the disease. Homozygosity mapping in a genetic isolate with PCH subtype 2 showed that a mutation in the tRNA splicing endonuclease (*TSEN*) subunit 54 gene is responsible for the disease in this family. Moreover, we identified additional mutations in *TSEN54*, *TSEN2* and *TSEN34* in other families with PCH type 2 and type 4. In **Chapter 2** we discuss these findings. **Chapter 3** describes strong genotype-phenotype correlations in a cohort of 169 patients with PCH. Patients with missense mutations are clinically and pathologically relatively mildly affected compared to patients who are compound heterozygote for missense and nonsense mutations. In addition, we identified more mutations in the *TSEN* genes responsible for PCH2 and PCH4. In the mitochondrial arginyl tRNA synthetase gene (*RARS2*) we identified mutations to be responsible for a rare form of PCH1 and for PCH6. **Chapter 4** describes the genetic characterisation of PCH type 5, a disease also caused by mutations in *TSEN54*. PCH5 has a severe phenotype with many similarities to PCH4. **Chapter 5** provides the first experimental evidence that loss of function mutations in *TSEN54* cause PCH. Morpholino knockdown of the zebrafish *tsen54* gene causes brain hypoplasia associated with increased cell death, without a defect in neurodevelopmental patterning, thus bearing comparison to PCH. Moreover zebrafish homozygous for a premature stop codon mutation in *tsen54* die during larval stages. **Chapter 5** also describes the consequences of *rars2* knockdown in zebrafish embryos, resulting in a similar neurological phenotype. Therefore *TSEN54* mediated PCH and *RARS2* mediated PCH possibly share a common disease pathway. **Chapter 6** presents experimental evidence on reduced tRNA splicing activity in patient fibroblasts. No defect in mRNA 3'end formation was observed. These data suggest that impaired tRNA splicing is the underlying disease mechanism in PCH. **Chapter 7** summarises all these findings and discusses the pathogenesis of the disease. Also new directions for further research are discussed.

Acknowledgements & Funding

We thank Dr. Paul Kasher for careful reading of the manuscript and helpful discussions. Financial support was kindly provided by the Hersenstichting Nederland KS2009(1)-81. Y.N. is supported by an AMC graduate school fellowship.

Reference List

1. Brun R: Zur Kenntnis der Bildungsfehler des Kleinhirns. Epikritische Bemerkungen zur Entwicklungspathologie, Morphologie und Klinik der umschriebenen Entwicklungshemmungen des Neozerebellums. Schweiz Arch Neurol Psychiatr 1917, 1:48-105.
2. Brouwer B: Hypoplasia ponto-neocerebellaris. Psychiatr Neurol (Amsterdam) 1924, 6:461-469.
3. Koster S: Two cases of hypoplasia ponto-neocerebellaris. Acta Psychiatr (Københ) 1926, 1:47-76.
4. Krause F: Über einen Bildungsfehler des Kleinhirns und einige faseranatomische Beziehungen des Organs. Zeitschrift der Gesammten Neurologie und Psychiatrie 1928, 119:788-815.
5. Biemond A.: Hypoplasia ponto-neocerebellaris, with malformation of the dentate nucleus. Folia Psychiatr Neurol Neurochir Neerl 1955, 58:2-7.
6. Norman RM: Cerebellar hypoplasia in Werdnig-Hoffmann disease. Arch Dis Child 1961, 36:96-101.
7. Goutieres F, Aicardi J, Farkas E: Anterior horn cell disease associated with pontocerebellar hypoplasia in infants. J Neurol Neurosurg Psychiatry 1977, 40:370-378.
8. Peiffer J, Pfeiffer RA: Hypoplasia ponto-neocerebellaris. J Neurol 1977, 215:241-251.
9. Barth PG, Vrensen GF, Uylings HB, Oorthuys JW, Stam FC: Inherited syndrome of microcephaly, dyskinesia and pontocerebellar hypoplasia: a systemic atrophy with early onset. J Neurol Sci 1990, 97:25-42.
10. Barth PG: Pontocerebellar hypoplasias. An overview of a group of inherited neurodegenerative disorders with fetal onset. Brain Dev 1993, 15:411-422.
11. Patel MS, Becker LE, Toi A, Armstrong DL, Chitayat D: Severe, fetal-onset form of olivopontocerebellar hypoplasia in three sibs: PCH type 5? Am J Med Genet A 2006, 140:594-603.
12. Edvardson S, Shaag A, Kolesnikova O, Gomori JM, Tarassov I, Einbinder T, Saada A, Elpeleg O: Deleterious mutation in the mitochondrial arginyl-transfer RNA synthetase gene is associated with pontocerebellar hypoplasia. Am J Hum Genet 2007, 81:857-862.
13. Anderson C, Davies JH, Lamont L, Foulds N: Early Pontocerebellar Hypoplasia with Vanishing Testes: A New Syndrome? Am J Med Genet Part A 2011, 155:667-672.
14. Albrecht S, Schneider MC, Belmont J, Armstrong DL: Fatal infantile encephalopathy with olivopontocerebellar hypoplasia and micrencephaly. Report of three siblings. Acta Neuropathol 1993, 85:394-399.
15. Barth PG, Blennow G, Lenard HG, Begeer JH, van der Kley JM, Hanefeld F, Peters AC, Valk J: The syndrome of autosomal recessive pontocerebellar hypoplasia, microcephaly, and extrapyramidal dyskinesia (pontocerebellar hypoplasia type 2): compiled data from 10 pedigrees. Neurology 1995, 45:311-317.
16. Chaves-Vischer V, Pizzolato GP, Hanquinet S, Maret A, Bottani A, Haenggeli CA: Early fatal pontocerebellar hypoplasia in premature twin sisters. Eur J Paediatr Neurol 2000, 4:171-176.

17. Goasdoue P, Rodriguez D, Moutard ML, Robain O, Lalande G, Adamsbaum C: Pontoneocerebellar hypoplasia: definition of MR features. Pediatr Radiol 2001, 31:613-618.

18. Steinlin M, Klein A, Haas-Lude K, Zafeiriou D, Strozzi S, Muller T, Gubser-Mercati D, Schmitt MT, Krageloh-Mann I, Boltshauser E: Pontocerebellar hypoplasia type 2: variability in clinical and imaging findings. Eur J Paediatr Neurol 2007, 11:146-152.

19. Barth PG, Aronica E, de Vries L, Nikkels PG, Scheper W, Hoozemans JJ, Poll-The BT, Troost D: Pontocerebellar hypoplasia type 2: a neuropathological update. Acta Neuropathol 2007, 114:373-386.

20. Namavar Y, Barth PG, Kasher PR, van Ruissen F., Brockmann K, Bernert G, Writzl K, Ventura K, Cheng EY, Ferriero DM et al.: Clinical, neuroradiological and genetic findings in pontocerebellar hypoplasia. Brain 2011, 134:143-156.

21. Rudnik-Schoneborn S, Sztriha L, Aithala GR, Houge G, Laegreid LM, Seeger J, Huppke M, Wirth B, Zerres K: Extended phenotype of pontocerebellar hypoplasia with infantile spinal muscular atrophy. Am J Med Genet A 2003, 117A:10-17.

22. Gorgen-Pauly U, Sperner J, Reiss I, Gehl HB, Reusche E: Familial pontocerebellar hypoplasia type I with anterior horn cell disease. Eur J Paediatr Neurol 1999, 3:33-38.

23. Ryan MM, Cooke-Yarborough CM, Procopis PG, Ouvrier RA: Anterior horn cell disease and olivopontocerebellar hypoplasia. Pediatr Neurol 2000, 23:180-184.

24. Szabo N, Szabo H, Hortobagyi T, Turi S, Sztriha L: Pontocerebellar hypoplasia type 1. Pediatr Neurol 2008, 39:286-288.

25. Okanishi T, Mori Y, Shirai K, Kobayashi S, Nakashima H, Kibe T, Yokochi K, Togari H, Nonaka I: Delayed gyration with pontocerebellar hypoplasia type 1. Brain Dev 2010, 32:258-262.

26. Barth PG, Ryan MM, Webster RI, Aronica E, Kan A, Ramkema M, Jardine P, Poll-The BT: Rhabdomyolysis in pontocerebellar hypoplasia type 2 (PCH-2). Neuromuscul Disord 2008, 18:52-58.

27. Cassandrini D, Biancheri R, Tessa A, Di RM, Di CM, Bruno C, Denora PS, Sartori S, Rossi A, Nozza P et al.: Pontocerebellar hypoplasia: clinical, pathologic, and genetic studies. Neurology 2010, 75:1459-1464.

28. Valayannopoulos V, Michot C, Rodriguez D, Hubert L, Saillour Y, Labrune P, de LJ, Brunelle F, Amiel J, Lyonnet S et al.: Mutations of TSEN and CASK genes are prevalent in pontocerebellar hypoplasias type 2 and 4. Brain 2011.

29. Graham JM, Jr., Spencer AH, Grinberg I, Niesen CE, Platt LD, Maya M, Namavar Y, Baas F, Dobyns WB: Molecular and neuroimaging findings in pontocerebellar hypoplasia type 2 (PCH2): is prenatal diagnosis possible? Am J Med Genet A 2010, 152A:2268-2276.

30. Rajab A, Mochida GH, Hill A, Ganesh V, Bodell A, Riaz A, Grant PE, Shugart YY, Walsh CA: A novel form of pontocerebellar hypoplasia maps to chromosome 7q11-21. Neurology 2003, 60:1664-1667.

31. Durmaz B, Wollnik B, Cogulu O, Li Y, Tekgul H, Hazan F, Ozkinay F: Pontocerebellar hypoplasia type III (CLAM): Extended phenotype and novel molecular findings. J Neurol 2009, 256:416-419.

32. Jacob FD, Hasal S, Goez HR: Pontocerebellar hypoplasia type 3 with severe vitamin A deficiency. Pediatr Neurol 2011, 44:147-149.

33. Kawagoe T, Jacob H: Neocerebellar hypoplasia with systemic combined olivo-ponto-dentatal degeneration in a 9-day-old baby: contribution to the problem of relations between malformation and systemic degeneration in early life. Clin Neuropathol 1986, 5:203-208.

34. Moerman P, Barth PG: Olivo-ponto-cerebellar atrophy with muscular atrophy, joint

contractures and pulmonary hypoplasia of prenatal onset. Virchows Arch A Pathol Anat Histopathol 1987, 410:339-345.

35. Park SH, Becker-Catania S, Gatti RA, Crandall BF, Emelin JK, Vinters HV: Congenital olivopontocerebellar atrophy: report of two siblings with paleo- and neocerebellar atrophy. Acta Neuropathol 1998, 96:315-321.

36. Pittella JE, Nogueira AM: Pontoneocerebellar hypoplasia: report of a case in a newborn and review of the literature. Clin Neuropathol 1990, 9:33-38.

37. Budde BS, Namavar Y, Barth PG, Poll-The BT, Nurnberg G, Becker C, van Ruissen F, Weterman MAJ, Fluiter K, te Beek E et al.: tRNA splicing endonuclease mutations cause pontocerebellar hypoplasia. Nat Genet 2008, 40:1113-1118.

38. Namavar Y, Chitayat D, Barth PG, van Ruissen F., de Wissel MB, Poll-The BT, Silver R, Baas F: TSEN54 mutations cause pontocerebellar hypoplasia type 5. Eur J Hum Genet 2011.

39. Rankin J, Brown R, Dobyns WB, Harington J, Patel J, Quinn M, Brown G: Pontocerebellar hypoplasia type 6: A British case with PEHO-like features. Am J Med Genet A 2010, 152A:2079-2084.

40. Simonati A, Cassandrini D, Bazan D, Santorelli FM: TSEN54 mutation in a child with pontocerebellar hypoplasia type 1. Acta Neuropathol 2011.

41. CBS. http://www.cbs.nl/nl-NL/menu/home/default.htm. 2011.

42. Renbaum P, Kellerman E, Jaron R, Geiger D, Segel R, Lee M, King MC, Levy-Lahad E: Spinal muscular atrophy with pontocerebellar hypoplasia is caused by a mutation in the VRK1 gene. Am J Hum Genet 2009, 85:281-289.

43. Dubowitz V, Daniels RJ, Davies KE: Olivopontocerebellar hypoplasia with anterior horn cell involvement (SMA) does not localize to chromosome 5q. Neuromuscul Disord 1995, 5:25-29.

44. Muntoni F, Goodwin F, Sewry C, Cox P, Cowan F, Airaksinen E, Patel S, Ignatius J, Dubowitz V: Clinical spectrum and diagnostic difficulties of infantile ponto-cerebellar hypoplasia type 1. Neuropediatrics 1999, 30:243-248.

45. Weinberg AG, Kirkpatrick JB: Cerebellar hypoplasia in Werdnig-Hoffmann disease. Dev Med Child Neurol 1975, 17:511-516.

46. Steiman GS, Rorke LB, Brown MJ: Infantile neuronal degeneration masquerading as Werdnig-Hoffmann disease. Ann Neurol 1980, 8:317-324.

47. de Leon GA, Grover WD, D'Cruz CA: Amyotrophic cerebellar hypoplasia: a specific form of infantile spinal atrophy. Acta Neuropathol 1984, 63:282-286.

48. Kamoshita S, Takei Y, Miyao M, Yanagisawa M, Kobayashi S, Saito K: Pontocerebellar hypoplasia associated with infantile motor neuron disease (Norman's disease). Pediatr Pathol 1990, 10:133-142.

49. Chou SM, Gilbert EF, Chun RW, Laxova R, Tuffli GA, Sufit RL, Krassikot N: Infantile olivopontocerebellar atrophy with spinal muscular atrophy (infantile OPCA + SMA). Clin Neuropathol 1990, 9:21-32.

50. Sztriha L, Johansen JG: Spectrum of malformations of the hindbrain (cerebellum, pons, and medulla) in a cohort of children with high rate of parental consanguinity. Am J Med Genet A 2005, 135:134-141.

51. Rudnik-Schoneborn S, Wirth B, Rohrig D, Saule H, Zerres K: Exclusion of the gene locus for spinal muscular atrophy on chromosome 5q in a family with infantile olivopontocerebellar atrophy (OPCA) and anterior horn cell degeneration. Neuromuscul Disord 1995, 5:19-23.

52. Grosso S, Mostadini R, Cioni M, Galluzzi P, Morgese G, Balestri P: Pontocerebellar

hypoplasia type 2: further clinical characterization and evidence of positive response of dyskinesia to levodopa. J Neurol 2002, 249:596-600.

53. Agamy O, Ben ZB, Lev D, Marcus B, Fine D, Su D, Narkis G, Ofir R, Hoffmann C, Leshinsky-Silver E et al.: Mutations disrupting selenocysteine formation cause progressive cerebello-cerebral atrophy. Am J Hum Genet 2010, 87:538-544.

54. Kaufmann R, Straussberg R, Mandel H, Fattal-Valevski A, Ben-Zeev B, Naamati A, Shaag A, Zenvirt S, Konen O, Mimouni-Bloch A et al.: Infantile cerebral and cerebellar atrophy is associated with a mutation in the MED17 subunit of the transcription preinitiation mediator complex. Am J Hum Genet 2010, 87:667-670.

55. van de Kamp JM, Lefeber DJ, Ruijter GJ, Steggerda SJ, den Hollander NS, Willems SM, Matthijs G, Poorthuis BJ, Wevers RA: Congenital disorder of glycosylation type Ia presenting with hydrops foetalis. J Med Genet 2007, 44:277-280.

56. Stibler H, Stephani U, Kutsch U: Carbohydrate-deficient glycoprotein syndrome--a fourth subtype. Neuropediatrics 1995, 26:235-237.

57. Denecke J, Kranz C, Kleist-Retzow JC, Bosse K, Herkenrath P, Debus O, Harms E, Marquardt T: Congenital disorder of glycosylation type Id: Clinical phenotype, molecular analysis, prenatal diagnosis, and glycosylation of foetal proteins. Pediat Res 2005, 58:248-253.

58. Kranz C, Sun L, Eklund EA, Krasnewich D, Casey JR, Freeze HH: CDG-Id in two siblings with partially different phenotypes. Am J Med Genet A 2007, 143A:1414-1420.

59. Hart CE, Race V, Achouri Y, Wiame E, Sharrard M, Olpin SE, Watkinson J, Bonham JR, Jaeken J, Matthijs G et al.: Phosphoserine aminotransferase deficiency: a novel disorder of the serine biosynthesis pathway. Am J Hum Genet 2007, 80:931-937.

60. Scaglia F, Wong LJ, Vladutiu GD, Hunter JV: Predominant cerebellar volume loss as a neuroradiologic feature of pediatric respiratory chain defects. Am J Neuroradiol 2005, 26:1675-1680.

61. de Koning TJ, de Vries LS, Groenendaal F, Ruitenbeek W, Jansen GH, Poll-The BT, Barth PG: Pontocerebellar hypoplasia associated with respiratory-chain defects. Neuropediatrics 1999, 30:93-95.

62. Somer M: Diagnostic criteria and genetics of the PEHO syndrome. J Med Genet 1993, 30:932-936.

63. Riikonen R: The PEHO syndrome. Brain Dev 2001, 23:765-769.

64. Kirschner J, Bonnemann CG: The congenital and limb-girdle muscular dystrophies: sharpening the focus, blurring the boundaries. Arch Neurol 2004, 61:189-199.

65. Muntoni F, Voit T: The congenital muscular dystrophies in 2004: a century of exciting progress. Neuromuscul Disord 2004, 14:635-649.

66. Najm J, Horn D, Wimplinger I, Golden JA, Chizhikov VV, Sudi J, Christian SL, Ullmann R, Kuechler A, Haas CA et al.: Mutations of CASK cause an X-linked brain malformation phenotype with microcephaly and hypoplasia of the brainstem and cerebellum. Nat Genet 2008, 40:1065-1067.

67. Jissendi-Tchofo P, Kara S, Barkovich AJ: Midbrain-hindbrain involvement in lissencephalies. Neurology 2009, 72:410-418.

68. Poirier K, Saillour Y, Bahi-Buisson N, Jaglin XH, Fallet-Bianco C, Nabbout R, Castelnau-Ptakhine L, Roubertie A, Attie-Bitach T, Desguerre I et al.: Mutations in the neuronal ss-tubulin subunit TUBB3 result in malformation of cortical development and neuronal migration defects. Hum Mol Genet 2010, 19:4462-4473.

69. Tischfield MA, Cederquist GY, Gupta ML, Jr., Engle EC: Phenotypic spectrum of the

tubulin-related disorders and functional implications of disease-causing mutations. Curr Opin Genet Dev 2011.

70. Messerschmidt A, Brugger PC, Boltshauser E, Zoder G, Sterniste W, Birnbacher R, Prayer D: Disruption of cerebellar development: potential complication of extreme prematurity. AJNR Am J Neuroradiol 2005, 26:1659-1667.

71. Messerschmidt A, Fuiko R, Prayer D, Brugger PC, Boltshauser E, Zoder G, Sterniste W, Weber M, Birnbacher R: Disrupted cerebellar development in preterm infants is associated with impaired neurodevelopmental outcome. Eur J Pediatr 2008, 167:1141-1147.

72. Trotta CR, Miao F, Arn EA, Stevens SW, Ho CK, Rauhut R, Abelson JN: The yeast tRNA splicing endonuclease: a tetrameric enzyme with two active site subunits homologous to the archaeal tRNA endonucleases. Cell 1997, 89:849-858.

73. Paushkin SV, Patel M, Furia BS, Peltz SW, Trotta CR: Identification of a human endonuclease complex reveals a link between tRNA splicing and pre-mRNA 3' end formation. Cell 2004, 117:311-321.

74. Trotta CR, Paushkin SV, Patel M, Li H, Peltz SW: Cleavage of pre-tRNAs by the splicing endonuclease requires a composite active site. Nature 2006, 441:375-377.

75. Hopper AK, Phizicky EM: tRNA transfers to the limelight. Genes Dev 2003, 17:162-180.

76. Genomic tRNA database. http://lowelab.ucsc.edu/GtRNAdb/. 2010.

77. Wickens M, Gonzalez TN: Molecular biology. Knives, accomplices, and RNA. Science 2004, 306:1299-1300.

78. Weitzer S, Martinez J: The human RNA kinase hClp1 is active on 3' transfer RNA exons and short interfering RNAs. Nature 2007, 447:222-226.

79. Trotta CR: Biochemistry: The big catch. Nature 2007, 447:156-157.

80. Weitzer S, Martinez J: hClp1: a novel kinase revitalizes RNA metabolism. Cell Cycle 2007, 6:2133-2137.

81. Kasher PR, Namavar Y, van Tijn P, Fluiter K, Sizarov A, Kamermans M, Grierson AJ, Zivkovic D, Baas F: Impairment of the tRNA-splicing endonuclease subunit 54 (tsen54) gene causes neurological abnormalities and larval death in zebrafish models of pontocerebellar hypoplasia. Hum Mol Genet 2011, 20:1574-1584.

82. Ten Donkelaar HJ, Lammens M, Wesseling P, Thijssen HO, Renier WO: Development and developmental disorders of the human cerebellum. J Neurol 2003, 250:1025-1036.

83. Antonellis A, Green ED: The role of aminoacyl-tRNA synthetases in genetic diseases. Annu Rev Genomics Hum Genet 2008, 9:87-107.

84. Park SG, Kim HJ, Min YH, Choi EC, Shin YK, Park BJ, Lee SW, Kim S: Human lysyl-tRNA synthetase is secreted to trigger proinflammatory response. Proc Natl Acad Sci U S A 2005, 102:6356-6361.

85. Hausmann CD, Ibba M: Aminoacyl-tRNA synthetase complexes: molecular multitasking revealed. FEMS Microbiol Rev 2008, 32:705-721.

86. Palioura S, Sherrer RL, Steitz TA, Soll D, Simonovic M: The human SepSecS-tRNASec complex reveals the mechanism of selenocysteine formation. Science 2009, 325:321-325.

87. Allmang C, Wurth L, Krol A: The selenium to selenoprotein pathway in eukaryotes: more molecular partners than anticipated. Biochim Biophys Acta 2009, 1790:1415-1423.

88. Bosl MR, Takaku K, Oshima M, Nishimura S, Taketo MM: Early embryonic lethality caused by targeted disruption of the mouse selenocysteine tRNA gene (Trsp). Proc Natl Acad Sci U S A 1997, 94:5531-5534.

89. Scheper GC, van der Klok T, van Andel RJ, van Berkel CG, Sissler M, Smet J, Muravina TI, Serkov SV, Uziel G, Bugiani M et al.: Mitochondrial aspartyl-tRNA synthetase deficiency causes leukoencephalopathy with brain stem and spinal cord involvement and lactate elevation. Nat Genet 2007, 39:534-539.

90. Park SG, Schimmel P, Kim S: Aminoacyl tRNA synthetases and their connections to disease. Proc Natl Acad Sci U S A 2008, 105:11043-11049.

91. Lukong KE, Chang KW, Khandjian EW, Richard S: RNA-binding proteins in human genetic disease. Trends Genet 2008, 24:416-425.

92. Cooper TA, Wan L, Dreyfuss G: RNA and disease. Cell 2009, 136:777-793.

93. Kolb SJ, Sutton S, Schoenberg DR: RNA processing defects associated with diseases of the motor neuron. Muscle Nerve 2010, 41:5-17.

94. Lemmens R, Moore MJ, Al-Chalabi A, Brown RH, Jr., Robberecht W: RNA metabolism and the pathogenesis of motor neuron diseases. Trends Neurosci 2010, 33:249-258.

95. Lee JW, Beebe K, Nangle LA, Jang J, Longo-Guess CM, Cook SA, Davisson MT, Sundberg JP, Schimmel P, Ackerman SL: Editing-defective tRNA synthetase causes protein misfolding and neurodegeneration. Nature 2006, 443:50-55.

96. Dittmar KA, Goodenbour JM, Pan T: Tissue-specific differences in human transfer RNA expression. PLoS Genet 2006, 2:e221.

97. Morgane PJ, Miller M, Kemper T, Stern W, Forbes W, Hall R, Bronzino J, Kissane J, Hawrylewicz E, Resnick O: The Effects of Protein Malnutrition on the Developing Central Nervous System in the Rat. Neuroscience & Biobehavioral Reviews 1978, 2:137-230.

98. De F, V, Varela O, Oropeza JJ, Bisiacchi B, Alvarez A: Effects of prenatal protein malnutrition on the electrical cerebral activity during development. Neurosci Lett 2010, 482:203-207.

99. Georgieff MK: Nutrition and the developing brain: nutrient priorities and measurement. Am J Clin Nutr 2007, 85:614S-620S.

100. Jordanova A, Irobi J, Thomas FP, Van Dijck P, Meerschaert K, Dewil M, Dierick I, Jacobs A, De Vriendt E, Guergueltcheva V et al.: Disrupted function and axonal distribution of mutant tyrosyl-tRNA synthetase in dominant intermediate Charcot-Marie-Tooth neuropathy. Nat Genet 2006, 38:197-202.

101. McLaughlin HM, Sakaguchi R, Liu C, Igarashi T, Pehlivan D, Chu K, Iyer R, Cruz P, Cherukuri PF, Hansen NF et al.: Compound heterozygosity for loss-of-function lysyl-tRNA synthetase mutations in a patient with peripheral neuropathy. Am J Hum Genet 2010, 87:560-566.

102. Belostotsky R, Ben-Shalom E, Rinat C, Becker-Cohen R, Feinstein S, Zeligson S, Segel R, Elpeleg O, Nassar S, Frishberg Y: Mutations in the mitochondrial seryl-tRNA synthetase cause hyperuricemia, pulmonary hypertension, renal failure in infancy and alkalosis, HUPRA syndrome. Am J Hum Genet 2011, 88:193-200.

103. Pierce SB, Chisholm KM, Lynch ED, Lee MK, Walsh T, Opitz JM, Li W, Klevit RE, King MC: Mutations in mitochondrial histidyl tRNA synthetase HARS2 cause ovarian dysgenesis and sensorineural hearing loss of Perrault syndrome. Proc Natl Acad Sci U S A 2011.

104. Popow J, Englert M, Weitzer S, Schleiffer A, Mierzwa B, Mechtler K, Trowitzsch S, Will CL, Luhrmann R, Soll D et al.: HSPC117 is the essential subunit of a human tRNA splicing ligase complex. Science 2011, 331:760-764.

105. Calvin K, Li H: RNA-splicing endonuclease structure and function. Cell Mol Life Sci 2008, 65:1176-1185.

Chapter 2

tRNA splicing endonuclease mutations cause pontocerebellar hypoplasia

Birgit S Budde*, Yasmin Namavar*, Peter G Barth, Bwee Tien Poll-The, Gudrun Nürnberg, Christian Becker, Fred van Ruissen, Marian AJ Weterman, Kees Fluiter, Erik T te Beek, Eleonora Aronica, Marjo S van der Knaap, Wolfgang Höhne, Mohammad Reza Toliat, Yanick J Crow, Maja Steinlin, Thomas Voit, Filip Roelens, Wim Brussel, Knut Brockmann, Marten Kyllerman, Eugen Boltshauser, Gerhard Hammersen, Michèl Willemsen, Lina Basel-Vanagaite, Ingeborg Krägeloh-Mann, Linda S de Vries, Laszlo Sztriha, Francesco Muntoni, Colin D Ferrie, Roberta Battini, Raoul CM Hennekam, Eugenio Grillo, Frits A Beemer, Loes ME Stoets, Bernd Wollnik, Peter Nürnberg & Frank Baas.

Published in 2008 in Nature Genetics 40: 1113-1118.

* these authors contributed equally to this work

Abstract

Pontocerebellar hypoplasias (PCH) represent a group of neurodegenerative autosomal recessive disorders with prenatal onset, atrophy or hypoplasia of the cerebellum, hypoplasia of the ventral pons, microcephaly, variable neocortical atrophy and severe mental and motor impairments. In two subtypes, PCH2 and PCH4, we identified mutations in three of the four different subunits of the tRNA-splicing endonuclease complex. Our findings point to RNA processing as a new basic cellular impairment in neurological disorders.

Introduction, results and discussion

On the basis of clinical criteria, five subtypes of autosomal recessive PCH have been classified. Type 1 (PCH1) (MIM60759), with anterior horn degeneration; type 2 (PCH2) (MIM277470), with chorea/ dystonia or spasticity; and type 4 (PCH4) (MIM225753), with more severe course and early lethality, also known as olivopontocerebellar hypoplasia, are more frequent than types 3 and 5, which have been reported in single families only [1–6]. Type 3 (MIM 608027) features microcephaly, seizures, hypotonia, hyper-reflexia, short stature and optic atrophy and maps to chromosome 7q11–21 [5]. In type 5, an early-lethal phenotype (MIM 610204), the cerebellar vermis is more affected than the hemipheres [1]. Gene defects are not known for any of these subtypes. However, a mutation of mitochondrial arginyl-tRNA synthethase was recently established to underlie a new subtype (PCH6) (MIM 611523), featuring cerebral atrophy, hypotonia, convulsions and multiple respiratory chain defects [7].

We examined 58 individuals with PCH from The Netherlands, other European countries, Brazil and Israel (Table 1). We classified 52 as PCH2 with typical clinical and magnetic resonance imaging (MRI) findings (Fig. 1a,b). We diagnosed three isolated cases of PCH1 and three as PCH4. Nine families bearing PCH2 came from the Volendam region of The Netherlands and are probably descendants of a single couple that lived in the seventeenth century (Suppl. Fig. 1). To identify the PCH2 locus we performed a genome-wide scan in families Am1 and Am1a from the Volendam region using 10K SNP arrays (Affymetrix). We identified linkage to chromosome 17q25 with a maximum lod score of 5.81 (Fig. 2a). Haplotype construction disclosed recombination events distal to rs2019877 and proximal to rs2889529, defining a disease interval of

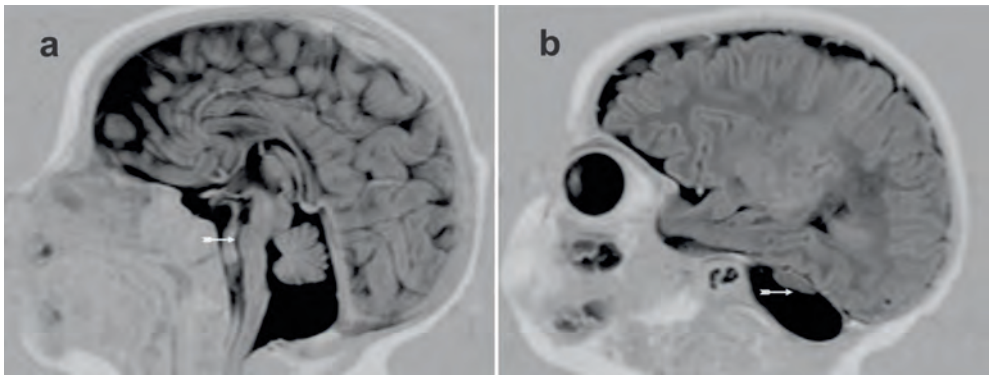

Figure 1. MRI of the brain of subject 2-2 of family Am1a (arrow in Fig. 2b) at 2 months of age. (a) Midsagittal image showing hypoplastic vermis and flat ventral pons (arrow). (b) Lateral sagittal image showing hypoplastic cerebellar hemisphere (arrow) leaving empty space in the posterior fossa.

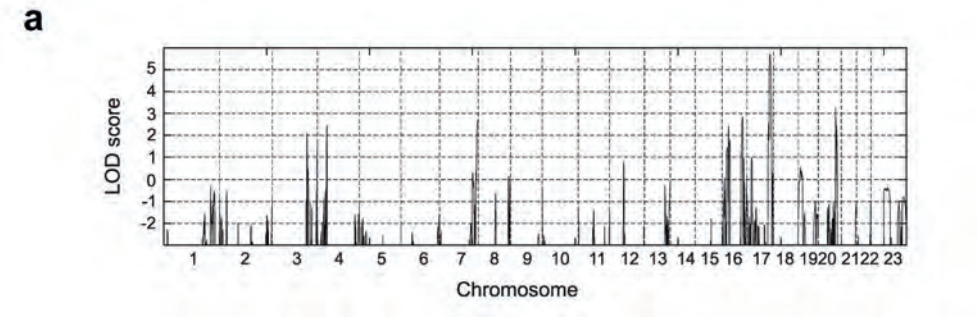

Figure 2. Genetic mapping of the PCH2 locus. (a) Multipoint linkage analysis of the genome-wide scan using the Affymetrix GeneChip Human Mapping 10KArray Xba131. Plot of additive lod calculations in families Am1 and Am1a is shown. (b) Haplotypes of the families Am1a and Am1 on chromosome 17q25. The disease-associated haplotype is boxed. Additional microsatellite markers and SNPs (rs numbers without an asterisk) were analysed to fine-map the candidate region identified by the genome-wide scan with SNPs (asterisks). The minimum disease-associated haplotype is defined by the markers D17S1301 and D17S937. Mutation site of *TSEN54*, grey shading.

13.4cM. By fine-mapping using microsatellite markers, we narrowed the PCH2 locus to an interval of 4.5cM between markers D17S1301 and D17S937 (Fig. 2b). This 2.7Mb region encompasses 85 genes. To further reduce the PCH2 critical interval we genotyped microsatellite markers in nine more families. In six families, part of the disease haplotype identified in families Am1 and Am1a was also transmitted to the affected offspring, confining the candidate interval to 3.4cM (Suppl. Fig. 2a). We prioritised the genes in this region on the basis of expression pattern and function and sequenced the entire coding region and intron-exon borders in 19 genes in five affected subjects and their parents (Suppl. Table 1). Segregation analysis of newly identified and genotyped SNPs confirmed linkage of this region of chromosome 17 with PCH2 in the Am1 and Am1a families (Fig. 2b). We identified four missense mutations. Three of them were homozygously present in our controls also. Only the AMC20 variant in the tRNA splicing endonuclease homolog 54 gene (*TSEN54*), that is c.919G>T of RefSeq NM_207346.2 was exclusively homozygous in our affected subjects. We therefore typed only the *TSEN54* c.919G>T variant in our remaining 47 subjects with PCH2. Among these, 42, all of European descent, were homozygous mutant, and five were homozygous wild-type (Table 1). We extensively genotyped 31 of the 47 individuals with PCH2 who were homozygous for the c.919G>T mutation and found them to share a 285kb SNP haplotype (Suppl. Fig. 2b). Thus, a single founder mutation event is the most likely explanation for the high number of individuals with PCH2 carrying the same c.919G>T mutation. We estimated that the mutation must have occurred at least 11 to 16 generations ago (see Supplementary Methods).

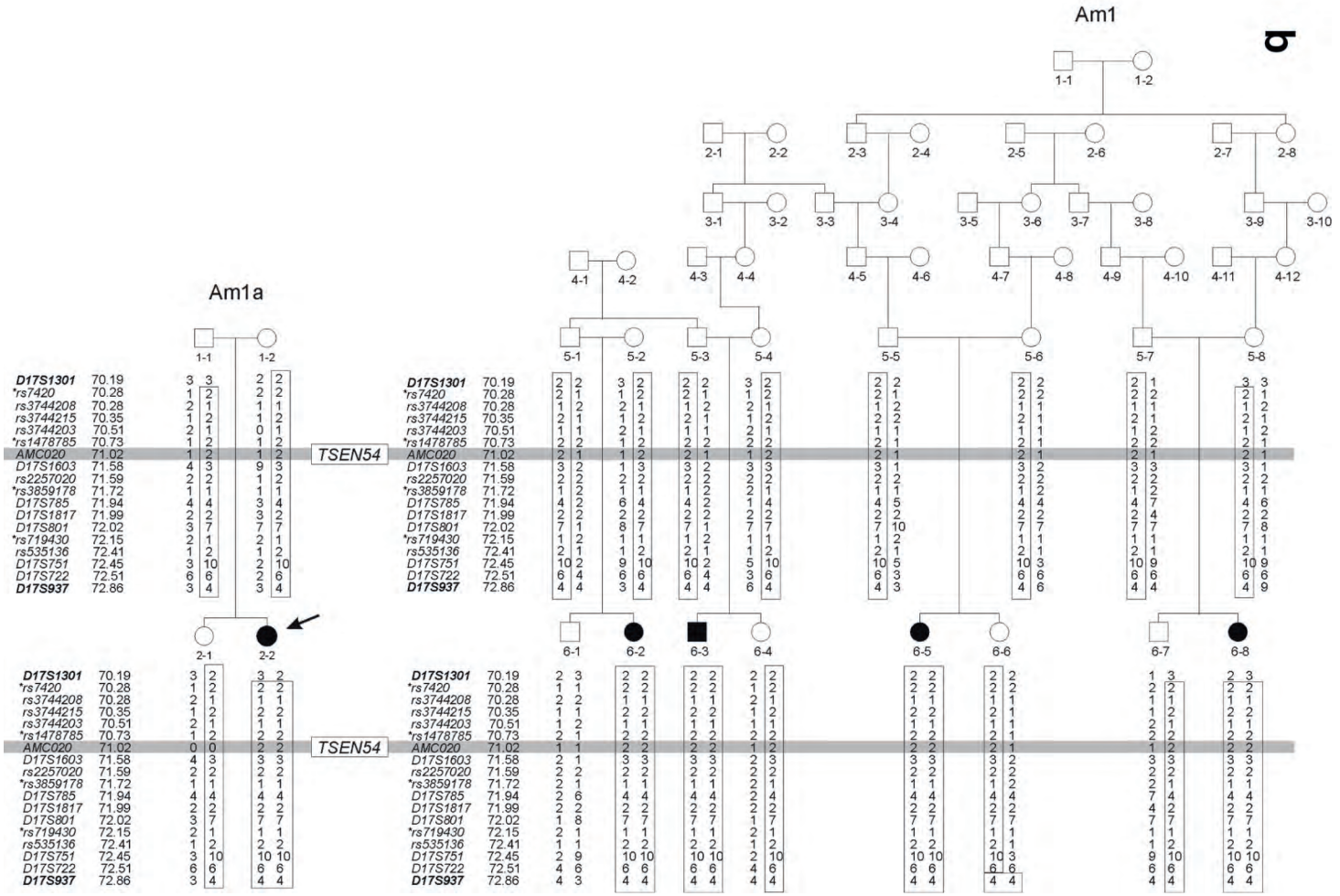
b
Am1
1-1
1-2
2-1
2-2
2-3
2-4
2-5
2-6
2-7
2-8
3-1
3-2
3-3
3-4
3-5
3-6
3-7
3-8
3-9
3-10
4-1
4-2
4-3
4-4
4-5
4-6
4-7
4-8
4-9
4-10
4-11
4-12
5-1
5-2
5-3
5-4
5-5
5-6
5-7
5-8
6-1
6-2
6-3
6-4
6-5
6-6
6-7
6-8
Am1a
1-1
1-2
2-1
2-2
D17S1301 70.19
*rs7420 70.28
rs3744208 70.28
rs3744215 70.35
rs3744203 70.51
*rs1478785 70.73
AMC020 71.02
D17S1603 71.58
rs2257020 71.59
*rs3859178 71.72
D17S785 71.94
D17S1817 71.99
D17S801 72.02
*rs719430 72.15
rs535136 72.41
D17S751 72.45
D17S722 72.51
D17S937 72.86
TSEN54

Table 1. Clinical data and mutations in subjects with PCH.

Phenotype Family code	m / f	Progressive micro-cephaly	MRI typical	Chorea/ dystonia	Swallowing disorder	Visual impair-ment	Optic atrophy	Spontaneous breath
PCH2								
Am1a, Am1c-e	3m, 5f	+	+	+	+	+	-	+
Am1b	2m	+	+	-	+	+	-	+
Am3	f	+	+	+	+	-	-	+
Am4	m	+	+	+	+	+	-	+
Am5	m	+	+	+	+	+	-	+
Am6	f	+	+	+	+	+		+
An1	m	+	+	+	+	+		+
Be1	1m, 1f	+	+	+	+	+	-	+
Es1	m	+	+	+	+	+	-	+
Fr1	m	+	+	+		+		+
Gb1	m	+	+	+	+	+	-	+
Ge1	1m, 1f	+	+	+	+	+	-	+
Gn2	f	+	+	+	+	+	-	+
Gn3	f	+	+	+	+	+	-	+
Gr1	m	+	+	+	+	+	-	+
Gr2	f	+	+	+	-	-	-	+
Je1	f	+	+	+	+	+	-	+
Lu2	f	+	+	+	+	+	-	+
Mc1	f	+	+	+	-	+	-	+
Mc2	f	+	+	3m -	+	+	-	+
Ms1	m	+	+	+	+	+		+
Ny1	m	+	+	+	+	+	-	+
Ny2	f	+	+	+	+	+		+
Ny3	m	+	+	+	+	+		+
Od1	f	+	+	+	+	+	-	+
Te1	2f	+	+	+	+	+	-	+
Tu1	2m	+	+	+	+	+	-	+
Tw1	m	+	+	+	+	+	-	+
Tw2	m	+	+	+	+	+		+
Uk1	m		+	+				+
Ut1	f	+	+	+	+	+	-	+
Ut2	f	+	+	+	+	+		+
Ut5	m	+	+	3m -	+	+	-	+
Zu2	2f	+	+	+	+		-	+
Le1	m	+	+	+	-	+	-	+
Hg1	m	+	+	+	-	+	-	+
Am2	m	+	+	+	-	-	-	+
Bx1	f	+	+	+	+	+		+
Pi1	f	+	+	+	+	+	+	+
PCH1								
Ae1	m		+	Hypotonia	+			-
Am7	m		+	Hypotonia	+			-
Lo2	f		+	Hypotonia	+			-
PCH4								
Br1	f		+	Hypertonia at birth	+			-
Ut4	m		+	Hypertonia at birth	+			-
Nu1	f		+	Hypertonia at birth	+			-

m, male; f, female; 3m-, not detectable at 3 months of age.

Congenital contracture/ polyhydramnios	Previous citations; remarks	Mutation in tRNA endonuclease subunit	Substitution
-/-	[3]	TSEN54	p.A307S, p.A307S
-/-	Spasticity	TSEN54	p.A307S, p.A307S
-/-	[3]	TSEN54	p.A307S, p.A307S
-/-		TSEN54	p.A307S, p.A307S
-/-		TSEN54	p.A307S, p.A307S
-/-		TSEN54	p.A307S, p.A307S
-/-		TSEN54	p.A307S, p.A307S
-/-		TSEN54	p.A307S, p.A307S
-/-		TSEN54	p.A307S, p.A307S
-/-		TSEN54	p.A307S, p.A307S
-/-		TSEN54	p.A307S, p.A307S
-/-		TSEN54	p.A307S, p.A307S
-/-		TSEN54	p.A307S, p.A307S
-/-		TSEN54	p.A307S, p.A307S
-/-	[3]	TSEN54	p.A307S, p.A307S
-/-	[3]	TSEN54	p.A307S, p.A307S
-/-		TSEN54	p.A307S, p.A307S
-/-	[3]	TSEN54	p.A307S, p.A307S
-/-		TSEN54	p.A307S, p.A307S
-/-		TSEN54	p.A307S, p.A307S
-/-		TSEN54	p.A307S, p.A307S
-/-		TSEN54	p.A307S, p.A307S
-/-		TSEN54	p.A307S, p.A307S
-/-		TSEN54	p.A307S, p.A307S
-/-		TSEN54	p.A307S, p.A307S
-/-		TSEN54	p.A307S, p.A307S
-/-		TSEN54	p.A307S, p.A307S
-/-		TSEN54	p.A307S, p.A307S
-/-		TSEN54	p.A307S, p.A307S
-/-		TSEN54	p.A307S, p.A307S
-/-	[3]	TSEN54	p.A307S, p.A307S
-/-		TSEN54	p.A307S, p.A307S
-/-		TSEN54	p.A307S, p.A307S
-/-		TSEN54	p.A307S, p.A307S
-/-		TSEN2	p.Y309C, p.Y309C
-/-		TSEN34	p.R58W, p.R58W
-/-	[3, 6, case 3]	None	
-/-	Affected brother: sex reversal	None	
-/-		None	
-/-	[15] Peripheral pareses	None	
-/+	[16] Peripheral pareses	None	
+/+	[17] Peripheral pareses	None	
-/+	Severe myoclonus	TSEN54	p.A307S, p.A307S, p.S93P
+/-	[6] Severe myoclonus	TSEN54	p.A307S, p.Q246X
-/+	Severe myoclonus	TSEN54	p.A307S, p.Q343X

Analysis of 451 Dutch and 279 German control DNA samples yielded no homozygous and only five Dutch and one German heterozygous genotypes. Additionally, we screened 136 healthy unrelated individuals from Volendam. Again, no homozygous mutants and only two heterozygous individuals were identified. Thus, the allele frequency of the c.919G>T variant in the PCH2 subjects is 0.884, counting the Volendam subjects as a single data point, and that in the control population is 0.004. These data strongly suggest that the *TSEN54* locus is responsible for most cases of PCH2. At the protein level, the *TSEN54* c.919G>T variant causes a substitution of alanine by serine at position 307 (p.A307S) (Suppl. Fig. 3a). This region of the protein is conserved in mammals and chicken but is not highly conserved in lower organisms (Suppl. Fig. 4). Therefore, the detrimental consequence of this exchange is difficult to deduce from the sequence alone. We obtained further evidence for a causative role when extending the *TSEN54* mutation screening to subjects with PCH1 and PCH4. Although we did not find *TSEN54* mutations in the three PCH1 cases, we identified the c.919G>T mutation in all three PCH4 cases. One individual was homozygous for the c.919G>T change, and two others were compound heterozygous for this change with either c.736C>T or c.1027C>T in addition to c.919G>T, both resulting in premature stop codons, at positions 246 or 343, respectively (Suppl. Fig. 3b,c). Compound heterozygosity was confirmed by testing the parents of one affected individual. DNA samples were unavailable for the parents of the other. The third subject with PCH4 carried an additional c.277T>C mutation on one of the two c.919G>T alleles, resulting in a second substitution at amino acid position 93 namely, from serine to proline (Suppl. Fig. 3d). The c.227T>C variant was not detected in 375 unrelated controls. Like Ala307, Ser93 is not highly conserved (Suppl. Fig. 4). However, this residue is situated in an antiparallel ß-sheet, and substitution by a proline at this position is very likely to hamper proper folding (see Supplementary Methods). The identification of nonsense mutations in *TSEN54* strongly supports our hypothesis that defects in *TSEN54* are causative in most cases of PCH2 and PCH4. Additionally, it points to a genotype–phenotype correlation, as the two truncating mutations, p.Q246X and p.Q343X, were found in the more severe cases of PCH4. The different mutational strengths may also explain the most obvious neuropathological difference between PCH2 and PCH4, namely the missing folia in the cerebellum in PCH4 (see Suppl. Fig. 5).

TSEN54 is part of a tRNA splicing endonuclease complex consisting of four subunits: TSEN2, TSEN15, TSEN34 and TSEN54 (Fig. 3) [8]. Therefore, we performed homozygosity mapping using Affymetrix 10K SNP arrays in three individuals with PCH2 in which no *TSEN54* mutations had been found. These three subjects were of Dutch, Italian and Pakistani origin and from consanguineous marriages. We detected a homozygous region of 17Mb on chromosome 3 around the *TSEN2* locus in the Pakistani subject. Sequence analysis of the coding region of *TSEN2* revealed a missense mutation (c.926A>G; RefSeq NM_025265.2) resulting in a substitution of tyrosine by cysteine at position 309 (Suppl. Fig. 3e). We sequenced DNA from 188 healthy Pakistani controls

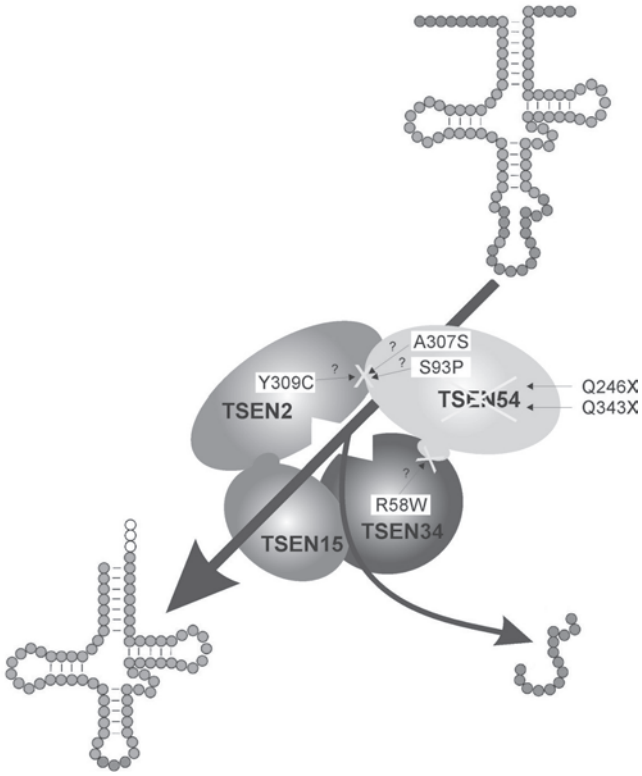

Figure 3. Model of human tRNA-splicing endonuclease (adapted from refs. [18,19]). The tetrameric enzyme complex consists of the two catalytic subunits, TSEN2 and TSEN34, and two structural subunits, TSEN15 and TSEN54. Identified mutations in the PCH families are indicated by the corresponding amino acid changes. Top right, unprocessed tRNA with intron and anticodon loop. After processing by the tRNA endonuclease, the intron is removed, resulting in the mature tRNA, bottom left. The processing of 5' leader and 3' trailer is preformed by other enzymes (see ref. [19] for details). For colour figure see page 166.

and did not find this variant. Additionally, 92 Dutch, 45 Chinese and 28 Palestinian controls showed only the wild-type sequence. Multiple sequence alignment of human *TSEN2* with the corresponding sequences of a broad range of other organisms showed that the Tyr309 position is strictly conserved (tyrosine or phenylalanine) within eukaryotic organisms (Suppl. Fig. 4). Comparison with structures available for highly homologous sequences suggests a role for Tyr309 in stabilization of domain orientation (Suppl. Fig. 6). Sequence analysis of the coding region of *TSEN34* revealed another homozygous missense mutation (c.172C>T; RefSeq NM_024075) in another subject with PCH2, of Turkish origin (family Hg1, Table 1 and Suppl. Fig. 3f). Arg58 is conserved in the closely related mammals. Within the vertebrates, this position is exchanged by small hydrophobic residues only (isoleucine, leucine). Therefore, exchange

for tryptophan in this position may well produce steric hindrance. Sequence analysis of unaffected controls yielded three heterozygotes in 139 DNA samples of Turkish origin and none in 91 Dutch samples.

In view of the identification of *TSEN* subunit mutations with PCH2 and PCH4, we determined the expression pattern of *TSEN54* in the developing brain (Fig. 4). *TSEN54* was highly expressed in neurons of the pons, cerebellar dentate and olivary nuclei during the second trimester of pregnancy, a determining period for the morphological development of these structures. Other brain regions show low or no staining (data not shown).

Here we report mutations in two catalytic subunits (*TSEN2* and *TSEN34*) and one noncatalytic subunit (*TSEN54*) of the tRNA splicing endonuclease (Fig. 3). The mutations p.Y309C in *TSEN2*, p.S93P and p.A307S in *TSEN54*, and p.R58W in *TSEN34* may disturb the interaction between the subunits, whereas the other three mutations are likely to result in reduced amounts of TSEN54. In human, tRNA genes occur with and without introns. For tRNA-Ile (codon TAT) and tRNA-Tyr (codons GTA and ATA), only intron-containing genes are present, whereas for tRNA-Pro, tRNA-Arg, tRNA-Leu, tRNA-Cys and tRNA-Trp, both intron-containing and intronless genes exist (http:// lowelab.ucsc.edu/GtRNAdb/). Because tRNAs are essential for cell survival, it is unlikely that the activity of the tRNA splicing endonuclease is completely abolished in PCH2 and PCH4, suggesting that the identified mutations result in partial loss of the ability to cleave pre-tRNAs by the endonuclease complex. However, RNA blot analysis of tRNA-Tyr from fibroblasts of three of the subjects homozygous for c.919C>T did not show unspliced products (data not shown). The high abundances of *TSEN54* mRNA in the developing pons, dentate and olivary nuclei are in line with the PCH2 phenotype. We propose that a functional endonuclease complex is essential for the development of these regions.

Notably, many neurological disorders are caused by mutations in genes involved in essential cellular processes: for example, mutations in the genes encoding subunits of the translation initiation factor *EIF2B* give rise to vanishing white matter disease, and defects in the mitochondrial translation machinery can lead to central nervous system disorders [9,10]. It is conceivable that the developing brain is extremely sensitive to changes affecting protein synthesis. Insufficient protein delivery in a certain timeframe could then lead to developmental disorders or degeneration. The identification of a mutation of the nuclear gene encoding mitochondrial arginyl-tRNA synthetase in PCH6 is in keeping with this hypothesis [7]. Our finding of *TSEN54* p.A307S, p.Q246X, p.Q343X and p.S93P; *TSEN34* p.R58W; and *TSEN2* p.Y309C substitutions in PCH2 and PCH4 reveals for the first time that mutations in genes involved in cytoplasmic tRNA splicing are associated with a human disease.

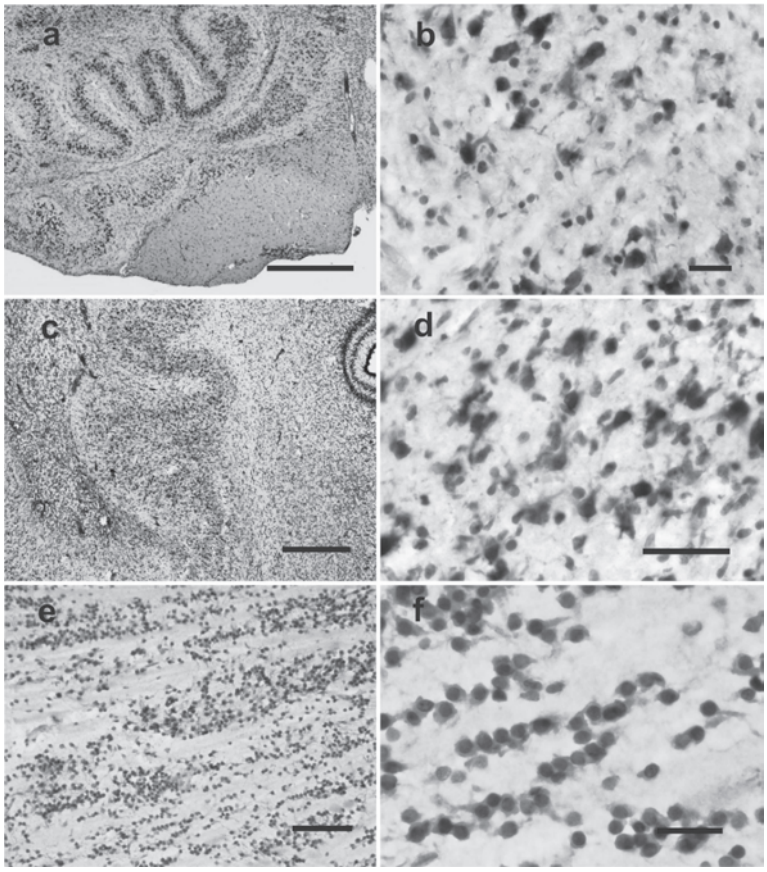

Figure 4. *TSEN54* expression in human foetal brain. (a,b) Inferior olivary nucleus at gestational age 23 weeks. The undulated structure can be seen in (a) including that in the medial accessory olivary nucleus. Scale bar, 500µm. (b) Higher magnification of (a) showing positive staining in individual neurons and surrounding dendrites. Scale bar, 25µm. (c,d) Cerebellar dentate nucleus at gestational age 23 weeks. (c) The upper half of the developing nucleus has the mature undulated form, while the lower half has the transitional compact form. Scale bar, 500µm. (d) Higher magnification of (c) showing positive staining in cytoplasma of individual neurons and surrounding dendrites. Scale bar, 50µm. (e,f) Ventral pons at gestational age, 21 weeks. (e) Groups of immature small neurons separated by bundles of nerve fibers. Scale bar, 100µm. (f) Higher magnification of (e) showing small neurons with positive staining of cytoplasm and dendrites. Scale bar, 25µm. For colour figure see page 167.

Methods

Classification of phenotypes

All affected subjects had an MRI pattern of pontocerebellar hypoplasia. Excluded were cases with cerebral cortical dysplasia or demyelination on MRI. We used sialotransferrin

electrophoresis to exclude congenital disorders of glycosylation, especially type CDG1A. Subjects admitted to the study were subclassified into three groups: PCH2, PCH4 (olivopontocerebellar hypoplasia) or PCH1.

Those with PCH2 had progressive microcephaly, as well as chorea/dystonia or spasticity. Those with PCH4 had clinical signs of prenatal functional neurological involvement, for example, polyhydramnios and/or contractures, while post-natal symptoms included severe generalised myoclonus, hypertonia and central respiratory failure leading to early death.

Neuropathological differences between PCH2 and PCH4 were incomplete folial development of the cerebellum in the former and absence of folia in the latter, with the exception of the nodulus and flocculus. Undulation of the inferior olivary nucleus was completely absent in PCH4 and partial in PCH2.

Individuals with PCH1 had spinal anterior horn involvement confirmed by autopsy or muscle biopsy. They had hypotonia from birth, inconsistent signs of prenatal functional neurological impairment, for example, polyhydramnios and/or contractures and postnatal weakness with respiratory failure.

Genome-wide linkage analysis

DNA was extracted from peripheral blood samples using standard methods. The genome-wide scan was performed by genotyping 16 individuals of Am1 and four individuals of Am1a using the GeneChip Human Mapping 10K Array Xba 131 (Affymetrix) according to manufactures guidelines. The mean intermarker distance was 210kb, equivalent to 0.32cM. Parametric linkage analysis was performed by a modified version of the program GENEHUNTER 2.1 through stepwise use of a sliding window with sets of 110 or 200 SNPs [11,12]. Haplotypes were reconstructed with GENEHUNTER 2.1 and presented graphically with HaploPainter [11,13]. All data handling was performed using the graphical user interface ALOHOMORA to facilitated linkage analysis with chip data [14].

Sequencing analysis

This was done using standard technology. See Supplementary Methods.

Analysis of *TSEN54* splicing.

We excluded the possibility that the *TSEN54* c.919G>T SNP affects mRNA splicing. Reverse transcriptase PCR on mRNA from an individual with PCH2 homozygous for p.A307S did not show evidence for altered splicing of exon 8. PCR with primers in exons 7 and 9 yielded only one fragment, containing exons 7, 8 and 9.

In situ hybridization for *TSEN54* using locked nucleic acid and 2'-O-methyl-RNA modified oligonucleotides

In situ hybridization for TSEN54 was done using 5'-fluorescein-labeled 19mer antisense oligonucleotides containing locked nucleic acid (LNA) and 2'-*O*-methyl (2OME)-RNA moieties. We designed two LNA/2OME probes, each targeting a unique sequence of *TSEN54* mRNA (NM_207346): 5'-TcuTucTcuTgcCauCucC-3' and 5'-TucTccTcu GggTauTggC-3' (where LNA residues are given in capital letters, 2OME-RNA in lower case). The oligonucleotides were synthesised by Ribotask ApS. Hybridizations were done on 12µm sections of paraffin-embedded material. In brief: sections were deparaffinized, treated with proteinase K (20µg/ml) for 5 min and postfixed with 4% paraformaldehyde in PBS for 10 min. Hybridizations were done at 60°C for 90 min in hybridization mix (50% (vol/vol) deionized formamide, 600mM NaCl, 10mM HEPES buffer, pH7.5, 1mM EDTA, x5 Denhardt's reagent and 200µg/ml denatured herring sperm DNA (D6898, Sigma)). The oligonucleotide concentration in the hybridization mix was 1µM. After hybridization the tissue sections were washed consecutively for 5 min with x2 SSC, x0.5 SSC and x0.2 SSC at 60°C. The hybridization signal was detected using a rabbit polyclonal antibody detecting both fluorescein and Oregon Green (A21253, Molecular Probes, Invitrogen) (1 h, 20°C, 1:100 dilution) and a horseradish peroxidase–labeled goat anti-rabbit polyclonal antibody (P0448 Dako) (1 h, 20°C, 1:100 dilution). The horseradish peroxidase was visualised using standard 3-amino-9-ethylcarbazole staining, and hematoxylin was used as a nuclear counterstain. As control for nonspecific binding, other similarly modified oligonucleotides were used. These probes were specific for other transcripts (*complement C6* and *miR134*). These oligonucleotides showed other staining patterns. The regions positive for *TSEN54* were negative for these probes (data not shown).

Acknowledgements

We thank E. Kirst, R. Niemiec and J. Benit-Deekman for technical assistance, P. de Knijff (Leiden University Medical Center) for the generous supply of control DNA samples and G.J. te Meerman for advice on estimation of mutation age. Financial support was given by Hersenstichting, Heijdeman-Teerhuis fonds, Stichting Irene Kinderziekenhuis, the German Ministry of Education and Research through the National Genome Research Network (01GR0416) and the Anton Meelmeijer Fund (F.B. and R.C.M.H.). We acknowledge the contribution of subject's data and blood samples by A.C.B. Peters, R.H.J.M. Gooskens and O. Van Nieuwenhuizen, Wilhelmina Childrens's Hospital, Utrecht; L. De Meirleir, University Hospital Vrije Universiteit Brussels; R. Korinthenberg, Universitatsklinikum Freiburg; J.H. Begeer, University Medical Center, Groningen; W. Deppe, Klinik Bavaria, Kreischa; G. Blennow, University Hospital Lund; H.G. Brunner and N. Knoers, University Medical Center St. Radboud, Nijmegen; A. Bohring, Westfalische Wilhelms-Universitat, Munster; M. Huppke, Elisabeth- Kinderkrankenhaus, Oldenburg; O. Debus, Marien Hospital, Vechta;

G. Hageman and R. Baarsma, Medisch Spectrum Twente, The Netherlands; S.A. Lynch, Institute of Human Genetics, New Castle upon Tyne; F. Cowan, Hammersmith Hospital London; M.A.J. de Koning-Tijssen, Academic Medical Center, Amsterdam; and E. Peeters, Juliana Childrens Hospital, The Hague. The authors wish to thank all the families who have voluntarily cooperated in this project.

Reference List

1. Patel MS, Becker LE, Toi A, Armstrong DL, Chitayat D: Severe, fetal-onset form of olivopontocerebellar hypoplasia in three sibs: PCH type 5? Am J Med Genet A 2006, 140:594-603.

2. Goutieres F, Aicardi J, Farkas E: Anterior horn cell disease associated with pontocerebellar hypoplasia in infants. J Neurol Neurosurg Psychiatry 1977, 40:370-378.

3. Barth PG, Blennow G, Lenard HG, Begeer JH, van der Kley JM, Hanefeld F, Peters AC, Valk J: The syndrome of autosomal recessive pontocerebellar hypoplasia, microcephaly, and extrapyramidal dyskinesia (pontocerebellar hypoplasia type 2): compiled data from 10 pedigrees. Neurology 1995, 45:311-317.

4. Albrecht S, Schneider MC, Belmont J, Armstrong DL: Fatal infantile encephalopathy with olivopontocerebellar hypoplasia and micrencephaly. Report of three siblings. Acta Neuropathol 1993, 85:394-399.

5. Rajab A, Mochida GH, Hill A, Ganesh V, Bodell A, Riaz A, Grant PE, Shugart YY, Walsh CA: A novel form of pontocerebellar hypoplasia maps to chromosome 7q11-21. Neurology 2003, 60:1664-1667.

6. Barth PG, Aronica E, de Vries L, Nikkels PG, Scheper W, Hoozemans JJ, Poll-The BT, Troost D: Pontocerebellar hypoplasia type 2: a neuropathological update. Acta Neuropathol 2007, 114:373-386.

7. Edvardson S, Shaag A, Kolesnikova O, Gomori JM, Tarassov I, Einbinder T, Saada A, Elpeleg O: Deleterious mutation in the mitochondrial arginyl-transfer RNA synthetase gene is associated with pontocerebellar hypoplasia. Am J Hum Genet 2007, 81:857-862.

8. Paushkin SV, Patel M, Furia BS, Peltz SW, Trotta CR: Identification of a human endonuclease complex reveals a link between tRNA splicing and pre-mRNA 3' end formation. Cell 2004, 117:311-321.

9. van der Knaap MS, Leegwater PA, Konst AA, Visser A, Naidu S, Oudejans CB, Schutgens RB, Pronk JC: Mutations in each of the five subunits of translation initiation factor eIF2B can cause leukoencephalopathy with vanishing white matter. Ann Neurol 2002, 51:264-270.

10. Scheper GC, van der Knaap MS, Proud CG: Translation matters: protein synthesis defects in inherited disease. Nat Rev Genet 2007, 8:711-723.

11. Kruglyak L, Daly MJ, Reeve-Daly MP, Lander ES: Parametric and nonparametric linkage analysis: a unified multipoint approach. Am J Hum Genet 1996, 58:1347-1363.

12. Strauch K, Fimmers R, Kurz T, Deichmann KA, Wienker TF, Baur MP: Parametric and nonparametric multipoint linkage analysis with imprinting and two-locus-trait models: application to mite sensitization. Am J Hum Genet 2000, 66:1945-1957.

13. Thiele H, Nurnberg P: HaploPainter: a tool for drawing pedigrees with complex haplotypes. Bioinformatics 2005, 21:1730-1732.

14. Ruschendorf F, Nurnberg P: ALOHOMORA: a tool for linkage analysis using 10K SNP

array data. Bioinformatics 2005, 21:2123-2125.

15. Sztriha L, Johansen JG: Spectrum of malformations of the hindbrain (cerebellum, pons, and medulla) in a cohort of children with high rate of parental consanguinity. Am J Med Genet A 2005, 135:134-141.

16. Barth PG: Pontocerebellar hypoplasias. An overview of a group of inherited neurodegenerative disorders with fetal onset. Brain Dev 1993, 15:411-422.

17. Muntoni F, Goodwin F, Sewry C, Cox P, Cowan F, Airaksinen E, Patel S, Ignatius J, Dubowitz V: Clinical spectrum and diagnostic difficulties of infantile ponto-cerebellar hypoplasia type 1. Neuropediatrics 1999, 30:243-248.

18. Hopper AK, Phizicky EM: tRNA transfers to the limelight. Genes Dev 2003, 17:162-180.

19. Trotta CR, Paushkin SV, Patel M, Li H, Peltz SW: Cleavage of pre-tRNAs by the splicing endonuclease requires a composite active site. Nature 2006, 441:375-377.

Supplementary methods

Estimation of mutation age by identity by descent (IBD)

If we assume that this haplotype is derived from a common ancestor we can make an estimate of the minimum age of this haplotype [5]. There is a relation between the number of meiotic steps until coalescence and the expected size of the shared haplotype surrounding the mutation when we assume that all individuals share an allele that has inherited from a common ancestor. The probability of recombination at Z basepairs from the mutation for a single meiosis is approximately $Z/10^8$, or 1% for a distance of 1cM. If there is a second meiosis the probability of no recombination at a distance of Z bases from the mutation is $(1\text{-}Z)^2$, and analogously for K meioses it is $(1\text{-}Z)^K$. A maximum likelihood estimator for the number of meioses separating all patients can be derived by finding that value of K for which the expected sharing is equal to the observed sharing. Because the haplotype decay occurs from the telomeric and the centromeric side, the cumulative probability distribution that the shared length is $>$ Q base pairs, can be found from the convolution of the telomeric and centromeric recombination probability functions. It is then found that the expected shared length surrounding a mutation that is IBD in all haplotypes is 200/K, where K is the number of meioses in the descent tree until coalescence, and the unit is centimorgan. If a mutation is rare, and only a very small fraction of all mutations is observed through a recessive disease, the descent tree will show long branches until coalescence occurs rapidly just after single introduction or mutation, whichever is the later event. This allows estimation of the age of a mutation from the shared length among all copies found, bearing in mind that the original mutation event cannot be dated, as this reasoning only applies to the events after coalescence to the single mutant from which all current mutants derive. Equating then K (the number of meioses) to the product of age A (in generations) and the number of copies found (c = 2* the number of patients), thus assuming fast initial multiplication of the mutation, we have to solve 200/(A*c) = 0.285 (285kb converted as 10^6 base pairs = 1% recombination).

This results in an estimate for A of 200/17.7 = 11.3 generations when we take all patients in account. However if we consider the Volendam families as one single case (i.e. 22 separate families) the value for A becomes 15.9. Therefore we conclude that the minimum age of the mutation is between 11 and 16 generations.

Sequencing analysis

Primer pairs for each exon including flanking intron sequences of a selected group of genes in the putative PCH2 locus were designed from genomic sequence using Primer 3 [2]. Primer sequences and PCR conditions are available upon request. PCR products were directly sequenced using ABI PRISM 3730 DNA Analyser and BigDye Terminator Cycle Sequencing Kit version 1.1 according to the protocols of the manufacturer

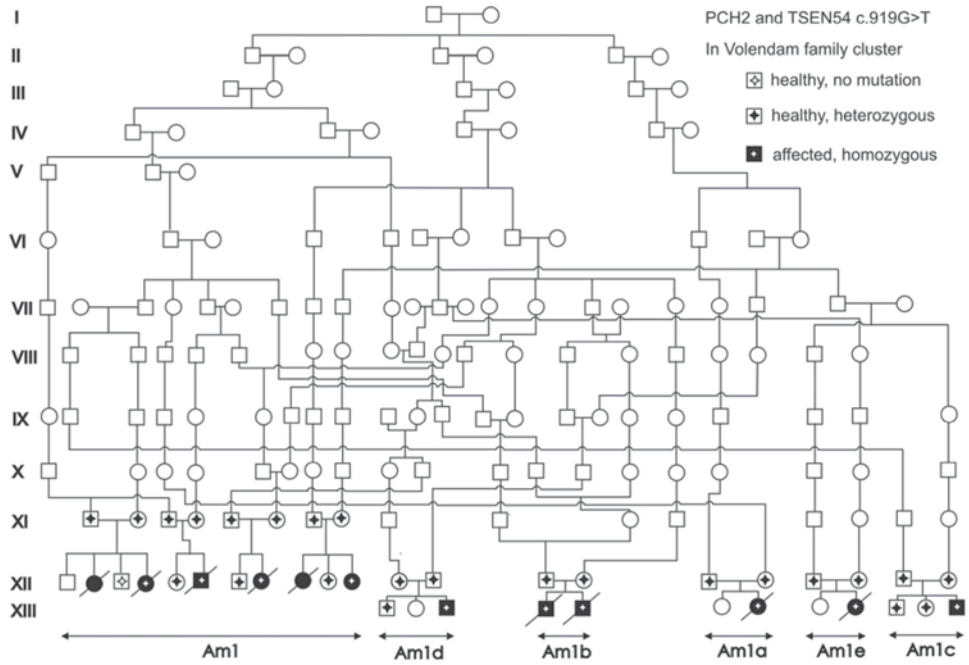

Supplementary Figure 1. Volendam family cluster with PCH2 tracing back to the 17th century. All affected individuals carry the homozygous p.A307S mutation of *TSEN54*. Family codes are given at the bottom of the drawing.

(Applied Biosystems, Foster City, CA).

Pyrosequencing analysis

German and Turkish controls were tested for the c.919G>T variation of *TSEN54* and c.172C>T variation of *TSEN34*, respectively by using pyrosequencing assays. PCR primers were designed using Primer SNP Design version 1.01 software (Biotage, Uppsala, Sweden). The following primers were used: for the *TSEN54* assay E8mu-tsen54-F 5'- BIOTIN-GTCACGGGAGCCGGTAAG, E8mu-tsen54-R 5'- GTGTG GCGGCTGTCTGAA and as internal primer E8mu-tsen54-S 5'- GTGGCGGCT GTCTGA and for the *TSEN34* assay TSEN34-2CT-F 5'- CTGCTGATGCC CGAAGAG, TSEN34-2CT-R 5'- BIOTIN-GGCGCTGACCAGAGTCAC, TSEN34-2CT-S 5'- TGATGCCCGAAGAGG. All PCR reactions were carried out with 6ng genomic DNA, 0.3nmol each of forward and reverse PCR primers, 0.5U Taq polymerase, 1.5mM $MgCl_2$. Pyrosequencing was carried out as defined by the supplier on a PSQ HS96A instrument (Biotage, Uppsala, Sweden). Samples were analysed with the PSQ HS96A version 1.2 software (Biotage, Uppsala, Sweden).

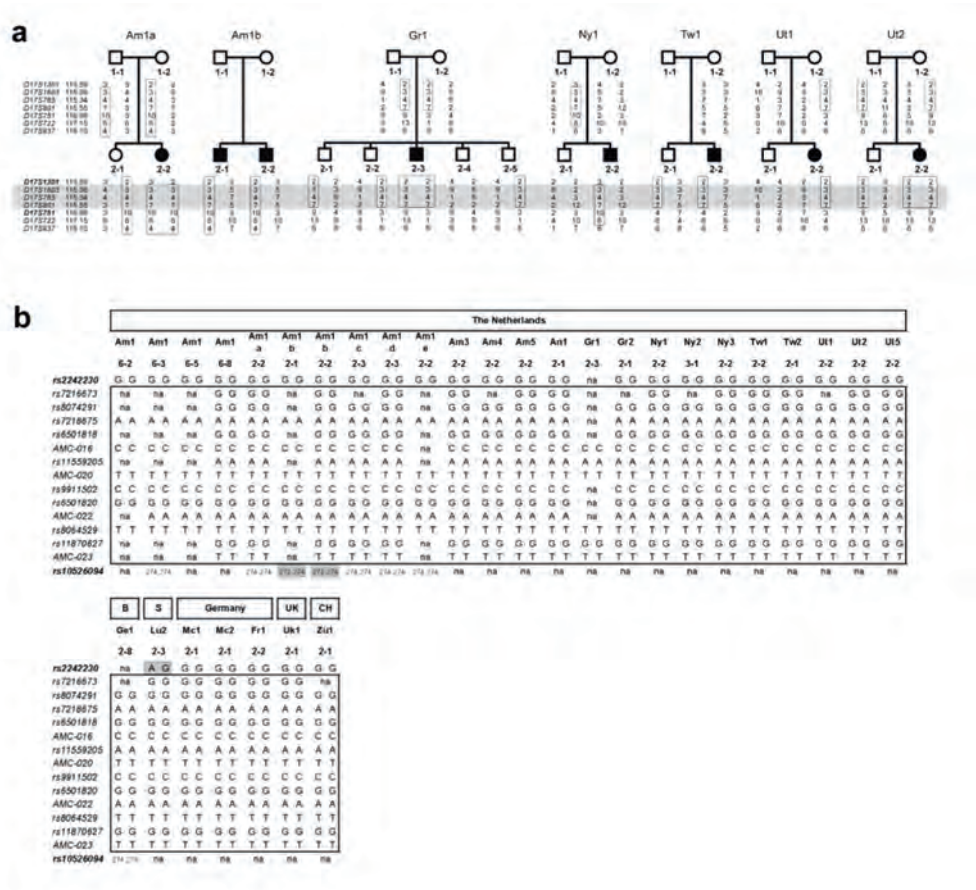

Supplementary Figure 2. Haplotypes of additional families on chromosome 17q25. (a) Haplotypes of six additional families from Volendam and other parts of the Netherlands. The shared disease haplotype of Am1a is boxed and the narrowed disease interval flanked by markers D17S1301 and D17S751 is highlighted in grey. (b) Haplotypes of 31 of 47 PCH2 patients homozygous for *TSEN54* c.919G>T (AMC-020). Country of origin, family code and patient ID are indicated in the top rows. Genotypes indicating a recombination are highlighted in grey. The shared homozygous region is flanked by rs2242230 (Lu2) and rs10526094 (Am 1b 2-1, 2-2). The distance between these markers is 285kb. The region shown is located between the microsatellite markers D17S1301 and D17S1603. Abbreviations are: na – not analysed, B – Belgium, S – Sweden, UK – United Kingdom, CH- Switzerland).

Discussion of the structural consequences of the identified mutations

Functional consequences of mutations in the involved proteins may be caused by different ways. By nonsense mutations leading to chain termination as it the case with the c.736C>T and c.1027C>T base exchanges in *TSEN54* most certainly there will be

no protein expression at all or no functional protein. Mutations of amino acid residues involved in the catalytic mechanism or within the interfaces of the heterotetramer may also seriously impair the function. But sequence alignment of *TSEN2*, *TSEN34* and *TSEN54* with the tRNA splicing enzymes of *Archaeglobus fulgidus* where residues in contact with RNA and possibly involved in the splicing mechanism are discussed on a structural basis [3] shows that those residues are not close to the positions shown here as mutated. Thus, the influence of the mutations p.S93P and p.A307S in *TSEN54* and p.Y309C in *TSEN2* may attributed to more subtle influences on local conformations or folding stabilities, as discussed below, thus influencing intramolecular functionality or intermolecular interactions between the four proteins involved or even with so far unknown additional protein factors.

Structural consequences of the missense mutations described here for the *TSEN2*

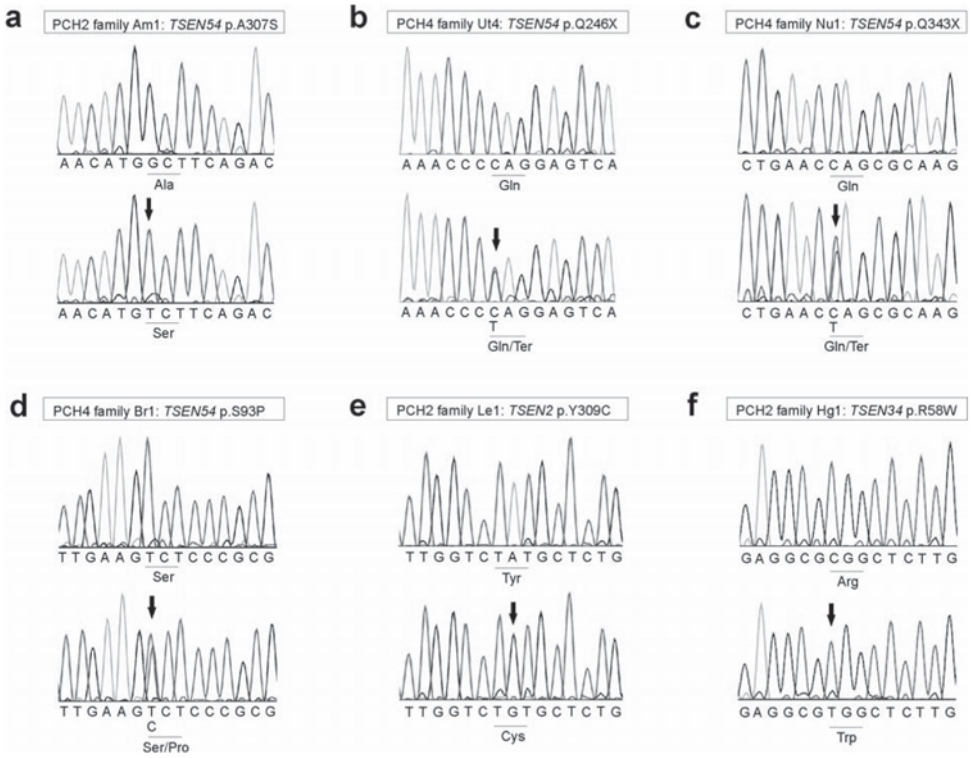

Supplementary Figure 3. *TSEN54*, *TSEN34* and *TSEN2* mutations in PCH families. (a-f) Chromatogram pairs are shown, one of an unaffected individual and the other of an affected patient. The arrow indicates the position of the homozygous and heterozygous mutations. The encoded amino acid is written below the nucleotide triplet. Family IDs, mutated genes and amino acid changes with the corresponding position in the protein sequence are given in the boxes above each chromatogram pair.

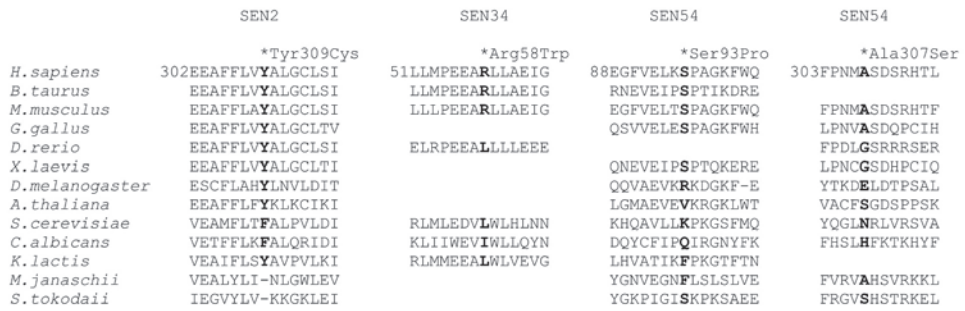

Supplementary Figure 4. Alignment of the mutated sequence regions of *TSEN2*, *TSEN34* and *TSEN54*. The corresponding regions of 12 different organisms are shown. The alignment includes the following amino acid sequences (first accession no.: SEN2 protein homologs, second: SEN34 protein homologs, third: SEN54 protein homologs): *Homo sapiens* Q8NCEO, Q9BSV6, Q7Z6J9; *Bos taurus* Q1PS47, Q3MHE1,Q17QY4; *Mus musculus* Q6P7W5, Q8BMZ5, Q8C2A2; *Gallus gallus* Q5ZIN2, --, PRK09297; *Danio rerio* Q08BW3, A2BIL9, Q504E6; *Xenopus laevis* Q6GPB4, --, Q6DE24; *Drosophila melanogaster* Q8IP11, --, Q9VTV4; *Arabidopsis thaliana* Q9M1E8, --, Q9M2L1; *Saccharomyces cerevisiae* P16658, P39707, QO2825; *Candida albicans* Q5AF73.

and *TSEN54* subunit of the RNA splicing complex may be discussed on the basis of structural homology considerations. Bujnicki and Rychlewski [4] show by careful sequence comparison that the folding of all four components of the yeast tRNA splicing endonuclease (which is homologous to the human complex) may be similar with the increased size of *TSEN54* mainly due to additional insertions between otherwise homologous sequence strains. The evolution of these complexes may have started with a homotetramer as known from the *M. jannaschii* complex via a heterodimeric tetramer as proposed for *H. volcanii* to the heterotetramer of yeast or higher organisms [5]. Thus, identification of mutated positions within sequence alignments with members of known structure may shed some light on the importance of these positions. A multiple sequence alignment of the corresponding sequence part of human *TSEN2* containing the p.Y309C mutation with those of a broad spectrum of other organisms show that the Y309 position is strictly conserved (Tyr of Phe) within eukaryotic organisms, but this residue is lacking in the archebacterial sequences (see Suppl. Fig. 4) pointing to an outer loop region within the structure. There are several structures reported for members of these RNA splicing complexes. For the human *TSEN2*, the highest sequence homology is found with splicing enzyme from *Sulfolobus tokodaii* which in the crystal structure (PDB code 2cv8) forms a noncrystallographic dimer. In this structure a lysine (K58) adjacent to the position corresponding to Y309 in human TSEN2 forms a salt bridge with a glutamic acid (E95). This salt bridge may help stabilise the proper orientation of two domains visible in the *Sulfolobus tokodaii* structure (Suppl. Fig. 6). In the human *TSEN2* sequence E95 corresponds to a histidine residue (H347) which may similarly stabilise domain positions by pi stacking interaction with Y309. A mutation of tyrosine 309 to cysteine will certainly abolish such interaction.

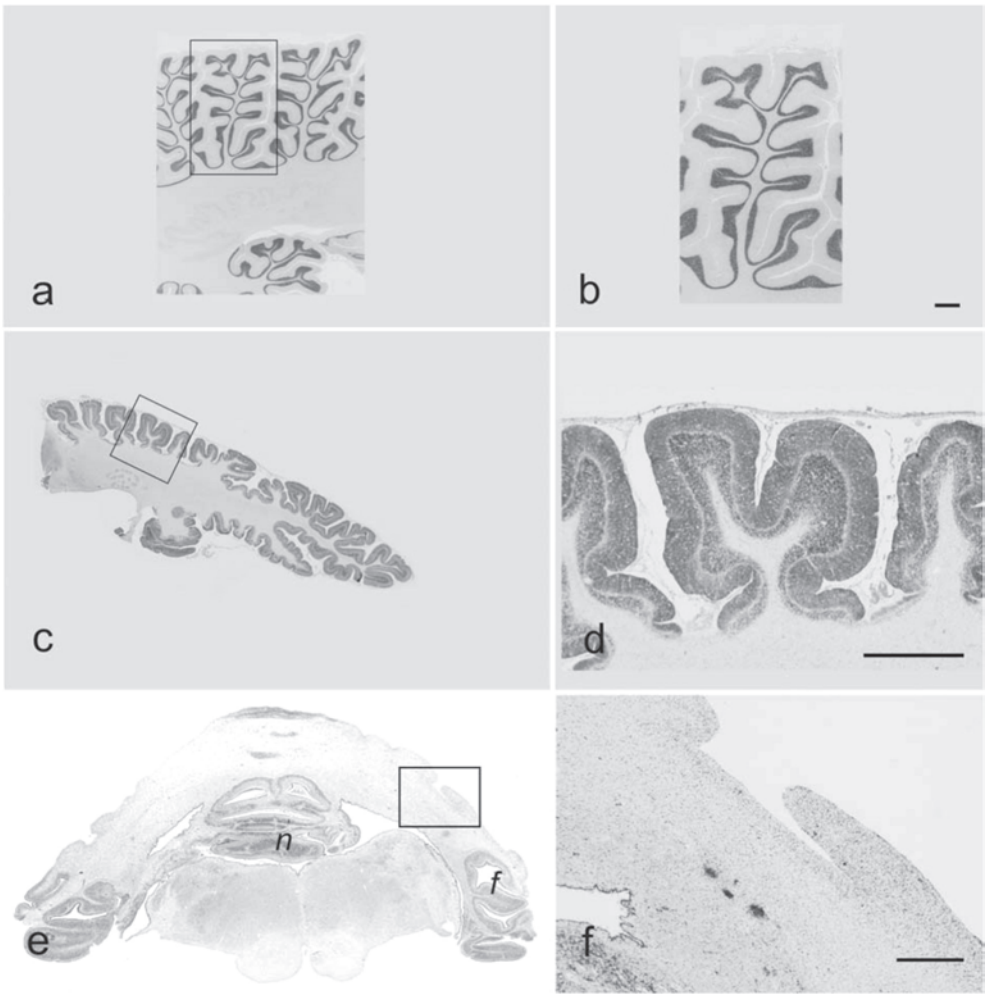

Supplementary Figure 5. Cerebellar cortex in PCH2 and PCH4 (OPCH). (a,b) Control male of 8 yr with accidental death. (c,d) Patient with PCH2 from Am1 family who died at 3yr, 7m. (e,f) Patient with PCH4 from Ut4 family who died two days old. All paraffin sections are stained for synaptophysin. Rectangles on the left side are magnified on the right side. Magnification bars represent 1mm. In control (a,b) a single folium within the rectangle has about 10 branchlets. In the PCH2 patient (c,d) folia are stunted and have few or no branchlets. Notice the loss of cortex between folia in (c). In the PCH4 patient (e,f) folia are rudimentary and denuded with complete loss of cortex except the nodulus (*n*) and flocculus (*f*). Adapted from Barth *et al.* [6], with permission. For colour figure see page 168.

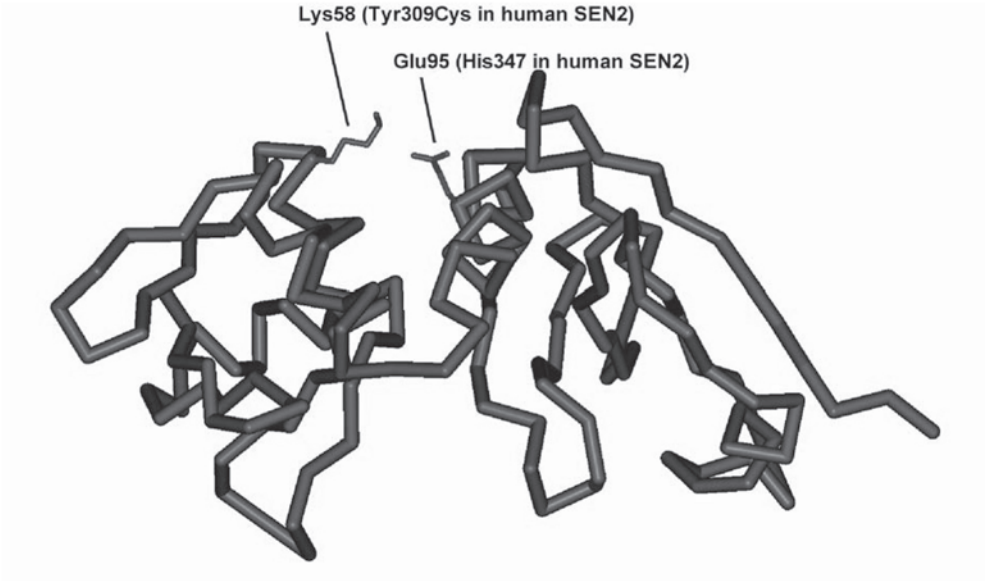

Supplementary Figure 6. Structure of the tRNA splicing enzyme from *Sulfolobus tokodaii* (PDB code 2cv8) with an electrostatic interaction at the position where a tyrosine is mutated to a cystein in the human sequence of *TSEN2*. The interacting residues Lys58 and Glu95 are indicated by a stick representation. The figure was drawn with ViewerPro 4.2 (Accelrys Inc.). It is a reduced representation of the structure (without side chains) showing only the C-alpha atom position of each amino acid.

The S93 mutation site in *TSEN54* should be solvent exposed as it follows from sequence alignment (Suppl. Fig. 4) and inspection of the homologous structures (in the *S. tokodaii* structure a short sequence stretch containing the equivalent residue position is omitted because there is no interpretable electron density). Otherwise it may interact with neighbouring subunits (as shown in the *M. jannaschii* structure, PDB code 1a79). Nevertheless, as follows from the *M. jannaschii* structure, it is situated in antiparallel ß-sheet where a substitution of the serine in the human sequence by a proline with another proline already adjacent to this position may restrict the available conformational space and such hamper a proper folding. In the case of the p.A307S mutation in the human *TSEN54* there is even a serine already present at this position in the *S. tokodaii* structure (see Suppl. Fig. 4) but the micro-environment of this residue which points into the inner part of the molecule shall certainly be different and thus cause a disadvantage of the larger serine residue over the alanine in the human TSEN54 structure. The *TSEN34* mutation p.R58W is in a region which is conserved in the closely related mammals (e.g. mouse and cow). A chicken sequence is not available for this protein. In other vertebrates, this position is exchanged by small hydrophobic residues only (Ile, Leu). Therefore the Trp exchange in this position may well produce sterical hindrance.

Supplementary Table 1. Genes analysed and new identified markers. For all genes the entire coding region and intron exon borders were sequenced.

Gene name	ENSEMBL gene ID	Novel Marker/ SNP	Nucleotide/AA change	Position in the gene	Physical position in bp
SLC9A3R1	ENSG00000109062				
NAT9	ENSG00000109065	AMC-001	beyond stopcodon insertion C	3'UTR	70277639
		AMC-002	intron 2 insertion ATAAA	intron 2	70282584
		AMC-003	UTR insertion GCCCC	5'UTR	70284369
		AMC-004	UTR G->A	5'UTR	70284642
		AMC-005	UTR C->T	5'UTR	70284705
GRIN2C	ENSG00000161509	AMC-006	intron 3 A->G	intron 3	70359549
		AMC-007	exon 2 G->A A8T	exon 2	70362805
HUMPPA/CDR2L	ENSG00000109089				
KCTD2	ENSG00000180901	AMC-008	intron 3 T->G	intron 3	70560842
		AMC-009	intron 5 C->T	intron 5	70570699
HN1	ENSG00000189159				
GGA3	ENSG00000125447	AMC-010	beyond stopcodon insertion GTGGGAG	exon 17	70745605
		AMC-011	beyond stopcodon insertion AGTGGGGGGTGGGG or AGTGGGG or GTGGGG	exon 17	70745613
		AMC 012	intron 4 T->G	intron 4	70751323
		AMC-013	intron 2 T->G	intron 1	70754526
SLC25A19	ENSG00000125454	CCG-001			
CASKIN2	ENSG00000177303				
TSEN54	ENSG00000182173	AMC-014	insertion exon 1 GGAGCC insertion EP	exon 1	71024245
		AMC-015	exon 3 T->C S93P	exon 3	71024740
		AMC-016	intron 4 C->A	intron 4	71025214
		AMC-017	intron 7 A->G	intron 7	71029350
		AMC-018	intron 7 G->A	intron 7	71029372
		AMC-019	exon 8 C->T Q246AMB	exon 8	71029493
		AMC-020	exon 8 G->T A307S	exon 8	71029676
		AMC-021	exon 8 C->T Q343AMB	exon 8	71029784
		AMC-022	exon 8 A->C Q389P	exon 8	71029923
		AMC-023	beyond stopcodon 11 T->C	exon 11	71032257
SRP68	ENSG00000167881				
GALR2	ENSG00000182687				
LGICZ1	ENSG00000186919				
FOXJ1	ENSG00000129654				
MFSD11	ENSG00000092931				
MGAT5B	ENSG00000167889	AMC-024	Exon 16 S2150S	exon16	72455746
		AMC-025	Intron 16 C->G	intron 16	72456309
CBX2	ENSG00000173894				
CBX4	ENSG00000141582				

Supplementary References

1. Te Meerman GJ, Van der Meulen MA, Sandkuijl LA: Perspectives of identity by descent (IBD) mapping in founder populations. Clin Exp Allergy 1995, 25 Suppl 2:97-102.
2. Rozen S, Skaletsky H: Primer3 on the WWW for general users and for biologist programmers. Methods Mol Biol 2000, 132:365-386.
3. Xue S, Calvin K, Li H: RNA recognition and cleavage by a splicing endonuclease. Science 2006, 312:906-910.
4. Bujnicki JM, Rychlewski L: Prediction of a common fold for all four subunits of the yeast tRNA splicing endonuclease: implications for the evolution of the EndA/Sen family. FEBS Lett 2000, 486:328-329.
5. Li H, Trotta CR, Abelson J: Crystal structure and evolution of a transfer RNA splicing enzyme. Science 1998, 280:279-284.
6. Barth PG, Aronica E, de Vries L, Nikkels PG, Scheper W, Hoozemans JJ, Poll-The BT, Troost D: Pontocerebellar hypoplasia type 2: a neuropathological update. Acta Neuropathol 2007, 114:373-386.

Chapter 3

Clinical, neuroradiological and genetic findings in pontocerebellar hypoplasia

Yasmin Namavar, Peter G. Barth, Paul R. Kasher, Fred van Ruissen, Knut Brockmann, Günther Bernert, Karin Writzl, Karen Ventura, Edith Y. Cheng, Donna M. Ferriero, Lina Basel-Vanagaite, Veerle R. C. Eggens, Ingeborg Krägeloh-Mann, Linda De Meirleir, Mary King, John M. Graham Jr, Arpad von Moers, Nine Knoers, Laszlo Sztriha, Rudolf Korinthenberg, PCH Consortium, William B. Dobyns, Frank Baas & Bwee Tien Poll-The.

Published in 2011 in Brain 134(1): 143-156.

Abstract

Pontocerebellar hypoplasia is a group of autosomal recessive neurodegenerative disorders with prenatal onset. The common characteristics are cerebellar hypoplasia with variable atrophy of the cerebellum and the ventral pons. Supratentorial involvement is reflected by variable neocortical atrophy, ventriculomegaly and microcephaly. Mutations in the transfer RNA splicing endonuclease subunit genes (*TSEN54*, *TSEN2*, *TSEN34*) were found to be associated with pontocerebellar hypoplasia types 2 and 4. Mutations in the mitochondrial transfer RNA arginyl synthetase gene (*RARS2*) were associated with pontocerebellar hypoplasia type 6. We studied a cohort of 169 patients from 141 families for mutations in these genes, of whom 106 patients tested positive for mutations in one of the *TSEN* genes or the *RARS2* gene. In order to delineate the neuroradiological and clinical phenotype of patients with mutations in these genes, we compared this group with 63 patients suspected of pontocerebellar hypoplasia who were negative on mutation analysis. We found a strong correlation ($P<0.0005$) between *TSEN54* mutations and a dragonfly-like cerebellar pattern on magnetic resonance imaging, in which the cerebellar hemispheres are flat and severely reduced in size and the vermis is relatively spared. Mutations in *TSEN54* are clinically associated with dyskinesia and/or dystonia and variable degrees of spasticity, in some cases with pure generalised spasticity. Nonsense or splice site mutations in *TSEN54* are associated with a more severe phenotype of more perinatal symptoms, ventilator dependency and early death. In addition, we present ten new mutations in *TSEN54*, *TSEN2* and *RARS2*. Furthermore, we show that pontocerebellar hypoplasia type 1 together with elevated cerebrospinal fluid lactate may be caused by *RARS2* mutations.

Introduction

Pontocerebellar hypoplasia (PCH) represents a group of autosomal recessive neurodegenerative disorders with prenatal onset, predominantly affecting growth and survival of neurons in the cerebellar cortex, the dentate, inferior olivary and ventral pontine nuclei. The variable involvement of supratentorial structures includes ventriculomegaly, neocortical atrophy and microcephaly. Radiologically and pathologically, all subtypes are characterised by hypoplasia and variable atrophy of the cerebellum and pons.

Six subtypes of PCH have so far been identified. Type 1 (MIM 607596) is characterised by additional loss of motor neurons in the spinal cord, morphologically similar to the hereditary spinal muscular atrophies [1-4]. Recently, an association with the vaccinia-related kinase 1 gene (*VRK1*) was reported in a single family with a mild variant of PCH type 1 [5]. In PCH type 2 (MIM 277470, 612389, 612390), the distinctive feature is dyskinesia and/or dystonia and, more rarely, pure spasticity [6]. PCH type 4 (MIM 225753), previously known as olivopontocerebellar hypoplasia, has a more severe course with prenatal onset of clinical symptoms such as polyhydramnios and contractures. Early postnatal death is often reported, usually due to primary respiratory insufficiency. Typical for PCH type 4 are the C-shaped inferior olives, indicating an earlier prenatal onset than seen in type 2 [7,8]. Neuropathologically, PCH type 4 and type 2 both display the fragmentation of the cerebellar dentate nuclei. Mutations in the transfer RNA splicing endonuclease subunit gene *TSEN54* are responsible for PCH type 2 and 4 in most European cases. All mutations identified in type 2 cases are missense mutations (*TSEN54*, *TSEN2*, *TSEN34*). In PCH type 4, nonsense and missense mutations have been identified together (*TSEN54*) [9].

PCH types 3, 5 and 6 (MIM 608027, 610204, 611523, respectively) are rare forms of PCH. Type 3, also known as cerebellar atrophy with progressive microcephaly, is associated with optic atrophy, seizures, hypotonia and short stature [10,11]. Type 3 is mapped to chromosome 7q (markers D7S802 and D7S630 define the borders of the region, but no gene has yet been identified [11]). Type 5 is characterised by intrauterine seizure-like activity and a predominantly affected vermis [12]. No associated locus has been identified. Type 6 has been reported in two families: one with associated mitochondrial respiratory chain abnormalities and the other with progressive encephalopathy, edema, hypsarrhythmia and optic atrophy-like features. Mutations in the nuclear encoded mitochondrial arginyl transfer RNA synthetase gene (*RARS2*) have been identified [13,14].

In this study, we investigated a cohort of 169 patients (141 families) who were referred to our laboratory for molecular genetic testing due to PCH. We screened the coding regions for *TSEN54*, *TSEN2*, *TSEN34*, *TSEN15*, *RARS2* and *VRK1* mutations. In order to define the phenotypical spectrum in patients with the common *TSEN54*

mutation, brain MRI and the clinical phenotype of patients with the common *TSEN54* mutation were compared with patients where we did not find a mutation. Here we show that on MRI, a dragonfly-like pattern of the cerebellum is significantly associated with the common homozygous p.A307S mutation in *TSEN54* (100%). The common mutation in *TSEN54* is associated with progressive microcephaly, severe lack of motor development, dyskinesia and/or dystonia, central visual impairment and impaired swallowing. These findings, together with a dragonfly-like cerebellum, are highly specific for PCH type 2 with the common mutation and can be implemented in the clinical and molecular diagnosis of type 2 patients. Compound heterozygotes with a nonsense mutation and a missense mutation in *TSEN54* are associated with a more severe phenotype with pre- and peri-natal onset of symptoms, such as polyhydramnios, contractures, dependence on mechanical ventilation (>1 day after birth) and early death.

Patients and methods

Patient cohort

For this study, we selected a group of 169 patients (141 families) referred for molecular genetic testing of PCH-associated genes. All patients who took part in our study were diagnosed with PCH by referring clinicians. Using these non-strict selection criteria, we aimed to include typical and atypical patients that represent the spectrum of cases submitted to laboratories performing genetic testing. Blood or genomic DNA samples were provided through neurology, paediatric and clinical genetic departments worldwide. Samples were submitted to our department for diagnostics and informed consent was obtained by referring physicians.

Genetic analysis

The coding regions and exon-intron boundaries of *TSEN54*, *TSEN34*, *TSEN2*, *TSEN15*, *RARS2* and *VRK1* were sequenced on both strands. If DNA levels were not sufficient, DNA was amplified with the GenomiPhi V2 DNA Amplification kit (GE Healthcare, Waukesha, USA) according to the manufacturer's protocol. For 28 cases, DNA from affected siblings was available. All coding regions and exon-intron boundaries for at least one case per family were sequenced. Once a mutation was found, it was verified in the affected sibling. Primer pair sequences, polymerase chain reaction (PCR) and sequence conditions are available upon request. PCR products were directly sequenced using BigDye Terminator sequencing kit and ABI PRISM 3730 DNA analyser (Applied Biosystems, Foster City, CA, USA) according to the manufacturer's protocol. Sequences were analysed using the CodonCode Software version 3.0.1 (Dedham, MA, USA). Possible variants were confirmed by re-sequencing a new PCR product.

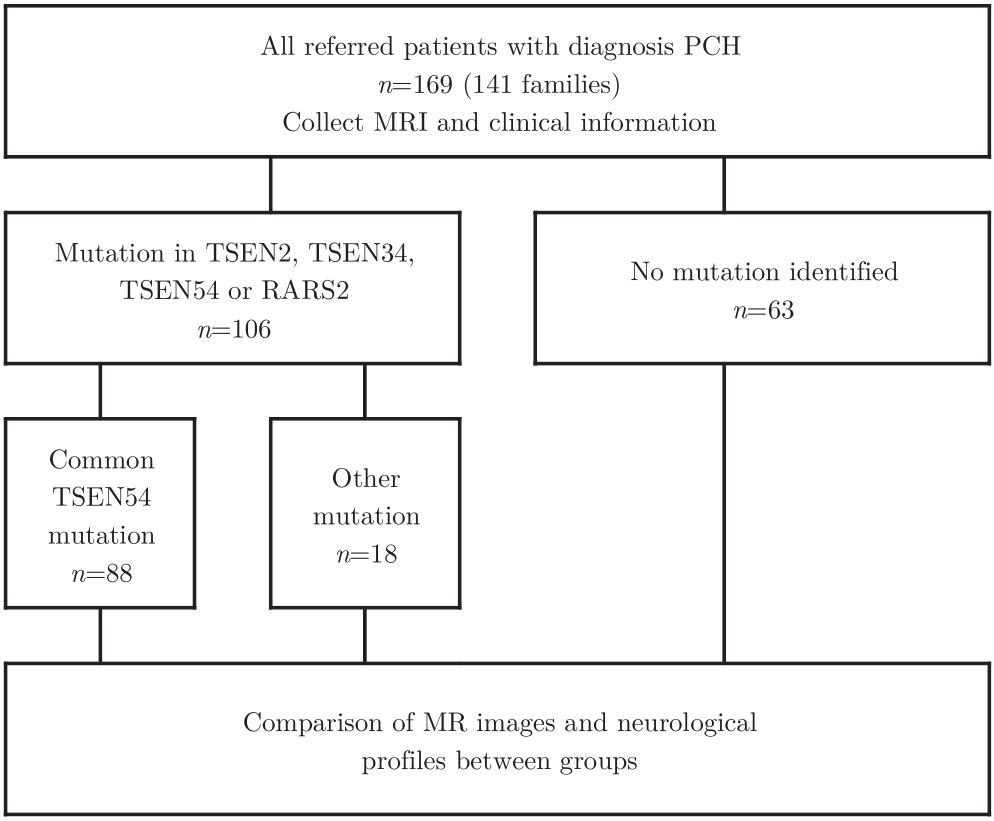

Figure 1. Study design.

When available, DNA from parents was analysed to confirm segregation. One hundred and sixty-seven control chromosomes (88 individuals) were screened to exclude polymorphisms. The study design is shown in Figure 1.

Clinical analysis

Detailed clinical information was available for 85 patients. This included pre- and perinatal morbidity and disease course (Table 1). Additional information requested by questionnaire included specific questions on (progressive) microcephaly, motor achievements, visual and feeding behaviour, speech and contractures.

Magnetic resonance imaging analysis

Complete magnetic resonance neuroimages (coronal, sagittal and axial sections) were available for 50 patients. Prior to DNA analysis, coronal, sagittal and axial MRIs were qualitatively analysed (by P.G.B. and B.T.P.T.). Cerebellum, pons, cerebral cortex, ventricles and myelination were analysed and divided into different categories (for

Table 1.

	Homozygous for *TSEN54* p.A307S		**No mutation identified**	
	(*n*=88)	**%**	**(*n*=63)**	**%**
Prematurity (<38 wks gestation)	11/63	17.5	10/29	34.5
Polyhydramnios	3/67	4.5	5/29	17.2
Jitteriness, clonus	45/50[a]	90	15/25	60
Congenital contractures	1/62	1.6	3/27	11.1
Microcephaly <-2SD	73/73	100	40/42	95.2
Progressive microcephaly	67/67[a] 1 ed	100	21/26 2 ed	80.8
Dyskinesia / dystonia	69/72[a,b]	95.8	20/34 3 ed	58.8
Pure spasticity	2/72[b]	2.8	3/32 3 ed	9.4
Impaired swallowing	68/69[a]	98.6	18/30	60.0
Central visual impairment	52/60[a] 2 ed	86.7	9/20 2 ed	45.0
Primary optic atrophy	0/59[a,c]	0	5/18	27.7
Epileptic seizures, all types	44/54	81.5	17/23 1 ed	73.9
Mechanical ventilation >l day after birth	4/64	6.3	8/27 1 ed	29.6
Median age at latest examination	34.5 mo (58 patients)		28 mo (34 patients)	
Survival range (median age of death)	2.5 wk till 31 yr[d] (50 mo, 18 patients)		1 day till 22 yr (6 mo, 13 patients)	
Hand control[e]	43 Nn[a] 10 I 2 ed		6 Nn 5 I 7 G 3 ed	
Postural antigravity control[f]	28 Nn[a] 17 S 1 T 1 Us 2 ed		9 Nn 5 S 1 T 1 H 7 Us 3 ed	

Table 1. Clinical symptoms in patients with the common mutation and in patients where no mutation was identified.

The number of patients with a symptom is given relative to all patients with information on this symptom. Percentages indicate the proportion of the patients with a symptom relative to all patients with symptom information. ed = early death.

a Significantly associated with the common mutation group, compared to cases where no mutation was identified. The absence of primary optic atrophy was also significantly associated with the mutation.

b One case did not exhibit dyskinesia, dystonia and spasticity, however, this case was <3 months at the time of the examination.

c One case had optic atrophy secondary to glaucoma. Primary optic atrophy was not reported in any of these cases.

d Patient is alive.

e Hand control: G = grasping; I = intentional; Nn = none.

f Postural antigravity control: H = with hip support; Nn = none; S = with shoulder support; T = with high thoracic support; Us = unsupported sitting.

further explanation see Tables 2 and 3 and Fig. 2a-d).

Statistical analysis

Fisher's exact test and Chi-square test for trend were used to test whether there were significant phenotypical differences between the different mutation groups and the group in whom no mutations were identified.

Results

We identified disease-causing mutations in 106 of the 169 patients, representing a mutation frequency of 62.7%. One hundred patients (59.2%) had a disease causing mutation in *TSEN54*. Eighty-eight of these patients were homozygous for the common mutation (p.A307S) in *TSEN54* (52.1%). MRI scans were available for evaluation from 50 individuals. Twenty of these 50 patients had the common mutation, in 13 cases we identified a rare mutation and in the remaining 17 of the 50 imaged cases we did not identify a mutation. All mutations that we identified were verified in 176 control chromosomes and none of them were found homozygous in healthy individuals. We also analysed, but did not identify, mutations in the candidate gene *TSEN15* and the *VRK1* gene.

TSEN54 common mutation

Neurological phenotype

Eighty-eight of 169 patients were homozygous for the common mutation (p.A307S) in *TSEN54* (52.1%). Due to the size of this group, we were able to redefine the phenotype in detail and compare with patients without mutations (Table 1). Pre- and peri-natal complications, such as polyhydramnios and contractures, were rare in patients with the common mutation. Neonatal irritability (jitteriness and/or clonus) and dyskinesia

Table 2. MRI findings in patients with the common mutation and in patients in whom no mutations were identified.

	TSEN54 p.A307S p.A307S (*n*=20)					No mutation identified (*n*=17)				
Morphological stage	0	1	2	3	4	0	1	2	3	4
Cerebellar hemispheres[a]	0	20	0	0	0	0	6	5	0	6
Pons[b]	0	4	16	-	-	2	12	3	-	-
Vermis folial atrophy[c,*]	9	10	0	-	-	6	6	3	2 afolial	-
Cerebral cortex[e]	12	4	4	0	-	11	2	3	1	-
Ventricles[f]	6	6	8	-	-	7	4	6	-	-

Reference sequences are NM_207346.2, NM_025265. 2, NM_024075.2 and NM_020320.3 (for *TSEN54*, *TSEN2*, *TSEN34* and *RARS2,* respectively).

a Based on coronal images, the cerebellar hemispheres were distinguished into different groups: (1) a dragonfly type, with flattened cerebellar hemispheres ('the wings') and a relatively preserved vermis ('the body'); (2) a butterfly type, with a small cerebellum where the proportional size of hemispheres and vermis is preserved; (3) a postnatal atrophy type; and (4) all cases that cannot be categorized under (1-3).

b Pons was scored as normal (0), attenuated (1) or flat (2).

c Vermal folia were scored as normal (0), atrophy (1) or severe atrophy (2).

d Cerebral cortex was scored as normal (0), mild atrophy with visible sulci (1), moderate or severe atrophy (2) or delayed maturation with immature aspect (3).

e Ventricles were scored as normal (0), anterior>posterior (1) or general dilatation (2).

*In one case it was not possible to determine the degree of folial atrophy in the vermis.

Table 3. MRI findings in patients with a rare mutation.

Family code	Gene	Mutation	Age (mean 12 weeks)	Cerebellar hemispheres[a]	Pons[b]	Vermis folial atrophy[c]	Cerebral cortex[d]	Ventricles[e]	Unusual findings
Ch1 II.1	TSEN54	p.E60AfsX109 p.A307S	8 days	4	1	1	3	0	Generally small cerebellum
Br1 II.2	TSEN54	p.S93P p.A307S p.A307S	6 days	1	1	1	3	2	
Se2 II.2	TSEN54	Splice site mutation p.A307S	2 days	1	1	1	3	0	
Dh1 II.1	TSEN54	p.G124V p.A307S	7 months	1	2	0	0	1	
Vi5 II.1	TSEN54	p.G124V p.A307S	10 months	3	2	0	1	1	
Ut4 II.1	TSEN54	p.Q246X p.A307S	3 days	1	2	0	3	2	Abnormal white matter sign. cerebellar hemispheres
Nu1 II.1	TSEN54	p.A307S p.Q343X	1-2 weeks	1	2	2	3	2	
Lj1 II.1	TSEN54	p.A307S p.Y513D	2 days	1	2	2	3	0	
Bd1 II.1	TSEN54	p.A307S p.P318QfsX23	10 months	1	2	0	0	1	
Gn6 II.1	TSEN54	p.A307S p.R353GfsX81	6 weeks	4	2	2	3	2	Generally small cerebellum
Pa1 II.3	TSEN2	p.Y309C splice site mutation	10 days	2	2	0	1	2	
Hg1 II.1	TSEN34	p.R58W p.R58W	1 year	2-3	1	1	0	2	
Ex1 II.1	RARS2	p.Q12R p.M342V	13 months	2	1	0	1	2	

Reference sequences are NM_207346.2, NM_025265. 2, NM_024075.2 and NM_020320.3 (for *TSEN54*, *TSEN2*, *TSEN34* and *RARS2*, respectively).
For explanation of footnotes a-e, see table 2.

and/or dystonia were associated with the presence of the common mutation ($P<0.005$ and <0.0001, respectively). Impaired swallowing contributing to failure to thrive and requiring nasogastric tube feeding or percutaneous endoscopic gastrostomy is frequently seen in patients with the common mutation ($P<0.0001$). Progressive microcephaly becomes more evident with increasing age and was associated with the common mutation ($P<0.005$) (Fig. 3) [15].

Impaired hand and head control and central visual impairment in the absence of primary optic atrophy were also strongly associated with the presence of the common mutation ($P<0.0005$). Primary optic atrophy was ultimately used as an exclusion criterion for the common mutation, as none of the patients with this mutation displayed such a phenotype. Taking all aforementioned criteria together, these characteristics fit with a PCH type 2 phenotype. Seizures were often reported, but were also present in the majority of patients in whom we did not identify a mutation ($P = 0.542$).

A wide range of life expectancy was reported. While one child died at the age of 2.5 weeks, one patient is now alive at 31 years of age.

We previously established the allele frequency of the common p.A307S mutation in German and Dutch individuals (n = 730) and identified 6 heterozygote genotypes [9]. Effects of the common mutation on protein function was predicted with Alamut software 1.5 (Interactive Biosoftware, Rouen France) (Tables 5 and 6) [9].

MRI analysis

Based on coronal images, we divided the cerebellar hemisphere pathology into four different categories (Table 2, Fig. 2a-d): (1) a dragonfly type, with flattened cerebellar hemispheres ('the wings') and a relatively preserved vermis ('the body'); (2) a butterfly type, with a small, normally proportioned cerebellum; (3) a postnatal atrophy type; and (4) the remainder of cases that cannot be categorized in (1-3) above. None of the images showed normal hemispheres. The dragonfly-like cerebellar hemispheres were significantly associated with the presence of the common mutation compared to cases where no mutation was identified ($P<0.0005$; Fig. 2a,b). All 20 cases with the common mutation had dragonfly-like hemispheres. Six of the 17 cases of the group without a mutation also showed this MRI phenotype.

The shape of the pons was divided into three different categories: (1) normal; (2) attenuated; or (3) flat. The degree of attenuation of the pons was significantly associated with the presence of the common mutation ($P<0.0005$; Fig. 4a).

The shape of the cerebellar folia in the vermis, the atrophy and/or maturity of the cerebral cortex and the size of the ventricles were not significantly associated with patients with a common mutation, compared to patients in whom no mutation was identified ($P = 0.213$, 0.871 and 0.573, respectively). The vermal folia and the cerebral

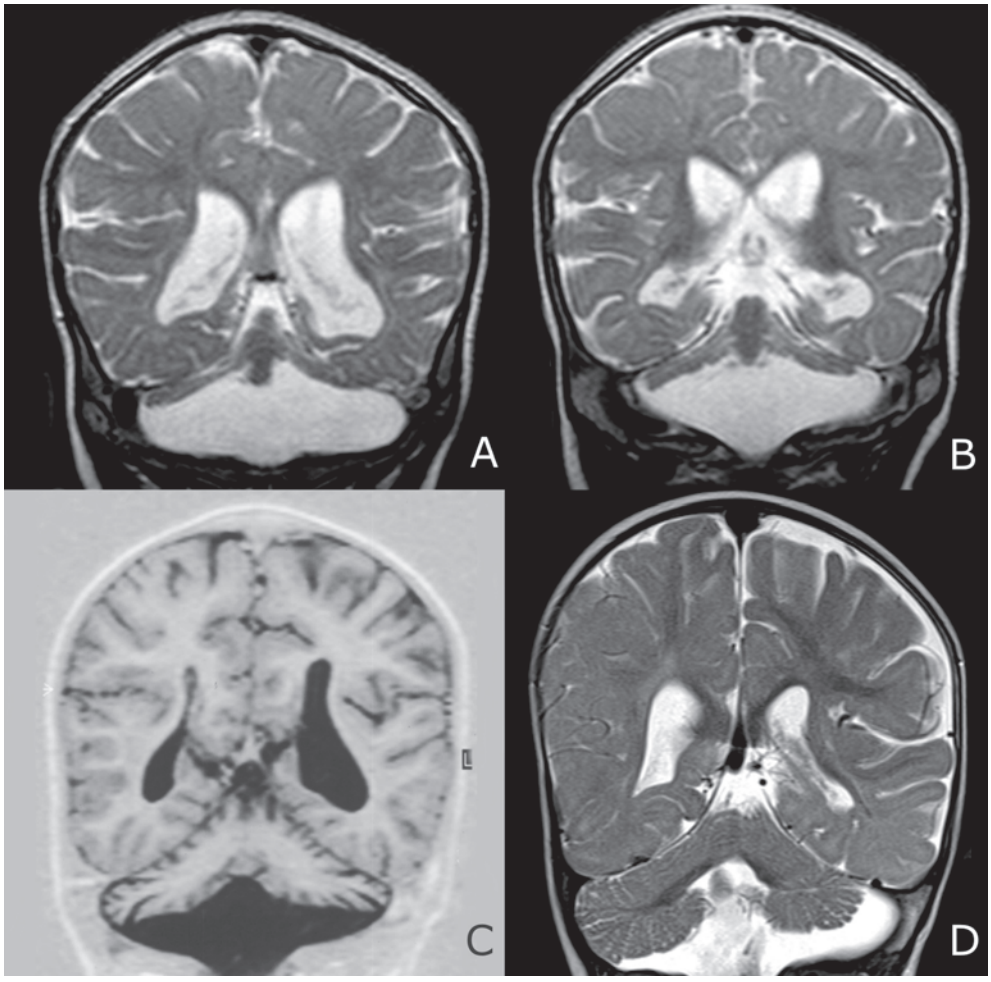

Figure 2. Examples of MRI scores of cerebellum. (a,b) Cerebellar hemisphere score 1: dragonfly type, with flat cerebellar hemispheres and a relatively spared cerebellar vermis (coronal sections, T_2-weighted, 9 months). Mild atrophy of the cerebral cortex with visible sulci. Homozygous for common *TSEN54* mutation. (c) Cerebellar hemisphere score 2: butterfly type, with hypoplastic cerebellar hemispheres. Decrease in size of the vermis is proportional to the diminution in size of the hemispheres (coronal section, T_1-weighted, 7 years). In addition, cerebellar cortical atrophy is seen, as well as mild atrophy of the cerebral cortex with visible sulci. No mutation identified. (d) Cerebellar hemisphere score 3: postnatal atrophy-like on the right side, combined with mild cerebellar hypoplasia on the left (coronal section, T_2-weighted, 10 months). In addition there is cerebral cortical atrophy with visible sulci. Heterozygote for uncommon *TSEN54* mutation (p.G124V) plus heterozygote for common *TSEN54* mutation.

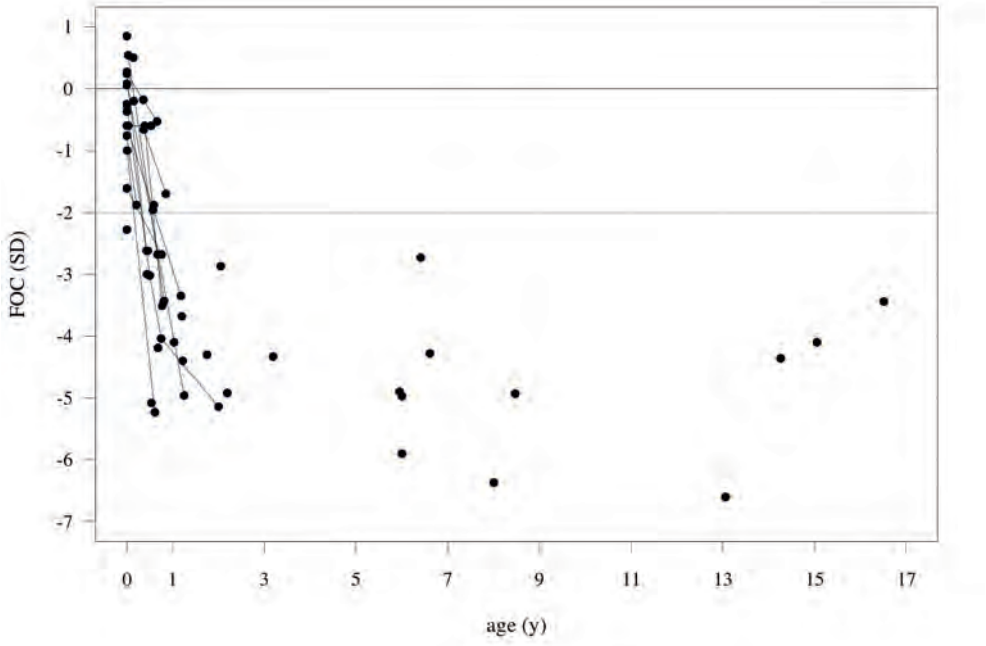

Figure 3. Progressive microcephaly in patients with the common mutation. Frontal-occipital circumference was measured in 38 cases (61 measurements). Measurements of individual patients are connected within the first 3 years of life to illustrate rates of progression. Reference measurements were used from Roche *et al.* [15].

cortex were relatively preserved. Also, no correlation was found between ventricular size and the presence of the common mutation. Generally, myelination of the cerebral hemispheres was delayed. No signs of demyelination were found.

Additional findings in the common mutation group

In eight patients (40%), mild to severe cerebral cortical atrophy was seen on MRI (Table 2, Fig. 5a). This phenomenon correlates with increasing age, suggesting that cortical atrophy might develop in all cases with PCH type 2.

One patient (Am1b II.1) had vermal and cerebellar hemispheric cysts (Fig. 5b,c). Autopsy of this patient revealed that the cysts were destructive [8]. We did not observe cysts in affected family members of this patient. However, cysts were found in one unrelated case where we did not find a mutation.

Genetic, clinical and neuroradiological findings in cases with a rare mutation

In 18 patients (17 families) of our cohort of 169 patients, we identified a rare combination of mutations in *TSEN54*, *TSEN34*, *TSEN2* or *RARS2*. In 10 patients we

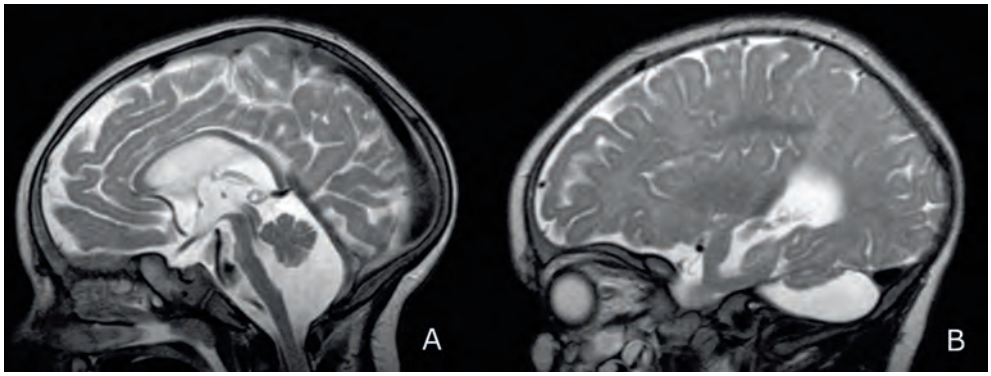

Figure 4. Typical MRI seen in the common mutation group. Flat ventral surface of the pons, cerebellar hemispheric and mild vermal hypoplasia. In this case without significant folial atrophy (sagittal sections, T_2-weighted, 9 months). The corpus callosum is too thin. Homozygous for common *TSEN54* mutation.

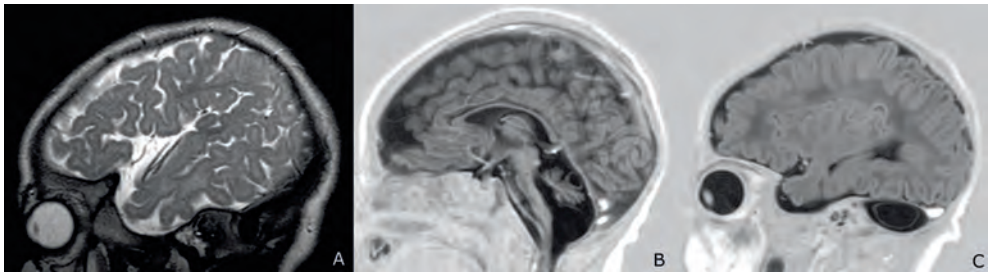

Figure 5. Additional findings in patients with the common mutation (a) Neocortical atrophy (sagittal view, T_2-weighted, 9 months). Homozygous for common *TSEN54* mutation. (b) Cerebellar vermal and (c) hemispheric cyst. Mid and lateral sagittal sections from Patient Am1b II.1 (T_1-weighted Inversion Recovery, 12 months). Homozygous for common *TSEN54* mutation.

observed a combination of mutations not previously published (Table 4). Effects of these mutations on protein function or transcription were predicted with Alamut software 1.5 (Interactive Biosoftware, Rouen France) (Tables 5 and 6).

Severe *TSEN54* mutations

Nine patients were compound heterozygote and we classified their combination of mutations as severe *TSEN54* mutations (Table 4). Of these, five (Ch1, Bd1, Ut4, Nu1, Gn6) carried a nonsense mutation plus a common mutation. Three individuals (Se1, Se2, Us15) carried a splice site mutation plus a common mutation. No RNA was available to test for splicing errors. *In silico* analysis suggests loss of a splice donor site in two patients (Se1 and Se2) and skipping of exon 10 in one patient (Us15). Segregation was confirmed by testing parental DNA.

Table 4. Clinical symptoms in patients with rare mutations in *TSEN54*, *TSEN34*, *TSEN2* or *RARS2*.

Family code	**Ch1 II.1**[d]	**Br1 II.2**	**Se2 II.2**	**Dh1 II.1**	**Vi5 II.1**	**Ut4 II.1**	**Nu1 II.1**
Gene	Tsen54	Tsen54	Tsen54	Tsen54	Tsen54	Tsen54	Tsen54
Mutation (allele A)	p.E60A fsX109	p.S93P p.A307S	p.A95A[e]	p.G124V	p.G124V	p.Q246X	p.A307S
Mutation (allele B)	p.A307S	p.A307S	p.A307S	p.A307S	p.A307S	p.A307S	p.Q343X
Pregnancy duration (weeks)	31	at term	34 5/7	40	u	38	35
Polyhydramnios	+	+	+	-	-	-	+
Jitteriness/clonus	+	+	+	-	u	+	+
Congenital contractures	+	-	+	-	-	+	-
Microcephaly	u	+	+	+	+	+	+
Progressive microcephaly	u	+	ed	+	+	ed	+
Dyskinesia/dystonia	ed	-	ed	+	+	ed	-
Pure spasticity	ed	-	ed	-	-	ed	+
Impaired swallowing	u	+	+	-	+	+	+
Central visual impairment	u	+	ed	-	+	ed	+
Primary optic atrophy	u	+	u	-	u	u	-
Epileptic seizures, all types	u	u	-	+	-	u	+
Mechanical ventilation >1 day after birth	+	+	+	-	-	+	+
Age at latest examination	9 d	u	6 d	4 yr	11 mo	2 d	8 mo
Age at death	9 d	3 mo	6 d	alive	alive	2 d	16 mo
Hand control[a]	ed	Nn	ed	G	I	ed	Nn
Postural antigravity control[b]	ed	Nn	ed	Us	Nn	ed	Nn

Reference sequences are NM_207346.2, NM_025265. 2, NM_024075.2 and NM_020320.3 (for *TSEN54*, *TSEN2*, *TSEN34* and *RARS2*, respectively).

Plus = Yes; Minus = No; u = unknown; ed = early death; wk = weeks; mo = months; yr = years.

a Hand control: G = grasping; I = intentional; Nn = none.

b Postural antigravity control: H = with hip support; Nn = none; S = with shoulder support; T = with high thoracic support; Us = unsupported sitting.

c Patient from Rankin *et al.* [14].

d DNA of patient was no longer available, therefore the genotype of the patient was predicted from sequencing parental DNA.

e Splice site mutation.

Se1 II.1	**Us15 II.1**	**Lj1 II.1**	**Bd1 II.1**	**Gn6 II.1**	**Le1 II.1**	**Pa1 II.1/II.3**	**Hg1 II.1**	**Ex1 II.1**[c]	**Sf1 II.1**
Tsen54	Tsen54	Tsen54	Tsen54	Tsen54	Tsen2	Tsen2	Tsen34	Rars2	Rars2
p.A307S	p.A307S	p.A307S	p.A307S	p.A307S	p.Y309C	p.Y309C	p.R58W	p.Q12R	p.Q12R
p.P417P[e]	c.1430+ 2T>A[e]	p.Y513D	p.P318Q fsX23	p.R353G fsX81	p.Y309C	c.960+ 1delGTAAG[e]	p.R58W	p.M342V	c.110+ 5A>G[e]
38	39	38 4/7	37 6/7	31	at term	39 4/7 / 39	u	at term	38
+	-	+	-	-	-	- / -	-	-	-
+	+	+	+	+	u	+ / +	u	+	-
+	+	+	-	+	-	- / -	-	u	+
+	u	+	+	+	+	+ / +	+	+	-
ed	u	+	+	+	+	+ / +	+	+	-
ed	ed	ed	-	+	+	+ / -	+	-	ed
ed	ed	ed	-	-	-	- / -	-	-	ed
u	+	+	+	+	-	+ / +	-	+	u
ed	ed	ed	+	u	+	+ / u	+	+	+
u	u	u	u	-	-	u / u	-	u	-
+	u	-	+	+	+	+ / -	+	+	u
ed	+	-	-	+	-	- / -	-	-	+
1 d	2 wk	3 wk	11 mo	6 wk	3 yr	4 yr / 1 mo	4 yr	2 yr	5 d
1 d	2 wk	6 wk	12 mo	alive	alive	both alive	alive	alive	6 d
ed	ed	Nn	Nn	u	G	Nn/Nn	Nn	u	ed
ed	ed	Nn	Nn	u	Us	Nn/Nn	Nn	S	ed

One patient (Br1) had three mutations in *TSEN54*, on one allele she had the common p.A307S mutation; on the second allele she also carried the p.A307S mutation plus another missense mutation, p.S93P [9].

All cases had severe congenital symptoms. One patient (Se2) was antenatally diagnosed with cerebellar hypoplasia (gestational age of 19 weeks). In five patients, polyhydramnios was reported ($P<0.05$) (Table 4). Contractures were reported in six patients ($P<0.005$) (Table 4). All but one case (Bd1) were dependent on mechanical ventilation ($P<0.01$). Severe myoclonus was reported in all of them and all but one died in their first year (range: 2 days–16 months, median age at death: 12 days). Additionally, one case (Gn6) is still alive (age at latest examination 6 weeks). In summary, patients who were compound heterozygote for a missense mutation plus nonsense or splice site mutations in *TSEN54* were more severely affected than patients homozygous for the common mutation. These patients fit a PCH type 4 phenotype, which includes early death, prolonged dependency on mechanical ventilation following birth, severe myoclonus, contractures and increased frequency of polyhydramnios. MRIs of these patients reveal pathology comparable to patients with the common mutation in *TSEN54* (Tables 2 and 3, Fig. 6a-c). The cerebellar hemispheres are similar, however the vermis is more frequently affected. The most striking difference, compared to the common mutation group and to patients without a mutation, is the immaturity of the cerebral cortex in this severely affected group ($P = 0.0003$ and 0.0012, respectively, Fig. 6a-c). In seven cases with PCH type 4 (Ch1, Se2, Ut4, Br1, Nu1, Us15, Gn6), the maturation of the cerebral cortex was underdeveloped for postconceptional age, with increased volume of extracerebral CSF and exceptionally large midline cava, most likely due to the lack of growth of the cerebral hemispheres.

Autopsy revealed similar pathology to the MRI. Olivopontocerebellar hypoplasia was observed in Patient Ut4 (Patient 7 and Patient Ut4 in [8] and [9] respectively), which included severely reduced folial development in the cerebellar hemispheres and the horseshoe appearance of the inferior olivary nucleus. Autopsy of Se2 revealed a similar pathology with additional severe cerebral immaturity and atrophy most pronounced in the frontal lobes. Motor neurons of the spinal anterior horns were intact.

Rare *TSEN54* missense mutations

Three patients were compound heterozygotes for missense mutations in *TSEN54* (Dh1, Vi5 and Lj1; Table 4). Two of these patients (Dh1, Vi5) carry the same combination of mutations (p.G124V and p.A307S). Compared to the common mutation group, Patient Dh1 is relatively well. She is able to sit unsupported, grasp, smile and socially interact with her parents. From this perspective it will be interesting to follow up Patient Vi5, who is still young (aged 11 months at last examination). With regard to her MRI, Patient Dh1 (Table 3) is similar to the common mutation group, which suggests that the degree of infratentorial involvement may not relate to postural motor control,

Table 5. Missense and nonsense mutations in pontocerebellar hypoplasia.

Gene	Nucleotide position	Protein position	Grantham score	Polyphen	Conservation amino acid	Other[a]
TSEN54	c.919G>T	p.A307S	99	Benign	Moderate conserved	-
TSEN54	c.371G>T	p.G124V	109	Probably damaging	Highly conserved	-
TSEN54	c.953delC	p.P318QfsX23	-	-	-	Truncated protein
TSEN54	c.736C>T	p.Q246X	-	-	-	Truncated protein
TSEN54	c.1537T>G	p.Y513D	160	Probably damaging	Highly conserved	-
TSEN54	c.1027C>T	p.Q343X	-	-	-	Truncated protein
TSEN54	c.178_215del	p.E60AfsX109	-	-	-	Truncated protein
TSEN54	c.277T>C	p.S93P	74	Possibly damaging	Highly conserved	-
TSEN54	c.1056_1057del	p.R353GfsX81	-	-	-	Truncated protein
TSEN34	c.172C>T	p.R58W	101	Probably damaging	Moderate conserved	-
TSEN2	c.926A>G	p.Y309C	194	Probably damaging	Moderate conserved	-
RARS2	c.35A>G	p.Q12R	43	Possibly damaging	Moderate conserved	-
RARS2	c.1024A>G	p.M342V	21	Probably damaging	Highly conserved	-

a Predictions were made with Alamut software 1.5 and Grantham score (Grantham, Science 1974)

Table 6. Splice site mutations in PCH.

Gene	Nucleotide position	Protein position	Splice site mutation[a]
TSEN54	c.1251A>G	p.P417P	Loss of a splice donor site
TSEN54	c.1430+2T>A	-	Skip of exon 10
TSEN54	c.285G>C	p.A95A	Loss of a splice donor site
TSEN2	c.960+1delGTAAG	-	Skip of exon 7
RARS2	c.110+5A>G	-	Skip of exon 2[b]

a Predictions were made with Alamut software 1.5 and Grantham score (Grantham, Science 1974).
b Edvardson *et al.* [13].

central visual impairment and intellectual performance. The MRI of Patient Vi5 shows postnatal atrophy of the cerebellar hemispheres (Table 3, Fig. 2d).

Patient Lj1 was compound heterozygote for the common mutation and the p.Y513D change. She had an early death PCH type 4 phenotype, similar to the severe *TSEN54* mutation group. This early postnatal death phenotype is associated with more severely affected cerebellar hemispheres, pons, vermis, cerebral cortex and ventricles than observed in cases with the common mutation (Table 3, Fig. 6a-c).

TSEN2 mutations

In two families (Table 4; Le1, Pa1) missense and splice site mutations in *TSEN2* were identified. In one patient (Le1, [9]) with a homozygous mutation in *TSEN2*, motor control (recorded as unsupported sitting and the ability to grasp objects) was better in comparison to the common *TSEN54* mutation group. Two siblings (Pa1 II.1 and II.3) match the common mutation group phenotype in all regards. Pa1 II.1 and II.3 carry a splice site mutation on one allele (c.960+1delGTAAG) and a missense mutation on the other allele (p.Y309C).

TSEN34 mutations

One patient (Table 4, Hg1) with a homozygous missense mutation in *TSEN34* was similar in symptomatology to the common *TSEN54* mutation group, except for the absence of dysphagia [9]. MRIs of this case show mild involvement of cerebellum and pons (similar to Fig. 2d).

RARS2 mutations

RARS2 mutations were found in two patients (Table 4). One case (Ex1, [14]) had progressive microcephaly, hypotonia, no dystonia/dyskinesia, impaired swallowing, seizures and lactic acidemia in the neonatal period. MRI findings were comparable to those published previously by others [13].

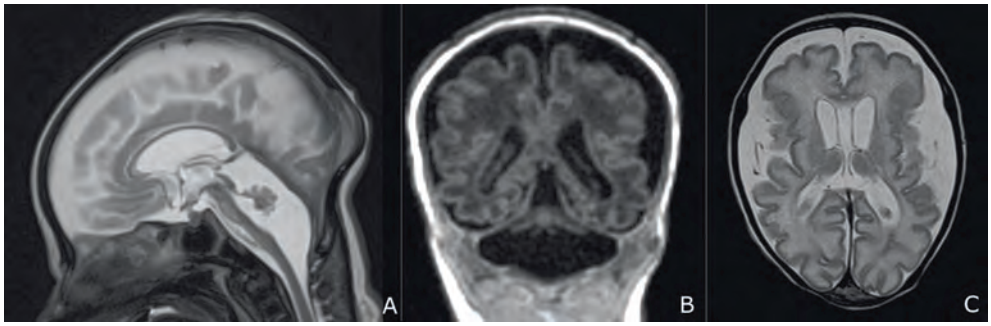

Figure 6. Typical findings in severe mutation group (PCH type 4 phenotype). (a) Showing flat lower surface of the pons and more severe involvement of vermis with extreme hypoplasia and moderate atrophy (midsagittal section, T_2-weighted, 31+5 weeks). Heterozygote for nonsense mutation in *TSEN54* (p.R353GfsX81) plus heterozygote for common *TSEN54* mutation. (b) Coronal image shows extremely small and flattened cerebellar hemispheres. The inferior vermis projects slightly below the hemispheres. Small appendages below the vermis possibly represent tonsils or flocculi, in this case (coronal view, T_1-weighted, 31+5 weeks). Heterozygote for nonsense mutation in *TSEN54* (p.R353GfsX81) plus heterozygote for common *TSEN54* mutation. (c) Increased extracerebral space, wide-open sylvian fossa and shallow frontal sulci indicating delay in neocortical maturation (axial T_2-weighted, 31+5 weeks). Heterozygote for nonsense mutation in *TSEN54* (p.R353GfsX81) plus heterozygote for common *TSEN54* mutation.

Table 7. Inclusion and exclusion criteria in negative mutation group.

Inclusion criteria
Jitteriness, clonus
Progressive microcephaly
Dyskinesia/dystonia
Impaired swallowing
Central visual impairment
MRI: Cerebellar hemisphere (score 1) [a]
MRI: Pons (score 1 or 2) [b]
Exclusion criterion
Primary optic atrophy

The above-mentioned characteristics were used as inclusion and exclusion criteria in order to study the negative mutation group more closely. Thirteen patients from the negative mutation group fit the PCH type 2 phenotype.

a Cerebellar hemisphere score as in Tables 2 and 3.

b Pons score as in Tables 2 and 3.

The other case (Sf1) had hypotonia, early lethality (age at death 6 days) and high CSF lactate levels, fitting a PCH type 6 phenotype. Post-mortem examination of this patient revealed a neuropathological profile that fits a PCH type 1 phenotype, with loss of spinal anterior horn cells and diffuse gliosis. Furthermore, flat cerebellar folia, loss of Purkinje cells and pontocerebellar hypoplasia were found.

PCH type 2 phenotype in the negative mutation group

We compared the group without mutations (63 patients) to the group with mutations, in order to find characteristics common to both groups, as well as atypical features. Using these criteria, only 13 individuals from the no-mutation group retained all the significant characteristics of the common *TSEN54* mutation group (Table 7). However, it must be stated that the clinical profile of the characteristics of these 13 individuals is incomplete.

Unidentified variants

Rare sequence variants were not likely to be pathogenic, since they were synonymous mutations, mutations in introns or untranslated regions, or mild amino acid substitutions (Suppl. Table 1).

Discussion

In this study, we investigated a cohort of 169 patients (141 families) clinically diagnosed with PCH and determined the contribution of five genes known to be involved in PCH (*TSEN54*, *TSEN2*, *TSEN34*, *RARS2* and *VRK1*). In addition, we sequenced candidate gene *TSEN15* for mutations, since this gene also encodes for a protein-subunit of the TSEN complex. We identified disease-causing mutations in 106 cases, representing a mutation frequency of 62.7%. In 100 patients we identified disease-causing mutations in *TSEN54* (59.2%). Eighty-eight of these patients had a homozygous p.A307S mutation in *TSEN54* (52.1%). Twelve cases had a rare combination of *TSEN54* mutations (7.1%). Three individuals carried mutations in *TSEN2* (1.8%). One patient had a mutation in *TSEN34* (0.6%). Two patients carried *RARS2* mutations (1.2%). In the genes *TSEN15* and *VRK1* no pathogenic mutations were found. Most alleles with the p.A307S *TSEN54* mutation were from patients of Northern European descent, including cases from the USA and Canada. Exceptional cases were from Israeli, Arab, Turkish and Ibero-American descent.

TSEN54 common mutation: PCH type 2

The common mutation group fits the PCH type 2 phenotype (Table 7), in which dyskinesia and/or dystonia and severe microcephaly are the major clinical hallmarks,

together with pontocerebellar hypoplasia. The presence of progressive microcephaly and the absence of primary optic atrophy can be considered distinctive features for the common mutation. Epileptic seizures are common in the PCH type 2 group (81.5%) and the probability of developing these increases with age. In some cases it may be difficult to differentiate between seizures and dyskinetic movements.

Life expectancy is difficult to predict as survival ranges from early postnatal (2.5 weeks) to adult death (one case alive at 31 years). Survival will be prolonged with better care such as tube feeding via percutaneous endoscopic gastrostomy and artificial ventilation. We show that the PCH type 2 phenotype is distinct and can be used to guide molecular diagnosis. All cases with the common mutation (100%) have a dragonfly-like phenotype on MRI, therefore MRI is recommended and helps in early diagnosis.

Severe *TSEN54* mutations: PCH type 4

Nine patients were considered to have a combination of missense and nonsense mutations in *TSEN54*, leading to more severe symptoms (Table 4) and early death (median age 12 days). These patients fit the PCH type 4 subtype.

MRI analysis of the *TSEN54* severe mutation group deviates in some regards from the common mutation group: analysis of seven cases reveals pericerebral CSF accumulation, persistently wide midline cava, delayed neocortical maturation and more severe involvement of the vermis (Fig. 6a-c). MRI analysis is therefore essential for diagnosis of PCH type 4.

RARS2 mutations causing a PCH type 1-like phenotype in one case

In one PCH type 1 case (confirmed by autopsy) we identified disease-causing mutations in *RARS2*. These mutations were not previously associated with PCH type 1, but *RARS2* mutations are associated with PCH type 6, featuring mild mitochondrial chain defects, hypotonia, progressive microcephaly and elevated CSF lactate levels. High CSF lactate is not reported in patients with a *TSEN* mutation. Autopsy was not performed on the previously published patients with PCH type 6 [13,14], and therefore a relationship between *RARS2* and PCH type 1 phenotype cannot be excluded until further cases have been studied.

TSEN2, *TSEN34* and rare *TSEN54* missense mutations

In seven cases of PCH (Le1, Pa1 II.1, Pa1 II.3, Hg1, Dh1, Vi5, Lj1) we identified rare missense mutations in *TSEN34* and *TSEN54*, and missense and splice site mutations in *TSEN2*. They fit the PCH type 2 phenotype; however Patient Dh1 has a mild clinical

phenotype compared to the common *TSEN54* mutation group. Since this group of patients is small in number, more individuals will be necessary to draw a specific phenotypical profile.

Unsolved cases

The mutation-negative group is phenotypically heterogeneous in contrast to the common mutation group. Only 13 of the 63 cases fulfilled the common mutation characteristics (criteria in Table 7). Information on some of these characteristics is missing in these 13 individuals, showing that sufficient clinical information and MRI are essential for confident clinical diagnosis and genetic analysis. Untranslated regions, introns or mutations in other genes may underlie the pathogenesis in these cases.

All patients referred by clinical geneticists or neurologists with the clinical or radiological diagnosis PCH were entered into this study reflecting common clinical practice. Taking these non-strict selection criteria into account, it remains possible that congenital glycosylation disorders, mitochondrial disorders or other diseases underlie the neurological findings in some of the unsolved cases [16-18]. In case of sensorineural hearing loss and a simplified gyral pattern, X-linked calcium/calmodulin-dependent serine protein kinase (*CASK*) mutations should be considered [19]. One should consider progressive encephalopathy, edema, hypsarrhythmia and optic atrophy syndrome when a case presents with these symptoms [20]. Stricter inclusion criteria might increase the percentage of mutation-positive cases.

Furthermore, the unsolved cases suffer from a higher rate of premature births (34.5%) than the common mutation group (17.5%). In these cases, the severe prematurity (<32 weeks) may be associated with pontocerebellar disruption, developmental delay and the occurrence of seizures [21]. Four (13.8%) of the unsolved cases were severely premature (born at 27 and 29 weeks, two others were born at 32 weeks). In the common *TSEN54* mutation group there were three cases (4.8%) with severe prematurity (one case at 29 weeks and twins at 30 4/7 weeks [22]).

Unclassified variants

In three cases, we cannot exclude that the missense mutations found on one allele are not associated with PCH (*TSEN54* p.N347Y, p.R374C and *TSEN34* p.R279C, Suppl. Table 1). Since it is not possible to detect large deletions by direct sequencing, we cannot rule out the possibility that these variants are pathogenic in combination with a deletion on the opposite allele.

Disease mechanism

It is difficult to define a common pathway in the different genes associated with PCH.

However all genes, apart from *VRK1*, play a role in protein synthesis and transfer RNA (tRNA) processing in particular. *RARS2* encodes for mitochondrial arginyl tRNA synthetase, which charges arginine to specific transfer RNAs during protein synthesis. *TSEN2*, *TSEN34*, *TSEN54* and *TSEN15* encode for the tRNA splicing endonuclease, which plays a role in intronic transfer RNA splicing (http://lowelab.ucsc.edu/GtRNAdb/) [23]. Alternative functions of these proteins might play a role in a common pathway responsible for PCH [23]. Other neurodegenerative diseases such as Charcot-Marie-Tooth disease and leukoencephalopathy with brainstem and spinal cord involvement and elevated lactate, are also associated with mutations in tRNA synthetase genes [24-27]. Patients with nonsense mutations in *TSEN54* show a more severe phenotype, which suggests that loss of function of the TSEN54 protein is the underlying disease mechanism. Further research is required to investigate why mutations in tRNA processing genes lead to PCH.

Conclusion

Here we present evidence that the common homozygous mutation in *TSEN54* can be predicted reliably from the PCH type 2 phenotype. There is a strong association with flat dragonfly-like cerebellar hemispheres, a flat pons, dyskinesia and/or dystonia, neonatal irritability, central visual impairment, the absence of optic atrophy and severe cognitive and motor impairment. More severe *TSEN54* mutations are associated with early postnatal death, contractures, polyhydramnios and ventilatory problems. MRI analysis reveals severe cerebral immaturity of the cortex, which assists in establishing a diagnosis of PCH type 4. Our data provide further evidence that PCH type 2 and 4 result from a common spectrum of mutations, mainly affecting *TSEN54*. The homogeneity of the phenotype, both from a clinical perspective and by neuroimaging, correlates strongly with the genotype and can facilitate early diagnosis and assist in molecular genetic testing. A clinical and/or neuroradiological PCH type 2 profile is shared with 13 unsolved cases, suggesting the involvement of other unidentified genes or the involvement of non-coding regions in the *TSEN* or *RARS2* genes in PCH. In addition, we show that PCH type 1 together with elevated CSF lactate may be caused by *RARS2* mutations. Together these data enhance the clinical description of PCH and will assist with the neuroradiological and genetic diagnosis of PCH.

Acknowledgements & Funding

We thank M.B. de Wissel-Dijns for technical assistance. We are grateful to Prof. J.M.B.V. de Jong, Prof. M. de Visser and K. Ritz for critical reading of the manuscript. We acknowledge the contribution of subject's data and DNA samples by S. Shallat, Peoria Medical Centre, Peoria, IL, USA; W. Deppe, Klinik Bavaria, Kreischa; H. Brunner, Radboud University Nijmegen; Miranda Splitt, The Institute For Human

Genetics, Newcastle upon Tyne, UK; Helen Cox, West Midlands Regional Clinical Genetics Service, Birmingham Womens Hospital, Edgbaston, Birmingham, UK; M. Steinlin, University Hospital, Bern; A. Bohring, Westfalische Wilhelms-Universitat, Munster, Germany; S. Gebre-Medhin, Universal Hospital, Lund, Sweden; K. Schoppmeyer, Universitatsklinikum Leipzig, Germany; D. Rowitch, Departments of Paediatrics, Neurosurgery and Howard Hughes Medical Institute, UCSF, San Francisco, USA; M. Koch, Neuropaediaty, Vestische Kinder-Jugendklinik, Datteln.

Financial support was kindly provided by the Hersenstichting Nederland KS2009(1)-81 and the AMC Graduate School, University of Amsterdam. Y.J.C. acknowledges the Manchester NIHR Biomedical Research Centre.

Reference List

1. Norman RM: Cerebellar hypoplasia in Werdnig-Hoffmann disease. Arch Dis Child 1961, 36:96-101.
2. Goutieres F, Aicardi J, Farkas E: Anterior horn cell disease associated with pontocerebellar hypoplasia in infants. J Neurol Neurosurg Psychiatry 1977, 40:370-378.
3. Barth PG: pontocerebellar hypoplasias. An overview of a group of inherited neurodegenerative disorders with foetal onset. Brain Dev 1993, 15:411-422.
4. Barth PG: pontocerebellar hypoplasia -- how many types? Eur J Paediatr Neurol 2000, 4:161-162.
5. Renbaum P, Kellerman E, Jaron R, Geiger D, Segel R, Lee M, King MC, Levy-Lahad E: Spinal muscular atrophy with pontocerebellar hypoplasia is caused by a mutation in the VRK1 gene. Am J Hum Genet 2009, 85:281-289.
6. Barth PG, Blennow G, Lenard HG, Begeer JH, van der Kley JM, Hanefeld F, Peters AC, Valk J: The syndrome of autosomal recessive pontocerebellar hypoplasia, microcephaly, and extrapyramidal dyskinesia (pontocerebellar hypoplasia type 2): compiled data from 10 pedigrees. Neurology 1995, 45:311-317.
7. Albrecht S, Schneider MC, Belmont J, Armstrong DL: Fatal infantile encephalopathy with olivopontocerebellar hypoplasia and micrencephaly. Report of three siblings. Acta Neuropathol 1993, 85:394-399.
8. Barth PG, Aronica E, de Vries L, Nikkels PG, Scheper W, Hoozemans JJ, Poll-The BT, Troost D: pontocerebellar hypoplasia type 2: a neuropathological update. Acta Neuropathol 2007, 114:373-386.
9. Budde BS, Namavar Y, Barth PG, Poll-The BT, Nurnberg G, Becker C, van Ruissen F, Weterman MAJ, Fluiter K, te Beek E et al.: tRNA splicing endonuclease mutations cause pontocerebellar hypoplasia. Nat Genet 2008, 40:1113-1118
10. Rajab A, Mochida GH, Hill A, Ganesh V, Bodell A, Riaz A, Grant PE, Shugart YY, Walsh CA: A novel form of pontocerebellar hypoplasia maps to chromosome 7q11-21. Neurology 2003, 60:1664-1667.
11. Durmaz B, Wollnik B, Cogulu O, Li Y, Tekgul H, Hazan F, Ozkinay F: pontocerebellar hypoplasia type III (CLAM): Extended phenotype and novel molecular findings. J Neurol 2009, 256:416-419.
12. Patel MS, Becker LE, Toi A, Armstrong DL, Chitayat D: Severe, fetal-onset form of

olivopontocerebellar hypoplasia in three sibs: pontocerebellar hypoplasia type 5? Am J Med Genet A 2006, 140:594-603.

13. Edvardson S, Shaag A, Kolesnikova O, Gomori JM, Tarassov I, Einbinder T, Saada A, Elpeleg O: Deleterious mutation in the mitochondrial arginyl-transfer RNA synthetase gene is associated with pontocerebellar hypoplasia. Am J Hum Genet 2007, 81:857-862.

14. Rankin J, Brown R, Dobyns WB, Harington J, Patel J, Quinn M, Brown G: pontocerebellar hypoplasia type 6: A British case with PEHO-like features. Am J Med Genet A 2010, 152A:2079-2084.

15. Roche AF, Mukherjee D, Guo SM, Moore WM. Head: Headcircumference reference data: birth to 18 years. Pediatrics 1987, 79:706-712

16. Denecke J, Kranz C, Kleist-Retzow JC, Bosse K, Herkenrath P, Debus O, Harms E, Marquardt T: Congenital disorder of glycosylation type Id: Clinical phenotype, molecular analysis, prenatal diagnosis, and glycosylation of foetal proteins. Pediat Res 2005, 58:248-253.

17. Scaglia F, Wong LJ, Vladutiu GD, Hunter JV: Predominant cerebellar volume loss as a neuroradiologic feature of pediatric respiratory chain defects. Am J Neuroradiol 2005, 26:1675-1680.

18. van de Kamp JM, Lefeber DJ, Ruijter GJ, Steggerda SJ, den Hollander NS, Willems SM, Matthijs G, Poorthuis BJ, Wevers RA: Congenital disorder of glycosylation type Ia presenting with hydrops foetalis. J Med Genet 2007, 44:277-280.

19. Najm J, Horn D, Wimplinger I, Golden JA, Chizhikov VV, Sudi J, Christian SL, Ullmann R, Kuechler A, Haas CA et al.: Mutations of CASK cause an X-linked brain malformation phenotype with microcephaly and hypoplasia of the brainstem and cerebellum. Nat Genet 2008, 40:1065-1067.

20. Somer M: Diagnostic criteria and genetics of the PEHO syndrome. J Med Genet 1993, 30:932-936.

21. Messerschmidt A, Brugger PC, Boltshauser E, Zoder G, Sterniste W, Birnbacher R, Prayer D: Disruption of cerebellar development: potential complication of extreme prematurity. AJNR Am J Neuroradiol 2005, 26:1659-1667.

22. Graham JM, Jr., Spencer AH, Grinberg I, Niesen CE, Platt LD, Maya M, Namavar Y, Baas F, Dobyns WB: Molecular and neuroimaging findings in pontocerebellar hypoplasia type 2 (pontocerebellar hypoplasia2): is prenatal diagnosis possible? Am J Med Genet A 2010, 152A:2268-2276.

23. Paushkin SV, Patel M, Furia BS, Peltz SW, Trotta CR: Identification of a human endonuclease complex reveals a link between tRNA splicing and pre-mRNA 3' end formation. Cell 2004, 117:311-321.

24. Seburn KL, Nangle La, Cox GA, Schimmel P, Burgess RW: An active dominant mutation of glycyl-tRNA synthetase causes neuropathy in a Charcot-Marie-Tooth 2D mouse model. Neuron 2006, 51:715-726

25. Scheper GC, van der Klok T, van Andel RJ, van Berkel CG, Sissler M, Smet J, Muravina TI, Serkov SV, Uziel G, Bugiani M et al.: Mitochondrial aspartyl-tRNA synthetase deficiency causes leukoencephalopathy with brain stem and spinal cord involvement and lactate elevation. Nat Genet 2007, 39:534-539.

26. Antonellis A, Green ED: The role of aminoacyl-tRNA synthetases in genetic diseases. Annu Rev Genomics Hum Genet 2008, 9:87-107.

27. Park SG, Schimmel P, Kim S: Aminoacyl tRNA synthetases and their connections to disease. Proc Natl Acad Sci U S A 2008, 105:11043-11049.

Supplementary Table 1. Unidentified variants.

Variant nr	Gene and region	Nucleotide change	Protein change
AMC-001	TSEN54 exon 1	c.3_8dup	p.E6_P7 dup
AMC-002	TSEN54 exon 7	c.568 G>A	p.V190M
AMC-003	TSEN54 intron 7	c.624-9G>A	-
AMC-004	TSEN54 exon 8	c.1039A>T	p.N347Y
AMC-005	TSEN54 exon 8	c.1120C>T	p.R374C
AMC-006	TSEN54 exon 8	c.1166A>C	p.Q389P
AMC-007	TSEN54 exon 11	c.1468C>T	p.R490W
AMC-008	TSEN54 3'UTR	*169T>C	n/a
AMC-009	TSEN2 5'UTR	c.-297C>T	n/a
AMC-010	TSEN2 5'UTR	c.-98_-96del	n/a
AMC-011	TSEN2 exon 2	c.108 A>G	p.E36E
AMC-012	TSEN2 exon 2	c.162G>A	p.A54A
AMC-013	TSEN2 intron 2	c.189+15C>T	n/a
AMC-014	TSEN2 intron 2	c.189+35G>A	n/a
AMC-015	TSEN2 intron 2	c.190-73A>G	n/a
AMC-016	TSEN2 intron 3	c.272-164G>T	n/a
AMC-017	TSEN2 intron 4	c.308+111T>C	n/a
AMC-018	TSEN2 exon 5	c.327G>A	p.E109E
AMC-019	TSEN2 exon 5	c.389A>C	p.K130T
AMC-020	TSEN2 intron 10	c.1249-34T>G	n/a
AMC-021	TSEN15 3'UTR	*30C>G	n/a
AMC-022	TSEN34 5'UTR	c.-98A>G	n/a
AMC-023	TSEN34 5'UTR	c.-5+72A>G	n/a
AMC-024	TSEN34 exon 2	c.62C>T	p.A21V
AMC-025	TSEN34 exon 2	c.99A>G	p.V33V
AMC-026	TSEN34 intron 4	c.746-60C>T	n/a
AMC-027	TSEN34 exon 5	c.835C>T	p.R279C
AMC-028	RARS2 intron 1	c.36+9C>A	n/a
AMC-029	RARS2 intron 3	c.213+48T>C	n/a
AMC-030	RARS2 exon 8	c.606C>T	p.L102L
AMC-031	RARS2 exon10	c.786T>C	p.Y262Y
AMC-032	RARS2 exon 13	c.1037C>T	p.T346I
AMC-033	RARS2 intron 14	c.1237+36dupA	n/a
AMC-034	RARS2 intron 17	c.1512-40_1512-39del	n/a
AMC-035	RARS2 intron 19	c.1651-51A>G	n/a

Appendix 1 - PCH consortium

Nathalie Van der Aa, Department of Medical Genetics, University and University Hospital Prins Boudewijnlaan 43, Edegem, Antwerp, Belgium. Willem F. M. Arts, Department of Paediatric Neurology, Erasmus Medical Center - Sophia Children's Hospital, P.O. Box 2060, 3000 CB Rotterdam, The Netherlands. Lesley C. Ades, Department of Clinical Genetics, The Children's Hospital at Westmead, Sydney Australia 2145, and Discipline of Paediatrics and Child Health, University of Sydney, Sydney Australia. Nadia Bahi-Buisson, Hopital Necker-Enfants Malades Universite Paris´Descartes Service de Neuropediatrie et Maladies Metaboliques, Paris, France. Roberta Battini, Department of Developmental Neuroscience, IRCCS Stella Maris, Calambrone, Pisa, Italy. Olaf Bodamer, Institute for Inherited Metabolic Diseases, Paracelsus Medical University and University Children's Hospital, Strubergasse 21, A-5020 Salzburg, Austria. Eugen Boltshauser, Department of Paediatric Neurology, Children's University Hospital, CH-8032 Zurich, Switzerland. Kym Boycott, Department of Genetics, Children's Hospital of Eastern Ontario, 401 Smyth Road, Ottawa, Ontario, K1H 8L1, Canada. Louise Brueton, West Midlands Regional Clinical Genetics service,Birmingham Womens Hospital, Edgbaston Birmingham, UK. Wim Brussel, Department of Pediatrics, Rijnstate Hospital, Wagnerlaan 55, 6815 AD Arnhem, The Netherlands. K. E. Chandler, GeneticMedicine, Manchester Academic Health Science Centre, Uni ersityof Manchester, Central Manchester University Hospitals NHS Foundation Trust, St. Mary's Hospital, Oxford Road, ManchesterM13 9WL, UK. Frances M. Cowan, Consultant/Hon. Senior Lecturer in Perinatal Neurology, Department of Paediatrics, Hammersmith Hospital, Imperial College London, DuCane Road, London W12 OHS, UK. Yanick Crow, Genetic Medicine, University of Manchester, Manchester Academic Health SciencCentre, Central Manchester Foundation Trust University Hospitals, Manchester, UK. Otfried Debus, Clemenshospital Childrens Hospital, Munster, Germany. Ercan Demir, Department of Pediatric Neurology, Gazi University, Ankara, Turkey, Gazi Universitesi T|p Fakultesi, Gazi Hastanesi, Cocuk Sagligi ve Hastaliklari ABD, Beşevler, Ankara, Turkey. Jacqueline Eason, Clinical Genetics Department, The Gables, Nottingham City Hospital Campus, Hucknall Road, Nottingham NG5 1PB, UK. Colin D. Ferrie, Department of Paediatric Neurology, Leeds General Infirmary, Leeds, UK. Richard B. Fisher, Consultant in Clinical Genetics, Northern Genetics Service, Teesside Genetics Unit, The James Cook University Hospital, Marton Road, Middlesbrough TS4 3BW, UK. Nicola Foulds, 1. Wessex Clinical Genetics Services, Southampton University Hospitals Trust, Southampton, UK. 2. Academic Unit of Genetic Medicine, Southampton University, Southampton, UK. Jeremy L. Freeman, Children's Neuroscience Centre, The Royal Children's Hospital Melbourne, 50 Flemington Road, Parkville, 3052, Victoria, Australia. Rob Gooskens, Rudolf Magnus Institute for Neuroscience, Department of Childneurology, University Medical Centre Utrecht, Lundlaan 6, 3584 EA Utrecht. Eugenio Grillo, Department of Neurology, Hospital Infantil Joana de Gusmao, Florianopolis, Santa Catarina, Brazil. Martin Haeussler, Fruehdiagnosezentrum Wuerzburg, Center for Social Pediatrics, University of Wuerzburg, Josef-Schneider-Strasse 2, 97080 Wuerzburg, Germany. Gerard Hageman, Department of Neurology, Medical Spectrum Twente, P.O. Box 50000, 7500 KA Enschede. Gerhard Hammersen, CNOPF'sche Kinderklinik, St. Johannis Muhlgasse 19, D-90419, Nurnberg, Germany. Denise Horn, Institute of Medical Genetics, Charite, University Medicineof Berlin, Augustenburger Platz 1, 13353 Berlin, Germany. ´Bertrand Isidor, Sevice de Genetique Medicale, CHU Nantes,Nantes. Marjo S. van der Knaap, Department of Child neurology,VU University Medical Center, De Boelelaan 1117, 1081 HVAmsterdam, The Netherlands. Wolfram Kress, Institute ofHuman Genetics, University of Wuerzburg, Biozentrum, AmHubland 97074 Wuerzburg, Germany. Peter M. Kroisel, Instituteof Human Genetics, Medical University of Graz, Harrachgasse 21, 8010 Graz, Austria. Marten Kyllerman, The Queen Silvia Children's Hospital, Gothenburg University, S-416 85 Goteborg, Sweden. A. M. A. Lachmeijer, Afdeling Klinische Genetica, VrijeUniversiteit medisch centrum, Polikiniek, Receptie D, De Boelelaan1117, 1081 HV, Amsterdam. Vincenzo Leuzzi, Department of Child Neurology and Psychiatry - La Sapienza Universita diRoma-Via dei Sabelli 108, 00141 Rome, Italy. Roelineke J.Lunsing, Department of Paediatric Neurology, University MedicalCentre Groningen, University of Groningen, Groningen, The Netherlands. George McGillivray, Murdoch Children's Research Institute, Royal Children's Hospital, Melbourne, Australia. Susanne Molmann, Ekenhoff 25, 49545 Tecklenburg. Francesco Muntoni, UCL Institute of Child Health and Great Ormond Street Hospital, Du Cane Road, London, UK. Andrea H. Nemeth, Churchill Hospital and University of Oxford, Churchill Drive, Headington, Oxford, OX37LJ. UK. Whitney Neufeld-Kaiser, University of Washington, Maternal Fetal Medicine and Medical Genetics, 1959 NE Pacific Street, Box 356159, Seattle, WA 98195-6159, USA. Onno van Nieuwenhuizen, Department of Child Neurology, Rudolf Magnus Institute for Neuroscience, Utrecht University, The Netherlands. Robert Ouvrier, Petre Foundation Professor of Paediatric Neurology, The University of Sydney and The Department of

Neurology, The Children's Hospital at Westmead, Hawkesbury Road, Westmead NSW 2145, Australia. Beatrix Palmafy, Bethesda Children Hospital, Department of Neurology Budapest Ilka u.57, 1043-Hungary. E.A.J. Peeters, Child Neurologist, Juliana Children Hospital, Sportlaan 600, 2566 MJ, The Hague, The Netherlands. Joanna J. Phillips, Division of Neuropathology, Department of Pathology, University of California, San Francisco, CA 94143, USA. Susan Price, Virtual Academic Unit, CDC, Northampton General Hospital, Northampton United Kingdom, NN1 5BD. Julia Rankin, Department of Clinical Genetics, Royal Devon and Exet NHS Foundation Trust (Heavitree), Gladstone Road, Exeter, X1´2ED, UK. Luc Regal, Pediatric Metabolic Center, University Hospital Leuven, Herestraat 49, 3000 Leuven, Belgium. J. F.de Rijk-van Andel, Department of Pediatric Neurology, AmphiaHospital location Langendijk, Langendijk 75, 4819 EV Breda The Netherlands. Filip Roelens, Child Neurology, H. Hart Hospital, Wilgenstraat 2, 8800 Roeselare Belgium. Joe C. Rutledge, University of Washington School of Medicine, Department of Laboratories, Seattle Children's Hospital, 4800 Sandpoint Way NE, Seattle, WA 98115 USA. Monique M. Ryan, Children's Neurosciences Centre, Royal Children's Hospital, Fleomington Road, Parkville, 3052 Victoria, Australia. Rainer Seidl,Department of Pediatrics, Division Neuropediatrics, Medical University Vienna, Waehringer Guertel 18-20, A-1090 Vienna, Austria. Nina C. Sellerer, Department of Biochemical Genetics, Dr von Hauner Children's Hospital Ludwig-Maximilians-University, Munich, Germany. Nora L. Shannon, Clinical GeneticsDepartment, The Gables, Nottingham City Hospital Campus, Hucknall Road, Nottingham NG5 1PB, UK. Deborah A. Sival, Department of Pediatrics, Beatrix Children's Hospital, University Medical Center Groningen University of Groningen, Hanzeplein 1, 9700RB, Groningen, The Netherlands. I. N. Snoeck,Department of Neuropediatrics, Haga Teaching Hospital/Juliana Children's Hospital, Sportlaan 600 2566 MJ, The Hague, The Netherlands. Rachel Straussberg, Sackler School of Medicine, TelAviv University, Tel Aviv, Israel. Marina A. J. Tijssen, Department of Neurology, Academic Medical Centre, University of Amsterdam, P.O. Box 22660, 1100 DD Amsterdam, The Netherlands. Patrick Verloo, Department of Child Neurology and Metabolic Diseases, University Hospital Ghent, Belgium. L. S. de Vries, Department Neonatology, Wilhelmina Children's Hospital, University Medical Centre, Utrecht, The Netherlands. David Wargowski, Director and Chief, Department of Pediatrics Clinic,Division of Genetics and Metabolism University of Wisconsin School of Medicine and Public Health, 1500 Highland AvenueMadison, Wisconsin 53705. Andrew N. Williams, Virtual Academic Unit, CDC, Northampton General Hospital, Northampton NN1 5BD, UK. Christian Windpassinger, Institute of Human Genetics, Medical University of Graz, Harrachgasse 21, 8010 Graz, Austria.

Reply: Mutations of TSEN and CASK genes are prevalent in pontocerebellar hypoplasias type 2 and 4

Yasmin Namavar, Peter G. Barth, Frank Baas & Bwee Tien Poll-The

Published in 2011 online in Brain
(doi:10.1093/brain/awr109).

Sir, Pontocerebellar Hypoplasia (PCH) type 2 caused by missense mutations in *TSEN54* is a distinct phenotype encompassing progressive microcephaly, swallowing problems and severe mental and motor impairments. None of the patients with PCH2 with missense mutations in *TSEN54* achieved unsupported walking or sitting, voluntary hand control was absent in almost all and higher visual functioning was absent or very limited. A common characteristic of PCH2 is the extrapyramidal dyskinesia, which often presents as severe chorea. In the more severe subtype PCH type 4 (due to compound heterozygosity of missense mutations plus nonsense or splice site mutations in *TSEN54*), the early lethality and prenatal symptoms like polyhydramnios, congenital contractures and the necessity for mechanical ventilation signify a more profound involvement. In both subtypes, MRI shows hypoplasia of the cerebellar hemispheres with relative sparing of the vermis and hypoplasia and atrophy of the ventral pons. Additionally, in PCH2 cases there is variable progressive atrophy of the cerebral cortex, delayed myelination and attenuation of the corpus callosum. In PCH4 impaired growth and maturation of the supratentorial parts of the brain results in increased pericerebral space and an immature aspect of the cerebral cortex. There is a remarkable coherence in the clinical presentation of cases with *TSEN54* mutations, resulting in either a PCH2 or a PCH4 phenotype, depending on the severity of their mutation (missense only in contrast to missense plus nonsense mutations).

CASK mutations result in a very broad phenotypical presentation [1,2,3]. The phenotypical spectrum reaches from FG syndrome (also known as Opitz-Kaveggia syndrome) with relative macrocephaly, congenital hypotonia, severe constipation and behavioural disturbances to a phenotype of mild mental retardation with relatively mild motor deficits and nystagmus to a phenotype of microcephaly, pontocerebellar hypoplasia, a simplified gyral pattern, sensorineural hearing loss and severe mental retardation. The *CASK* gene is located on the X-chromosome; therefore hemizygous missense mutations in boys are less severe than nonsense mutations, with even early lethality in these boys (prenatal or neonatal). Nonsense mutations in girls are always *de novo* with a severe disease course as a consequence [1]. The hemizygous missense mutation, p.R28L in *CASK* results in FG syndrome in one Italian family, mothers of the affected males are healthy or only have mitigated clinical features [2]. In all the published cases with a *CASK* mutation, the corpus callosum is normal in size and shape [4].

The findings of Valayannopoulus *et al.* [5] support our findings that the common (p.A307S) mutation in *TSEN54* (identified in three patients) is associated with a "dragonfly-like" cerebellar pattern on MRI [6]. Additionally the authors report three girls with *de novo* nonsense *CASK* mutations. Two of them had a butterfly-like cerebellar phenotype and one (Patient 8) displayed a dragonfly-like cerebellar pattern on MRI. This important finding shows the possibility of *CASK* involvement in the cases where we could not identify a mutation [6]. By any means, this requires further investigation. On closer examination the phenotypical overlap between *TSEN54* and

CASK cases is especially present in neonates and infants with *TSEN54* mutations in which cerebral atrophy is still not apparent. The authors propose the absence of optic atrophy as a characteristic difference, as this is common in *CASK* carriers but absent in patients with *TSEN54* mutations [1]. Also it would be of interest to know whether the cases with a *CASK* mutation presented by Valayannopoulus and colleagues [5] suffered from sensorineural hearing loss, as this feature is also described in *CASK* carriers and absent in *TSEN54* carriers [1]. Another characteristic that can help in distinguishing between *CASK* and *TSEN54* mutations is the number of complexity gyri, reduction of those gyri is not observed in the latter, but has been observed in patients with *CASK* mutations [1]. Finally there is the "outcome" as reported by Valayannopoulus *et al.* [5] and the motor development in particular, that seems to be better in *CASK* carriers; whereas all three *CASK* cases were able to stand unsupported none of the *TSEN54* cases showed such a development [6].

Still, although it is tempting to do, we plead for prudence in making a diagnostic algorithm. Next to *CASK*, there are several other genes to consider: e.g *RARS2* and *VRK1* are associated with PCH type 6 and an atypical presentation of PCH type 1, respectively [7,8]. *MED17* and *SEPSECS* mutations can give a phenotype of cerebello-cerebral atrophy, which could potentially be difficult to distinguish from PCH. Therefore it remains important to carefully examine patients, both clinically and neuroradiologically [9,10]. One thing that perhaps can help in making a distinction between patients with *CASK* mutations and patients with *TSEN54* mutations is that the underlying disease mechanism in patients with *CASK* mutations is a neuronal migration deficit while *TSEN*-mediated PCH is a progressive neurodegenerative disorder [11]. The *CASK* gene is encoding for a calcium/calmodulin-dependent serine protein kinase that is involved in signaling in both, pre- and post synapses, and is involved in the interaction with TBR1 (T-box brain gene 1) in such a way that it enhances *TBR1* transcription. TBR1 is involved in regulating the expression of the extracellular matrix protein Reelin (RELN) [12]. Reelin is essential for normal neuronal migration, since *RELN* mutations are responsible for lissenencephaly and pontocerebellar hypoplasia [13]. The better clinical outcome of *CASK* mutation carriers supports the hypothesis that *CASK* is solely a developmental disorder, whereas *TSEN54*-mediated PCH is a neurodegenerative disorder with cell death, resulting in progressive neuronal atrophy and no development [14].

Nowadays the list of genes responsible for various types of pontocerebellar hypoplasia and related disorders is rapidly growing. With careful clinical and neuroradiological examination and testing of several genes it will be hopefully possible to make a molecular diagnosis in most cases with such a phenotype.

Reference List

1. Najm J, Horn D, Wimplinger I, Golden JA, Chizhikov VV, Sudi J, Christian SL, Ullmann R, Kuechler A, Haas CA et al.: Mutations of CASK cause an X-linked brain malformation phenotype with microcephaly and hypoplasia of the brainstem and cerebellum. Nat Genet 2008, 40:1065-1067.

2. Piluso G, D'Amico F, Saccone V, Bismuto E, Rotundo IL, Di DM, Aurino S, Schwartz CE, Neri G, Nigro V: A missense mutation in CASK causes FG syndrome in an Italian family. Am J Hum Genet 2009, 84:162-177.

3. Hackett A, Tarpey PS, Licata A, Cox J, Whibley A, Boyle J, Rogers C, Grigg J, Partington M, Stevenson RE et al.: CASK mutations are frequent in males and cause X-linked nystagmus and variable XLMR phenotypes. Eur J Hum Genet 2010, 18:544-552.

4. Takanashi J, Arai H, Nabatame S, Hirai S, Hayashi S, Inazawa J, Okamoto N, Barkovich AJ: Neuroradiologic features of CASK mutations. AJNR Am J Neuroradiol 2010, 31:1619-1622.

5. Valayannopoulos V, Michot C, Rodriguez D, Hubert L, Saillour Y, Labrune P, de LJ, Brunelle F, Amiel J, Lyonnet S et al.: Mutations of TSEN and CASK genes are prevalent in pontocerebellar hypoplasias type 2 and 4. Brain 2011.

6. Namavar Y, Barth PG, Kasher PR, van Ruissen F., Brockmann K, Bernert G, Writzl K, Ventura K, Cheng EY, Ferriero DM et al.: Clinical, neuroradiological and genetic findings in pontocerebellar hypoplasia. Brain 2011, 134:143-156.

7. Edvardson S, Shaag A, Kolesnikova O, Gomori JM, Tarassov I, Einbinder T, Saada A, Elpeleg O: Deleterious mutation in the mitochondrial arginyl-transfer RNA synthetase gene is associated with pontocerebellar hypoplasia. Am J Hum Genet 2007, 81:857-862.

8. Renbaum P, Kellerman E, Jaron R, Geiger D, Segel R, Lee M, King MC, Levy-Lahad E: Spinal muscular atrophy with pontocerebellar hypoplasia is caused by a mutation in the VRK1 gene. Am J Hum Genet 2009, 85:281-289.

9. Agamy O, Ben ZB, Lev D, Marcus B, Fine D, Su D, Narkis G, Ofir R, Hoffmann C, Leshinsky-Silver E et al.: Mutations disrupting selenocysteine formation cause progressive cerebello-cerebral atrophy. Am J Hum Genet 2010, 87:538-544.

10. Kaufmann R, Straussberg R, Mandel H, Fattal-Valevski A, Ben-Zeev B, Naamati A, Shaag A, Zenvirt S, Konen O, Mimouni-Bloch A et al.: Infantile cerebral and cerebellar atrophy is associated with a mutation in the MED17 subunit of the transcription preinitiation mediator complex. Am J Hum Genet 2010, 87:667-670.

11. Barth PG, Vrensen GF, Uylings HB, Oorthuys JW, Stam FC: Inherited syndrome of microcephaly, dyskinesia and pontocerebellar hypoplasia: a systemic atrophy with early onset. J Neurol Sci 1990, 97:25-42.

12. Hsueh YP: The role of the MAGUK protein CASK in neural development and synaptic function. Curr Med Chem 2006, 13:1915-1927.

13. Hong SE, Shugart YY, Huang DT, Shahwan SA, Grant PE, Hourihane JO, Martin ND, Walsh CA: Autosomal recessive lissencephaly with cerebellar hypoplasia is associated with human RELN mutations. Nat Genet 2000, 26:93-96.

14. Kasher PR, Namavar Y, van Tijn P, Fluiter K, Sizarov A, Kamermans M, Grierson AJ, Zivkovic D, Baas F: Impairment of the tRNA-splicing endonuclease subunit 54 (tsen54) gene causes neurological abnormalities and larval death in zebrafish models of pontocerebellar hypoplasia. Hum Mol Genet 2011, 20:1574-1584.

Chapter 4

TSEN54 mutations cause pontocerebellar hypoplasia type 5

Yasmin Namavar, David Chitayat, Peter G. Barth,
Fred van Ruissen, Marit B. de Wissel, Bwee Tien Poll-The,
Rachel Silver & Frank Baas.

Published in 2011 in the European Journal of Human Genetics 19: 724-726.

Abstract

Pontocerebellar hypoplasia (PCH) is a group of autosomal recessive neurodegenerative disorders characterised by prenatal onset of stunted brain growth and progressive atrophy predominantly affecting cerebellum, pons, and olivary nuclei, and to a lesser extent also the cerebral cortex. Six subtypes (PCH1-6) were described and genes for four types (PCH1, 2, 4 and 6) were identified. Mutations in the tRNA splicing endonuclease subunit (*TSEN*) genes 54, 2 and 34 are found in PCH2 and PCH4. One family with severe prenatal onset of PCH has been the only representative of PCH5 published so far and the molecular genetic status of PCH5 has not been ascertained until now. We screened the previously reported PCH5 family for mutations in the *TSEN54* gene. The PCH5 patient was found to be the result of compound heterozygosity for the common *TSEN54* mutation (p.A307S) plus a novel splice site mutation. The mutations associated with PCH5 are similar to what has been reported in PCH4. Thus PCH5, PCH4 and PCH2 represent a spectrum of clinical manifestations caused by different mutations in the *TSEN* genes. We therefore propose to classify PCH2, PCH4 and PCH5 as *TSEN* mutation spectrum disorders.

Introduction

Pontocerebellar hypoplasias (PCHs) are a group of lethal autosomal recessive disorders characterised by prenatal onset of stunted growth and atrophy of the cerebellum, pons, and olivary nuclei. Six subtypes have been identified so far, each with a distinct pathology and clinical presentation. Microcephaly and delayed development are features of all subtypes. Life expectancy is difficult to predict as survival ranges from early death (1 day) to adult death [1]. Mutations in different genes have been identified in four of them; PCH1, PCH2, PCH4 and PCH6 [1-4].

PCH2 is the most common subtype and is characterised by jitteriness and the development of dyskinesia and choreatic movements. Other criteria include swallowing problems, central visual failure and the absence of primary optic atrophy. Patients usually die during childhood. Mutations in genes encoding the tRNA splicing endonuclease complex (TSEN) are responsible for PCH2. In most cases an alanine to serine substitution (p.A307S) in *TSEN54* is found, whereas rare cases show mutations in *TSEN2* and *TSEN34* [1,3,5].

PCH4 presents a more severe form of PCH including hypertonia and severe clonus and usually more pronounced cerebellar hypoplasia (see Table 1). Nine cases of genetically confirmed PCH4 have been described so far, of which eight were compound heterozygote for a nonsense mutation or a splice site mutation and the common p.A307S missense mutation in the *TSEN54* gene [1]. One case carried a rare missense mutations for *TSEN54* on one allele (p.S93P) in addition to homozygozity for the common p.A307S mutation. Thus, a reduced amount of, or aberrant, TSEN54 protein is present in PCH4 patients, resulting in a more severe phenotype in comparison with PCH2. In seven of eight PCH4 cases, the Magnetic Resonance Imaging (MRI) scans showed immaturity of the cerebral cortex with underdeveloped cerebral hemispheres and increased extracerebral cerebrospinal fluid volume. The cerebellar pathology in PCH4 is also more severe compared to PCH2. In addition to the severely affected cerebellar hemispheres, six out of eight cases showed mild or severe atrophy of the cerebellar vermis [1].

In 2006, Patel *et al.* presented a family with a new PCH type identified as PCH5, with foetal seizures and on autopsy marked degeneration of the cerebellar vermis [6]. The parents were healthy and non-consanguineous, with three children affected with severe olivopontocerebellar hypoplasia (OPCH), two healthy siblings and a miscarriage at 12 weeks gestation. The pedigree was consistent with an autosomal recessive mode of inheritance. All affected cases suffered from intra-uterine seizure-like movements, recognised by the mother as rhythmic movements and confirmed on foetal ultrasound. Patient 1 died from apnea at the age of 3 days after withdrawal of care. She suffered from generalised hypertonia, sustained clonus and respiratory distress. The pregnancies with patient 2 and 3 were terminated at 27 and 20 weeks, respectively, following the

finding of clearly visible cerebellar hypoplasia on ultrasound. Autopsies done on these three affected cases revealed immature neurons in the pons, with gliosis and apoptosis in patient 1 and 2 and a C-shaped inferior olive present in all cases [6]. The cerebellar vermis and hemispheres were severely reduced. The vermis showed absence and immaturity of Purkinje cells and distinct focal absence of the external granule cell layer. Based on the clinical and pathological manifestations Patel *et al.* proposed that this family constitute a new subtype of PCH, PCH5 [6].

Methods

To test whether PCH5 is part of the *TSEN* mutation spectrum, we tested patient 1 from the report of Patel *et al.* for *TSEN54* mutations with parental consent [6]. PCR products were sequenced using the Big Dye Terminator Sequencing kit and ABI PRISM 3730XL DNA Analyser (Applied Biosystems, Foster City, CA, USA). Codon Code Software version 3.5.6. (CodonCode Corporation, Dedham, MA, USA) was used to analyse the sequenced samples.

Results and discussion

Analysis of patient 1 and his parents showed that the index case was a compound heterozygote for two *TSEN54* mutations. One allele carried the common PCH associated mutation c.919G>T, p.A307S and the other a splice site mutation; c.468+2T>C. This variant was not found in 176 control chromosomes. Homozygosity for the p.A307S *TSEN54* mutation results in PCH2 [3]. The c.468+2T>C is located in the donor splice site of intron 5, which makes skipping of exon 5 likely. This was confirmed with Alamut software, this tool uses four different splice site prediction algorithms (www.interactive-biosoftware.com/alamut.html). The character of these mutations is similar to those reported in PCH4. Comparing the clinical and pathological features of PCH5 with a genetically confirmed group of PCH4 patients showed that the findings are similar [1]. For example the inferior olivary nuclei in the PCH5 family, reported by Patel *et al.* showed a C-shaped structure similar to what is reported in PCH4 [6-9]. The absence of the external granular layer in the vermis and cerebellar hemispheres described in PCH5 is focal and is similar to the segmental loss of cerebellar cortex typically seen in PCH2 and PCH4 [8]. In the PCH5 cases, the vermis was noted to be more affected than the hemispheres; however, since the vermal cortex is only relatively spared in PCH4 cases there is no essential difference. In our recent study, six out of eight PCH4 cases, on whom brain MRI was available, also showed mild or severe atrophy of the cerebellar vermal folia [1]. The prenatal seizure-like activity observed in the PCH5 cases is similar to the severe neonatal clonus seen in PCH4 [9]. Although milder, the clinical findings in PCH2 are similar to what is reported in PCH4 and PCH5 [10]. Early postnatal lethality due to hypoventilation, as observed in the

Table 1. *TSEN*-mutation-spectrum and clinical manifestations.

PCH subtype	**MIM**	**Distinguishing clinical features**	**Lethality**	**Pathology of cerebellum, olivary nucleus, pons**	**Gene**	**Ref.**
PCH2	277470, 612389, 612390	*Neonatal period*: clonus, impaired swallowing. *Infancy and later*: chorea, variable spastic pareses; progressive microcephaly. *MRI*: variable neocortical atrophy, pontocerebellar hypoplasia.	Infancy and childhood. Adolescence reached in some cases.	*Cerebellar hypoplasia:* hemispheres >> vermis. Segmental degeneration of cortex. Fragmentation of cerebellar dentate nucleus. *Olivary nucleus:* neuron loss and decreased folding. *Pons:* progressive loss of ventral nuclei and transverse fibers.	*TSEN54,* p.A307S/A307S most common. Rarely: Other *TSEN54* missense mutations. *TSEN2, TSEN34* mutations.	[1,3,8,10,11]
PCH4	225753	*Neonatal period*: hypertonia, severe clonus, polyhydramnios and/or contractures; primary hypoventilation. *MRI*: delayed neocortical maturation, pontocerebellar hypoplasia; micrencephaly on autopsy.	Early postnatal death from apnea	*Cerebellar hypoplasia:* hemispheres >> vermis, areas of stunted or absent folial development. Cerebellar dentate nucleus present as tiny remnants *Olivary nucleus:* absent folding and gliosis. *Pons:* loss of ventral nuclei and transverse fibers.	*TSEN54* Compound heterozygosity for p.A307S plus nonsense or splice site mutations.	[1,3,7-9]
PCH5	611523	*Prenatal/neonatal period*: clonus or seizures. *Neonatal period*: persistent clonus. Micrencephaly and pontocerebellar hypoplasia on autopsy	Early postnatal death from apnea	*Cerebellar hypoplasia:* cortical involvement as in PCH4, but vermal cortex more extensively affected than hemispheric cortex; subtotal loss of cerebellar dentate nucleus. *Olivary nucleus:* absent folding. *Pons:* loss of ventral nuclei and transverse fibers.	*TSEN54* Compound heterozygosity for p.A307S plus splice site mutation.	[6] this paper.

firstborn of the PCH5 family, is also commonly observed in PCH4 [1].

Thus, our molecular genetic findings and the phenotype in PCH5 are similar to that of PCH4. Since PCH2 is also caused by mutations in one of the TSEN subunits, we propose that PCH2, PCH4 and PCH5 will be united as a spectrum of clinical manifestations caused by different mutations in the *TSEN* genes (Table 1). We, therefore, propose to reassign PCH2, PCH4 and PCH5 as TSENopathies.

Acknowledgements

Financial support was kindly provided by the Hersenstichting Nederland KS2009(1)-81.

Reference List

1. Namavar Y, Barth PG, Kasher PR, van Ruissen F., Brockmann K, Bernert G, Writzl K, Ventura K, Cheng EY, Ferriero DM et al.: Clinical, neuroradiological and genetic findings in pontocerebellar hypoplasia. Brain 2011, 134:143-156.

2. Edvardson S, Shaag A, Kolesnikova O, Gomori JM, Tarassov I, Einbinder T, Saada A, Elpeleg O: Deleterious mutation in the mitochondrial arginyl-transfer RNA synthetase gene is associated with pontocerebellar hypoplasia. Am J Hum Genet 2007, 81:857-862.

3. Budde BS, Namavar Y, Barth PG, Poll-The BT, Nurnberg G, Becker C, van Ruissen F, Weterman MAJ, Fluiter K, te Beek E et al.: tRNA splicing endonuclease mutations cause pontocerebellar hypoplasia. Nat Genet 2008, 40:1113-1118.

4. Renbaum P, Kellerman E, Jaron R, Geiger D, Segel R, Lee M, King MC, Levy-Lahad E: Spinal muscular atrophy with pontocerebellar hypoplasia is caused by a mutation in the VRK1 gene. Am J Hum Genet 2009, 85:281-289.

5. Cassandrini D, Biancheri R, Tessa A, Di RM, Di CM, Bruno C, Denora PS, Sartori S, Rossi A, Nozza P et al.: Pontocerebellar hypoplasia: clinical, pathologic, and genetic studies. Neurology 2010, 75:1459-1464.

6. Patel MS, Becker LE, Toi A, Armstrong DL, Chitayat D: Severe, fetal-onset form of olivopontocerebellar hypoplasia in three sibs: PCH type 5? Am J Med Genet A 2006, 140:594-603.

7. Albrecht S, Schneider MC, Belmont J, Armstrong DL: Fatal infantile encephalopathy with olivopontocerebellar hypoplasia and micrencephaly. Report of three siblings. Acta Neuropathol 1993, 85:394-399.

8. Barth PG, Aronica E, de Vries L, Nikkels PG, Scheper W, Hoozemans JJ, Poll-The BT, Troost D: Pontocerebellar hypoplasia type 2: a neuropathological update. Acta Neuropathol 2007, 114:373-386.

9. Chaves-Vischer V, Pizzolato GP, Hanquinet S, Maret A, Bottani A, Haenggeli CA: Early fatal pontocerebellar hypoplasia in premature twin sisters. Eur J Paediatr Neurol 2000, 4:171-176.

10. Barth PG, Blennow G, Lenard HG, Begeer JH, van der Kley JM, Hanefeld F, Peters AC, Valk J: The syndrome of autosomal recessive pontocerebellar hypoplasia, microcephaly, and extrapyramidal dyskinesia (pontocerebellar hypoplasia type 2): compiled data from 10

pedigrees. Neurology 1995, 45:311-317.

11. Steinlin M, Klein A, Haas-Lude K, Zafeiriou D, Strozzi S, Muller T, Gubser-Mercati D, Schmitt MT, Krageloh-Mann I, Boltshauser E: Pontocerebellar hypoplasia type 2: variability in clinical and imaging findings. Eur J Paediatr Neurol 2007, 11:146-152.

Chapter 5

Impairment of the tRNA splicing endonuclease subunit 54 gene causes neurological abnormalities and larval death in zebrafish models of pontocerebellar hypoplasia

Paul R Kasher, Yasmin Namavar, Paula van Tijn, Kees Fluiter, Aleksander Sizarov, Maarten Kamermans, Andrew J Grierson, Danica Zivkovic & Frank Baas.

Published in 2011 in Human Molecular Genetics 20(8): 1574-1584.

Abstract

Pontocerebellar hypoplasia (PCH) represents a group (PCH1-6) of neurodegenerative autosomal recessive disorders characterised by hypoplasia and/or atrophy of the cerebellum, hypoplasia of the ventral pons, progressive microcephaly and variable neocortical atrophy. The majority of PCH2 and PCH4 cases are caused by mutations in the *TSEN54* gene; one of the four subunits comprising the tRNA splicing endonuclease (TSEN) complex. We hypothesised that *TSEN54* mutations act through a loss of function mechanism. At 8 weeks of gestation, human *TSEN54* is expressed ubiquitously in the brain, yet strong expression is seen within the telencephalon and metencephalon. Comparable expression patterns for *tsen54* are observed in zebrafish embryos. Morpholino (MO) knockdown of *tsen54* in zebrafish embryos results in loss of structural definition in the brain. This phenotype was partially rescued by co-injecting the MO with human *TSEN54* mRNA. A developmental patterning defect was not associated with *tsen54* knockdown; however, an increase in cell death within the brain was observed, thus bearing resemblance to PCH pathophysiology. Additionally, *N*-methyl-*N*-nitrosourea mutant zebrafish homozygous for a *tsen54* premature stop-codon mutation die within 9 days post-fertilization. To determine whether a common disease pathway exists between *TSEN54* and other PCH-related genes, we also monitored the effects of mitochondrial arginyl-tRNA synthetase (*rars2*; PCH1 and PCH6) knockdown in zebrafish. Comparable brain phenotypes were observed following the inhibition of both genes. These data strongly support the hypothesis that *TSEN54* mutations cause PCH through a loss of function mechanism. Also we suggest that a common disease pathway may exist between *TSEN54*- and *RARS2*-related PCH, which may involve a tRNA processing-related mechanism.

Introduction

Pontocerebellar hypoplasia (PCH) represents a group of neurodegenerative autosomal recessive disorders characterised by severe mental and motor impairments. The disease is associated with prenatal onset, hypoplasia/atrophy of the cerebellum, hypoplasia of the ventral pons, progressive microcephaly and variable neocortical atrophy. The median life expectancy is 50 months [1]; however, in rare cases, the most severe forms can lead to fatality during early post-natal periods. To date, six subtypes of PCH (PCH1-6) have been distinguished based on varying clinical and pathological features [1-6].

Mutations in three of the four subunit genes comprising the tRNA splicing endonuclease (TSEN) complex are responsible for PCH2 and PCH4 [1,2]. The TSEN complex is a heterotetramic enzyme comprised of two structural subunits, TSEN54 and TSEN15, and two catalytic subunits, TSEN2 and TSEN34 [7,8]. Mutations in the *TSEN54* subunit gene are the most frequent cause of PCH2 and PCH4, and a common mutation (p.A307S) has been identified in the majority of patients. A homozygous p.A307S mutation is strongly associated with a PCH2 phenotype. The p.A307S mutation occurring compound heterozygous with a *TSEN54* null allele is associated with a severe PCH4 phenotype [1]. Other less common *TSEN54* mutations, as well as rare mutations occurring in the *TSEN2* and *TSEN34* subunit genes have also been identified in PCH2 and PCH4 cases [1,2].

tRNAs play an essential role in protein synthesis where the anticodon of a mature tRNA molecule recognises and interacts with the codon displayed by the mRNA. Through the activity of the ribosome, this process allows condensation of the tRNA-specific amino acid with the peptide chain on the adjacent tRNA [9]. Part of the maturation process is the removal of an intronic sequence that exists within the anticodon loop of some tRNA genes. Splicing of the intron is performed through a composite active site of the TSEN complex [8]. In humans, only 6.2% of tRNA genes contain an intron and therefore require TSEN function for maturation and exposure of the anticodon, necessary for downstream translation. Multiple genes exist for each tRNA and in some circumstances the vast majority or all tRNA genes for a particular codon are intron-containing. For example, in humans, 13 of the 14 genes encoding tRNA-Tyr (GTA) contain an intron. Therefore, a defective TSEN complex is likely to lead to a shortage of tRNA Tyrosine. Other examples exist including tRNA-Ile (TAT), tRNA-Leu (CAA) and tRNA-Arg (TCT). More details can be viewed at http://lowelab.ucsc.edu/GtRNAdb/.

In most cases, PCH4 patients, who are more severely affected than PCH2 patients, have a null allele and a missense mutation in the *TSEN54* subunit gene [1]. This genotype-phenotype observation supports a hypothesis for a loss of TSEN function in PCH2 and PCH4 pathophysiology. The TSEN complex is not only involved in tRNA

splicing. It also plays a role in mRNA 3' end formation [7]. Therefore, it is possible that other functions of the TSEN complex may play a role in the disease pathogenesis of PCH2 and PCH4 cases.

How mutations in a gene involved with tRNA splicing and protein synthesis can lead to a brain-specific defect is unclear. *TSEN54* is expressed throughout the body; however, there are differences in expression levels between various tissues (http://www.genecards.org/cgi-bin/carddisp.pl?gene=TSEN54& search=tsen54).
Strong *TSEN54* mRNA expression has been observed in neuronal populations in the developing cerebellum, pons and olivary nuclei at 23 weeks of gestation [2]. This and the selective degeneration in PCH could suggest that TSEN activity is required at high levels in the brain structures affected in the disease. At 23 weeks of gestation, the brain has already significantly increased in volume and is well established neuroanatomically [10]. Neonatal ultrasound analysis in PCH2 patients reveals that the cerebellum develops as normal to gestation week 29; however, from gestation week 31, cerebellar hypoplasia can be observed [11]. In addition, cell death in the pons has been reported in PCH patients at low levels following pathological examination [5]. It is likely that high levels of degeneration are present during the time course of disease; however, most cells will have degenerated at the time of death and are thus unavailable for post-mortem analysis.

As PCH is a rare and lethal neurodegenerative disorder, patient material is scarce. To further understand the role of TSEN in the pathophysiology of PCH, a disease model is required. Zebrafish are now a well-established tool used to model various neurodegenerative disorders [12]. In this current study, we have utilised two separate genetic approaches to produce zebrafish models of *TSEN54*-related PCH. These include an antisense morpholino (MO) oligonucleotide-induced knockdown of *tsen54* and also an *N*-methyl-*N*-nitrosourea (ENU) mutagenesis strategy to produce a zebrafish strain harbouring a *tsen54* premature stopcodon mutation. Here, we show that the knockdown of *tsen54* results in brain hypoplasia and loss of structural definition in the brain, which is associated with increased cell death but not a developmental patterning defect, whereas genetic knockout of *tsen54* is lethal. Additionally, the knockdown of the mitochondrial arginyl-tRNA synthetase *(rars2*) gene, (*RARS2* mutations cause PCH1 and PCH6) [1,4,13] results in a phenotype that is comparable with *tsen54* depletion. Using these novel disease models of PCH, we provide the first evidence in an experimental model that *TSEN54* mutations act through a loss of function mechanism and that a common disease pathway may exist between PCH subtypes due to either *TSEN54* or *RARS2* mutations.

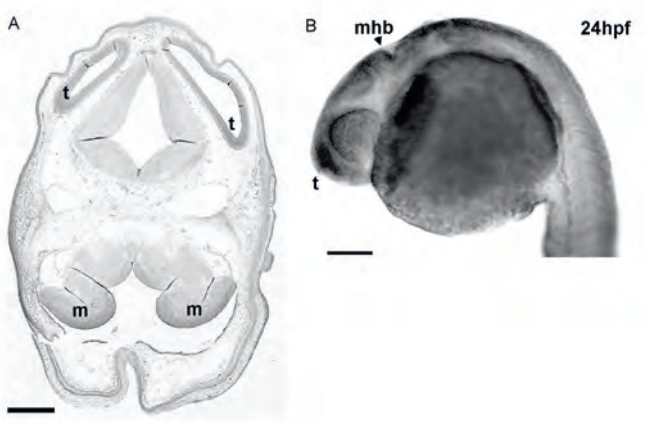

Figure 1. *TSEN54* expression is ubiquitous but strong in the brain in human and zebrafish early stages of neurodevelopment. (a) *TSEN54 in situ* hybridization within transverse section of a human foetal brain at 8 weeks prenatal age. *TSEN54* mRNA is widely expressed throughout brain and head tissue, but strongly expressed in the developing metancephalon (m) and telencephalon (t). Scale bar = 1mm. (b) Lateral view of *tsen54* whole-mount *in situ* hybridization in zebrafish embryo. Ubiquitous *tsen54* mRNA expression pattern is observed at 24 hpf in zebrafish embryos, with the strongest expression observed within the brain, especially the telencephalon (t) and mid-hindbrain boundary (mhb). Scale bar = 200µm. For colour figure see page 169.

Results

TSEN54 expression during early development in human and zebrafish

To examine *TSEN54* expression during early brain development, we performed *in situ* hybridization on 8-week-old human foetal brain sections using *TSEN54*-specific locked nucleic acid/2'-O-methyl RNA (LNA/2OME) probes. *TSEN54* mRNA is expressed throughout the brain at this early stage, with high levels of expression observed within the developing telencephalon and metencephalon (Fig. 1a). During normal development, the metencephalon later forms the pons and cerebellum [14]. Analysis of other tissues shows relatively high *TSEN54* expression in spinal cord and liver, whereas expression in other tissues was low (Suppl. Fig. 1). We next examined the expression pattern of zebrafish *tsen54* in embryos at 24 h post-fertilization (hpf). The zebrafish *TSEN54* orthologue (also known as zgc: 109927; accession number: NM_001020529) shares 46% identity to the human gene. As shown in Figure 1b, *tsen54* expression is ubiquitous, with strong expression in the brain within the telencephalon and midhindbrain boundary (MHB). *tsen54* is also expressed ubiquitously during early embryogenesis in zebrafish as observed from the 8-cell stage to the somite stages (Suppl. Fig. 2).

MO knockdown of *tsen54* causes loss of structural integrity in the zebrafish brain

As *TSEN54*-related PCH is inherited in an autosomal recessive manner, the biological mechanism underlying the disease is likely to be associated with a loss of TSEN54 function. To test this hypothesis in a model system, we were interested in monitoring the effects of knocking down the zebrafish *tsen54* gene using an antisense MO oligonucleotide approach. In comparison to wild-type (WT) un-injected (Fig. 2a) and control MO (CoMO)-injected embryos (Fig. 2b) at 24 hpf, injection of 2.5ng *tsen54* translation blocking (ATG) MO (Fig. 2c) resulted in abnormalities within the head including brain hypoplasia and loss of structural integrity inside the brain. Clear structural definition of the MHB (denoted by an asterisk) was apparent in the control embryos (Fig. 2a,b); however, this structure appeared aberrant in *tsen54* morphants (Fig. 2c,d). In zebrafish embryos, the MHB is a key structure involved with the neuronal migration and the development of the cerebellum [15]. To exclude the possibility that the effect was due to a nonspecific effect and to confirm specific targeting of the MO [16], we designed a second *tsen54* MO that targeted the exon 8 splice donor site of the *tsen54* gene. As shown in Figure 2d, we observe comparable brain hypoplasia and reduced structural definition in splice-site morphants. Reverse transcriptase-polymerase chain reaction (RT-PCR) of cDNA synthesised from WT, CoMO and splice-site morphant embryos confirmed abnormal splicing of the *tsen54* gene in the morphants (Fig. 2g). To further confirm that the phenotype was directly attributable to the knockdown of *tsen54*, we attempted to rescue the brain phenotype associated with *tsen54* depletion by co-injecting the ATG MO with human *TSEN54* mRNA. As shown in Figure 2e, injection of 233pg human *TSEN54* mRNA alone produced no effects upon brain structure. Co-injection of *tsen54* ATG MO and human *TSEN54* mRNA resulted in a partial rescue of the brain phenotype observed with MO only (Fig. 2f). Co-injected embryos display generally milder brain hypoplasia and more clearly defined brain structure when compared with ATG alone (Fig. 2c). We next quantified the proportion of brain phenotypes associated with each treatment at 24 hpf (Fig. 2h). Brain phenotypes were classified as either normal (appeared as WT), mild (slight brain hypoplasia, slight reduction in structural definition in the brain) or severe (severe brain hypoplasia, complete loss of brain structural definition). As expected, predominantly normal brain phenotypes were associated with both control groups (WT un-injected, human *TSEN54* mRNA only). Knockdown of *tsen54* with the ATG MO was associated with a mostly severe brain phenotype (76%), although mild (13%) and normal (11%) brain phenotypes were also observed to a lesser extent. Co-injection of the ATG MO with human *TSEN54* mRNA resulted in a striking reduction in the proportion of embryos displaying a severe brain phenotype (8%) and a shift to a predominantly mild (67%) brain phenotype. Indeed, the percentage of normal brain phenotypes also increased (25%) within the rescue group. Therefore, human TSEN54 is capable of partially rescuing the brain phenotype associated with the loss of *tsen54* translation, thus confirming specific targeting of the MO.

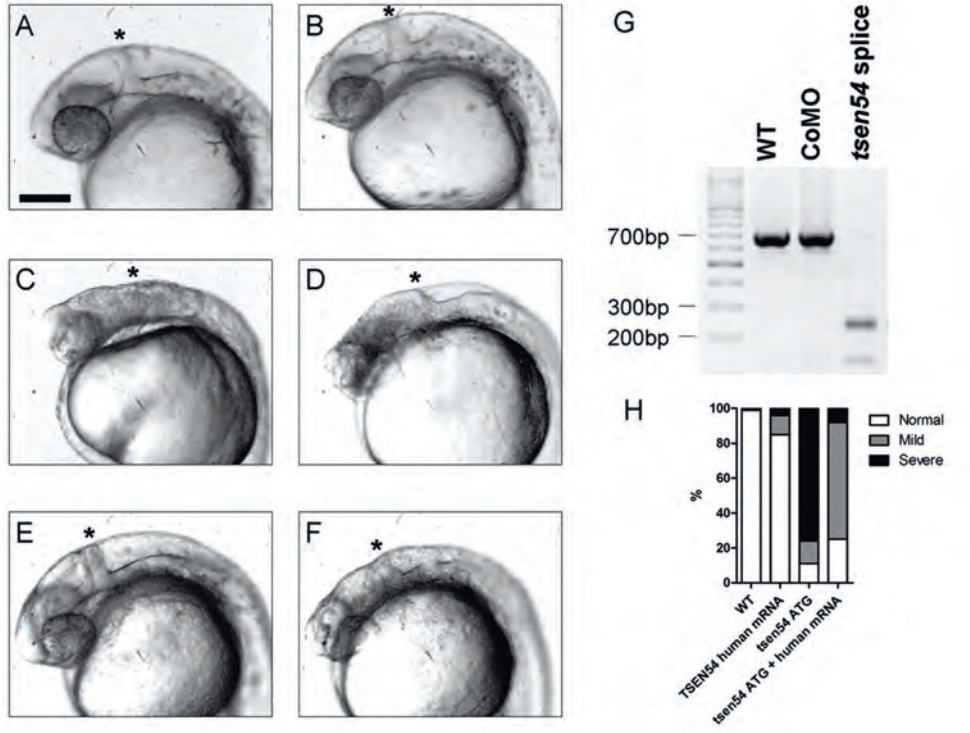

Figure 2. Disruption of *tsen54* translation causes brain hypoplasia and loss of structural definition in the MHB in zebrafish embryos. (a-f) Lateral views of head and brain regions of *tsen54* MO and human *TSEN54* mRNA-injected zebrafish embryos at 24 hpf. Asterisks denote the MHB. (a) WT un-injected embryo; (b) CoMO-injected embryo; (c) *tsen54* ATG MO-injected embryo; (d) *tsen54* exon 8 splice donor site MO-injected embryo; (e) human *TSEN54* mRNA-injected embryo; (f) rescued embryo co-injected with *tsen54* ATG MO and human *TSEN54* mRNA. Scale bar = 200µm. (g) RT–PCR using primers located in exons 7 and 10 in *tsen54* cDNA synthesised from RNA extractions from WT un-injected embryos, CoMO-injected embryos and *tsen54* exon 8 splice donor site MO-injected embryos. RT–PCR using samples from control embryos produced a band of 696bp in length. Shorter products observed in splice MO-injected embryos indicate abnormal splicing of the *tsen54* gene. (h) Quantification of phenotypes observed in WT un-injected embryos, human *TSEN54* mRNA-injected embryos, *tsen54* ATG MO-injected embryos and rescued embryos co-injected with ATG MO and human mRNA. For each group, 50–100 embryos were analysed. Embryos were classified as displaying normal (white), mild (grey) or severe (black) phenotypes. There is a shift from a predominantly severe phenotype in the *tsen54* ATG MO group to a predominantly mild phenotype in ATG MO and human *TSEN54* mRNA co-injection group, thus illustrating the partial rescue of the brain phenotype associated with the loss of *tsen54*. For colour figure see page 170.

Inhibition of *tsen54* translation produces a brain defect which is not associated with a developmental patterning deficiency

PCH is characterised by hypoplasia and atrophy of the cerebellar hemispheres, hypoplasia of the pons and a general delay of neurodevelopment [17]. To determine whether the brain phenotype caused by *tsen54* knockdown in zebrafish embryos was associated with a developmental brain patterning defect, we performed *in situ* hybridization on whole-mount embryos at 24 hpf using *fgf8* (fibroblast growth factor 8) and *otx2* (orthodenticle homeobox 2) RNA probes as markers of brain development. In zebrafish brain, *fgf8* is expressed in the MHB and plays a role in the maintenance and development of this region, which includes the cerebellum [18]. In addition, *fgf8* is also expressed within the telencephalon and optic vesicles [19]. *Otx2* plays a role in early regionalisation of the mesencephalon and indeed is expressed within fore-midbrain regions during early development in zebrafish [20]. Abnormal localization of the expression of these genes within morphants would suggest a defect in the developmental patterning of these brain regions. As shown in Figure 3a, embryos injected with human *TSEN54* mRNA alone show normal expression patterning of *fgf8*. When the brain was observed from a dorsal perspective (Fig. 3d), the expression of *fgf8* appeared as a 'horseshoe with a peak' pattern in control embryos. MO knockdown of *tsen54* was not associated with abnormal patterning (Fig. 3b), as *Fgf8* expression was correctly observed within the MHB and telencephalon. However, compared with controls, the MHB appeared compressed, thus reflecting the brain hypoplasia associated with *tsen54* knockdown. This result is further supported when observing the dorsal view of the morphant brain where the 'peak' of the 'horseshoe' was absent from the MHB (Fig. 3e, arrow). Loss of this horseshoe peak was reversed, to a certain extent, by co-injecting the *tsen54* ATG MO with human *TSEN54* mRNA, further confirming specific gene targeting (Fig. 3c and f). Similarly, *tsen54* knockdown did not result in abnormal patterning of the fore-midbrain as localization of *otx2* expression was comparable between morphants (Fig. 3h) and controls (Fig. 3g). However, the brain hypoplasia phenotype was further illustrated by the reduction in intensity and extent of the *otx2* expression pattern in morphants compared with controls (Fig. 3j,k), which could be partially rescued by the introduction of human *TSEN54* mRNA (Fig. 3i and l).

Brain phenotype caused by *tsen54* knockdown is associated with increased cell death

As the brain phenotype caused by *tsen54* knockdown was not associated with a neurodevelopmental patterning defect, we next monitored the levels of neurodegeneration in the brains of morphant embryos. Embryos were incubated with acridine orange, a vital dye that binds to nucleic acids in damaged cells [21]. The numbers of fluorescing cells within the brain were counted from 10 to 20 embryos per group (at 24 hpf). Low numbers of fluorescing cells were counted in the brains of WT embryos (Fig. 4a and e; 55.5 ± 4; mean ± SEM) and *TSEN54* mRNA-injected embryos (Fig. 4b and e; 80.7 ± 7). In comparison to both of the control groups,

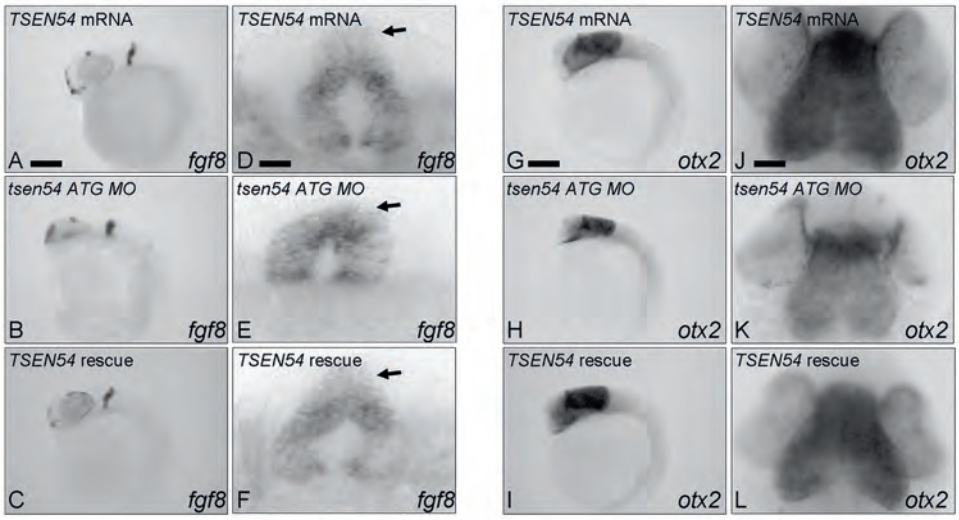

Figure 3. Knockdown of zebrafish *tsen54* results in a brain defect that is not associated with abnormal developmental patterning. Whole-mount *in situ* hybridization using *fgf8* (a-f) and *otx2* (g-l) DIG RNA probes in 24 hpf embryos injected with human *TSEN54* mRNA alone (a,d,g,j), *tsen54* ATG MO (b,e,h,k) and *tsen54* ATG MO with human *TSEN54* mRNA rescue (c,f,i,l). Lateral views are presented in (a-c) for *fgf8* staining and (g-i) for *otx2* staining (scale bar = 200µm). Dorsal views are presented in (d-f) for *fgf8* staining (scale bar = 30µm) and (j-l) for *otx2* staining (scale bar = 50µm). Results reveal brain hypoplasia is evident in *tsen54* morphants, as indicated by the loss of the *fgf8* 'horseshoe peak' expression pattern (arrows) however, developmental patterning of the MHB (*fgf8*) and fore-midbrain (*otx2*) are normal. Co-injection of the ATG MO with *TSEN54* human mRNA is capable of partially rescuing the brain hypoplasia phenotype, thus confirming specific targeting of the MO. For colour figure see page 171.

injection of the *tsen54* ATG MO resulted in a significant increase in the number of fluorescing cells within the brain (Fig. 4c and e; 242.9 ± 16; $P<0.0001$). Co-injection of *tsen54* ATG MO with human *TSEN54* mRNA resulted in a significant reduction in the numbers of fluorescing cells in comparison to the *tsen54* ATG injection only group (Fig. 4d and e; 173.9 ± 7.8; $P = 0.0005$); however, the number of fluorescing cells in this group was still significantly greater than that of both control groups ($P<0.0001$). Therefore, this result further confirms that human TSEN54 is capable of partially rescuing the brain phenotype associated with *tsen54* knockdown.

A homozygous premature stop-codon mutation within *tsen54* causes early lethality in zebrafish

Antisense MO oligonucleotides allow a highly efficient means of knocking down gene function during early embryonic development; however, the effects diminish after a few days post-fertilization (dpf) [12]. Therefore, we generated a stable zebrafish model that harboured a mutation within the *tsen54* gene in order to study the survival rates. We

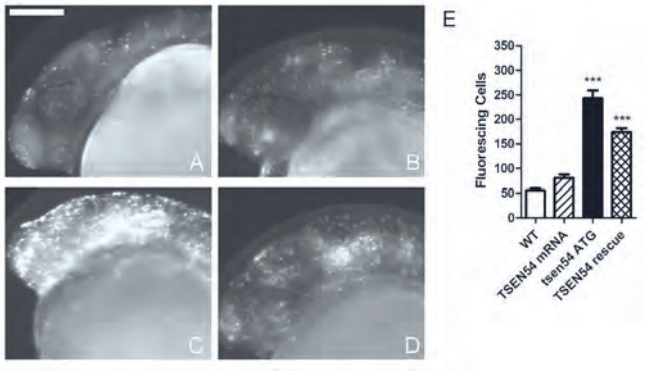

Figure 4. *tsen54* knockdown is associated with increased cell death in the brain. (a-d) Lateral view of brains of live zebrafish embryos (24 hpf) incubated with acridine orange in (a) WT un-injected, (b) human *TSEN54* mRNA alone, (c) *tsen54* ATG MO and (d) *tsen54* ATG MO co-injected with human *TSEN54* mRNA rescue groups. Scale bar = 200µm. (e) Quantification of fluorescing cells from each group (n = 10-20). Dead cells were counted from the tip of the forebrain to the ear, excluding the eye. Injection of *tsen54* ATG MO resulted in a significant increase in the number of dead cells within the brain. Co-injection of the ATG MO with human *TSEN54* mRNA resulted in a significant decrease in cell death (*** $P<0.0005$).

screened the zebrafish ENU mutagenesis DNA archive at the Hubrecht Laboratories, Utrecht [22], and identified a heterozygous C>T substitution in exon 8 of the *tsen54* gene (c.682C>T; Fig. 5a). The position of this mutation translates as the conversion of an arginine to a premature stop codon at amino acid position 228 (p.R228X). Heterozygotes from the F2 progeny were identified by genotyping and the mutation was backcrossed onto a WT AB background for five generations to reduce the number of potentially confounding ENU mutations [23]. All mutants from this breeding programme were subsequently referred to as $tsen54^{R228X}$. As PCH is an autosomal recessive disease, we next performed an in-cross between heterozygous mutants to test for homozygosity. Embryos resulting from the in-cross were genotyped at 1, 2 and 3 weeks post-fertilization. All three genotypes were present after 1 week; however, at 2 weeks post-fertilization, $tsen54^{R228X-/-}$ animals were absent, suggesting that homozygosity was lethal during the larval stages (data not shown). To determine the precise time point at which the lethality of $tsen54^{R228X-/-}$ larvae occurred, we performed a survival analysis. As shown in Fig. 5b, larvae obtained from a control WT TL in-cross showed 72% survival after 3 weeks, whereas only 45% of the $tsen54^{R228X+/+}$ embryos survived to 21 dpf, probably due to the retention of an ENU mutation on the $tsen54^{R228X+/+}$ background. Of the $tsen54^{R228X+/-}$ heterozygous embryos, 62% survived to 21 dpf. Confirming our observations on the lethality of homozygosity for the mutation, all $tsen54^{R228X-/-}$ larvae had died by 9 dpf (Fig. 5b).

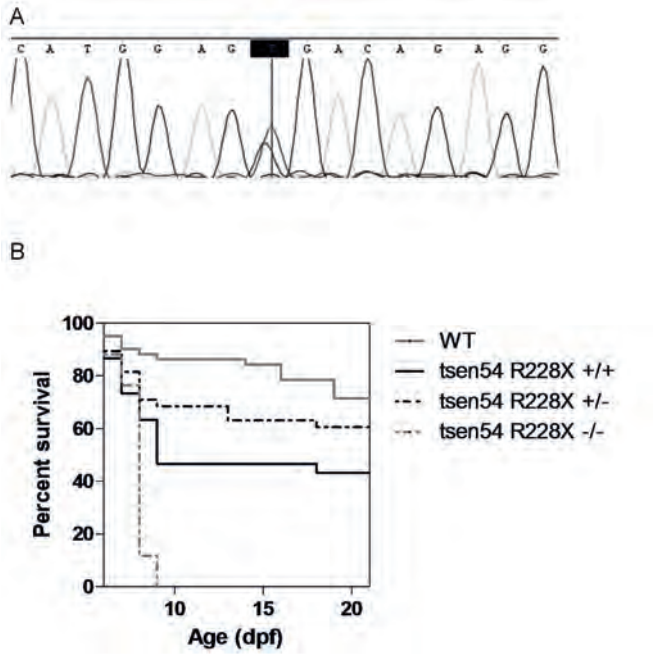

Figure 5. A homozygous premature stop-codon mutation within *tsen54* causes early lethality in zebrafish larvae. (a) Sequence trace obtained from the individual heterozygous c.682C>T *tsen54* mutant (hu5985). Translation of this base pair substitution leads to the p.R228X mutation. The mutation was subsequently backcrossed onto a WT background for five generations. (b) Progeny from a *tsen54* $^{R228X+/-}$ in-cross were observed for 3 weeks post-fertilization to test for homozygosity. Survival was plotted using the Kaplan-Meier curves. By 9 dpf, 100% of the *tsen54*$^{R228X-/-}$ (grey dotted line) larvae had died. In comparison, 45% and 62% of the *tsen54*$^{R228X+/+}$ (black line) and *tsen54*$^{R228X+/-}$ (black dotted line) survived to the 3 weeks post-fertilization time point, respectively. As a comparison to general ENU mutant survival, 72% WT TL larvae (grey line) were observed to survive to the 21 dpf stage. For colour figure see page 172.

Disruption of the *rars2* gene results in a brain phenotype comparable with *tsen54* morphants

Mutations in the nuclear-encoded *RARS2* gene are found in PCH1 and PCH6 [1,4,13]. RARS2 plays a role in the aminoacylation of mitochondrial tRNA-Arg [4]. Thus, a common disease mechanism related to tRNA processing may account for different PCH subtypes caused by mutations in *TSEN54* or *RARS2*. Similar to *tsen54*, *rars2* is expressed ubiquitously at 24 hpf but strong within the head and brain [24].

To test the effects of *rars2* inhibition, we injected zebrafish embryos with MOs designed to target the *rars2* ATG start site and the exon 6 splice donor site. As shown in Figure 6c and d, knockdown of *rars2* with both MOs results in brain hypoplasia and loss of structural definition within the brain in comparison to control embryos (Fig. 6a,b). RT-PCR reveals that abnormal splicing of *rars2* occurred in the splice-site

morphants (Fig. 6g). Co-injection of human *RARS2* mRNA with the *rars2* ATG MO resulted in partial recovery of the brain phenotype, thus confirming specific targeting of gene knockdown (Fig. 6e,f and h). Whole-mount *in situ* hybridization using *fgf8* (Suppl. Fig. 3a-f) and *otx2* (Suppl. Fig. 3g-l) RNA probes further illustrates the brain hypoplasia phenotype observed in *rars2* morphants. Similar to *tsen54* knockdown, developmental patterning of the MHB and the fore-midbrain regions was not affected. Furthermore, *rars2* knockdown was associated with a significant increase in cell death within the brains of morphant embryos (Suppl. Fig. 4c and e) when compared with both control groups ($P<0.0001$; Suppl. Fig. 4a,b and e). The number of dead cells was significantly reduced when human *RARS2* mRNA was co-injected with the *rars2* ATG MO ($P = 0.0005$; Suppl. Fig. 4d,e). Taken together, these observations reveal phenotypic comparisons between *rars2* and *tsen54* morphants, suggesting a common disease pathway may exist between two separate genes in the pathogenesis of distinct subtypes of PCH.

Discussion

In this study, we show that the inhibition of *tsen54* in zebrafish leads to neurological abnormalities and is lethal, thus bearing similarities to the disease characteristics associated with PCH. In addition, these data strongly support the hypothesis that *TSEN54* mutations cause the disease through a loss of function mechanism. A strong and specific expression pattern for *TSEN54* in developing human cerebellar neurons at gestation week 23 has been reported previously [2]. Here, we show that *TSEN54* mRNA is ubiquitously expressed in the brain at 8 weeks of development with strong expression observed within the developing metencephalon and telencephalon. The metencephalonic region of the developing brain eventually forms the pons and cerebellum [25]. Abnormalities in both of these regions are the hallmark features of PCH pathology as all six subtypes of PCH are characterised by hypoplasia and variable atrophy of the cerebellum and pons [1-6]. The telencephalon gives rise to the cerebral cortex and basal ganglia within the cerebral hemispheres [26]. Cerebral cortical atrophy has been reported in 40% of *TSEN54*-related PCH patients, a feature that correlates with increasing age, suggesting all patients would display such a phenotype if survival rates were higher [1]. Cerebral immaturity is also a key feature for PCH4 diagnosis [1]. Also, although less common, microglial and astrocytic pathology have also been reported in the basal ganglia in PCH2 [17]. Therefore, strong *TSEN54* expression is apparent in those brain regions affected in PCH during the earlier stages of neurodevelopment. In zebrafish, we observed a ubiquitous expression pattern of *tsen54*; however, strongest expression was detected within the brain at 24 hpf, in particular the telencephalon and MHB. Ubiquitous *tsen54* expression observed as early as the 8-cell stage is compatible with an essential function of this gene during development. Our data confirm results from previous studies in zebrafish embryos using *tsen54* RNA probes [24]. Importantly,

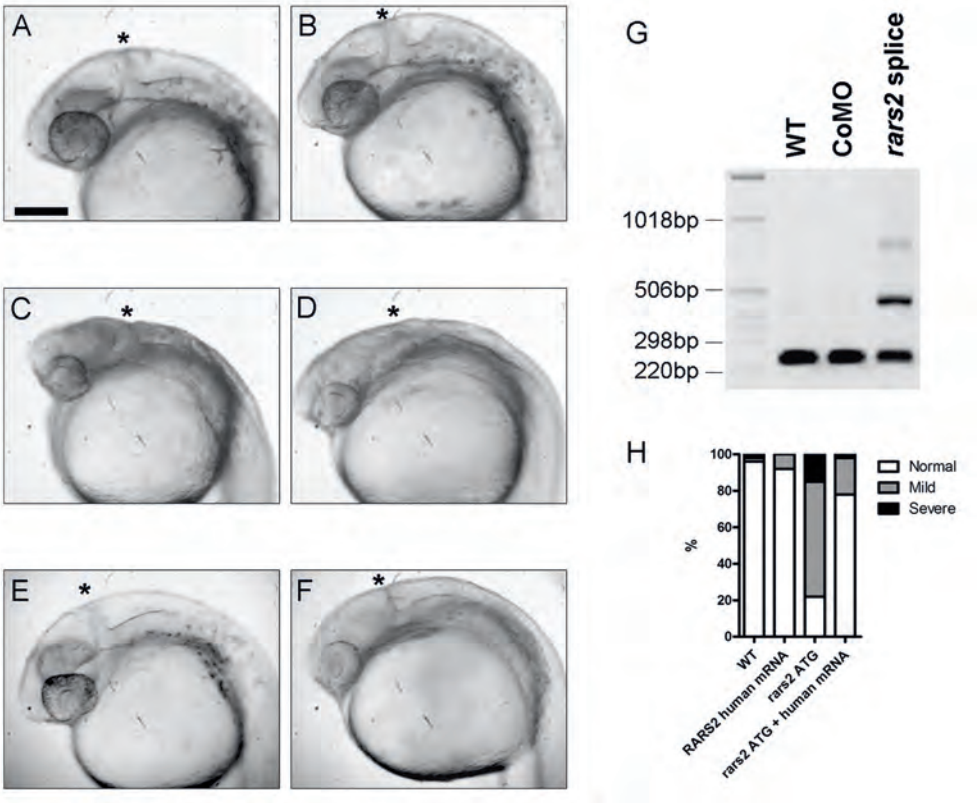

Figure 6. Disruption of *rars2* gene results in brain phenotype comparable with *tsen54* knockdown. (a-f) Head and brain regions of *rars2* MO and human *RARS2* mRNA-injected zebrafish embryos at 24 hpf. Asterisks denote the MHB. (a) WT un-injected embryo; (b) CoMO-injected embryo; (c) *rars2* ATG MO-injected embryo; (d) *rars2* exon 6 splice donor site MO-injected embryo; (e) human *RARS2* mRNA-injected embryo; (f) rescued embryo co-injected with *rars2* ATG MO and human *RARS2* mRNA. Scale bar = 200µm. (g) RT-PCR using primers located in exons 3 and 6 in *rars2* cDNA synthesised from RNA extractions from WT un-injected embryos, CoMO-injected embryos and *rars2* exon 6 splice donor site MO-injected embryos. RT-PCR using samples from control embryos produced a band of 246bp in length. Larger products observed in splice MO-injected embryos indicate abnormal splicing of the *rars2* gene. (h) Quantification of phenotypes observed in WT un-injected embryos, human *RARS2* mRNA-injected embryos, *rars2* ATG MO-injected embryos and rescued embryos co-injected with ATG MO and human mRNA. For each group, 50-100 embryos were analysed. Embryos were classified as displaying normal (white), mild (grey) or severe (black) phenotypes. There is a shift from a predominantly mild-severe phenotype in the *rars2* ATG MO group to a predominantly normal phenotype in ATG MO and human *RARS2* mRNA co-injection group, thus illustrating the partial rescue of the brain phenotype associated with the loss of *rars2*. For colour figure see page 173.

a comparable *TSEN54* expression pattern is observed in humans and zebrafish during early neurodevelopmental stages.

Although obvious anatomical differences exist between the species, comparisons can be made between the brain phenotypes observed in *tsen54* morphant zebrafish embryos and *TSEN54*-related PCH. The presence of progressive microcephaly and cortical shrinkage is a distinctive pathology associated with a PCH2 phenotype [1]. Therefore, the observation of brain hypoplasia in zebrafish embryos following *tsen54* knockdown is an expected phenotype. A general neurodevelopmental delay and immaturation of the brain is also associated with the disease [1]. PCH is considered a neurodevelopmental, neurodegenerative disorder, however, in contrast to other neurodevelopmental disorders such as lissencephaly [27], a brain patterning defect is not associated with PCH. Here, we tested for neurodevelopmental abnormalities in our *tsen54* MO knockdown model by monitoring the expression of *fgf8* and *otx2*. Expression of these genes was observed within the appropriate regions for this developmental stage thus indicating that a brain patterning deficiency was not associated with a loss of *tsen54*. Low levels of cell death within the pons have been reported in few PCH patients [5]. However, as PCH is a neurodegenerative disorder occurring during early brain development, it is likely that high levels of cell death occur during earlier time points of the disease, rendering these cells unavailable for post-mortem analysis. Indeed, a significant increase in the number of acridine orange fluorescing cells was evident in the brains of *tsen54* morphants. Therefore, these data suggest that the brain phenotype caused by the loss of tsen54 function is due to an increased activation of processes leading to cell death and neurodegeneration. It should be noted that not all tissues with high expression of *TSEN54* are affected in PCH patients. Since we show here that PCH is in fact a neurodegenerative disease and not a developmental defect *per se*, other factors must determine the tissue-specific defect. A possible explanation could be a large demand for specific tRNAs for protein synthesis during a specific time in development. As discussed in more detail below, if this demand is not met, cells may degenerate.

The majority of *TSEN54*-related PCH patients die within the first decade of life [1]. In the most severe cases, a *TSEN54* null allele occurring compound heterozygous with the common p.A307S mutation can lead to early post-natal death [1,2]. We identified the *tsen54*^{R228X} ENU mutation and as expected heterozygous mutants were viable. It is likely that possessing two copies of a premature stop-codon mutation leads to a non-functional or absent protein; thus, we predicted that the loss of *tsen54* would be lethal. To date, no patients have been identified that harbour homozygous premature stop-codon mutations in *TSEN54*. Due to the potential severity of this type of mutation, it is possible that these patients never survive through prenatal stages. A *tsen54*$^{R228X+/-}$ in-cross produced the expected mendelian ratios (observed following genotyping at 5 dpf), however by 9 dpf, all *tsen54*$^{R228X-/-}$ larvae had died. In comparison, 45% of *tsen54*$^{R228X+/+}$ and 62% of *tsen54*$^{R228X+/-}$ survived beyond the 21 dpf time-point. These data therefore strongly suggest that homozygosity of the *tsen54* premature stop-codon

mutation is larval lethal in this model. The absence of a brain phenotype (data not shown) and the survival up to 9 dpf in the *tsen54*$^{R228X-/-}$ mutants may be explained by the persistence of maternal tsen54 protein during embryogenesis [28]. Extensive characterisation of the *tsen54*$^{R228X-/-}$ mutant line is necessary to fully establish this model as a tool to study the disease mechanisms underlying *TSEN54*-related PCH.

In both human and zebrafish, the loss of *TSEN54/tsen54* function results in a severe region-specific neurological phenotype. Due to the primary function of the TSEN complex, these observations therefore suggest that a high level of tRNA splicing activity is required within these brain regions during development. Demand for such activity suggests that there is a larger proportion of intron-containing tRNA genes expressed within these regions. Intron-containing tRNA genes are rare in vertebrates (only 6.2% in humans); therefore, tRNA splicing activity is only required for a small proportion of tRNA genes. However, reduced tRNA splicing activity may still lead to a reduction in the availability of specific tRNAs, e.g. tRNA Tyrosine, where 13 of the 14 tRNA-Tyr (GTA) genes contain an intron. In zebrafish, there is ~20-fold more tRNA genes present in comparison to human; however, intron-containing tRNA genes still only represent 6.6% of the total (http://lowelab.ucsc.edu/GtRNAdb/). As in humans, the vast majority of zebrafish tRNA-Tyr (GTA) genes contain an intron (225 out of 236). Hypothetically, therefore, it is reasonable to suggest that in both species, the loss of tRNA splicing function could lead to a reduction in the availability of tRNA-Tyr. If the expression levels of intron-containing tRNA genes are higher in specific brain structures, then a depletion of tyrosine and/or other amino acids could explain the brain-specific degeneration observed in *TSEN54*-related PCH and the zebrafish *tsen54* knockdown model. Due to extensive secondary and tertiary structures, little is known about the spatio-temporal expression levels of different tRNA genes. However, one study has revealed that the expression levels of different human tRNA genes vary greatly between tissues that may reflect translational control based on the availability of certain tRNAs [29]. Future experiments may benefit from examining the levels of intron-containing tRNA genes within the cerebellum and pons in comparison to other tissues. An alternative suggestion for specific susceptibility of the cerebellum and pons in the pathogenesis of PCH may relate to an alternative function of TSEN. For example, the human TSEN complex has been shown to associate with factors involved with pre-mRNA 3' end formation [7]. Therefore, it is feasible that this and/or other currently unknown functions relating to RNA processing may exist for TSEN.

As the *RARS2* gene plays a role in the aminoacylation of mitochondrial tRNA-Arg [4] and mutations in this gene are found in PCH1 and PCH6 [1,4,13], we tested whether the knockdown of *rars2* in zebrafish resulted in a similar phenotype to *tsen54* inhibition. Comparable phenotypes were observed between the *rars2* and *tsen54* groups. The obvious functional link between TSEN54 and RARS2 is an involvement with tRNA processing. Although specific phenotypical differences exist between *TSEN54*- and *RARS2*-related PCH, all patients display hypoplasia and variable atrophy of the

cerebellum and pons. The comparable brain phenotype observed following *tsen54* and *rars2* knockdown therefore provides evidence in a model system that a common disease pathway may exist between PCH subtypes. As for *TSEN54*, aminoacyl tRNA synthetases (ARSs) are also expressed ubiquitously in humans [30]. In zebrafish at 24 hpf, *rars2* is ubiquitously expressed; however, strongest expression is observed within the brain [24]. Mutations in various cytoplasmic and mitochondrial ARS genes have been identified in leukoencephalopathy (*DARS2*) [31] and different subtypes of Charcot-Marie-Tooth disease (*GARS* [32], *YARS* [33], *KARS* [34]). Recently, mutations in *SEPSECS*, a protein involved with the synthesis of the amino acid selenocysteine, have been reported to cause progressive cerebello-cerebral atrophy, a neurodevelopmental disorder with comparable phenotypic features to PCH [35]. Taken together with our data, these studies suggest different neuronal populations at different stages of life are susceptible to disruption of specific amino acid availability. Defects in tRNA splicing and tRNA aminoacylation caused by the loss of TSEN54 and RARS2 function, respectively, may ultimately reduce the availability of functionally charged tRNA. Therefore, a common disease pathway involving TSEN54 and RARS2 may relate to the abnormal processing of cytoplasmic and mitochondrial tRNAs within the brain. We cannot yet, however, rule out the potential for alternative functions of these genes in the pathogenesis of PCH. Nevertheless, the identification of a mutation in *MED17* [36], encoding a subunit of the mediator complex involved with transcription pre-initiation, in patients with cerebral and cerebellar atrophy (CCA) supports the hypothesis that an unmet demand for protein synthesis at a specific moment in development is the underlying cause of cerebellar atrophy or hypoplasia in CCA and PCH.

Materials and methods

Zebrafish stocks and maintenance

All zebrafish (*Danio rerio*) procedures were approved by the Academic Medical Center Animal Ethics Committee and experiments complied with standard animal care guidelines. Breeding and maintenance of all zebrafish stocks was performed as described by others [37]. WT TL zebrafish strains were crossed to generate embryos for MO and RNA injections, as well as *in situ* hybridizations. ENU mutant zebrafish lines were maintained on a mixed AB/TL background. Fertilized embryos were collected and staged according to the standard guidelines [38].

In situ hybridization using LNA/2OME-modified oligonucleotides to detect *TSEN54* expression in human foetal sections

Human embryonic tissue was collected and prepared for histological analyses as described [39]. Use of the human embryos for research was approved by the Ethical

Committee of the University of Amsterdam, the Netherlands. Pre-hybridization conditioning and hybridization using a human *TSEN54* specific, fluorescein-labelled LNA/2OME probe (5'- TcuTucTcuTgcCauCucC -3'; where LNA residues are given in capital letters and 2OME in lower case) was performed as described previously [2]. Probes were synthesised by Ribotask ApS, Odense, Denmark. Hybridization signal was detected by incubating the sections in blocking buffer containing anti-fluorescein-Alkaline phosphatase (AP) Fab fragments (1:1000; Roche, Lewes, UK) for 1 h at room temperature. AP signal was detected by using VECTOR Blue AP Substrate Kit (Vector, Burlingame, CA, USA).

Zebrafish whole-mount *in situ* hybridization using LNA/2OME probes

Embryos were dechorionated, fixed in 4% paraformaldehyde (PFA) in 0.1% phosphate buffered saline-Tween (PBST) and stored in methanol at -20°C till further use. Pre-hybridization conditioning and hybridization using a zebrafish *tsen54* specific, fluorescein-labelled LNA/2OME probe (5'-TauCugTccCgcTccCucT-3'; Ribotask ApS) was performed on whole embryos as described by others [40]. Hybridization signal was detected by incubating the embryos in blocking buffer containing anti-fluorescein-AP Fab fragments (1:2000; Roche) with agitation overnight at 4°C. AP staining was performed using 5-bromo-4-chloro-3-indolyl phosphate/nitro blue tetrazolium substrate.

MO injections

MOs (Gene-tools, LLC, Philomath, OR, USA) were designed around the start codon (ATG) and the exon 8 splice donor site of the zebrafish *tsen54* gene (ATG: 5'-CTTGCCTCTTTCTGAAAAACCCATC-3'; Ex8splice: 5'-TAGTGTAAAGTACAT CTTACGGTGT-3'). For the zebrafish *rars2* gene, MOs were designed against the ATG and the exon 6 splice donor sequence (ATG: 5'-CACTCCTCCTGAAAAAACAC GCCAT-3'; Ex6splice: 5'- CACACACACAGTAAACTGACCTGAA -3'). Standard CoMOs were also provided by Gene-tools. Using fine glass needles and a microinjector (World Precision Instruments, Sarasota, FL, USA), 1–4-cell stage embryos were injected directly into the yolk sac with 2.5ng ATG MO, 3.2ng splice MO or 6.6ng CoMO. Embryos were allowed to recover in E3 medium stored at 28°C before fixation at various time points.

Human mRNA *in vitro* transcription and injections

Human *TSEN54* cDNA cloned into the pCMV-SPORT6 vector (NIH_MGC_71) and human *RARS2* cDNA cloned into the pOTB7 vector (NIH_MGC_44) were obtained from the Mammalian Gene Collection (NIH, Bethesda, USA). The *TSEN54* insert was excised using *Xho*I and *Eco*RI; the *RARS2* insert was excised using *Bam*HI and *Xho*I.

Both cDNA sequences were ligated into separate pCS2+ vectors. The *TSEN54* and *RARS2* constructs were linearized with Asp718 and Not1, respectively, and *in vitro* transcription was performed using the SP6 mMESSAGE mMACHINE kit (Ambion, Warrington, UK). For injections, 233 or 555pg of *TSEN54* and *RARS2* mRNA, respectively, was injected per embryo either alone as a control or in combination with the ATG MO. For each group, 50–100 embryos at 24 hpf were classified and counted as displaying phenotypes described as either normal (appeared as WT), mild (slightly smaller head, slightly reduced brain structure definition) or severe (small head, complete loss of brain structural definition).

RT–PCR

To confirm specific targeting of the splice MO, total RNA was extracted from 50 injected embryos using TRIzol (Invitrogen, Germany) and chloroform for phase separation and isopropanol precipitation. For the reverse transcription reaction, 1µg of RNA was mixed with 125pmol/µl OligodT_{12}-VN and denatured for 10 min at 72°C. First-strand cDNA was synthesised using SuperscriptII enzyme (Invitrogen) and incubating at 42°C for 1 h. For *tsen54* ex8 splice MO, a region of 696bp spanning exons 7 and 10 was amplified using the following primers: 5'-CAGCATCGGACAA ACAGAAG-3' and 5'-ACTGGTCTGACGGGGACA-3' (Sigma-Aldrich). For *rars2* ex6 splice MO, a region of 246bp spanning exons 3 and 6 was amplified using the following primers: 5'-GAGACCTGCAGAACACCACA-3' and 5'-AACTTCTTGGCGATGT TTGG-3' (Sigma-Aldrich).

Whole-mount *in situ* hybridization using DIG-labelled RNA probes

Fgf8 [18] and *otx2* [20] were linearized with *Eco*RV and *Eco*RI, respectively, and digoxigenin (DIG)-RNA probes were synthesised using the SP6/T7 polymerase RNA labelling kit (Roche). Zebrafish embryos (24–30 hpf) were dechorionated, fixed overnight at 4°C in 4% PFA in 0.1% PBST and stored in methanol at -20°C till further use. Whole-mount *in situ* hybridization was performed as described by others [41].

In vivo cell death assay

Live embryos were incubated for 30 min in the dark at 28°C in water containing 2µg/ml acridine orange (Sigma-Aldrich). Embryos were washed five times in water prior to imaging. The numbers of fluorescing cells in focus were counted within the brain in a region encapsulating the tip of the forebrain to the ear. Dying cells within the eye were omitted from the analysis. Fluorescing cells were counted in 10-20 embryos/larvae per condition. The mean number of fluorescing cells ± standard error was plotted. One-way ANOVA with the Newman-Keuls multiple comparisons test was performed for statistical analysis.

ENU mutagenesis screen

ENU mutation screening was performed using a TILLING (targeting induced local lesions IN genomics) approach with a frozen archive of genomic DNA derived from mutagenized F1 zebrafish at the Hubrecht Institute, Utrecht, the Netherlands, as described previously [42]. Exon 8 of the *tsen54* gene was amplified using the following nested PCR primers (Primer 1: 5'-GGGACTTCAGCAGCATTAG-3'; Primer 2: 5'-AGGAGATCTGAGCGTTTGG-3'; Primer 3: 5'-CCAGTCTTTACCCAGTCACC-3'; Primer 4: 5'-CTTCCAACAATCTTTCTTTCC-3'; Sigma-Aldrich). The first PCR was performed using primers 1 and 4. The second PCR was performed using primers 2 and 3, which contained universal M13 forward (M13F) and M13 reverse (M13R) adaptor sequences at their 5' ends, respectively. Mutation detection and verification was therefore performed by sequencing the internal nested PCR product using M13F (5'-TGTAAAACGACGGCCAGT-3'; Sigma-Aldrich) and M13R primers (5'-AGGAAA CAGCTATGACCAT-3'; Sigma-Aldrich). PCR products were sequenced as described previously [1].

Taqman genotyping

Following identification of the individual heterozygous c.682C>T *tsen54* mutant (hu5985) in the live F1 library, the mutation was backcrossed onto a WT AB background for five generations to reduce the number of potentially confounding ENU mutations. For each subsequent generation, genotyping was performed using a Taqman single nucleotide polymorphism (SNP) genotyping approach (Applied Biosystems, Warrington, UK). Briefly, fish were anaesthetized in 250mg/l tricaine (MS-222; Sigma-Aldrich), and a small portion of the caudal fin was removed with a scalpel. Fin clips were digested with lysis buffer containing 0.1mg/ml of proteinase K at 60°C for 1 h. Following DNA quantification, 10ng of DNA was added to 1×5µl of Roche Fast-Start universal probe mix (Roche) containing 40× Taqman SNP assay probe (designed and generated by Applied Biosystems; FAM and VIC dye-labelled). Real-time PCR was then performed using a Roche LightCycler 480 for 40 cycles (denatured at 95°C for 15 s, annealed/amplified at 60°C for 1 min). Allelic discrimination was analysed using the Roche LightCycler software version 1.5.

Survival analysis in *tsen54*^{R228X} mutant zebrafish

Progenies from an in-cross mating of *tsen54*$^{R228X+/-}$ adults were raised for 3 weeks. Dead larvae were removed from the tank twice daily and DNA was extracted immediately before freezing. At 21 dpf, all surviving larvae were humanely sacrificed and DNA was extracted. All dead and surviving embryos were genotyped as described above. Survival of *tsen54*$^{R228X-/-}$ larvae was examined using the Kaplan-Meier analysis (Graphpad Prism, version 5) to produce survival curves for each genotype. Similarly, progenies from an in-cross mating of WT TL adults were raised for 3 weeks and dead larvae were counted on a daily basis for survival analysis.

Acknowledgements

We would like to thank C. van Rooijen and W. de Graaf for technical assistance with zebrafish maintenance and M. Brand and E. Weinberg for providing RNA probes. We would also like to thank E. Cuppen and H. van Roekel for support with ENU TILLING.

Funding

We would like to thank ZF Health for funding the ENU TILLING library and support by the 'Internationale Stichting Alzheimer Onderzoek' (ISAO #07508 and #09506) to P.T. and D.Z.. Y.N. is supported by an AMC graduate school fellowship.

Reference List

1. Namavar, Y., Barth, P.G., Kasher, P.R., van Ruissen, F., Brockmann, K., Bernert, G., Writzl, K., Ventura, K., Cheng, E.Y., Ferriero, D.M. et al.: Clinical, neuroradiological and genetic findings in pontocerebellar hypoplasia 2011. Brain, 134: 143– 156.
2. Budde, B.S., Namavar, Y., Barth, P.G., Poll-The, B.T., Nurnberg, G., Becker, C., van Ruissen, F., Weterman, M.A., Fluiter, K., te Beek, E.T. et al.: tRNA splicing endonuclease mutations cause pontocerebellar hypoplasia. Nat. Genet. 2008, 40: 1113– 1118.
3. Durmaz, B., Wollnik, B., Cogulu, O., Li, Y., Tekgul, H., Hazan, F. and Ozkinay, F.: Pontocerebellar hypoplasia type III (CLAM): extended phenotype and novel molecular findings. J. Neurol. 2009, 256: 416– 419.
4. Edvardson, S., Shaag, A., Kolesnikova, O., Gomori, J.M., Tarassov, I., Einbinder, T., Saada, A. and Elpeleg, O.: Deleterious mutation in the mitochondrial arginyl-transfer RNA synthetase gene is associated with pontocerebellar hypoplasia. Am. J. Hum. Genet. 2007, 81: 857– 862.
5. Patel, M.S., Becker, L.E., Toi, A., Armstrong, D.L. and Chitayat, D.: Severe, fetal-onset form of olivopontocerebellar hypoplasia in three sibs: PCH type 5? Am. J. Med. Genet. A, 2006, 140: 594– 603.
6. Renbaum, P., Kellerman, E., Jaron, R., Geiger, D., Segel, R., Lee, M., King, M.C. and Levy-Lahad, E.: Spinal muscular atrophy with pontocerebellar hypoplasia is caused by a mutation in the VRK1 gene. Am. J. Hum. Genet. 2009, 85: 281–289.
7. Paushkin, S.V., Patel, M., Furia, B.S., Peltz, S.W. and Trotta, C.R.: Identification of a human endonuclease complex reveals a link between tRNA splicing and pre-mRNA 3' end formation. Cell 2004, 117: 311–321.
8. Trotta, C.R., Paushkin, S.V., Patel, M., Li, H. and Peltz, S.W.: Cleavage of pre-tRNAs by the splicing endonuclease requires a composite active site. Nature 2006, 441: 375– 377.
9. Hopper, A.K. and Phizicky, E.M. tRNA transfers to the limelight. Genes Dev. 2003, 17: 162–180.
10. Huang, H., Xue, R., Zhang, J., Ren, T., Richards, L.J., Yarowsky, P., Miller, M.I. and Mori, S.: Anatomical characterization of human foetal brain development with diffusion tensor magnetic resonance imaging. J. Neurosci. 2009, 29: 4263– 4273.
11. Graham, J.M. Jr., Spencer, A.H., Grinberg, I., Niesen, C.E., Platt, L.D., Maya, M.,

Namavar, Y., Baas, F. and Dobyns, W.B.: Molecular and neuroimaging findings in pontocerebellar hypoplasia type 2 (PCH2): is prenatal diagnosis possible? Am. J. Med. Genet. A 2010, 152: 2268– 2276.

12. Bandmann, O. and Burton, E.A.: Genetic zebrafish models of neurodegenerative diseases. Neurobiol. Dis. 2010, 40: 58– 65.

13. Rankin, J., Brown, R., Dobyns, W.B., Harington, J., Patel, J., Quinn, M. and Brown, G.: Pontocerebellar hypoplasia type 6: a British case with PEHO-like features. Am. J. Med. Genet. A 2010, 152A: 2079– 2084.

14. Parisi, M.A. and Dobyns, W.B.: Human malformations of the midbrain and hindbrain: review and proposed classification scheme. Mol. Genet. Metab. 2003, 80: 36– 53.

15. Koster, R.W. and Fraser, S.E.: Direct imaging of in vivo neuronal migration in the developing cerebellum. Curr. Biol. 2001, 11: 1858– 1863.

16. Eisen, J.S. and Smith, J.C.: Controlling morpholino experiments: don't stop making antisense. Development 2008, 135: 1735–1743.

17. Barth, P.G., Aronica, E., de Vries, L., Nikkels, P.G., Scheper, W., Hoozemans, J.J., Poll-The, B.T. and Troost, D.: Pontocerebellar hypoplasia type 2: a neuropathological update. Acta Neuropathol. 2007, 114: 373–386.

18. Reifers, F., Bohli, H., Walsh, E.C., Crossley, P.H., Stainier, D.Y. and Brand, M. Fgf8 is mutated in zebrafish acerebellar (ace) mutants and is required for maintenance of midbrain-hindbrain boundary development and somitogenesis. Development 1998, 125: 2381– 2395.

19. Picker, A. and Brand, M.: Fgf signals from a novel signaling center determine axial patterning of the prospective neural retina. Development 2005, 132: 4951– 4962.

20. Li, Y., Allende, M.L., Finkelstein, R. and Weinberg, E.S. Expression of two zebrafish orthodenticle-related genes in the embryonic brain. Mech. Dev. 1994, 48: 229– 244.

21. van Ham, T.J., Mapes, J., Kokel, D. and Peterson, R.T.: Live imaging of apoptotic cells in zebrafish. FASEB J.2010, 24: 4336–4342.

22. de Bruijn, E., Cuppen, E. and Feitsma, H.: Highly efficient ENU mutagenesis in zebrafish. Methods Mol. Biol.2009, 546: 3–12.

23. Keays, D.A., Clark, T.G. and Flint, J.: Estimating the number of coding mutations in genotypic- and phenotypic-driven N-ethyl-N-nitrosourea (ENU) screens. Mamm. Genome 2006, 17: 230– 238.

24. Thisse, B. and Thisse, C.: Fast release clones. A high throughput expression analysis. ZFIN direct data submission, http://zfin.org. 2004.

25. Sarnat, H.B., Benjamin, D.R., Siebert, J.R., Kletter, G.B. and Cheyette, S.R.: Agenesis of the mesencephalon and metencephalon with cerebellar hypoplasia: putative mutation in the EN2 gene—report of 2 cases in early infancy. Pediatr. Dev. Pathol. 2002, 5: 54–68.

26. Xuan, S., Baptista, C.A., Balas, G., Tao, W., Soares, V.C. and Lai, E.: Winged helix transcription factor BF-1 is essential for the development of the cerebral hemispheres. Neuron 1995, 14: 1141–1152.

27. Yamada, M., Yoshida, Y., Mori, D., Takitoh, T., Kengaku, M., Umeshima, H., Takao, K., Miyakawa, T., Sato, M., Sorimachi, H. et al.: Inhibition of calpain increases LIS1 expression and partially rescues in vivo phenotypes in a mouse model of lissencephaly. Nat. Med. 2009, 15: 1202–1207.

28. Wagner, D.S., Dosch, R., Mintzer, K.A., Wiemelt, A.P. and Mullins, M.C.: Maternal control of development at the midblastula transition and beyond: mutants from the zebrafish II. Dev. Cell 2004, 6: 781– 790.

29. Dittmar, K.A., Goodenbour, J.M. and Pan, T.: Tissue-specific differences in human transfer RNA expression. PLoS Genet. 2006, 2: e221.

30. Antonellis, A. and Green, E.D.: The role of aminoacyl-tRNA synthetases in genetic diseases. Annu. Rev. Genomics Hum. Genet. 2008, 9: 87–107.

31. Scheper, G.C., van der Klok, T., van Andel, R.J., van Berkel, C.G., Sissler, M., Smet, J., Muravina, T.I., Serkov, S.V., Uziel, G., Bugiani, M. et al.: Mitochondrial aspartyl-tRNA synthetase deficiency causes leukoencephalopathy with brain stem and spinal cord involvement and lactate elevation. Nat. Genet. 2007, 39: 534 –539.

32. Antonellis, A., Ellsworth, R.E., Sambuughin, N., Puls, I., Abel, A., Lee-Lin, S.Q., Jordanova, A., Kremensky, I., Christodoulou, K., Middleton, L.T. et al.: Glycyl tRNA synthetase mutations in Charcot-Marie-Tooth disease type 2D and distal spinal muscular atrophy type V. Am. J. Hum. Genet. 2003, 72: 1293– 1299.

33. Jordanova, A., Irobi, J., Thomas, F.P., Van Dijck, P., Meerschaert, K., Dewil, M., Dierick, I., Jacobs, A., De Vriendt, E., Guergueltcheva, V. et al.: Disrupted function and axonal distribution of mutant tyrosyl-tRNA synthetase in dominant intermediate Charcot-Marie-Tooth neuropathy. Nat. Genet. 2006, 38: 197– 202.

34. McLaughlin, H.M., Sakaguchi, R., Liu, C., Igarashi, T., Pehlivan, D., Chu, K., Iyer, R., Cruz, P., Cherukuri, P.F., Hansen, N.F. et al.: Compound heterozygosity for loss-of-function lysyl-tRNA synthetase mutations in a patient with peripheral neuropathy. Am. J. Hum. Genet. 2010, 87: 560– 566.

35. Agamy, O., Ben, Z.B., Lev, D., Marcus, B., Fine, D., Su, D., Narkis, G., Ofir, R., Hoffmann, C., Leshinsky-Silver, E. et al.: Mutations disrupting selenocysteine formation cause progressive cerebello-cerebral atrophy. Am. J. Hum. Genet. 2010, 87: 538– 544.

36. Kaufmann, R., Straussberg, R., Mandel, H., Fattal-Valevski, A., Ben-Zeev, B., Naamati, A., Shaag, A., Zenvirt, S., Konen, O., Mimouni-Bloch, A. et al.: Infantile cerebral and cerebellar atrophy is associated with a mutation in the MED17 subunit of the transcription preinitiation mediator complex. Am. J. Hum. Genet. 2010, 87: 667– 670.

37. Klooster, J., Yazulla, S. and Kamermans, M.: Ultrastructural analysis of the glutamatergic system in the outer plexiform layer of zebrafish retina. J. Chem. Neuroanat. 2009, 37: 254 –265.

38. Kimmel, C.B., Ballard, W.W., Kimmel, S.R., Ullmann, B. and Schilling, T.F.: Stages of embryonic development of the zebrafish. Dev. Dyn. 1995, 203: 253–310.

39. Sizarov, A., Anderson, R.H., Christoffels, V.M. and Moorman, A.F.: Three-dimensional and molecular analysis of the venous pole of the developing human heart. Circulation 2010, 122: 798– 807.

40. Kloosterman, W.P., Wienholds, E., de Bruijn, E., Kauppinen, S. and Plasterk, R.H.: In situ detection of miRNAs in animal embryos using LNA-modified oligonucleotide probes. Nat. Methods 2006, 3: 27–29.

41. Thisse, C. and Thisse, B.: High-resolution in situ hybridization to whole-mount zebrafish embryos. Nat. Protoc. 2008, 3: 59– 69.

42. Wienholds, E., van Eeden, F., Kosters, M., Mudde, J., Plasterk, R.H. and Cuppen, E.: Efficient target-selected mutagenesis in zebrafish. Genome Res. 2003, 13: 2700–2707.

Supplementary figures

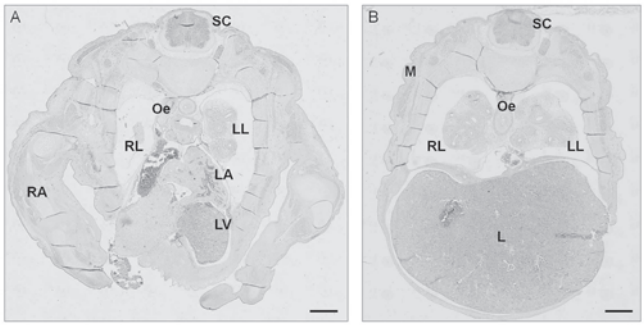

Supplementary Figure 1. *TSEN54* expression within other human foetal tissues. Relatively high *TSEN54* expression was observed in human foetal spinal cord and liver, whereas comparatively low expression levels were observed in other tissues. SC = spinal cord; L = liver; Oe = oesophagus; M = muscle; LL = left lung; RL = right lung; LA = left atrium; LV = left ventricle; RA = right arm. Scale bar = 500µm. For colour figure see page 174.

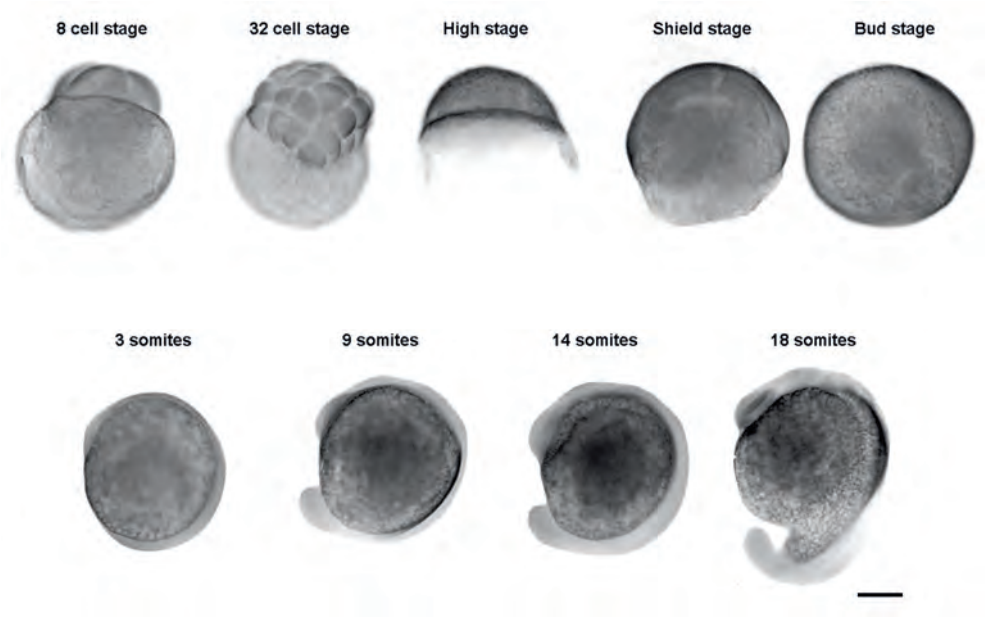

Supplementary Figure 2. *tsen54* expression is ubiquitous during early embryogenesis in the zebrafish. Ubiquitous *tsen54* mRNA expression pattern is observed in zebrafish embryos from the 8-cell stage to the somite stages. Scale bar = 200µm. For colour figure see page 174.

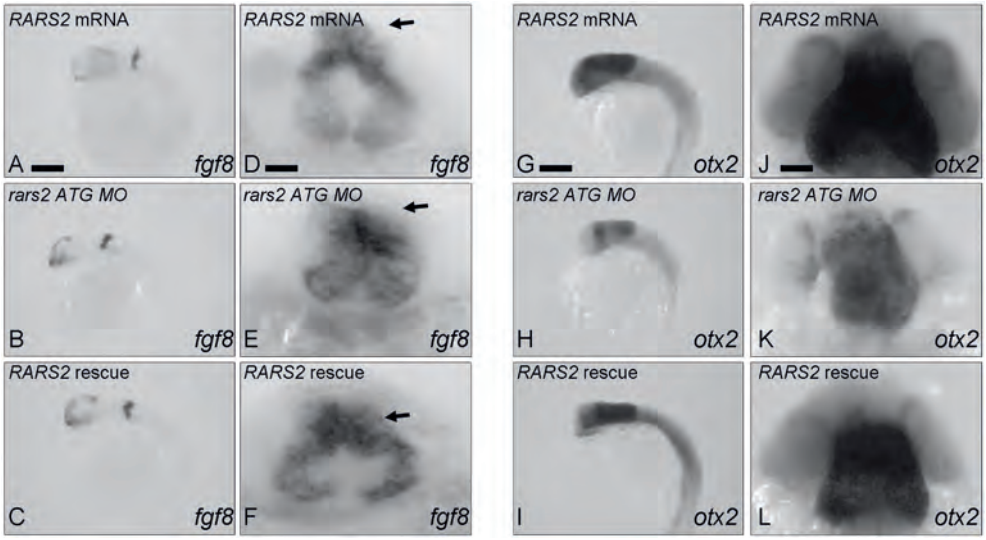

Supplementary Figure 3. Disruption of *rars2* gene results in brain phenotype comparable to *tsen54* knockdown. Whole mount *in situ* hybridization using *fgf8* (a-f) and *otx2* (g-l) DIG RNA probes in 24hpf embryos injected with human *RARS2* mRNA alone (a,d,g,j), *rars2* ATG MO (b,e,h,k) and *rars2* ATG MO with human *RARS2* mRNA rescue (c,f,i,l). Lateral views are presented in (a-c) for *fgf8* staining and (g-i) for *otx2* staining (scale bar = 200µm). Dorsal views are presented in (d-f) for *fgf8* staining (scale bar = 30µm) and (j-l) for *otx2* staining (scale bar = 50µm). Results reveal brain hypoplasia is evident in *rars2* morphants, as indicated by loss of the *fgf8* 'horse-shoe peak' expression pattern (arrows) however, developmental patterning of the mid-hindbrain boundary (*fgf8*) and fore-midbrain (*otx2*) are normal. Co-injection of the ATG MO with *RARS2* human mRNA is capable of partially rescuing the brain hypoplasia phenotype, thus confirming specific targeting of the MO. For colour figure see page 175.

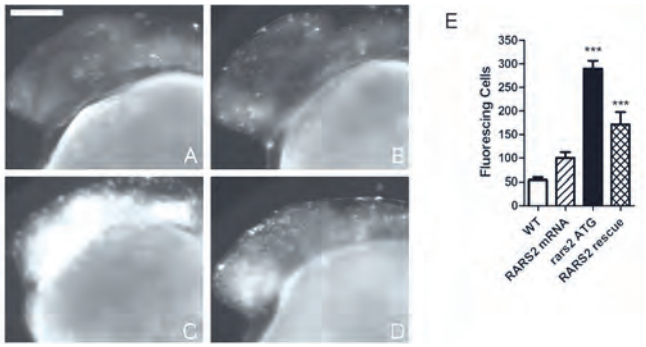

Supplementary Figure 4. Disruption of *rars2* gene results in brain phenotype comparable to *tsen54* knockdown. (a-d) Lateral view of brains of live zebrafish embryos (24 hpf) incubated with acridine orange in (a) WT un-injected, (b) human *RARS2* mRNA alone, (c) *rars2* ATG MO and (d) *rars2* ATG MO plus human *RARS2* mRNA rescue groups. Scale bar = 200µm. (e) Quantification of fluorescing cells from each group (n = 10-20). Dead cells were counted from the tip of the forebrain to the ear, excluding the eye. Injection of *rars2* ATG MO resulted in a significant increase in the number of dead cells within the brain. Co-injection with human *RARS2* mRNA resulted in a significant decrease in cell death (*** = $P<0.0005$).

Chapter 6

Functional studies on the tRNA splicing endonuclease complex in pontocerebellar hypoplasia

This work is done in collaboration with the Institute of Molecular Biotechnology of the Austrian Academy of Sciences, Dr. Bohr Gasse 3, A-1030 Vienna, Austria.

Abstract

Mutations in three of the four subunit genes of the tRNA splicing endonuclease are responsible for most types of Pontocerebellar Hypoplasia (PCH). Pontocerebellar Hypoplasia is a neurodegenerative disease characterised by hypoplasia of cerebellum and pons. Patients display disturbed motor coordination, progressive microcephaly, mental retardation and seizures. PCH type 2 is the relatively milder variant of PCH, caused by missense mutations. PCH type 4 is more severe and is caused by nonsense plus missense mutations. The tRNA splicing endonuclease is involved in splicing of intron-containing tRNAs and has also been implicated in mRNA 3'end formation. Therefore either impaired tRNA splicing or impaired mRNA 3'end formation could be responsible for PCH, or both. In this chapter we try to distinguish between these possibilities. We analysed the tRNA splicing activity of PCH2 fibroblasts in an *in vitro* assay. Nuclear extracts of PCH2 and PCH4 cases showed reduced tRNA splicing activity. PCH4 extracts showed less activity than PCH2 extracts, which is in line with the mutations in these disorders; missense mutations and nonsense versus homozygous missense mutations. No evidence was found for impaired mRNA 3'end formation both *in vitro* and *in vivo*. We propose that impaired tRNA splicing causes PCH.

Introduction

Pontocerebellar Hypoplasia (PCH) is a group (PCH1-7) of neurodegenerative disorders associated with early onset of hypoplasia and atrophy of cerebellum and pons, progressive microcephaly and variable neocortical atrophy. Mutations in the tRNA splicing endonuclease (TSEN) complex can cause at least 4 different PCH subtypes; PCH1, PCH2, PCH4 and PCH5 [1-3]. Three (TSEN54, TSEN2 or TSEN34) of the four subunits of the TSEN complex (the fourth subunit being TSEN15) are associated with any of these PCH subtypes. PCH4/PCH5 is caused by a combination of a null allele and a missense mutation in *TSEN54*, giving rise to a severe phenotype of perinatal symptoms and early lethality. A milder phenotypic profile with less perinatal complications, longer survival and dyskinetic movement disturbances are characteristics of PCH2. PCH2 is caused by missense mutations in *TSEN54* [4]. This genotype-phenotype correlation (e.g. a more severe phenotype caused by compound heterozygosity for a missense mutations and a null allele) suggests that the disease mechanism of PCH acts through loss of TSEN54 function. This hypothesis is supported by zebrafish models for PCH: Following *tsen54* targeted knockdown by antisense morpholinos loss of structural definition and head hypoplasia in zebrafish embryos was observed, sharing similarities with the brain phenotype observed in PCH. This knockdown could be rescued by co-injecting human *TSEN54*. Moreover zebrafish homozygous for a nonsense mutation (c.682C>T, p.R228X) in *tsen54* are lethal 9 days post fertilization [5]. How *TSEN54* mutations give rise to PCH is still unknown. In this chapter we want to investigate how the TSEN complex is involved in PCH by examining its different functions and expression in PCH.

TSEN54 and TSEN15 are the two structural subunits of the TSEN complex and TSEN2 and TSEN34 are the two catalytic subunits [6]. Following removal of the 5' leader and 3' trailer sequences, addition of a CCA tail and various modifications, maturation of tRNAs requires intron removal. There are multiple gene copies for each tRNA; for certain tRNA species up to 43 genes per isotype. Only a small proportion (6.3%) of these human tRNA genes is intron-containing. The intron, located within the anticodon loop of the tRNA, is not removed by the conventional splicing machinery, but by the endonucleolytic activity of the TSEN complex. tRNAs are genomically encoded by genes with and without introns. A few tRNAs e.g. all tRNA-Gly are only encoded by genes lacking introns. For some other tRNA species the majority of the tRNA genes are intron-containing: For example, 13 of the 14 tRNA-Tyr (GTA) genes contain an intron [7].

In yeast pre-tRNA-Tyr splicing is greatly depending on Sen function [8]. A defect in Sen function significantly affects the amount of functional tRNAs and would have a pronounced effect on protein synthesis. Our previous study in PCH showed that mutated *TSEN54* (homozygous for c.919G>T, p.A307S) fibroblasts do not accumulate pre-tRNA-Tyr, so no defect in tRNA maturation could be detected [2]. In order to test

the *in vitro* activity of the tRNA splicing endonuclease in *TSEN54* mutated fibroblasts and compare this with wild-type fibroblasts, an *in vitro* tRNA splicing assay was performed. Here we show that tRNA splicing activity is reduced in *TSEN54* mutated fibroblasts, compared to the control fibroblast lines.

The TSEN-complex is also thought to be involved in mRNA 3'end processing. An *in vitro* study showed that depletion of *TSEN2* in HEK293 cells resulted in extended sequences downstream of the cleavage and polyadenylation sequence of the *GAPDH* (glyceraldehyde-3-phosphate dehydrogenase) and *EF1A* (eukaryotic translation elongation factor 1 alpha) transcripts, using both a ribonuclease protection assay and quantitative Polymerase Chain Reaction (qPCR) [9]. Two isoforms of *TSEN2*, one containing exon 7 (wild-type) and one without exon 7 (Δex7) were described [9]. The composition of the TSEN complex containing TSEN2 Δex7 is different compared to wild-type TSEN with reduced levels of TSEN15 and TSEN34 being observed in the TSEN2 Δex7 associated complex. This TSEN2 Δex7-complex might have another function since it is ubiquitously expressed and its endonucleolytic activity is retained. Moreover it is not able to cleave tRNAs properly. The TSEN2 Δex7 protein associates stronger than wild-type TSEN2 with Symplekin and CstF64, factors involved in mRNA 3'end processing [9,10]. It is possible that only this TSEN2 Δex7 isoform plays a role in mRNA 3'end formation. In order to test whether PCH patients accumulate downstream mRNA 3'regions due to aberrant TSEN54 function, we determined the amount of downstream 3'ends of the *GAPDH* transcript and compared these with a region prior to the cleavage and polyadenylation site. A significant inter-individual variation was observed, but no significant effect could be detected on mRNA 3'end formation in fibroblasts of patients with a *TSEN54* mutation compared to controls. To test *in vivo* whether tsen54 or tsen2 function is involved in mRNA 3'end formation we down-regulated *tsen54* and *tsen2* by morpholino injections in zebrafish embryos and measured efficiency of mRNA 3'ends formation. Downregulation of *tsen2* and not *tsen54* affected mRNA 3'end processing in the *gapdh* transcript. We did not find evidence for tsen2 involvement in two other zebrafish transcripts.

As we only found a clear effect on tRNA splicing and not on mRNA 3'end formation, we also determined the expression of *TSEN2* exon 7 in different tissues including cerebellum and compared this with the constitutive exon 2. We found high expression of exon 2 and also of exon 7 in cerebellum, compared to other tissues.

We were interested to know whether more genes involved in the tRNA maturation pathway would be affected in PCH. Genes involved with tRNA ligation were also candidate genes for PCH. In our remaining "unsolved" PCH cases we screened three genes of this pathway, like the human cleavage and polyadenylation factor I and tRNA kinase (*CLP1*), the tRNA phosphotransferase (*TRPT1*) and the tRNA ligase (*HSPC117*) for mutations. No mutations were identified in any of these genes in our unsolved PCH cohort.

Methods

tRNA splicing activity assay

For fibroblasts of all subjects and/or parents of subjects, informed consent for research purposes was obtained. The fibroblasts of the control subjects were either healthy adult subjects or aged-matched subjects with unrelated disease. Nuclear extracts were isolated from fibroblasts cultured in DMEM (Dulbecco's Modified Eagle Medium, Invitrogen) with L-Glutamin (Sigma-Aldrich) supplemented with 10% foetal calf serum (Sigma-Aldrich) and penicillin/streptomycin (Sigma-Aldrich). Cell pellets were harvested and resuspended in phosphate buffered saline (PBS) and centrifuged for 5 minutes at 1500 rpm. Cell pellets were resuspended in 1 pellet volume of buffer A (10mM HEPES-KOH pH8.0, 1mM $MgCl_2$, 10mM KCl, 1mM DTT) and incubated on ice for 15 minutes. Cells were lysed through a 25 gauge needle and a 1ml syringe filled with Buffer A. Lysates were centrifuged for 20 seconds at 13000 rpm and afterwards the pellet was resuspended in 2/3 pellet volumes of Buffer B (20mM HEPES-KOH pH8.0, 1.5mM $MgCl_2$, 25% glycerol, 420mM NaCl, 0.2mM EDTA, 1mM DTT and 0.1mM AEBSF), small magnetic stirrers were transferred to each sample and samples were stirred for 30 minutes on ice. Suspensions were centrifuged at 12000 rpm for 10 minutes at 4°C; afterwards the supernatant was microdialyzed (Millipore Billerica, MA, USA) against Buffer C (30mM HEPES-KOH pH7.4, 100mM KCl, 5mM $MgCl_2$, 10% glycerol, 1mM DTT and 0.1mM AEBSF) for 1 hour at 4°C. At least 2.5µl of 1.5mg/ml protein was required for the cleavage assay. Extracts were frozen with liquid nitrogen and stored at -80°C.

Saccharomyces cerevisiae pre-tRNA-Phenylalanine (Phe) was amplified by PCR. Primer pairs were used as previously described by Weitzer *et al.* [11]. The forward primer sequence included a T7-RNA polymerase promoter: 5'- AATTTAATACG ACTCACTATAGGGGATTTAGCTCAGTTGGG -3' and the reverse primer sequence: 5'- TGGTGGGAATTCTGTGGATCGAAC -3'. 3 pmol of the PCR product was incubated in the MEGAshorscript T7 Kit (Ambion, Warrington, UK) according manufacturer's protocol. α-^{32}P-Guanine-TP (GTP) was included in the *in vitro* transcription reaction to radioactively bodylabel the pre-tRNA and extracted subsequently by running the product on a 10% denaturing acrylamide gel. The pre-tRNA was eluted in water and final concentration was made to 0.3M NaCl. RNA was precipitated with 3 volumes 100% ethanol for at least 1 hour at -20°C and the RNA pellet was dissolved in water to a final concentration of 1µM.

0.5µl of 1µM pre-tRNA was denatured at 100°C for 1 minute and cooled down again to room temperature. 2.5µl of the nuclear extract, 2µl Buffer D (100mM KCl, 5.75mM MgCl2, 2.5mM DTT, 5mM ATP pH 8.0, 6.1mM Spermidine-HCl pH8.0) and 0.5µl of 1µM pre-tRNA were mixed and incubated at 30°C for 15, 30 or 45 minutes. The reaction was stopped in 150µl of proteinase K buffer (140µl of 200mM Tris-HCl pH7.5,

25mM EDTA pH8.0, 300mM NaCl and 2% SDS plus 6.86ml of 100mg Proteinase K in 7.14ml Proteinase K storage buffer (50mM Tris-HCl pH8.0, 5mMCaCl2, 50% glycerol)) for 20 minutes at 65°C. RNA was phenol/chloroform extracted and precipitated by adding 3 volumes of 100% ethanol. Pellets were dissolved in formamide loading buffer containing xylene cyanol and bromophenol blue. Products were separated on a 10% denaturing acrylamide gel and visualized by Phosphorimaging.

qPCR for mRNA 3'end formation in patients

Fibroblasts were lysed in TRIzol (Invitrogen, Carlsbad, CA, USA) and sheared through a 27 gauge needle. RNA was isolated by chloroform extraction and isopropanol precipitation and dissolved in RNase free water. cDNA was synthesised from 5µg of RNA with 0.125 U random hexamer primers (pdN6) (Roche Applied Science, Penzberg, Upper Bavaria, Germany) in a 15µl reaction. For purification purposes cDNA was precipitated with 3 volumes of 100% ethanol and dissolved in 15µl H2O. 1µl cDNA was used in a 10µl reaction containing SYBR Green I Master Mix (Roche Applied Science). Two primer pairs were designed for the housekeeping transcript GAPDH. One primer pair was designed upstream of the polyadenylation signal, targeting the terminal exon and the 3'UTR of *GAPDH* (forward: 5'– GGCCTCCAAGGAGTAAGACC-3', reverse: 5'–AGGGACTCCCAGCAGTG –3'). The second primer pair was designed to overlap the polyadenylation signal and the region downstream of the polyadenylation signal (forward: 5'- CCTTGTCATGTACCATCAATAAAG -3', reverse: 5'- TGCCC CAGACCCTAGAATAA -3'). Downstream *GAPDH* regions were normalized against *GAPDH* 3'UTR regions. 18S ribosomal RNA (*RN18S1*) was used as an additional control for normalizing purposes. Minus Reverse Transcriptase samples were used as a control to test for genomic DNA contamination. Data were analysed using LinRegPCR analysis software [12].

qPCR for mRNA 3'end formation in zebrafish embryos

All zebrafish (*Danio rerio*) procedures were approved by the Academic Medical Center Animal Ethics Committee and experiments complied with standard animal care guidelines. Breeding and maintenance of all zebrafish stocks were performed as described previously [13]. Wild type (WT) TL zebrafish strains were crossed to generate embryos for morpholino injections. Fertilized embryos were collected and staged according to standard guidelines [14]. Morpholinos (MOs; Gene-tools, LLC, Philomath, OR, USA) were designed around the exon 3 splice donor site (5'- ACT TCTTTTTTTGTGTCTTACTTA -3') of the zebrafish *tsen2* gene. *Tsen54* splice site morpholinos were designed and used as described previously [5]. Standard control MOs (CoMO) were also provided by Gene-tools. Using fine glass needles and a microinjector (World Precision Instruments, Sarasota, FL, USA), 1-4 cell stage embryos were injected directly into the yolk sac with 6.6ng and 3.2ng splice MO or 6.6ng CoMO.

Total RNA was extracted from 50 injected embryos 24 hpf using TRIzol (Invitrogen) and chloroform for phase separation and isopropanol precipitation. cDNA was synthesised with random hexamer primers from 5µg of RNA as described above. 1µl cDNA was used in a 10µl reaction containing SYBR Green I Master Mix (Roche Applied Science). Two primer pairs were designed for the zebrafish housekeeping transcripts *gapdh*. One primer pair was designed upstream of the polyadenylation signal, targeting the terminal exon and the 3'UTR of *gapdh* (forward: 5'- GCAACC GTGTATGTGACCTG -3', reverse: 5'- GGAGAATGGTCGCGTATCAA -3'). The second primer pair was designed to overlap the polyadenylation signal and the region downstream of the polyadenylation signal (forward: 5'- TCTGTTAACAACTT GCGATGG -3', reverse: 5'- TTGCACCGAACAAGCTATTG -3'). Downstream *gapdh* regions were normalized against *gapdh* 3'UTR regions. Similarly, primers were designed for two other housekeeping transcripts, *actin* and *hprt1* (hypoxanthine phosphoribosyltransferase). One primer pair for *hprt1* and *actin* targeting its UTR (*hprt1* forward: 5'- GTGTGATTAGTGACAGTGGGAAA-3', *hprt1* reverse: 5'- CATTCAGATGCTCATGTTCCA-3', *actin* forward: 5'- TCCATCCTGGCTTCTCT GTC -3', *actin* reverse: 5'- AAGCACTTCCTGTGGACGAT-3') and one pair overlapping the polyadenylation signal (*hprt1* forward: 5'- GCAACCAATGTTGCCA AGAA-3', *hprt1* reverse: 5'- TCAAGACAGGATTTGCAAAGAA-3', *actin* forward: 5'- CAGTCTCTCAGCCGTACATTTG-3', *actin* reverse: 5'- GCAAGAGAAGACCCAA AACA-3'). Minus Reverse Transcriptase samples were used as a control to test for genomic DNA contamination. Data were analysed using LinRegPCR analysis software [12].

qPCR for *TSEN2* isoform analysis

Blood-, heart-, cerebellum-, hippocampus-, primary motor cortex- and somatosensory cortex samples were obtained from human control subjects. Informed consent for research purposes was obtained for all subjects. Sections were cut and dissolved in TRIzol Reagent (Invitrogen) for subsequent RNA isolation. RNA was isolated using RNeasy Mini protocol for QIAcube instrument (Qiagen, Venlo, The Netherlands) or using the PAXgene system (Qiagen) for blood samples. cDNA was synthesised from 1µg of RNA with oligodT_{12}-VN primers in a 15µl reaction. cDNA samples were 1:10 diluted and 1µl was used in a 10µl reaction containing SYBR Green I Master mix (Roche Applied Science). Primer pairs for the constitutive exon 2 (forward exon 2 primer: 5'- TGGCAGAAGCAGTTTTCCAT -3', reverse exon 2 primer: 5'- GGTCCTGA CCAAAAGGGATT -3') and the alternatively spliced exon 7 were designed. As exon 7 is only 51 nucleotides, the reverse primer extended into exon 8 (forward exon 7 primer 5'- TGGTCTATGCTCTGGGATGTT -3', reverse exon 8 primer 5'- GCT TTCCAGAGCTTCACTATCG -3'). *TSEN2* qPCRs were normalized to *GAPDH*. Data were analysed using LinRegPCR analysis software [12].

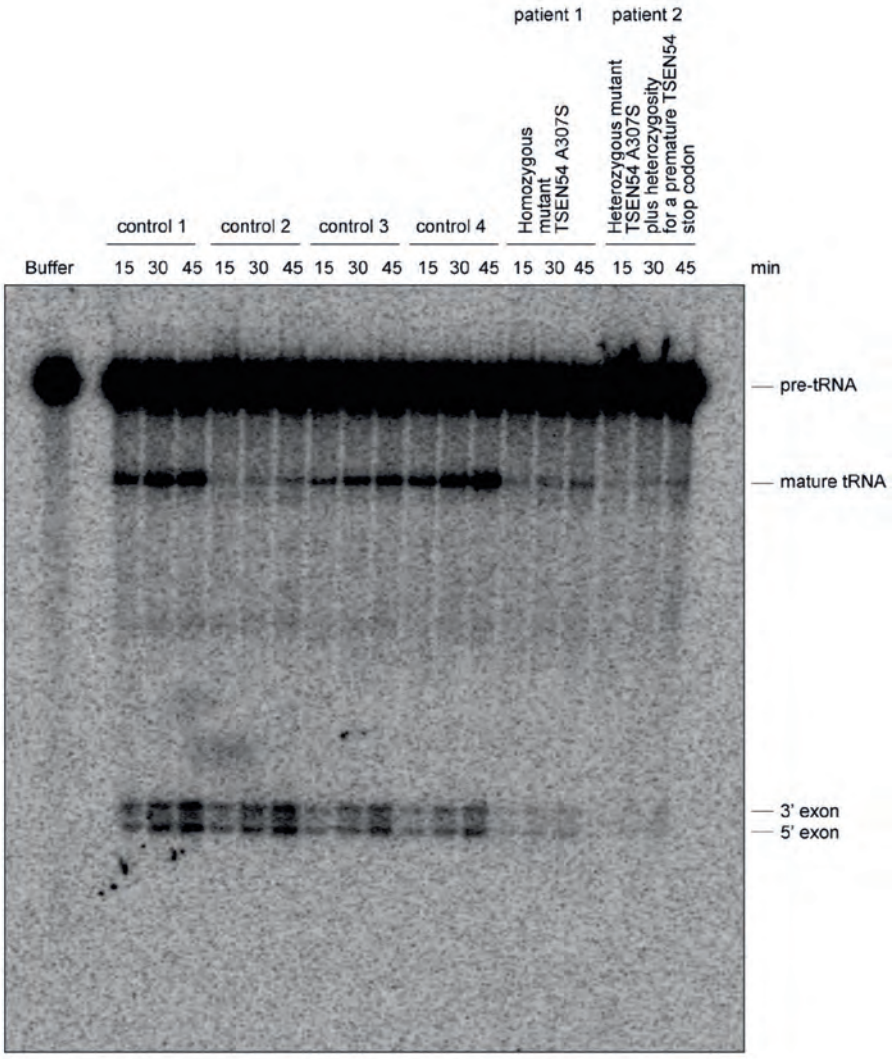

Figure 1. PCH2 nuclear extracts show reduced tRNA cleavage *in vitro*. A body-labeled pre-tRNA-Phe was incubated with nuclear extracts derived from control and PCH2 patient fibroblast cell lines. Samples were taken at the indicated time points and generation of tRNA exons was monitored by electrophoresis and detected by Phosphorimaging.

Mutation screen

We screened PCH cases referred to our laboratory for molecular genetic testing and negative on *TSEN* mutation analysis. Samples were submitted to our department for diagnostics and informed consent was obtained by referring physicians. The coding regions of *CLP1*, *TRPT1* and *HSPC117* were sequenced. If DNA levels were not

sufficient, DNA was amplified with the GenomiPhi V2 Amplification kit (GE Healthcare, Waukesha, USA) according to manufacturer's protocols. Primer pair sequences, PCR and sequence conditions are available upon request. PCR products were directly sequenced using BigDye Terminator sequencing kit and ABI PRISM 3730 DNA analyser (Applied Biosystems, Foster City, CA, USA). Sequences were analysed using the CodonCode Software version 3.5.6 (Dedham, MA, USA). Seventeen PCH patients were screened for *CLP1* and *TRPT1* mutations and 88 PCH patients were screened for *HSPC117* mutations.

Results

tRNA splicing activity assay

The enzymatic activity of the tRNA splicing endonuclease was examined in fibroblast extracts derived from four control subjects and two PCH subjects (Fig. 1). Patient 1 carried the common homozygous missense mutation in *TSEN54* (c.919G>T, p.A307S), Patient 2 was compound heterozygous for the common missense mutation in *TSEN54* and a heterozygous deletion leading to a premature termination signal (c.953delC, p.P318QfsX23). Both patients show reduced tRNA exon-generation in the tRNA splicing assay compared to controls, this effect was larger in Patient 2.

A follow-up experiment confirmed this result in three other patients (Patient 3, 4, 5) all carrying the homozygous c.919G>T (p.A307S) *TSEN54* mutation (Fig. 2a,b) and showed no impaired tRNA exon generation in three different control subjects (Control 7, 8, 9). In addition no reduced tRNA splicing activity was observed in a healthy heterozygous carrier of the c.919G>T *TSEN54* mutation, confirming that disruption of both alleles is required to develop PCH (Control 6).

Moreover we performed the same experiment in a case with PCH type 1 (Fig. 2a,b). A characteristic of PCH1 is additional loss of motor neurons in the anterior horns of the spinal cord. This patient has been screened for mutations in the different *TSEN* (*TSEN54*, *2*, *34*, *15*) genes and other PCH associated genes (*RARS2* and *VRK1*) but no mutation was identified [2]. In order to test whether TSEN-function was affected in this case with PCH1 (Control 5) we performed the same assay, but no reduced tRNA splicing activity could be measured, indicating that impaired tRNA splicing is not underlying PCH1 in this case.

mRNA 3'end formation analysis

As the TSEN complex is also involved in the processing of mRNA 3'ends we were interested to know whether PCH patients accumulated 3'ends. We tested nine patients

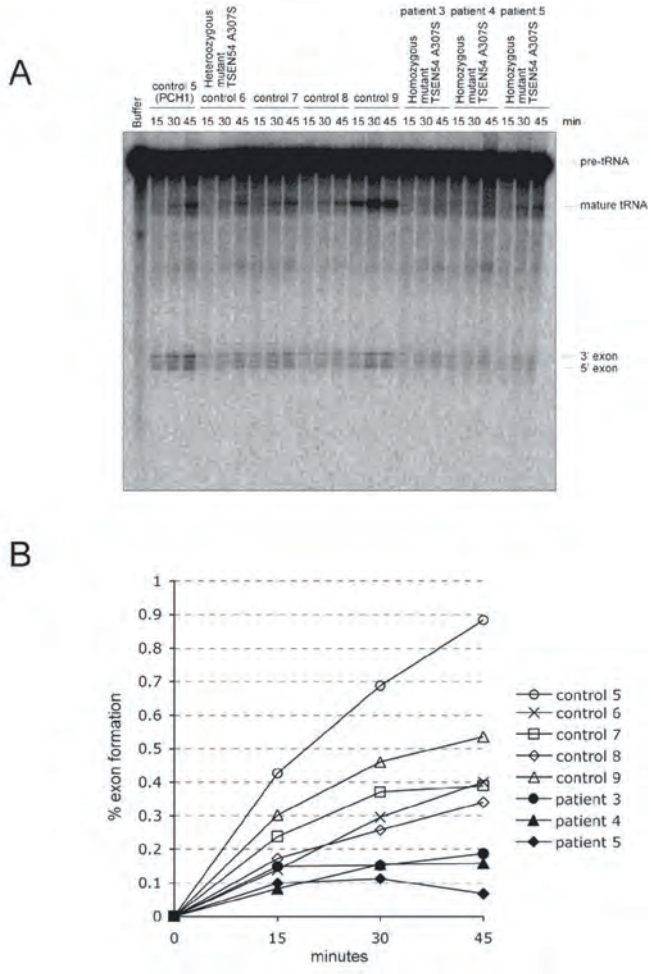

Figure 2. PCH2 nuclear extracts show reduced tRNA cleavage *in vitro*. (a) Nuclear extracts from control and PCH2 patient cell lines were incubated with a bodylabeled pre-tRNA-Phe. Samples were taken at the indicated time points and generation of tRNA exons was monitored by electrophoresis and detected by Phosphorimaging. (b) Quantification of tRNA exon levels (in % of the input pre-tRNA).

harbouring a *TSEN54* mutation and compared this with nine controls. We amplified the region overlapping the cleavage and polyadenylation signal in *GAPDH* and compared this to a region upstream to this signal. No significant effects in mRNA 3'end regions could be detected between fibroblast samples of patients and controls in *GAPDH* (Fig. 3).

In order to determine if tsen54 function is involved in mRNA 3'end formation *in vivo* we down-regulated *tsen54* in zebrafish embryos and compared *gapdh*, *hprt1* and

actin mRNA 3'ends with those mRNA 3'ends of *tsen2* down-regulated zebrafish. In zebrafish no evidence was found for involvement of tsen54 in mRNA 3'end processing. However an involvement of tsen2 in 3'end processing could be confirmed for *gapdh* (Fig. 4a), as higher levels of 3'ends were observed in morphants injected with the high dose of MO compared to the low dose tsen2 morphants and controls. No differences in 3'end formation were observed in tsen2 morphants for *hprt1* and *actin* (Fig. 4b,c).

TSEN2 isoform analysis

Expression of *TSEN2* exon 7 and a constitutive exon (exon 2) were determined by qPCR. Expression was determined in blood, heart, cerebellum, hippocampus and primary motor cortex of different control subjects. Of each tissue three control samples were available, only of the primary motor cortex just two samples were available. The three different tissue samples were not available from the same three individuals. Higher expression of *TSEN2* exon 2 in cerebellum was found compared to hippocampus, primary motor cortex, heart and blood (Fig. 5b). We found a similarly high expression for exon 7 in the cerebellum, but with generally lower levels of exon 7 expression among all tissue types (Fig. 5a).

Mutation analysis

In mammals there are two pathways of tRNA ligation: the yeast-like pathway and the Archaea-like pathway. pre-tRNA cleavage by TSEN generates a 2'- 3' cyclic phosphate at the 3' splice site and a 5'-OH group at the 5' splice site. In the yeast-like pathway the requirement for exon ligation by a yet to be identified ligase is the prior phosphorylation of the 5'-OH group of the 3' exon by CLP1 and opening of the 2'- 3'

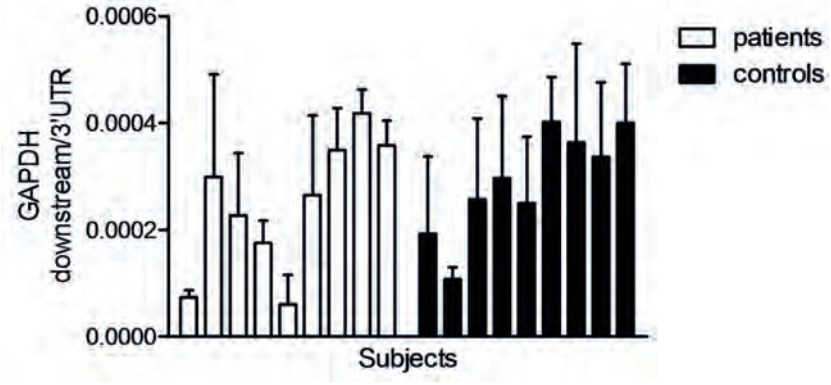

Figure 3. Expression analysis of *GAPDH* mRNA 3'ends normalized to its own transcript. No significant effects in mRNA 3'end regions could be detected between fibroblast samples of patients and controls in *GAPDH*.

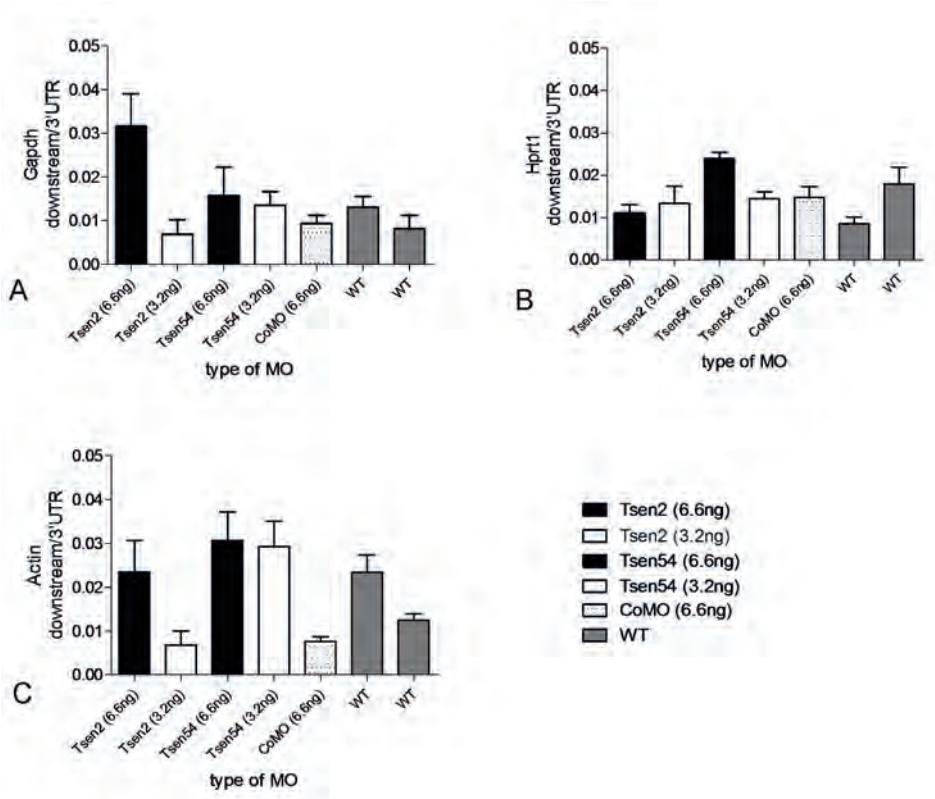

Figure 4. (a) Expression analysis of *gapdh* mRNA 3'ends normalized to its own transcript. No significant effects in mRNA 3'end regions could be detected between *tsen54* downregulated zebrafish embryos and controls (control morpholino injected fish and wild-type uninjected fish) in *gapdh*. More 3'ends of *gapdh* were observed in zebrafish embryos treated with a high dosage of *tsen2* morpholino. (b) Expression analysis of *hprt1* mRNA 3'ends normalized to its own transcript. No significant effects in mRNA 3'end regions could be detected between *tsen2* and *tsen54* downregulated zebrafish embryos and controls (control morpholino injected fish and wild-type uninjected fish) in *hprt1*. (c) Expression analysis of *actin* mRNA 3'ends normalized to its own transcript. No significant effects in mRNA 3'end regions could be detected between *tsen2* and *tsen54* downregulated zebrafish embryos and controls (control morpholino injected fish and wild-type uninjected fish) in *actin*.

cyclic phosphate of the 5' exon by an unknown diesterase (CPD) activity. The 5'-phosphate of the 3' exon is subsequently used for the ligation. A phosphotransferase (TRPT1) transfers the 2'-phosphate that arises after CPD activity to NAD. The Archaea-like ligation pathway involves a direct ligase (HSPC117) activity that joins the tRNA half-molecules using the phosphate of the 2'–3' cyclic phosphate as the junction phosphate [15,16]. In order to test these candidate genes in our cohort of unsolved PCH cases we screened, but did not identify mutations in the coding regions of *CLP1*, *TRPT1* and *HSPC117* in these cases.

Discussion

There are two known functions of the TSEN complex. The first and best studied function is the role of the TSEN complex in the intron removal of tRNAs. The tRNA splicing activity assay showed reduced tRNA exon generation in patients with a *TSEN54* mutation compared to controls. This effect was largest in Patient 2, who carried a null allele plus a missense mutation in *TSEN54*. Patient 1, 3, 4 and 5 were all homozygous for the c.919G>T (p.A307S) mutation in *TSEN54* and also showed reduced tRNA exon generation compared to controls. These findings are in line with the more severe phenotype observed in PCH4, in which there is a null allele plus a

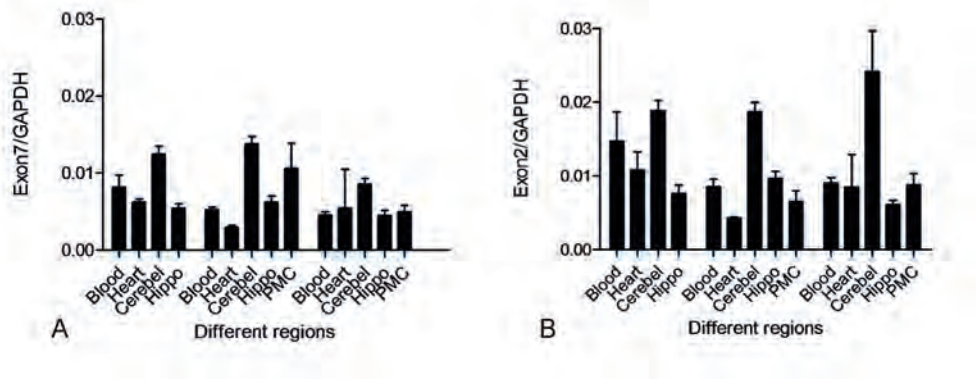

Figure 5. Expression profile of (a) exon 7 and (b) exon 2 of *TSEN2*. Higher expression of *TSEN2* exon 2 in cerebellum (Cerebel) can be observed compared to hippocampus (Hippo), primary motor cortex (PMC), heart and blood. A similar expression pattern for was observed, but with lower levels of exon 7 overall.

missense mutation which supports the loss of function hypothesis. Moreover a PCH1 case negative in *TSEN* mutation analysis did not show reduction in tRNA exon generation. This finding makes it unlikely that this PCH1 case carries an unidentified mutation in one of the non-coding regions of the *TSEN* genes or a transcriptional regulator of the TSEN complex. Depending on availability of patient fibroblasts, the tRNA splicing activity assay could be used as a diagnostic read-out to examine whether a patient would carry a *TSEN* mutation or not.

The second function of the TSEN complex is its role in mRNA 3'end processing. Although it is known that the TSEN complex associates with several factors involved in mRNA 3'end processing, direct involvement has only been confirmed once for TSEN2 [9]. Knock-down of *TSEN2* resulted in increased downstream *GAPDH* and *EF1a*

mRNA 3'ends. There was no effect of TSEN54 on mRNA 3'end formation, as we could not detect more *GAPDH* mRNA 3'ends in *TSEN54* mutated fibroblasts compared to controls. RNA derived from fibroblasts might not be the most suitable source for such an assay. The large inter-individual variation in expression is a problem, but no significant difference between nine patients and nine controls could be detected (Fig. 3). Patient 2 carrying one null allele and one mutated allele (second bar of Fig. 3) also did not show a significant effect on mRNA 3'end formation. *In vivo* experiments in zebrafish confirmed this result, as no accumulation of mRNA 3'ends in *tsen54* deprived zebrafish embryos was observed in any of the three tested transcripts. Evidence for a role of tsen2 (in the higher MO dose treated fish) in mRNA 3'end formation was confirmed in the *gapdh* transcript which agrees with has been found following *in vitro* knockdown of *TSEN2* in HEK293 cells. It is unclear why the *actin* and *hprt1* transcripts did not show this effect. Perhaps the effect observed in *gapdh* is due to variation and not due to *tsen2* knockdown. Another explanation could be that the regulation of 3'end processing of *hprt1* and *actin* is not regulated by tsen2. Furthermore it remains possible that qPCR is not sensitive enough to detect small differences in 3'ends. RNA-Seq of the transcriptome or a kinetic assay assessing the activity of the TSEN complex in 3'end processing might be an alternative method to detect such changes [11]. It is also possible that polyadenylation occurs but at a less efficient rate, meaning that a further downstream cleavage and polyadenylation site will be used, rather than the canonical AAUAA sequence. If this is the case, a Serial Analysis of Gene Expression (SAGE) will give more insight into whether there is accumulation of such ends compared to controls.

The TSEN2 wild-type protein is related to tRNA splicing, the Δex7 protein is associated with mRNA 3'end formation [9]. Expression analysis of *TSEN2* showed high expression in cerebellum compared to blood, heart, primary motor cortex and hippocampus. A strong cerebellar expression pattern for *TSEN54* at gestation week 8 and week 23 has been reported previously [2,5]. Both *TSEN2* exons, exon 2 and exon 7, had increased expression in cerebellum. As one can expect this expression is larger for TSEN2 wild-type as the constitutive exon 2 will be measured twice, in the wild-type and Δex7 transcript. Interestingly, the only two published *TSEN2* mutations in PCH compromise exon 7. One of them is a homozygous missense mutation (c.926A>G, p.Y309C) [2]. The other mutation is a heterozygous splice site mutation (c.960+ 1delGTAAG) identified in combination with the previous reported missense mutation (p.Y309C) [4]. The splice site mutation is predicted to lead to a skipping of exon 7, but no RNA was available to test this. We can conclude that an undisrupted exon 7 is necessary for normal development, meaning that the *TSEN2* Δex7 isoform is not affected in PCH. In line with this, the only effect we could measure was on tRNA splicing activity. We therefore propose impaired tRNA splicing as the pathomechanism underlying PCH.

In this chapter we show that a reduction in tRNA exon generation can be measured

in PCH fibroblasts. These data do not support impairment of mRNA 3' formation as a mechanism underlying PCH. Altogether this data is in advance of the hypothesis that loss of tRNA splicing is the underlying disease mechanism in PCH.

Reference List

1. Simonati A, Cassandrini D, Bazan D, Santorelli FM: TSEN54 mutation in a child with pontocerebellar hypoplasia type 1. Acta Neuropathol 2011.
2. Budde BS, Namavar Y, Barth PG, Poll-The BT, Nurnberg G, Becker C, van Ruissen F, Weterman MAJ, Fluiter K, te Beek E et al.: tRNA splicing endonuclease mutations cause pontocerebellar hypoplasia. Nat Genet 2008, 40:1113-1118.
3. Namavar Y, Chitayat D, Barth PG, van Ruissen F., de Wissel MB, Poll-The BT, Silver R, Baas F:TSEN54 mutations cause pontocerebellar hypoplasia type 5. Eur J Hum Genet 2011.
4. Namavar Y, Barth PG, Kasher PR, van Ruissen F., Brockmann K, Bernert G, Writzl K, Ventura K, Cheng EY, Ferriero DM et al.: Clinical, neuroradiological and genetic findings in pontocerebellar hypoplasia. Brain 2011, 134:143-156.
5. Kasher PR, Namavar Y, van Tijn P, Fluiter K, Sizarov A, Kamermans M, Grierson AJ, Zivkovic D, Baas F: Impairment of the tRNA-splicing endonuclease subunit 54 (tsen54) gene causes neurological abnormalities and larval death in zebrafish models of pontocerebellar hypoplasia. Hum Mol Genet 2011, 20:1574-1584.
6. Trotta CR, Miao F, Arn EA, Stevens SW, Ho CK, Rauhut R, Abelson JN: The yeast tRNA splicing endonuclease: a tetrameric enzyme with two active site subunits homologous to the archaeal tRNA endonucleases. Cell 1997, 89:849-858.
7. Genomic tRNA database. http://lowelab.ucsc.edu/GtRNAdb/. 2010.
8. Trotta CR, Paushkin SV, Patel M, Li H, Peltz SW: Cleavage of pre-tRNAs by the splicing endonuclease requires a composite active site. Nature 2006, 441:375-377.
9. Paushkin SV, Patel M, Furia BS, Peltz SW, Trotta CR: Identification of a human endonuclease complex reveals a link between tRNA splicing and pre-mRNA 3' end formation. Cell 2004, 117:311-321.
10. Takagaki Y, Manley JL: Complex protein interactions within the human polyadenylation machinery identify a novel component. Mol Cell Biol 2000, 20:1515-1525.
11. Weitzer S, Martinez J: The human RNA kinase hClp1 is active on 3' transfer RNA exons and short interfering RNAs. Nature 2007, 447:222-226.
12. Ruijter JM, Ramakers C, Hoogaars WM, Karlen Y, Bakker O, van den Hoff MJ, Moorman AF: Amplification efficiency: linking baseline and bias in the analysis of quantitative PCR data. Nucleic Acids Res 2009, 37:e45.
13. Klooster J, Yazulla S, Kamermans M: Ultrastructural analysis of the glutamatergic system in the outer plexiform layer of zebrafish retina. J Chem Neuroanat 2009, 37:254-265.
14. Kimmel CB, Ballard WW, Kimmel SR, Ullmann B, Schilling TF: Stages of embryonic development of the zebrafish. Dev Dyn 1995, 203:253-310.
15. Popow J, Englert M, Weitzer S, Schleiffer A, Mierzwa B, Mechtler K, Trowitzsch S, Will CL, Luhrmann R, Soll D et al.: HSPC117 is the essential subunit of a human tRNA splicing ligase complex. Science 2011, 331:760-764.
16. Filipowicz W, Shatkin AJ: Origin of splice junction phosphate in tRNAs processed by HeLa cell extract. Cell 1983, 32:547-557.

Chapter 7

Summary and discussion

Summary and discussion

Pontocerebellar Hypoplasia (PCH) is a group (PCH1-7) of neurodegenerative disorders with early onset of stunted brain growth with progressive atrophy affecting cerebellum, pons, olivary nuclei and, to a lesser degree, the cerebral cortex. Clinically, patients from all subtypes have disturbed motor coordination, progressive microcephaly, mental retardation and seizures. Life expectancy ranges from neonatal death to death in adulthood in rare occasions. Most patients die during infancy. Prior to the identification of genes in PCH, a subdivision of five PCH subtypes was made, PCH1 to PCH5 [1-3].

PCH1 has been characterised as morphologically similar to spinal muscular atrophy type 1, but with hypoplasia of cerebellum and variable involvement of pons and cerebrum. There is hypotonia, due to spinal cord involvement [4]. PCH2 is the most common subtype of PCH and has been associated with movement disturbances like chorea and extrapyramidal dyskinesias [5]. PCH3 has been described in three families only and presents with cerebellar atrophy, short stature, hypotonia and primary optic atrophy [6]. PCH4 and PCH5 have been characterised with a prenatal onset of symptoms like polyhydramnios, contractures and severe neonatal clonus. Neuropathologically, the olivary nuclei are C-shaped and the ventral pons and cerebellum are more severely affected than in the other subtypes [7]. Since 2007 two more subtypes were added, meaning that the term PCH now denotes a group of seven disorders with hypoplasia of pons and cerebellum. In 2007, PCH6 has been described as a disorder with severe encephalopathy with mild respiratory chain abnormalities and elevated cerebrospinal fluid (CSF) lactate, moreover the first PCH associated gene was identified. PCH6 is caused by mutations in the nuclear encoded mitochondrial arginyl-tRNA synthetase gene (*RARS2*) [8]. PCH7 has recently been described in one case with PCH and additional genital abnormalities [9].

In 2008, we identified the molecular basis of PCH2 by linkage analysis in a large family with PCH2. This family was part of a genetic Dutch isolate in which PCH was previously described [5]. All 10 affected family members were homozygous carriers of the c.919G>T (p.A307S) mutation in the tRNA splicing endonuclease subunit 54 gene (*TSEN54*). *TSEN54* mutations were also found in 37 of the other PCH2 cases. Analysis of the other tRNA splicing endonuclease subunit genes in the remaining PCH2 cases (without *TSEN54* mutations) revealed missense mutations in *TSEN2* and *TSEN34*. This strongly suggested that *TSEN* mutations are responsible for PCH2.

Analysis of PCH1 and PCH4 cases revealed that *TSEN54* mutations were also found in PCH4 cases. These mutations were more severe than the mutations seen in PCH2; two PCH4 cases were compound heterozygous for a nonsense mutation plus a missense mutation and one PCH4 case carried three missense mutations in *TSEN54*. Neuropathological comparison of PCH2 and PCH4 showed that in PCH4 cerebellar folia are virtually absent, whereas the PCH2 cerebellum only showed diminished folia.

The truncating mutations seen in PCH4 in combination with a more severe phenotype of perinatal complications like polyhydramnios and contractures imply that loss of TSEN function is most likely the underlying disease mechanism in PCH2 and PCH4. High expression of *TSEN54* was noted in neurons of pons, cerebellar dentate nucleus and olivary nuclei during the second trimester of the pregnancy.

The tRNA splicing endonuclease complex is involved in splicing of intron-containing tRNAs. Only a small minority (6%) of tRNAs requires intron removal by the endonuclease. Another function of the TSEN complex is thought to involve mRNA 3'end processing, as *in vitro* knockdown of *TSEN2* resulted in an accumulation of 3'ends in two different transcripts [10].

Northern blot analysis of tRNA-Tyr in fibroblast samples of PCH2 cases with a *TSEN54* mutation, failed to show a defect in maturation, suggesting that under the conditions of *in vitro* culture of fibroblasts the *TSEN54* mutations did not abolish tRNA maturation. A complete block in tRNA-Tyr maturation was not expected since a completely non-functional TSEN complex is not likely to be compatible with life.

RARS2, mutated in PCH6, is also involved in tRNA processing. RARS2 is involved in charging arginine (Arg) to its mitochondrial (mt)-tRNA-Arg. In *RARS2* mutated fibroblasts, a reduction in the amount of the mt-tRNA-Arg was observed. Nevertheless the residual mt-tRNA-Arg transcript was almost completely charged, suggesting that uncharged mt-tRNA-Arg is unstable [8].

Following the identification of genes in PCH2, PCH4 and PCH6 an extensive genotype-phenotype study has been performed in all cases (169 patients) that were referred to our laboratory for PCH diagnostics in order to capture the complete spectrum of the disease. In these cases we screened the *TSEN* genes (*TSEN54*, *2*, *34*, *15*), the *RARS2* gene and the Vaccinia Related Kinase 1 gene (*VRK1*), the latter associated with an atypical presentation of PCH1 [8,11]. Analysis of patients for which clinical information and Magnetic Resonance Imaging (MRI) were available, confirmed that the common *TSEN54* mutation was associated with extrapyramidal dyskinesias and/or spasticity and progressive microcephaly, as was previously described as PCH2 [1]. Moreover the c.919G>T (p.A307S) mutation was associated with flat dragonfly-like cerebellar hemispheres. Cases with more severe mutations in *TSEN54* (nonsense or splice site) in combination with a missense mutation have a PCH4 phenotype. Analysis of this large cohort allowed us to conclude that in the PCH4 cases more supratentorial involvement was present; a severe delay in the maturation of neocortex was found in combination with craniocerebral dysproportion presumably due to prenatal onset of diminished brain growth. In a minority of the PCH cases mutations were found in *RARS2* and *TSEN2*. In a large group of 63 cases no mutations were found, however only in 13 of them sufficient clinical information was available to state that these cases fulfill our criteria for PCH, thus, mutations in other genes or in non-coding regions of

TSEN genes could underlie PCH in these patients.

Identification of the genes for PCH2 and PCH4 allowed us to screen PCH5 too. In 2006, PCH5 was described in a single family as a separate PCH subtype with intrauterine seizures and marked degeneration of the cerebellar vermis as distinguishing features. However after closer examination of our large series of PCH4 patients, we noted that some PCH4 cases also had severe vermal involvement and the neonatal clonus was similar to the seizure-like activity observed in PCH5. Genetic analysis of this PCH5 family showed that the mutational spectrum was similar to PCH4. The proband of the PCH5 family was compound heterozygous for a splice site mutation and the common mutation in *TSEN54*. Thus PCH5 and PCH4 are identical disorders.

In order to study the disease mechanism leading to PCH we developed a zebrafish model for PCH. Zebrafish embryos 24 hours post fertilization showed strong *tsen54* expression in brain, mostly in telencephalon and mid-hindbrain, comparable with high expression of *TSEN54* in telencephalon and metencephalon in an 8 week old human embryo. Downregulation of either *tsen54* or *rars2* with antisense oligonucleotides resulted in brain hypoplasia with loss of structural definition of the mid-hindbrain boundary and increased cell death. This phenotype could be partially rescued by co-injecting human *TSEN54* and *RARS2* mRNA respectively. Analysis of the expression of specific neurodevelopmental markers including fibroblast growth factor (*fgf8*) and orthodenticle homeobox 2 (*otx2*) revealed that the brain structures had developed normally in the morphant embyros. In addition, increased cell death was observed within the brains of the *tsen54* and *rars2* morphants. Taken together, these data agree with the suggestion that PCH is a neurodegenerative disease rather than a developmental migration disorder. Germline knockout fish were isolated from a *N*-methyl-*N*-nitrosourea (ENU) mutant zebrafish library. Zebrafish homozygous for a *tsen54* premature stop-codon mutation did not show overt defects in brain development but die 9 days post fertilization, confirming that TSEN54 is essential for survival. We assume that stable *tsen54* knockout fish survive the first week on maternal *TSEN54* mRNA and/or tRNAs derived from the oocyte.

The TSEN complex is not only involved in tRNA splicing, it has also been implicated in mRNA 3'end formation [10]. Therefore either impaired tRNA splicing or impaired mRNA 3'end formation could be responsible for PCH, or both. To distinguish between these possibilities we analysed the tRNA splicing activity of PCH2 fibroblasts in an *in vitro* assay. Nuclear extracts of PCH2 and PCH4 cases showed reduced tRNA processing. PCH4 extracts showed less activity than PCH2 extracts, which is in line with the mutations in these disorders; missense mutations and nonsense versus homozygous missense mutations. No evidence was found for impaired mRNA 3'end formation in PCH, *in vitro* and *in vivo*.

In summary, we have shown that mutations in *TSEN54*, *TSEN2* and *TSEN34* can

result in PCH2, PCH4 and PCH5. We also show that loss of TSEN54 function is responsible for a phenotype of neurodegeneration, probably due to reduced tRNA splicing metabolism.

Implications

In this thesis we tried to identify genes responsible for PCH and to understand the pathogenesis of the disease. Identification of genes involved in PCH provided new insight into the clinical spectrum of the disease which resulted in some discussion about the nomenclature of the PCH subtypes. Should we adhere to the clinical classification or move to a genetic classification? There is a certain variation in the clinical spectrum of PCH caused by the same mutation, but the differences are not that large.

PCH classification and nomenclature

The identification of genes in PCH showed that there was considerable overlap of the clinical phenotype with the genetic classification. *RARS2* mutations have been found in PCH1 and PCH6, but are still very rare compared to *TSEN* mutations. Patients with *RARS2* mutations have elevated CSF lactate levels and mild mitochondrial chain abnormalities, accompanied with the PCH phenotype. Almost all PCH2 cases with identified mutations have *TSEN54* mutations [7,12]. PCH4 and PCH5 are also caused by *TSEN54* mutations [7,13]. In one PCH1 family *TSEN54* mutations were identified too [14]. Mutations in two other tRNA splicing endonuclease subunit genes (*TSEN2* and *TSEN34*) were found to be responsible for PCH2 in rare occasions [12]. Therefore we propose a new classification for disorders caused by *TSEN* mutations; the TSENopathies. Valayannopoulus *et al.* show that *CASK* mutations can give a cerebellar dragonfly-like phenotype similar to the dragonfly-phenotype observed in *TSEN54* mutated patients [15]. However, *CASK* mutations can lead to a spectrum of disorders, ranging from FG syndrome with relative macrocephaly and behavioural disturbances to an X-linked disorder with microcephaly and hypoplasia of pons and cerebellum [16,17]. This shows that the presence of cerebellar hypoplasia (with or without pontine involvement) is not exclusive for the diagnosis PCH. It is important to keep in mind that hypoplasia of pons and cerebellum can be a symptom of several genetic and non-genetic disorders. It seems that we are moving into a new era of PCH classification, in which the current non-genetic classification does not necessarily fit as neatly. Indeed, as it is likely that more mutations will be identified in *TSEN54*, *TSEN2*, *TSEN34*, *RARS2* or *CASK*, the appearance of several different clinical presentations will add further complexity to the categorization on a non-genetic basis. Furthermore the genetic basis in PCH3, PCH7 and the majority of the PCH1 cases has not been discovered yet. Hopefully genes responsible for these subtypes will be found soon, adding to the fast growing list of genes responsible for various types of disorders with hypoplasia of pons and cerebellum. With careful clinical practice, meticulous neurological and radiological

examination and testing of candidate genes it will be hopefully possible to make a molecular diagnosis in most cases with pontocerebellar hypoplasia.

Pathomechanism

It is not yet clear how mutations in the *TSEN* and *RARS2* genes lead to a specific neurodegenerative disorder. It is tempting to point in the direction of impaired protein synthesis and impaired tRNA processing in PCH. Even though protein synthesis is the one thing that the TSEN complex and RARS2 have in common and although tRNA splicing (necessary for translation) is reduced in PCH, it does not explain everything. There are several different diseases known with mutations in protein synthesis genes, leading to other diseases than PCH. For example the white matter disease leukoencephalopathy with brain stem and spinal cord involvement and lactate elevation (LBSL) is caused by mutations in the mitochondrial aspartyl-tRNA synthetase (*DARS2*) [18]. Not all disorders with tRNA synthetase mutations have a neuronal phenotype as mutations in the mitochondrial seryl-tRNA synthetase gene (*SARS2*) result in a non-neurological multisystem disease with Hyperuricemia, Pulmonary Hypertension, Renal Failure and Alkalosis (HUPRA-syndrome) [19]. This suggests that tRNA synthetases can also have alternative functions [20].

Even if impaired protein synthesis is indeed the reason why patients develop PCH, it is not understood how and why the brain is specifically affected. Electron Microscopy of a biopsy taken from the cortex of a PCH2 case at the age of 16 months (homozygous for the common mutation in *TSEN54*) showed highly dense (opaque) Endoplasmic Reticulum (ER) and studded ribosomes accumulating at the ER membrane. Mitochondria and Golgi-complex showed normal morphology [5]. Perhaps the impaired supply of mature tRNAs will lead to an accumulation of ribosomes at mRNA transcripts. As a disease mechanism for *TSEN* mediated PCH we propose that impaired tRNA splicing potentially leads to impaired tRNA formation which could delay protein synthesis significantly, specifically in those cases in which there is a high demand.

Future directions

The big question is why only the brain is affected by tRNA splicing endonuclease mutations. Defects in protein synthesis in cases in which there is a high demand, is a likely explanation. However we cannot exclude that there is a brain specific alternative function for the TSEN complex. The TSEN complex might be involved in splicing or cleavage of other (brain-specific) RNA species. High-throughput sequencing of RNA isolated by crosslinking immunoprecipitation (HITS-CLIP) might identify novel RNA species processed by the TSEN complex [21]. To distinguish between these options one should study tRNA splicing in neuronal tissue. Zebrafish neurons homozygous for *tsen54* mutations are suitable or induced pluripotent stem cell (iPS) technology might be a good tool to convert patient fibroblasts to neuronal cells.

If reduced tRNA splicing is indeed the limiting factor, it should be possible to rescue the lethality associated with the homozygous p.R228X *tsen54* mutant zebrafish by the expression of a transgene containing mature tRNA genes which do not require intronic splicing [22,23]. If it is possible to promote survival in these fish using this approach, it is very likely that impaired tRNA splicing is indeed disease causing in PCH.

Even then it is not understood how impaired tRNA splicing leads to neurodegeneration. Metabolic labelling experiments should provide more insight into the amount of protein synthesis and amino acid turnover in the brain. Maybe higher protein metabolism is required in developing brain tissue. Once we have a greater understanding for the cause of PCH, a search for intervention mechanisms in PCH can be started.

Reference List

1. Barth PG: Pontocerebellar hypoplasias. An overview of a group of inherited neurodegenerative disorders with fetal onset. Brain Dev 1993, 15:411-422.
2. Barth PG: Pontocerebellar hypoplasia -- how many types? Eur J Paediatr Neurol 2000, 4:161-162.
3. Patel MS, Becker LE, Toi A, Armstrong DL, Chitayat D: Severe, fetal-onset form of olivopontocerebellar hypoplasia in three sibs: PCH type 5? Am J Med Genet A 2006, 140:594-603.
4. Norman RM: Cerebellar hypoplasia in Werdnig-Hoffmann disease. Arch Dis Child 1961, 36:96-101.
5. Barth PG, Vrensen GF, Uylings HB, Oorthuys JW, Stam FC: Inherited syndrome of microcephaly, dyskinesia and pontocerebellar hypoplasia: a systemic atrophy with early onset. J Neurol Sci 1990, 97:25-42.
6. Rajab A, Mochida GH, Hill A, Ganesh V, Bodell A, Riaz A, Grant PE, Shugart YY, Walsh CA: A novel form of pontocerebellar hypoplasia maps to chromosome 7q11-21. Neurology 2003, 60:1664-1667.
7. Namavar Y, Barth PG, Kasher PR, van Ruissen F., Brockmann K, Bernert G, Writzl K, Ventura K, Cheng EY, Ferriero DM et al.: Clinical, neuroradiological and genetic findings in pontocerebellar hypoplasia. Brain 2011, 134:143-156.
8. Edvardson S, Shaag A, Kolesnikova O, Gomori JM, Tarassov I, Einbinder T, Saada A, Elpeleg O: Deleterious mutation in the mitochondrial arginyl-transfer RNA synthetase gene is associated with pontocerebellar hypoplasia. Am J Hum Genet 2007, 81:857-862.
9. Anderson C, Davies JH, Lamont L, Foulds N: Early Pontocerebellar Hypoplasia with Vanishing Testes: A New Syndrome? Am J Med Genet Part A 2011, 155:667-672.
10. Paushkin SV, Patel M, Furia BS, Peltz SW, Trotta CR: Identification of a human endonuclease complex reveals a link between tRNA splicing and pre-mRNA 3' end formation. Cell 2004, 117:311-321.
11. Renbaum P, Kellerman E, Jaron R, Geiger D, Segel R, Lee M, King MC, Levy-Lahad E: Spinal muscular atrophy with pontocerebellar hypoplasia is caused by a mutation in the

VRK1 gene. Am J Hum Genet 2009, 85:281-289.

12. Budde BS, Namavar Y, Barth PG, Poll-The BT, Nurnberg G, Becker C, van Ruissen F, Weterman MAJ, Fluiter K, te Beek E et al.: tRNA splicing endonuclease mutations cause pontocerebellar hypoplasia. Nat Genet 2008, 40:1113-1118.

13. Namavar Y, Chitayat D, Barth PG, van Ruissen F., de Wissel MB, Poll-The BT, Silver R, Baas F: TSEN54 mutations cause pontocerebellar hypoplasia type 5. Eur J Hum Genet 2011.

14. Simonati A, Cassandrini D, Bazan D, Santorelli FM: TSEN54 mutation in a child with pontocerebellar hypoplasia type 1. Acta Neuropathol 2011.

15. Valayannopoulos V, Michot C, Rodriguez D, Hubert L, Saillour Y, Labrune P, de LJ, Brunelle F, Amiel J, Lyonnet S et al.: Mutations of TSEN and CASK genes are prevalent in pontocerebellar hypoplasias type 2 and 4. Brain 2011.

16. Najm J, Horn D, Wimplinger I, Golden JA, Chizhikov VV, Sudi J, Christian SL, Ullmann R, Kuechler A, Haas CA et al.: Mutations of CASK cause an X-linked brain malformation phenotype with microcephaly and hypoplasia of the brainstem and cerebellum. Nat Genet 2008, 40:1065-1067.

17. Piluso G, D'Amico F, Saccone V, Bismuto E, Rotundo IL, Di DM, Aurino S, Schwartz CE, Neri G, Nigro V: A missense mutation in CASK causes FG syndrome in an Italian family. Am J Hum Genet 2009, 84:162-177.

18. Scheper GC, van der Klok T, van Andel RJ, van Berkel CG, Sissler M, Smet J, Muravina TI, Serkov SV, Uziel G, Bugiani M et al.: Mitochondrial aspartyl-tRNA synthetase deficiency causes leukoencephalopathy with brain stem and spinal cord involvement and lactate elevation. Nat Genet 2007, 39:534-539.

19. Belostotsky R, Ben-Shalom E, Rinat C, Becker-Cohen R, Feinstein S, Zeligson S, Segel R, Elpeleg O, Nassar S, Frishberg Y: Mutations in the mitochondrial seryl-tRNA synthetase cause hyperuricemia, pulmonary hypertension, renal failure in infancy and alkalosis, HUPRA syndrome. Am J Hum Genet 2011, 88:193-200.

20. Park SG, Schimmel P, Kim S: Aminoacyl tRNA synthetases and their connections to disease. Proc Natl Acad Sci U S A 2008, 105:11043-11049.

21. Licatalosi DD, Mele A, Fak JJ, Ule J, Kayikci M, Chi SW, Clark TA, Schweitzer AC, Blume JE, Wang X et al.: HITS-CLIP yields genome-wide insights into brain alternative RNA processing. Nature 2008, 456:464-469.

22. Kasher PR, Namavar Y, van Tijn P, Fluiter K, Sizarov A, Kamermans M, Grierson AJ, Zivkovic D, Baas F: Impairment of the tRNA-splicing endonuclease subunit 54 (tsen54) gene causes neurological abnormalities and larval death in zebrafish models of pontocerebellar hypoplasia. Hum Mol Genet 2011, 20:1574-1584.

23. Genomic tRNA database. http://lowelab.ucsc.edu/GtRNAdb/. 2010.

Summary (Dutch)

Nederlandse samenvatting

Pontocerebellar Hypoplasie (PCH) is een groep van zeven (PCH1-7) neurodegeneratieve aandoeningen die al start voor de geboorte en zich uit in hypoplasie en atrofie van de hersenen, met nadruk op het cerebellum, de pons, de olijfkernen en in mindere mate ook de cerebrale cortex. Patiënten uit alle subtypes hebben centrale motorische stoornissen, progressieve microcefalie, cognitieve defecten en epilepsie. De levensverwachting varieert van sterfte in de neonatale periode tot in de volwassen periode. De meeste patiënten sterven echter tijdens de kinderjaren. Voorafgaand aan de identificatie van de genen verantwoordelijk voor PCH bestond er al een onderverdeling in vijf subtypes, namelijk PCH1-5 [1-3], gebaseerd op voor elk subtype unieke verschijnselen.

PCH1 heeft naast de gemeenschappelijke kenmerken van de PCH groep, degeneratie van de spinale motorische voorhoorncellen welke histologisch sterk lijkt op de Spinale Musculaire Atrofie groep, overigens zonder de moleculair-genetische afwijkingen van deze groep van aandoeningen. De hypotonie en spierzwakte die gezien wordt bij PCH1 berust op deze degeneratie [4].

PCH2 is het meest voorkomende PCH subtype en uit zich in motorische stoornissen, zoals chorea en extrapiramidale dyskinesieën, naast wisselende spasticiteit [5]. PCH3 is slechts beschreven in drie families en kenmerkt zich door cerebellaire atrofie, een korte gestalte, hypotonie en primaire opticus atrofie [6]. PCH4 en PCH5 worden getypeerd door een prenatale aanvang van de symptomen, zoals polyhydramnions, contracturen en een ernstige neonatale clonus. De olijfkernen hebben een immature C-vorm zonder undulaties en de ventrale pons en het cerebellum zijn zwaarder getroffen dan bij de andere subtypen [7]. Sinds 2007 zijn er twee subtypen bijgekomen. In 2007 werd PCH6 voor het eerst beschreven als een encefalopathie, met ademhalingsketen defecten en een verhoogd lactaatgehalte in de liquor cerebrospinalis. [8]. PCH7 werd onlangs beschreven in een patiënt met PCH met daarnaast bestaande genitale afwijkingen, leidend tot progressieve involutie van de mannelijke genitalia [9].

Met behulp van koppelingsonderzoek hebben wij in 2008 de genetische basis in een grote familie met PCH2 kunnen vinden. Deze Nederlandse familie was onderdeel van een genetisch gesloten gemeenschap waar PCH al eerder was beschreven [1]. Alle tien getroffen familieleden waren homozygote dragers van de c.919G>T (p.A307S) mutatie in het tRNA splicing endonuclease subunit 54 gen (*TSEN54*). *TSEN54* mutaties werden ook gevonden in 37 andere PCH2 patiënten. Twee andere PCH2 patiënten (zonder *TSEN54* mutaties) bleken mutaties in twee andere tRNA splicing endonuclease subunit genen te hebben, namelijk in *TSEN2* en *TSEN34*. Na sequentie analyse van deze genen in PCH1 en PCH4 patiënten, bleek dat *TSEN54* mutaties ook werden gevonden in PCH4.

Deze PCH4 mutaties zijn ernstiger dan de mutaties die bij PCH2 patiënten waren gevonden; twee PCH4 patiënten waren compound heterozygoot voor een nonsense mutatie (een mutatie die resulteert in een stop-codon) plus een aminozuursubstitutie en bij één PCH4 patiënt werden drie aminozuursubstituties in *TSEN54* gevonden. Ook fenotypische verschillen tussen PCH2 en PCH4 zijn gradueel, met de ernstiger vormen bij PCH4. Zo blijkt bij neuropathologische vergelijking van PCH2 en PCH4 dat de cerebellaire folia nagenoeg afwezig zijn bij PCH4, terwijl bij PCH2 het cerebellum minder folia heeft dan normaal, maar meer dan bij PCH4 worden gevonden. De ernstigere mutaties bij PCH4 patiënten in combinatie met een ernstiger fenotype met perinatale complicaties, zoals polyhydramnions en contracturen, ondersteunen de hypothese dat het verlies van TSEN functie het onderliggende ziektemechanisme is in PCH2 en PCH4. *In situ* hybridisatie toonde hoge expressie van *TSEN54* mRNA in neuronen van de pons, de nucleus dentatus en de olijfkeren tijdens het tweede trimester van de zwangerschap.

Het tRNA splicing endonuclease complex is betrokken bij de splicing van intron-bevattende tRNAs. Slechts een kleine minderheid (6%) van de tRNA's hebben een intron. Bij een andere studie resulteerde *in vitro* knockdown van *TSEN2* in een accumulatie van mRNA 3'uiteindes van twee verschillende transcripten; daarom wordt gedacht dat het TSEN complex tevens betrokken is bij mRNA 3'eindformatie [10]. Northern blot analyse van tRNA-Tyrosine (Tyr) in fibroblasten van PCH2 patiënten met een *TSEN54* mutatie laten geen maturatie defect zien. Dit suggereert dat *TSEN54* mutaties *in vitro* niet tot een tRNA maturatie probleem leiden, tenminste niet in fibroblasten. Een compleet maturatie defect in tRNA-Tyr werd niet verwacht, omdat een volledig niet-functionerend TSEN complex waarschijnlijk niet verenigbaar is met het leven. De vraag naar het mechanisme dat *in vivo* leidt tot de ziekteverschijnselen bij *TSEN54* mutaties is dus nog niet éénduidig beantwoord.

Mutaties in het gen dat codeert voor het mitochondriale arginine-tRNA synthetase (RARS2) liggen ten grondslag aan PCH6. RARS2, is ook betrokken bij het verwerken van tRNAs. RARS2 speelt een rol bij de aminoacylatie van Arginine (Arg) aan het mitochondriale-tRNA-Arg. In *RARS2* gemuteerde fibroblasten, werd een reductie van mt-tRNA-Arg waargenomen. Toch was deze residuele mt-tRNA-Arg bijna volledig geaminoacyleerd, wat suggereert dat het niet-geaminoacyleerde mt-tRNA-Arg instabiel is [8].

Na identificatie van de genen in PCH2, PCH4 en PCH6 werd door ons een uitgebreide studie verricht naar de correlatie tussen genotype en fenotype bij alle 169 patienten. Dit materiaal werd in ons laboratorium onderzocht op PCH genen. In deze 169 patiënten hebben wij de *TSEN* genen (*TSEN54*, *2*, *34*, *15*), het *RARS2* gen, en het Vaccinia Related Kinase 1 gen (*VRK1*) gescreend op mutaties [8]. Mutaties in *VRK1* zijn geassocieerd met een atypische variant van PCH1 [11]. Analyse van die patiënten waarvan ook klinische informatie en Magnetic Resonance Imaging (MRI) beschikbaar

was, bevestigde dat de c.919G>T (p.A307S) *TSEN54* mutatie sterk geassocieerd is met extrapiramidale dyskinesieën en/of spasticiteit en progressieve microcefalie, zoals eerder was beschreven bij PCH2 [1]. Bovendien is de c.919G>T (p.A307S) mutatie geassocieerd met een platte libelachtige vorm van de cerebellaire hemisferen met relatieve sparing van de vermis. Patiënten met de meer ernstige mutaties in *TSEN54* (nonsense of splice site mutaties) in combinatie met een aminozuursubstitutie hebben een PCH4 fenotype. Deze grote patiëntengroep maakte het mogelijk te concluderen dat er bij PCH4 sprake is van meer supratentoriële betrokkenheid met daarbij een ernstige vertraging in de maturatie van de neocortex, in combinatie met een relatief verhoogde hoeveelheid liquor. In een minderheid van de PCH patiënten werden mutaties gevonden in *RARS2* en *TSEN2*. In 63 patiënten werden geen mutaties gevonden; maar in deze restgroep was van slechts 13 patiënten voldoende klinische informatie beschikbaar om de klinische diagnose PCH te ondersteunen. Ergo kunnen mutaties in andere genen of in niet-coderende regio's van *TSEN* genen ten grondslag liggen aan PCH bij deze patiënten.

Identificatie van de genen voor PCH2 en PCH4 stelde ons ook in staat om PCH5 te bestuderen. In 2006 werd PCH5 beschreven in één familie als een apart subtype van PCH met intra-uteriene convulsies en degeneratie van de cerebellaire vermis als onderscheidend kenmerk. Na bestudering van onze grote groep PCH4 patiënten stelden we vast dat sommige PCH4 patiënten, net als de PCH5 patiënten, deze ernstige betrokkenheid van de vermis hebben en dat de neonatale clonus die bij PCH4 gezien werd vergelijkbaar is met de intra-uteriene convulsies die PCH5 patiënten hebben. DNA analyse van deze PCH5 familie toonde aan dat het mutatie-profiel ook vergelijkbaar is met het mutatie-profiel bij PCH4. De proband van de PCH5 familie was compound heterozygoot voor een splice site mutatie en de c.919G>T (p.A307S) mutatie in *TSEN54*. PCH5 en PCH4 zijn dus identieke aandoeningen.

Met het oog op het ziektemechanisme dat tot PCH leidt, hebben wij een zebravismodel voor PCH ontwikkeld. Zebravisembryo's lieten 24 uur na de bevruchting een sterke *tsen54* expressie zien in de hersenen, voornamelijk in het telencephalon en de "mid-hindbrain boundary", vergelijkbaar met hoge expressie van *TSEN54* in het telencephalon en metencephalon in een humaan embryo van 8 weken. Downregulatie van of *tsen54* of *rars2* met antisense oligonucleotiden resulteerde in hersenhypoplasie met het verlies van de "mid-hindbrain boundary" en een verhoogde celdood. Dit fenotype kon gedeeltelijk worden gered door het co-injecteren van respectievelijk het humane *TSEN54* en *RARS2* mRNA. De expressie van ontwikkelingsmarkers zoals fibroblast growthfactor (*fgf8*) en orthodenticle homeobox 2 (*otx2*) toonde expressie in de juiste regio's in de antisense-behandelde vis. Het normale patroon van deze ontwikkelingsmarkers en de verhoogde celdood suggereren dat PCH een neurodegeneratieve ziekte is en geen migratiestoornis. Kiembaan-knockout-vissen waren geïsoleerd uit een *N*-methyl-*N*-nitrosourea (ENU) mutant zebravis-database. Zebravissen, homozygoot voor een *tsen54* nonsense mutatie, vertoonden vroeg in de

ontwikkeling geen duidelijke stoornissen in de ontwikkeling van de hersenen, maar stierven 9 dagen na de bevruchting, waaruit blijkt dat TSEN54 essentieel is om te overleven. We gaan ervan uit dat stabiele *tsen54* knockout-vissen in de eerste week overleven dankzij de aanwezigheid van het maternale *TSEN54* mRNA en/of tRNA's afkomstig van de eicel.

Wij hebben ook bekeken of het TSEN complex betrokken is bij mRNA 3'eindformatie [10]. Dus ofwel een verminderde tRNA splicing, ofwel een verminderde mRNA 3'eindformatie zou verantwoordelijk kunnen zijn voor de ontwikkeling van PCH, of beide. Om onderscheid te kunnen maken tussen deze mogelijkheden analyseerden we de tRNA splicing activiteit van PCH2 fibroblasten in een *in vitro* assay. Nucleaire extracten van PCH2 en PCH4 patiënten vertoonden verminderde tRNA splicing. PCH4 extracten bleken minder activiteit dan PCH2 extracten te vertonen. Dit is in overeenstemming met de mutaties in deze aandoeningen; aminozuursubstituties en nonsense mutaties versus homozygote aminozuursubstituties. We hebben echter geen bewijs kunnen vinden voor verminderde mRNA 3'-eindformatie in PCH *in vitro* en *in vivo*.

Samengevat kon door ons worden aangetoond dat mutaties in *TSEN54*, *TSEN2* en *TSEN34* kunnen resulteren in PCH2, PCH4 en PCH5. Ook toonden we aan dat het verlies van TSEN54 functie verantwoordelijk is voor een fenotype van neurodegeneratie, waarschijnlijk ten gevolge van een verminderd tRNA splicing metabolisme.

Referenties

1. Barth PG: Pontocerebellar hypoplasias. An overview of a group of inherited neurodegenerative disorders with fetal onset. Brain Dev 1993, 15:411-422.
2. Barth PG: Pontocerebellar hypoplasia -- how many types? Eur J Paediatr Neurol 2000, 4:161-162.
3. Patel MS, Becker LE, Toi A, Armstrong DL, Chitayat D: Severe, fetal-onset form of olivopontocerebellar hypoplasia in three sibs: PCH type 5? Am J Med Genet A 2006, 140:594-603.
4. Norman RM: Cerebellar hypoplasia in Werdnig-Hoffmann disease. Arch Dis Child 1961, 36:96-101.
5. Barth PG, Vrensen GF, Uylings HB, Oorthuys JW, Stam FC: Inherited syndrome of microcephaly, dyskinesia and pontocerebellar hypoplasia: a systemic atrophy with early onset. J Neurol Sci 1990, 97:25-42.
6. Rajab A, Mochida GH, Hill A, Ganesh V, Bodell A, Riaz A, Grant PE, Shugart YY, Walsh CA: A novel form of pontocerebellar hypoplasia maps to chromosome 7q11-21. Neurology 2003, 60:1664-1667.
7. Namavar Y, Barth PG, Kasher PR, van Ruissen F., Brockmann K, Bernert G, Writzl K, Ventura K, Cheng EY, Ferriero DM et al.: Clinical, neuroradiological and genetic findings in pontocerebellar hypoplasia. Brain 2011, 134:143-156.

8. Edvardson S, Shaag A, Kolesnikova O, Gomori JM, Tarassov I, Einbinder T, Saada A, Elpeleg O: Deleterious mutation in the mitochondrial arginyl-transfer RNA synthetase gene is associated with pontocerebellar hypoplasia. Am J Hum Genet 2007, 81:857-862.

9. Anderson C, Davies JH, Lamont L, Foulds N: Early Pontocerebellar Hypoplasia with Vanishing Testes: A New Syndrome? Am J Med Genet Part A 2011, 155:667-672.

10. Paushkin SV, Patel M, Furia BS, Peltz SW, Trotta CR: Identification of a human endonuclease complex reveals a link between tRNA splicing and pre-mRNA 3' end formation. Cell 2004, 117:311-321.

11. Renbaum P, Kellerman E, Jaron R, Geiger D, Segel R, Lee M, King MC, Levy-Lahad E: Spinal muscular atrophy with pontocerebellar hypoplasia is caused by a mutation in the VRK1 gene. Am J Hum Genet 2009, 85:281-289.

Colour plates

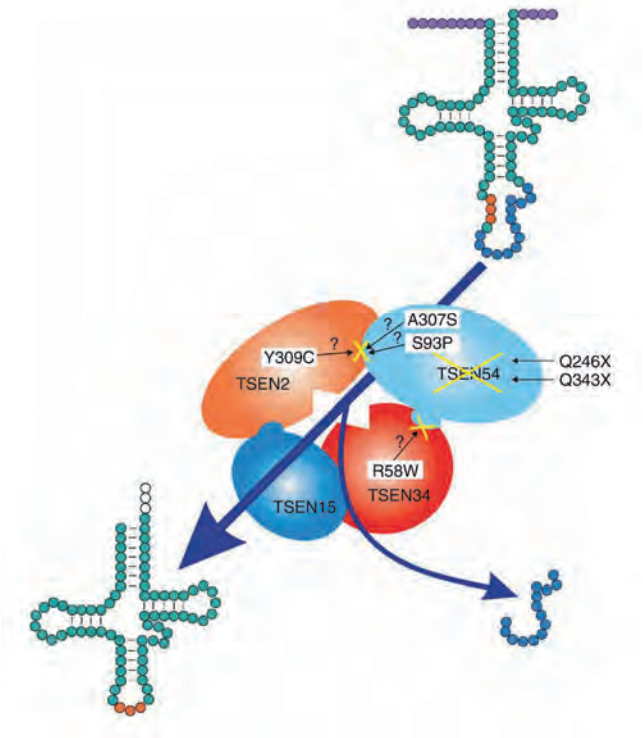

Figure 3. Model of human tRNA-splicing endonuclease (adapted from [18] and [19]). The tetrameric enzyme complex consists of the two catalytic subunits, TSEN2 and TSEN34, and two structural subunits, TSEN15 and TSEN54. Identified mutations in the PCH families are indicated by the corresponding amino acid changes. Top right, unprocessed tRNA with intron (blue) and anticodon loop (orange). After processing by the tRNA endonuclease, the intron is removed, resulting in the mature tRNA, bottom left. The processing of 5' leader and 3' trailer (purple) is preformed by other enzymes (see ref. [19] for details).

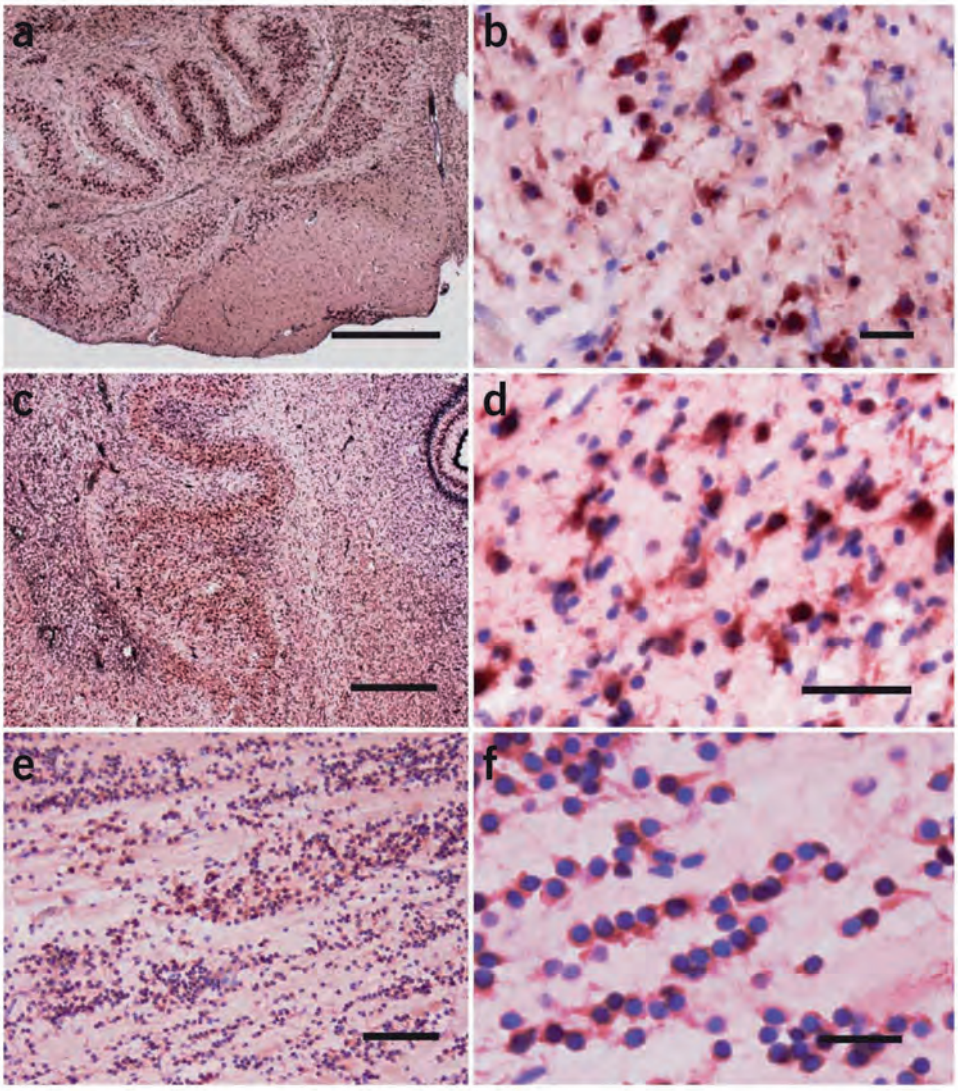

Figure 4. *TSEN54* expression in human foetal brain. (a,b) Inferior olivary nucleus at gestational age 23 weeks. The undulated structure can be seen in (a) including that in the medial accessory olivary nucleus. Scale bar, 500µm. (b) Higher magnification of (a) showing positive staining in individual neurons and surrounding dendrites. Scale bar, 25µm. (c,d) Cerebellar dentate nucleus at gestational age 23 weeks. (c) The upper half of the developing nucleus has the mature undulated form, while the lower half has the transitional compact form. Scale bar, 500µm. (d) Higher magnification of (c) showing positive staining in cytoplasma of individual neurons and surrounding dendrites. Scale bar, 50µm. (e,f) Ventral pons at gestational age, 21 weeks. (e) Groups of immature small neurons separated by bundles of nerve fibers. Scale bar, 100µm. (f) Higher magnification of (e) showing small neurons with positive staining of cytoplasm and dendrites. Scale bar, 25µm.

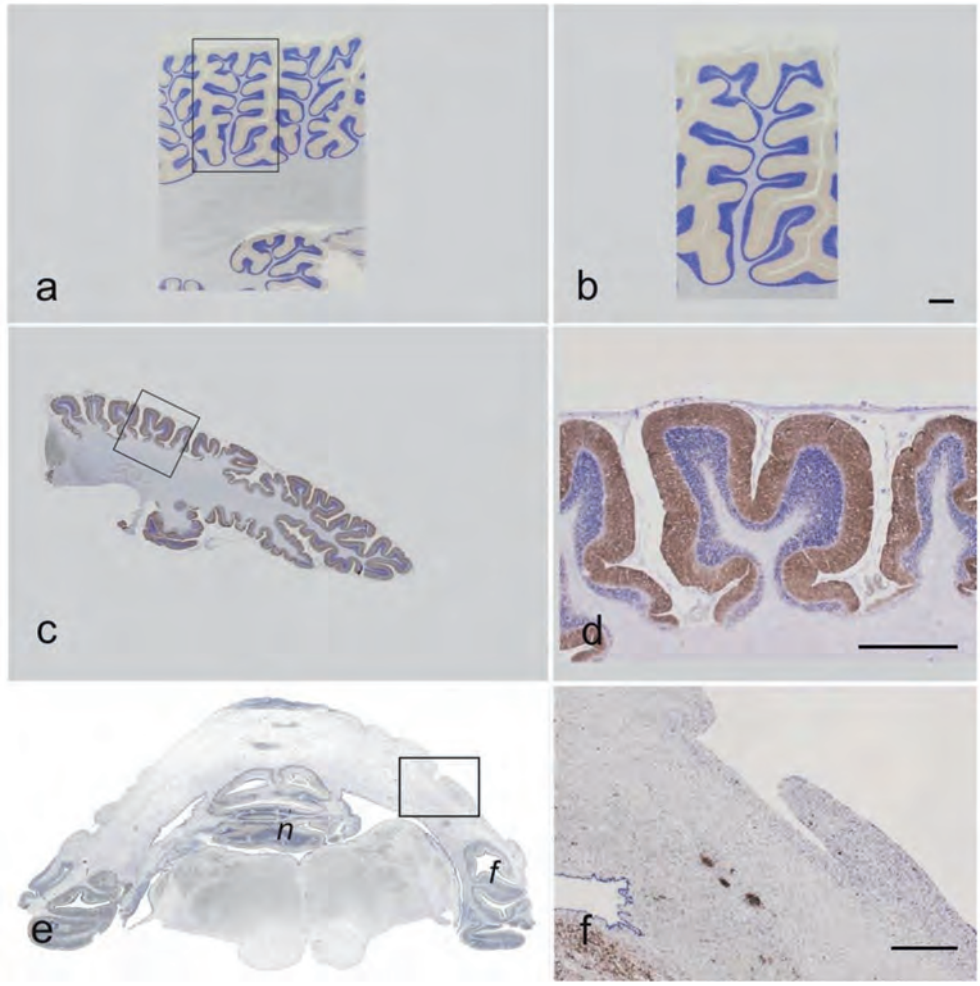

Supplementary Figure 5. Cerebellar cortex in PCH2 and PCH4 (OPCH). (a,b) Control male of 8 yr with accidental death. (c,d) Patient with PCH2 from Am1 family who died at 3 yr, 7m. (e,f) Patient with PCH4 from Ut4 family who died two days old. All paraffin sections are stained for synaptophysin. Rectangles on the left side are magnified on the right side. Magnification bars represent 1mm. In control (a,b) a single folium within the rectangle has about 10 branchlets. In the PCH2 patient (c,d) folia are stunted and have few or no branchlets. Notice the loss of cortex between folia in (c). In the PCH4 patient (e,f) folia are rudimentary and denuded with complete loss of cortex except the nodulus (*n*) and flocculus (*f*). Adapted from Barth *et al.* [6], with permission.

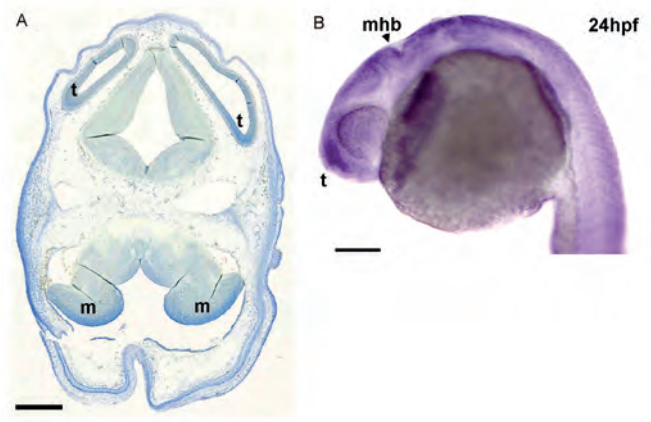

Figure 1. *TSEN54* expression is ubiquitous but strong in the brain in human and zebrafish early stages of neurodevelopment. (a) *TSEN54 in situ* hybridization within transverse section of a human foetal brain at 8 weeks prenatal age. *TSEN54* mRNA is widely expressed throughout brain and head tissue, but strongly expressed in the developing metancephalon (m) and telencephalon (t). Scale bar = 1mm. (b) Lateral view of *tsen54* whole-mount *in situ* hybridization in zebrafish embryo. Ubiquitous *tsen54* mRNA expression pattern is observed at 24 hpf in zebrafish embryos, with the strongest expression observed within the brain, especially the telencephalon (t) and mid-hindbrain boundary (mhb). Scale bar = 200µm.

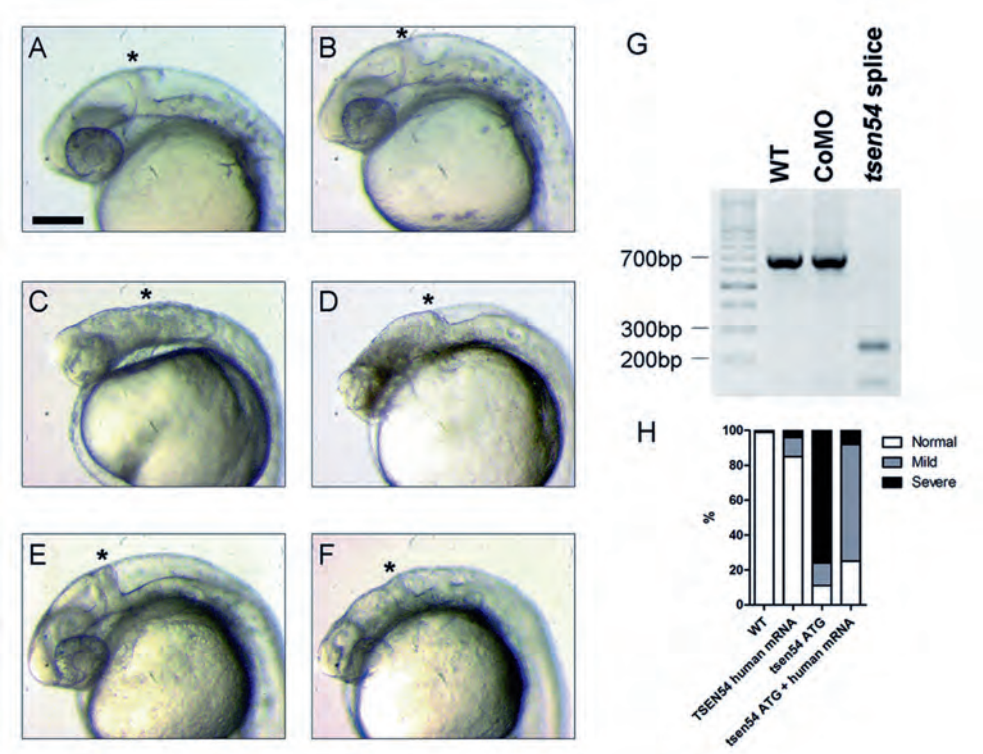

Figure 2. Disruption of *tsen54* translation causes brain hypoplasia and loss of structural definition in the MHB in zebrafish embryos. (a-f) Lateral views of head and brain regions of *tsen54* MO and human *TSEN54* mRNA-injected zebrafish embryos at 24 hpf. Asterisks denote the MHB. (a) WT un-injected embryo; (b) CoMO-injected embryo; (c) *tsen54* ATG MO-injected embryo; (d) *tsen54* exon 8 splice donor site MO-injected embryo; (e) human *TSEN54* mRNA-injected embryo; (f) rescued embryo co-injected with tsen54 ATG MO and human *TSEN54* mRNA. Scale bar = 200µm. (g) RT-PCR using primers located in exons 7 and 10 in *tsen54* cDNA synthesised from RNA extractions from WT un-injected embryos, CoMO-injected embryos and *tsen54* exon 8 splice donor site MO-injected embryos. RT-PCR using samples from control embryos produced a band of 696bp in length. Shorter products observed in splice MO-injected embryos indicate abnormal splicing of the *tsen54* gene. (h) Quantification of phenotypes observed in WT un-injected embryos, human *TSEN54* mRNA-injected embryos, *tsen54* ATG MO-injected embryos and rescued embryos co-injected with ATG MO and human mRNA. For each group, 50-100 embryos were analysed. Embryos were classified as displaying normal (white), mild (grey) or severe (black) phenotypes. There is a shift from a predominantly severe phenotype in the *tsen54* ATG MO group to a predominantly mild phenotype in ATG MO and human *TSEN54* mRNA co-injection group, thus illustrating the partial rescue of the brain phenotype associated with the loss of tsen54.

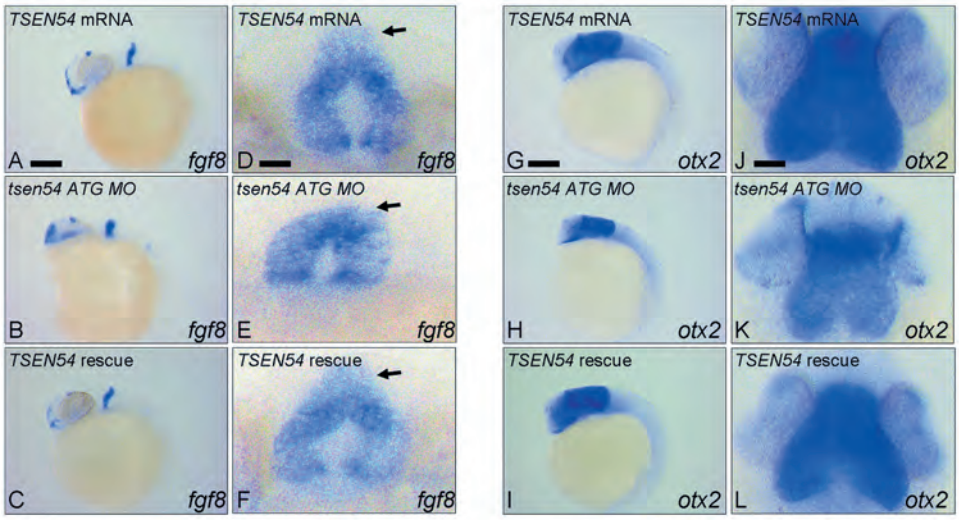

Figure 3. Knockdown of zebrafish *tsen54* results in a brain defect that is not associated with abnormal developmental patterning. Whole-mount *in situ* hybridization using *fgf8* (a-f) and *otx2* (g-l) DIG RNA probes in 24 hpf embryos injected with human *TSEN54* mRNA alone (a,d,g,j), *tsen54* ATG MO (b,e,h,k) and *tsen54* ATG MO with human *TSEN54* mRNA rescue (c,f,i,l). Lateral views are presented in (a-c) for *fgf8* staining and (g-i) for *otx2* staining (scale bar = 200µm). Dorsal views are presented in (d-f) for *fgf8* staining (scale bar = 30µm) and (j-l) for *otx2* staining (scale bar = 50µm). Results reveal brain hypoplasia is evident in *tsen54* morphants, as indicated by the loss of the *fgf8* 'horseshoe peak' expression pattern (arrows) however, developmental patterning of the MHB (*fgf8*) and fore-midbrain (*otx2*) are normal. Co-injection of the ATG MO with *TSEN54* human mRNA is capable of partially rescuing the brain hypoplasia phenotype, thus confirming specific targeting of the MO.

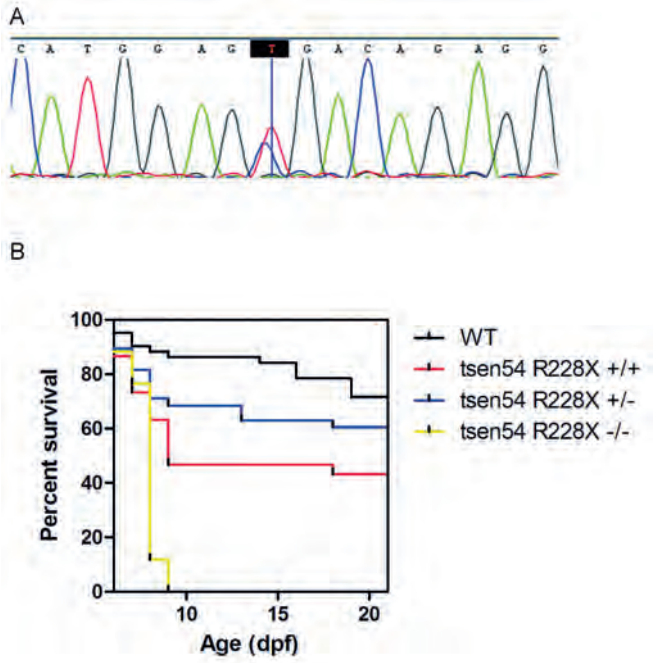

Figure 5. A homozygous premature stop-codon mutation within *tsen54* causes early lethality in zebrafish larvae. (a) Sequence trace obtained from the individual heterozygous c.682C>T *tsen54* mutant (hu5985). Translation of this base pair substitution leads to the p.R228X mutation. The mutation was subsequently backcrossed onto a WT background for five generations. (b) Progeny from a *tsen54*$^{R228X+/-}$ in-cross were observed for 3 weeks post-fertilization to test for homozygosity. Survival was plotted using the Kaplan-Meier curves. By 9 dpf, 100% of the *tsen54*$^{R228X-/-}$ (yellow line) larvae had died. In comparison, 45% and 62% of the *tsen54*$^{R228X+/+}$ (red line) and *tsen54*$^{R228X+/-}$ (blue line) survived to the 3 weeks post-fertilization time point, respectively. As a comparison to general ENU mutant survival, 72% WT TL larvae (black line) were observed to survive to the 21 dpf stage.

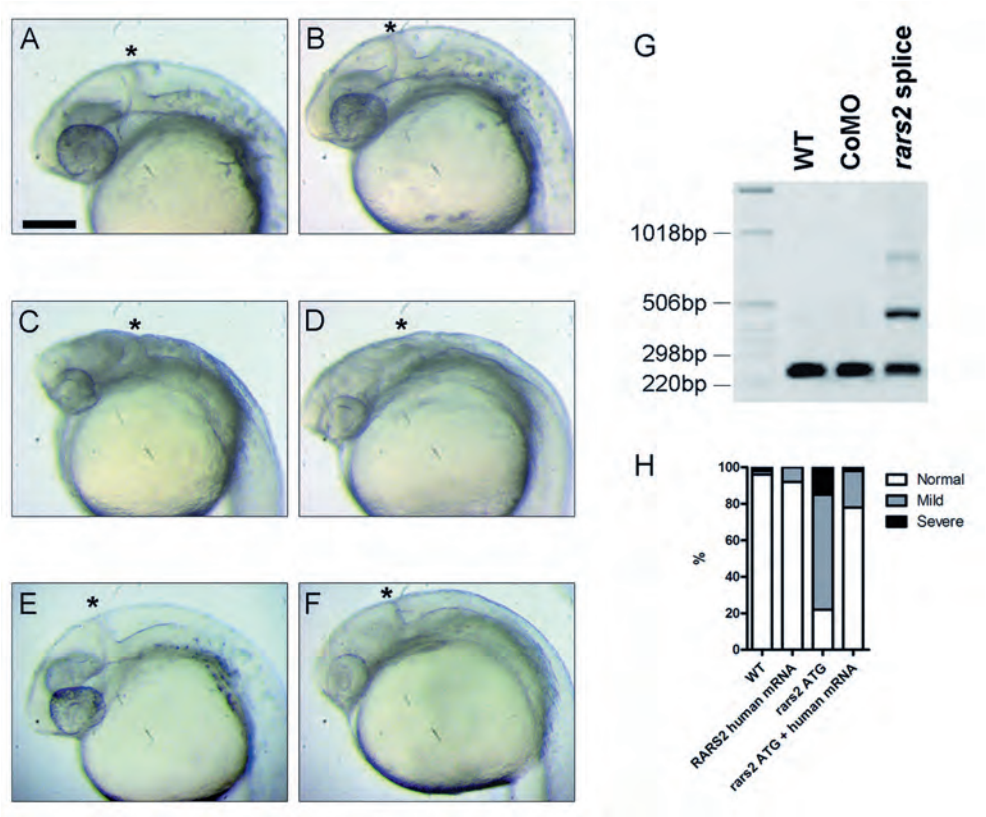

Figure 6. Disruption of *rars2* gene results in brain phenotype comparable with *tsen54* knockdown. (a-f) Head and brain regions of *rars2* MO and human *RARS2* mRNA-injected zebrafish embryos at 24 hpf. Asterisks denote the MHB. (a) WT un-injected embryo; (b) CoMO-injected embryo; (c) *rars2* ATG MO-injected embryo; (d) *rars2* exon 6 splice donor site MO-injected embryo; (e) human *RARS2* mRNA-injected embryo; (f) rescued embryo co-injected with *rars2* ATG MO and human *RARS2* mRNA. Scale bar = 200µm. (g) RT-PCR using primers located in exons 3 and 6 in *rars2* cDNA synthesised from RNA extractions from WT un-injected embryos, CoMO-injected embryos and *rars2* exon 6 splice donor site MO-injected embryos. RT-PCR using samples from control embryos produced a band of 246bp in length. Larger products observed in splice MO-injected embryos indicate abnormal splicing of the *rars2* gene. (h) Quantification of phenotypes observed in WT un-injected embryos, human *RARS2* mRNA-injected embryos, *rars2* ATG MO-injected embryos and rescued embryos co-injected with ATG MO and human mRNA. For each group, 50-100 embryos were analysed. Embryos were classified as displaying normal (white), mild (grey) or severe (black) phenotypes. There is a shift from a predominantly mild-severe phenotype in the *rars2* ATG MO group to a predominantly normal phenotype in ATG MO and human *RARS2* mRNA co-injection group, thus illustrating the partial rescue of the brain phenotype associated with the loss of rars2.

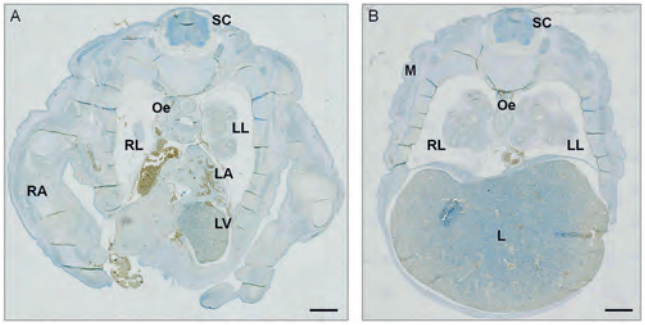

Supplementary Figure 1. *TSEN54* expression within other human foetal tissues. Relatively high *TSEN54* expression was observed in human foetal spinal cord and liver, whereas comparatively low expression levels were observed in other tissues. SC = spinal cord; L = liver; Oe = oesophagus; M = muscle; LL = left lung; RL = right lung; LA = left atrium; LV = left ventricle; RA = right arm. Scale bar = 500µm.

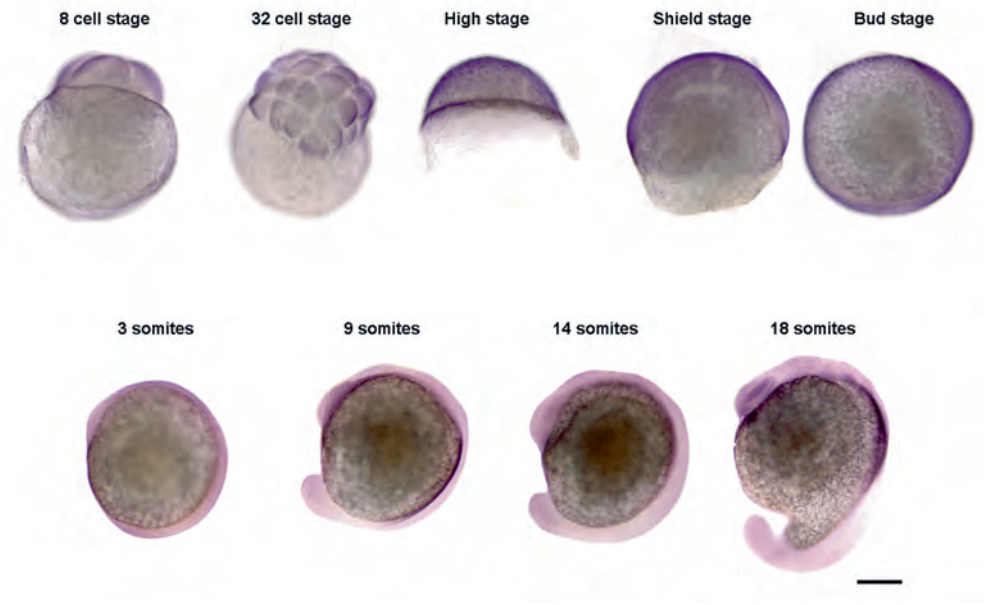

Supplementary Figure 2. *Tsen54* expression is ubiquitous during early embryogenesis in the zebrafish. Ubiquitous *tsen54* mRNA expression pattern is observed in zebrafish embryos from the 8-cell stage to the somite stages. Scale bar = 200µm.

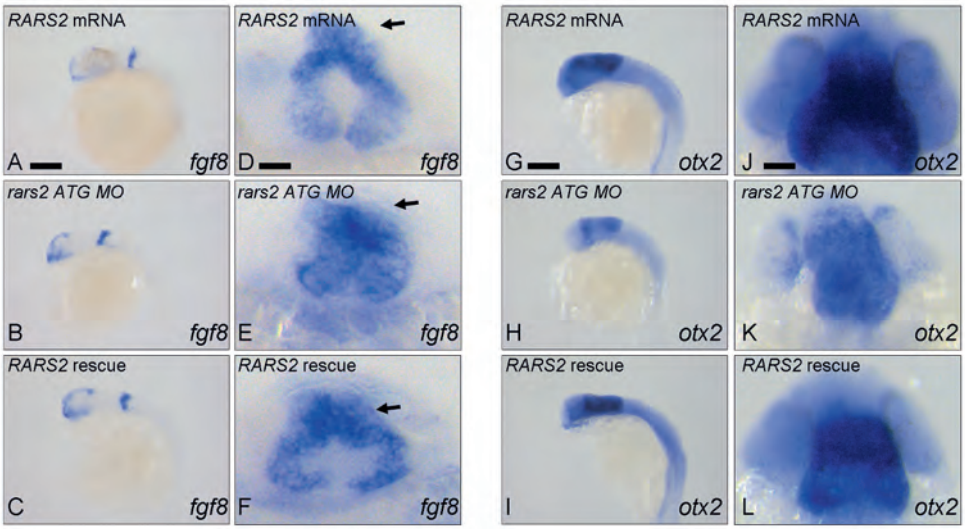

Supplementary Figure 3. Disruption of *rars2* gene results in brain phenotype comparable to *tsen54* knockdown. Whole mount *in-situ* hybridization using *fgf8* (a-f) and *otx2* (g-l) DIG RNA probes in 24 hpf embryos injected with human *RARS2* mRNA alone (a,d,g,j), *rars2* ATG MO (b,e,h,k) and *rars2* ATG MO with human *RARS2* mRNA rescue (c,f,i,l). Lateral views are presented in (a-c) for *fgf8* staining and (g-i) for *otx2* staining (scale bar = 200µm). Dorsal views are presented in (d-f) for *fgf8* staining (scale bar = 30µm) and (j-l) for *otx2* staining (scale bar = 50µm). Results reveal brain hypoplasia is evident in *rars2* morphants, as indicated by loss of the *fgf8* 'horse-shoe peak' expression pattern (arrows) however, developmental patterning of the mid-hindbrain boundary (*fgf8*) and fore-midbrain (*otx2*) are normal. Co-injection of the ATG MO with *RARS2* human mRNA is capable of partially rescuing the brain hypoplasia phenotype, thus confirming specific targeting of the MO.

Acknowledgements

Dankwoord - Acknowledgements

In de eerste plaats wil ik alle patiënten en familieleden bedanken voor hun medewerking, dit onderzoek was niet mogelijk geweest zonder hun bijdrage. De afgelopen jaren heb ik met veel plezier aan dit proefschrift gewerkt. Zowel dit onderzoek als dit plezier rusten op de wetenschappelijke en vriendschappelijke hulp van vele mensen. Helaas kan ik niet iedereen noemen, maar dat betekent niet dat ik niet dankbaar ben aan iedereen die hierbij betrokken was!

Mijn bijzondere dank gaat uit naar Professor Dr. F. Baas. Beste Frank, dankjewel! Alles wat ik nu weet over genetica en moleculaire biologie heb jij mij geleerd. Dank voor jouw steun, enthousiasme, kritische vragen en dat je altijd open stond voor wetenschappelijke discussies. Dank voor jouw interesse en voor het geloven in mij, zelfs voordat ik er zelf in geloofde.

Mijn dank gaat ook uit naar Professor Dr. P.G. Barth. Beste Peter, dankuwel voor uw geduld! Ik heb veel van u geleerd. U hebt ervoor gezorgd dat mijn focus bij de geneeskunde bleef liggen. Anderzijds was er altijd veel interesse van uw kant voor mijn labwerk. Dankuwel voor alle enerverende discussies over onze gemeenschappelijke interesse of misschien wel onze gemeenschappelijke obsessie, PCH.

Beste Professor Dr. B.T. Poll-The, beste Bwee Tien, dankuwel voor het vertrouwen en de vrijheid die ik heb gekregen. Dank dat u mij meenam de kliniek in en uitnodigde op congressen en patiëntenbijeenkomsten. Dankuwel voor de klinische verbreding die u mij hierbij gaf. Ik koester onze gesprekken en discussies in de auto en natuurlijk de tip om te gaan hardlopen! Ik kijk ernaar uit om u tegen te komen in de kliniek.

Of course I would like to acknowledge the reading committee: Prof. Hennekam, Prof. van der Knaap, Dr. Martinez, Prof. Oostra, Prof. van Schaik and Prof. Wanders for reviewing my thesis and participating in my defense. Thank you!

My gratitude goes to the Martinez group from the IMBA in Vienna. Dr. Javier Martinez and Dr. Stefan Weitzer, thank you for a fruitful and promising collaboration. Thank you very much for the warm welcome I received in Vienna. Thank you for teaching me, as a medical student, hard-core tRNA experiments. Johannes thanks for endless tRNA processing discussions, they helped me a lot!

Beste Professor M. de Visser, dat dit avontuur bij u is begonnen, in het derde jaar van mijn studie, ben ik niet vergeten. Dank voor uw hulp in het allereerste begin, maar natuurlijk ook voor het lezen van mijn “geno-pheno”-manuscript en uw motiverende woorden bij presentaties.

My daily support came from some very good friends in the lab.

Paul Kasher, dear Paul, I liked it how we were a very good team, how we talked about science and how we could also talk about other stuff. Meaning: birds, badgers, clowns, Papa Lazarou, a fine selection of sandwiches, shepherd's pie and science jokes. You taught me how to stay cool and how to plan my experiments well. For the future I hope we will meet each other again in a lab and I am sure we will keep on seeing each other in the UK or in Amsterdam, or wherever. SUPERBEDANKT!

Lieve Katja, I cherish our morning moments which usually started with a cup of coffee or tea and then we discussed our plans for the day. Thank you so much for always being there for me. I feel you are my true PhD friend: we have been through all the courses and congresses together. I will most certainly miss you being around. Not only because I will miss your help but also because I have to miss the gezelligheid. And thanks for being my paranimf!

Lieve Jelly, vanaf de eerste dag waren we matties aka "soulmates". Altijd heb jij tijd gemaakt om écht te luisteren. Jouw gezelligheid, positiviteit, interesse en oprechtheid waren recept voor een geweldige tijd! Dankjewel voor het hooghouden van deze moraal, ook op stressvolle dagen. Ook bedankt voor alle nuttige en minder nuttige email-alerts en jouw hulp bij de afronding van mijn proefschrift en de voorbereidingen op mijn verdediging. Ik zal je missen!

Lieve Olaf, wij wisten wel beter. Nu moet ik de grote-mensen-wereld weer in, zonder jouw hulp, een veilige vraagbaak, een koffiemaatje, een sparringspartner, een vier-handen-op-jouw-buik-gevoel, een dankbaar publiek voor al mijn grappen, een luisterend oor. Olaf, dankjewel!

Lieve Martin, sorry dat ik altijd jouw lunch op at! Dankjewel dat jij er bent, voor alle broodjes kaas, het temperen van mijn kuren, het opruimen van de brokken, alle ontspanning en je hulp bij proeven. Dankjewel voor superveel hulp!

Anneloor, dank voor jouw stimulerende woorden, kritische vragen en het zelfvertrouwen dat je me gaf en natuurlijk voor het beantwoorden van al mijn RNA vragen. Fred, dank voor jouw hulpvaardigheid bij al mijn database en genetica vragen. Marian, bedankt voor het wegwijsmaken tijdens de vroege dagen en het delen van het A307S-eureka-moment toen Frank op vakantie was. Jeroen, tot in het einde der dagen heb ik jou vermoeid met vragen, met name als ik weer eens een RA-periode had, dank voor je niet-aflatende hulp. Rob, dankjewel voor het geen enkele kans onbenut laten om mij te plagen en natuurlijk voor het aanleren van tal van basisskills in het lab. Wiep, dank voor jouw vertrouwen in mijn kunnen, de inspiratie voor de fundamentele biologie en het aanzetten van kritisch denken. Prof. Dr. V. de Jong, beste Vianney, dankuwel voor het kritisch lezen van mijn manuscripten, uw motiverende woorden en uw spannende verhalen.

Alle andere aio's wens ik een mooie afronding van jullie tijd hier. Diana, de laatste loodjes, ik weet zeker dat het goed komt en heb zin in jouw verdediging! Joeri, never a dull moment, succes met de afronding van jouw PhD. Judith en Nawal, jullie zijn nog maar net begonnen, geniet ervan! Veerle, bedankt voor alle gezongen liedjes en alle NERD-grapjes omtrent het getal 54 en oranjeSLM, maar ook bedankt voor de fijne samenwerking. Barbara jouw lach en oprechte interesse voor je omgeving zal ik koesteren en ik hoop dat als ik eenmaal dokter ben, ik net zo goed kan luisteren als jij! Hyung, het was super om naast jou te zitten en heerlijk om de dag te beginnen met "how do you like your eggs in the morning", wat mis ik dat!

José, Valeria, Sidhartha and Marleen, my PhD colleagues from the very first moments. José the best PhD advice came from you: try to become an expert on your topic. I tried and I hope that I succeeded, thanks for your support. Valeria, thank you for being such a fine example and always happy to help! Sid, bedankt dat jij mij binnen no-time thuis hebt laten voelen op de afdeling en voor alle vertrouwdheid! Marleen, bedankt voor de gezellige tijd in de aio-kamer en bij alle willekeurige borrels.

Ruud, bedankt voor al jouw hulp in het lab, jouw vogelverhalen en twee superleuke culinaire weekenden! Marit bedankt voor al jouw PCR-hulp-bij-ongeluk. Kees dank voor jouw kritische vragen, jouw RNA-liefde en de Keesipedia. Line, leuk dat ik op precies dezelfde datum verdedig als jij, ik neem aan dat dat iets goeds betekent! Natuurlijk ook alle andere (ex)collega´s en studenten bedankt voor de goede sfeer en hulp in het lab, Lou, Ted, Ferry, Susan, Mia, Carin, Marja, Lydia, Coby, Justus, Thijs, Theo, Anna, Jules, Regien, Marylla, Jan-Willem, Monique, Linda, Maaike, Marieke, Paul (Klarenbeek), Rebecca, Esther, Elsmarieke, Jenny, Ana, Oscar, Bart Andre en Martina.

Natuurlijk is er ook nog dat andere front, zonder wie ik het niet gekund had! Lieve Papa en Mama, ik ben blij dat ik dit met jullie kan delen. Dank jullie wel voor het leren van een wetenschappelijk-kritsche blik en voor al jullie hulp bij de afronding van deze fase en bij de start van een nieuwe fase. Ik weet dat jullie trots op mij zijn, ik houd van jullie en jullie mening zal altijd belangrijk voor mij zijn. Lieve Reza, ik ben altijd zo trots op jou! Dankjewel dat je vaak zo lief bent en je daarbij toch dikwijls hardop afvroeg of ik toch geen workaholic werd, maar ook dat je mij al heel vroeg buiten de hokjes leerde denken. Dankje voor al het plezier en jouw zorgen!

Lieve Oma, dankuwel dat u altijd voor mij klaar staat. Ook bedankt voor al uw steun, interesse, liefde en levenswijsheid. Wat fijn dat u altijd zo dichtbij bent! Marian, dankjewel voor jouw niet-aflatende steun, ook op grijze dagen.

Lieve Kim, dankjewel voor jouw onvoorwaardelijkheid. Je bent er altijd voor mij. Wat zou ik zonder jou moeten!? Dankjewel voor jouw steun, liefde, enorme hulp, maar ook voor alle gesprekken over essentiële en minder essentiële zaken die wel uitvoerige analyses vereisen.

De familie van Leeuwen, en dan vooral lieve Francien en Gerrit! Dank jullie wel voor alle warmte en het geluk om zo dichtbij te mogen zijn. Lieve Narda, wat heerlijk dat jij precies leuk vindt, wat ik verschrikkelijk vind! Dankjewel voor jouw hulp en warmte!

Lieve Wiebe, samen zijn we groot geworden. De keus om aan het promotie-onderzoek te beginnen heb ik samen met jou en mede dankzij jou gemaakt. Dankjewel voor al jouw hulp en jouw enorme steun! Ook bedankt voor alle "this is how it's made's" en hulp bij het lezen van menig artikel! Jelle, dankjewel voor tientallen pannenkoeken, honderden koppen koffie en thee, altijd teveel gebakken eieren, twee toiletbrillen, kilometers rondjes Sloterpark, westerns of andere slechte films, het delen van spannende en minder spannende verhalen en het opvangen van heel wat stress, ook bij het maken van dit proefschrift! Eefje! Dankjewel dat je zo ontzettend lief voor mij bent. Heerlijk dat we weer samen in het AMC zijn en ik kijk al uit naar jouw verdediging. Lieve Michiel, superfijn dat je de laatste twee jaar weer zo dichtbij was. Wat een enorme motivator ben jij (heb je dat wel door?). Dankjewel voor het hebben kunnen delen van deze tijd. Anouk! Yes! Al bijna 3 jaar houden wij de zwemspirit high (en daarmee het fysiek afbeulen). Dankjewel voor alle gesprekken voor, tijdens, en na het zwemmen. Jesse, lieve Jes, wij vinden steeds een nieuwe weg om onze vriendschap te vieren zonder dat dat ons ooit moeite kost. Ik weet zeker dat dit voor de toekomst ook goed komt. Gek genoeg ben jij voor mij een rustpunt, dankjewel.

Dank aan alle lieve mensen, met het gevaar hier incompleet te zijn: Bernard, Thomas, Vincent, Renske, Nadia, Arcinio, Jenny, Margriet, Flo, Danny, Siân.

Anieke, Marieke, Rob, Ben. Jongens wat een heerlijkheid. Dank jullie wel voor alle ontspanning! Wat moet een mens zonder ontspanning? En een mens moet toch ook eten? En op vakantie, en vooruit, ook vogelen, tekenen, koffie drinken, de hondenmand in, af en toe naar Texel en vooral veel samen. Gelukkig hoefden we voor de rest heel weinig en konden we overal keihard dwarsdoorheen genieten. Ik heb zo'n zin in de toekomst, met jullie, als voortzetting van deze tijd!
Lieve Marieke, dankjewel voor jouw wijsheid op precies de goede momenten, jouw relativeringskunst, jouw goede zorgen bij ziekte en alle veiligheid! Dankjewel voor de ontspanning die er is bij jou thuis, met alle goede dingen van het leven (met of zonder klei). Lieve Ben, wat fijn dat je erbij bent en wat bijzonder dat het vanaf het begin af aan meteen al zo goed en vertrouwd is. Lieve Anieke, dankjewel! Met jou bij mij in de buurt komt alles altijd goed en lukt het mij om de wereld zonnig in te zien. Je geeft me rust en vertrouwen. Ik ben zo blij met al jouw hulp in mijn leven (wat echt heel veel is) en omdat je mijn paranimf wilt zijn en dat je mijn biografie wilde schrijven! Wat fijn dat alles altijd zo leuk is op deze manier. Lieve Rob, je staat zelfs in mijn biografie! Je bent the R in mijn leven. Dankjewel voor jouw gigantische hulp, niet in de minste plaats bij stressbestrijding, de lay-out en het maken van dit proefschrift (wat is het ontzettend mooi geworden!), maar ook bij het doormaken van ieder willekeurig life-event. Rob, dankjewel!

List of publications

List of publications

Namavar Y, Barth PG, Poll-The BT and Baas F: Classification, diagnosis and potential mechanisms in pontocerebellar hypoplasia. The Orphanet Journal of Rare Diseases 2011, 6:50.

Namavar Y, Barth PG, Baas F and Poll-The BT: Reply: Mutations of TSEN and CASK genes are prevalent in pontocerebellar hypoplasias type 2 and 4. Brain 2011, online (doi:10.1093/brain/awr109).

Namavar Y, Chitayat D, Barth PG, van Ruissen F, de Wissel MB, Poll-The BT, Silver R, Baas F: TSEN54 mutations cause pontocerebellar hypoplasia type 5. Eur J Hum Genet 2011.

Namavar Y, Barth PG, Kasher PR, van Ruissen F, Brockmann K, Bernert G, Writzl K, Ventura K, Cheng EY, Ferriero DM, Basel-Vanagaite L, Eggens VR, Krägeloh-Mann I, De Meirleir L, King M, Graham JM Jr, von Moers A, Knoers N, Sztriha L, Korinthenberg R, PCH Consortium, Dobyns WB, Baas F, Poll-The BT: Clinical, neuroradiological and genetic findings in pontocerebellar hypoplasia. Brain 2011, 134:143-156.

Kasher PR, Namavar Y, van Tijn P, Fluiter K, Sizarov A, Kamermans M, Grierson AJ, Zivkovic D, Baas F: Impairment of the tRNA-splicing endonuclease subunit 54 (tsen54) gene causes neurological abnormalities and larval death in zebrafish models of pontocerebellar hypoplasia. Hum Mol Genet 2011, 20:1574-1584.

Graham JM, Jr., Spencer AH, Grinberg I, Niesen CE, Platt LD, Maya M, Namavar Y, Baas F, Dobyns WB: Molecular and neuroimaging findings in pontocerebellar hypoplasia type 2 (PCH2): is prenatal diagnosis possible? Am J Med Genet A 2010, 152A:2268-2276.

Namavar Y, Barth PG & Baas F: Pontocerebellar Hypoplasia Type 2 and Type 4. Pagon RA, Bird TD, Dolan CR, Stephens K, editors. Seattle (WA): University of Washington, Seattle. GeneReviews, 2009.

Budde BS*, Namavar Y*, Barth PG, Poll-The BT, Nürnberg G, Becker C, van Ruissen F, Weterman MA, Fluiter K, te Beek ET, Aronica E, van der Knaap MS, Höhne W, Toliat MR, Crow YJ, Steinling M, Voit T, Roelenso F, Brussel W, Brockmann K, Kyllerman M, Boltshauser E, Hammersen G, Willemsen M, Basel-Vanagaite L, Krägeloh-Mann I, de Vries LS, Sztriha L, Muntoni F, Ferrie CD, Battini R, Hennekam RC, Grillo E, Beemer FA, Stoets LM, Wollnik B, Nürnberg P, Baas F: tRNA splicing endonuclease mutations cause pontocerebellar hypoplasia. Nat Genet 2008, 40:1113-1118.

*Equally contributed

Biography

Biography – Yasmin Namavar

After growing up and receiving her secondary school education in Uithoorn, Yasmin (born 1983) went to study in Amsterdam. Somehow it was fortunate that because of the lottery system, she was not immediately admitted to the Medicine studies. Instead, Yasmin studied Biomedical Sciences for one year, with the first course being on genetics, a subject that proved to be an essential red thread for her academic career, unwinding in this thesis. Ever since the first days at university (and already before that, in secondary school), Rob was present at Yasmin's side (himself being a hard-core ecologist, they still shared their first courses in Biology). At the same time, new people appeared in her close surroundings and some would stick around tightly throughout the wild period of undergraduate studies and the more serious times of Masters and graduate studies.

The second year at university however, Yasmin was accepted for the medicine studies and she would be distracted by pathological phenomena and a wide array of syndromes and palindromes for the next three-and-a-half years, before she would be back in the lab and discover her fascination for running gels and analysing blots. During her five months internship at the lab with Professor Shaw's group in Sheffield, she met her future collaborator and companion in discovering the inner workings of Tsen54, Paul Kasher.

At the end of the theoretical part of her Medicine studies, marked with an MSc degree, Yasmin received the AMC PhD scholarship for excellent students, which was followed in a year by the second publication award of the AMC. In addition to these distinctions she was awarded with the best oral presentation prize at a national genetics conference in 2011, for her presentation: *The role of the tRNA splicing endonuclease in Pontocerebellar Hypoplasia.* It seems strange to characterise a colourful person like Yasmin by listing the prizes she received in her field of study. Still stranger may be to emphasise those achievements without highlighting something from her list of publications. But space is limited (and one could argue that the publications have received enough space and emphasis in the remainder of this book) and I think that the awards and distinctions shortly described here, can illustrate Yasmin's everlasting ambition and endurance in trying to get to the bottom of the problem she is studying. Yasmin has shown that through hard, intelligent work, in combination with a passionately intense focus, it was possible to solve a part of the complex puzzle that forms the human brain.

The academic achievement stands by itself, but in a biography, let the author be allowed some final points of personal observation: Courage, intelligence and humor, these nouns hardly cover a glimpse of her personality, but as adjectives they could be considered the themes or volumes in a more extended biography.

By Anieke van Leeuwen